

# Springer Tracts in Modern Physics

## Volume 201

Managing Editor: G. Höhler, Karlsruhe

Editors: J. Kühn, Karlsruhe

Th. Müller, Karlsruhe

A. Ruckenstein, New Jersey

F. Steiner, Ulm

J. Trümper, Garching

P. Wölflie, Karlsruhe

Available online at  
**SpringerLink.com**

Starting with Volume 165, Springer Tracts in Modern Physics is part of the [SpringerLink] service. For all customers with standing orders for Springer Tracts in Modern Physics we offer the full text in electronic form via [SpringerLink] free of charge. Please contact your librarian who can receive a password for free access to the full articles by registration at:

[springerlink.com](http://springerlink.com)

If you do not have a standing order you can nevertheless browse online through the table of contents of the volumes and the abstracts of each article and perform a full text search.

There you will also find more information about the series.

**Springer**

*Berlin*

*Heidelberg*

*New York*

*Hong Kong*

*London*

*Milan*

*Paris*

*Tokyo*

# Springer Tracts in Modern Physics

---

Springer Tracts in Modern Physics provides comprehensive and critical reviews of topics of current interest in physics. The following fields are emphasized: elementary particle physics, solid-state physics, complex systems, and fundamental astrophysics.

Suitable reviews of other fields can also be accepted. The editors encourage prospective authors to correspond with them in advance of submitting an article. For reviews of topics belonging to the above mentioned fields, they should address the responsible editor, otherwise the managing editor.

See also [springeronline.com](http://springeronline.com)

## Managing Editor

Gerhard Höhler

Institut für Theoretische Teilchenphysik

Universität Karlsruhe

Postfach 69 80

76128 Karlsruhe, Germany

Phone: +49 (7 21) 6 08 33 75

Fax: +49 (7 21) 37 07 26

Email: [gerhard.hoehler@physik.uni-karlsruhe.de](mailto:gerhard.hoehler@physik.uni-karlsruhe.de)

[www-tpp.physik.uni-karlsruhe.de/](http://www-tpp.physik.uni-karlsruhe.de/)

## Elementary Particle Physics, Editors

Johann H. Kühn

Institut für Theoretische Teilchenphysik

Universität Karlsruhe

Postfach 69 80

76128 Karlsruhe, Germany

Phone: +49 (7 21) 6 08 33 72

Fax: +49 (7 21) 37 07 26

Email: [johann.kuehn@physik.uni-karlsruhe.de](mailto:johann.kuehn@physik.uni-karlsruhe.de)

[www-tpp.physik.uni-karlsruhe.de/~jk](http://www-tpp.physik.uni-karlsruhe.de/~jk)

Thomas Müller

Institut für Experimentelle Kernphysik

Fakultät für Physik

Universität Karlsruhe

Postfach 69 80

76128 Karlsruhe, Germany

Phone: +49 (7 21) 6 08 35 24

Fax: +49 (7 21) 6 07 26 21

Email: [thomas.muller@physik.uni-karlsruhe.de](mailto:thomas.muller@physik.uni-karlsruhe.de)

[www-ekp.physik.uni-karlsruhe.de](http://www-ekp.physik.uni-karlsruhe.de)

## Fundamental Astrophysics, Editor

Joachim Trümper

Max-Planck-Institut für Extraterrestrische Physik

Postfach 16 03

85740 Garching, Germany

Phone: +49 (89) 32 99 35 59

Fax: +49 (89) 32 99 35 69

Email: [jtrumper@mpe-garching.mpg.de](mailto:jtrumper@mpe-garching.mpg.de)

[www.mpe-garching.mpg.de/index.html](http://www.mpe-garching.mpg.de/index.html)

## Solid-State Physics, Editors

Andrei Ruckenstein

*Editor for The Americas*

Department of Physics and Astronomy

Rutgers, The State University of New Jersey

136 Frelinghuysen Road

Piscataway, NJ 08854-8019, USA

Phone: +1 (732) 445 43 29

Fax: +1 (732) 445-43 43

Email: [andreib@physics.rutgers.edu](mailto:andreib@physics.rutgers.edu)

[www.physics.rutgers.edu/people/pips/Ruckenstein.html](http://www.physics.rutgers.edu/people/pips/Ruckenstein.html)

Peter Wölfle

Institut für Theorie der Kondensierten Materie

Universität Karlsruhe

Postfach 69 80

76128 Karlsruhe, Germany

Phone: +49 (7 21) 6 08 35 90

Fax: +49 (7 21) 69 81 50

Email: [woelfle@tkm.physik.uni-karlsruhe.de](mailto:woelfle@tkm.physik.uni-karlsruhe.de)

[www-tkm.physik.uni-karlsruhe.de](http://www-tkm.physik.uni-karlsruhe.de)

## Complex Systems, Editor

Frank Steiner

Abteilung Theoretische Physik

Universität Ulm

Albert-Einstein-Allee 11

89069 Ulm, Germany

Phone: +49 (7 31) 5 02 29 10

Fax: +49 (7 31) 5 02 29 24

Email: [frank.steiner@physik.uni-ulm.de](mailto:frank.steiner@physik.uni-ulm.de)

[www.physik.uni-ulm.de/theo/qc/group.html](http://www.physik.uni-ulm.de/theo/qc/group.html)

Andrey Grozin

# Heavy Quark Effective Theory

With 72 Figures



Springer

**Andrey Grozin**

Budker Institute of Nuclear Physics  
630090 Novosibirsk, Russia  
E-mail: A.G.Grozin@inp.nsk.su

Cataloging-in-Publication Data applied for

**Physics and Astronomy Classification Scheme (PACS):**

**12.39.Hg, 12.38.Bx**

**ISSN print edition: 0081-3869**

**ISSN electronic edition: 1615-0430**

**ISBN 3-540-20692-2 Springer-Verlag Berlin Heidelberg New York**

This work is subject to copyright. All rights are reserved, whether the whole or part of the material is concerned, specifically the rights of translation, reprinting, reuse of illustrations, recitation, broadcasting, reproduction on microfilm or in any other way, and storage in data banks. Duplication of this publication or parts thereof is permitted only under the provisions of the German Copyright Law of September 9, 1965, in its current version, and permission for use must always be obtained from Springer-Verlag. Violations are liable for prosecution under the German Copyright Law.

Springer-Verlag is a part of Springer Science+Business Media

[springeronline.com](http://springeronline.com)

© Springer-Verlag Berlin Heidelberg 2004  
Printed in Germany

The use of general descriptive names, registered names, trademarks, etc. in this publication does not imply, even in the absence of a specific statement, that such names are exempt from the relevant protective laws and regulations and therefore free for general use.

Typesetting: by the author using a Springer L<sup>A</sup>T<sub>E</sub>X macro package

Cover concept: eStudio Calamar Steinen

Cover production: *design & production* GmbH, Heidelberg

Printed on acid-free paper SPIN: 10791166 56/3141/jl 543210

## Preface

Heavy quark physics is one of the most rapidly progressing areas of high energy physics, both experimentally and theoretically. Experiments at the B-factories at SLAC and KEK are producing a lot of information about decays of B-mesons, with high statistics and low systematic errors. Therefore, a better theoretical understanding of the properties of B-mesons is very important. An understanding of strong-interaction effects in weak decays is necessary for extracting fundamental electroweak parameters (such as elements of the Kobayashi–Maskawa mixing matrix) from experimental data on these decays. Moreover, investigation of the B-meson – the simplest non-trivial hadron, the QCD hydrogen atom – is interesting in its own right.

In this book, we shall discuss properties of hadrons with a single heavy quark, b or c; the t quark decays before it can form a hadron, and it is not interesting for our purposes. In the case of hadrons containing a c quark,  $\Lambda_{\text{QCD}}/m_c$  corrections can be rather large. The applicability of the theory for hadrons containing b is much better. The physics of mesons consisting of a heavy quark and a heavy antiquark ( $\bar{c}c$ ,  $\bar{b}b$ ,  $\bar{b}c$ ) is essentially different, and will not be discussed here. Note that  $B_c$  mesons can be, to some approximation, described by the methods discussed in this book. However, the expansion parameter  $m_c/m_b \approx 1/3$  is not very small, and the accuracy would be poor.

Heavy quark effective theory (HQET) is an effective field theory constructed to reproduce the results of QCD for problems with a single heavy quark with mass  $m$ , expanded to some order  $(k/m)^n$ , where  $k \ll m$  is the characteristic momentum in the problem. To the leading order in  $1/m$ , it has symmetries which are not explicit in the original QCD Lagrangian. These symmetries relate various matrix elements involving heavy hadrons. HQET considerably simplifies lattice simulations with heavy quarks. The considerable progress in the theory of hadrons containing a heavy quark during the last decade is largely due to HQET.

In this book, we shall discuss the properties of HQET as a quantum field theory and the methods used for calculating Feynman diagrams in HQET. Some knowledge of QCD (see, e.g., the textbook [15]) is needed for understanding the text. However, knowledge of methods of calculation of multiloop diagrams is not assumed. We shall discuss such methods for QCD and HQET in parallel (see [9] for more details).

Chapter 1 gives an overview of basic experimental facts about mesons and baryons containing a b or c quark and a qualitative discussion of some of their properties. Then the HQET Lagrangian (Chaps. 2–4) and bilinear quark currents (Chaps. 5–7) are discussed in detail. Finally, Chap. 8 discusses some facts and hypotheses about the behaviour of perturbative series in HQET at high orders.

We shall discuss a few of the most fundamental applications in great detail, rather than provide a long list of results without derivations. Some of the material in this book was used in lecture courses, and all calculations were actually performed in the classroom. Such an explicit approach should be appropriate for those readers who wish to develop skills for solving similar problems. Results which cannot be derived during a lecture are in most cases not included. Readers who want to do non-trivial calculations are advised to use computer algebra (see, e.g., [8]).

Larger areas which are omitted from this book, owing to space and time constraints, are inclusive decays of heavy hadrons (see, e.g., [16, 1, 17]) and their interactions with soft pions (see, e.g., [20, 2]). Remarkable progress has been made in recent years in both of these areas. Also, we shall not discuss other effective field theories, such as non-relativistic QCD (used for heavy-quark–antiquark systems) and soft-collinear effective theory (used for decays of hadrons containing a heavy quark producing energetic light hadrons). These theories are under active development, and a firm knowledge of a simpler effective theory, HQET, is invaluable for understanding these more complicated theories.

For more information about applications of HQET, see the book [13] and the reviews [1, 3, 4, 5, 6, 7, 10, 11, 12, 14, 16, 17, 18, 19].

I am grateful to P.A. Baikov, A.E. Blinov, D.J. Broadhurst, K.G. Chetyrkin, A. Czarnecki, A.I. Davydychev, G.P. Korchemsky, J.G. Körner, S.A. Larin, T. Mannel, K. Melnikov, S.V. Mikhailov, M. Neubert, T. van Ritbergen, V.A. Smirnov, F.V. Tkachov, N.G. Uraltsev, A.I. Vainshtein, and O.I. Yakovlev for numerous illuminating discussions of problems discussed in this book.

Novosibirsk, February 2004

*Andrey Grozin*

## References

1. I. Bigi, M.A. Shifman, N.G. Uraltsev: Annu. Rev. Nucl. Part. Sci. **47**, 591 (1997)
2. R. Casalbuoni, A. Deandrea, N. Di Bartolomeo, R. Gatto, F. Feruglio, G. Nardulli: Phys. Rep. **281**, 145 (1977)

3. A.F. Falk: ‘The Heavy Quark Expansion of QCD’, in *The Strong Interaction, from Hadrons to Partons*, ed. by J. Chan, L. DePorcel, L. Dixon, SLAC-R-508 (SLAC, Stanford 1997) p. 43; ‘The CKM Matrix and the Heavy Quark Expansion’, in *Flavor Physics for the Millennium*, ed. by J.L. Rosner (World Scientific, Singapore 2001) p. 379
4. J.M. Flynn, N. Isgur: *J. Phys. G* **18**, 1627 (1992)
5. H. Georgi: ‘Heavy Quark Effective Field Theory’, in *Perspectives in the Standard Model*, ed. by R.K. Ellis, C.T. Hill, J.D. Lykken (World Scientific, Singapore 1992) p. 589
6. B. Grinstein: ‘Lectures on Heavy Quark Effective Theory’, in *High Energy Phenomenology*, ed. by M.A. Perez, R. Huerta (World Scientific, Singapore 1992) p. 161; *Annu. Rev. Nucl. Part. Sci.* **42**, 101 (1992); ‘An Introduction to the Theory of Heavy Mesons and Baryons’, in *CP Violation and the Limits of the Standard Model*, ed. by J.F. Donoghue (World Scientific, Singapore 1995) p. 307; ‘An Introduction to Heavy Mesons’, in *6 Mexican School of Particles and Fields*, ed. by J.C. D’Olivo, M. Moreno, M.A. Perez (World Scientific, Singapore 1995) p. 122; ‘Introduction to Heavy Flavors’, in *Advanced School on Quantum Chromodynamics*, ed. by S. Peris, V. Vento (Universitat Autònoma de Barcelona, Barcelona 2001) p. 115
7. A.G. Grozin: *Introduction to the Heavy Quark Effective Theory, Part 1*. Preprint BudkerINP 92-97 (Novosibirsk 1992), hep-ph/9908366
8. A.G. Grozin: *Using REDUCE in High Energy Physics* (Cambridge University Press, Cambridge 1997)
9. A.G. Grozin: *Int. J. Mod. Phys. A*, to be published; hep-ph/0307297
10. F. Hussain, G. Thompson: ‘An Introduction to the Heavy Quark Effective Theory’, in *Summer School in High Energy Physics and Cosmology*, ed. by E. Gava, A. Masiero, K.S. Narain, S. Randjbar-Daemi, Q. Shafi (World Scientific, Singapore 1995) p. 45
11. N. Isgur, M.B. Wise: ‘Heavy Quark Symmetry’. In *Heavy Flavours*, ed. by A.J. Buras, M. Lindner (World Scientific, Singapore 1992) p. 234
12. T. Mannel: *Chin. J. Phys.* **31**, 1 (1993); ‘Heavy Quark Mass Expansion in Quantum Chromodynamics’, in *QCD – 20 Years Later*, ed. by P.M. Zerwas, H.A. Kastrup (World Scientific, Singapore 1993) v. 2, p. 634; *J. Phys. G* **21**, 1007 (1995); ‘Review of Heavy Quark Effective Theory’, in *Heavy Quarks at Fixed Target*, ed. by L. Kopke (INFN, Frascati 1997) p. 107; *Rep. Prog. Phys.* **60**, 1113 (1997)
13. A.V. Manohar, M.B. Wise: *Heavy Quark Physics* (Cambridge University Press, Cambridge 2000)
14. M. Neubert: *Phys. Rep.* **245**, 259 (1994); ‘Heavy Quark Masses, Mixing Angles, and Spin Flavor Symmetry’, in: *The Building Blocks of Creation: from Micro-fermis to Megaparsecs*, ed. by S. Raby, T. Walker (World Scientific, Singapore 1994) p. 125; *Int. J. Mod. Phys. A* **11**, 4173 (1996); ‘Heavy Quark Effective Theory’, in *Effective Theories and Fundamental Interactions*, ed. by A. Zichichi (World Scientific, Singapore 1997) p. 98; ‘Heavy Quark Effective Theory’, in *Non-Perturbative Particle Theory and Experimental Tests*, ed. by M. Jamin, O. Nachtmann, G. Domokos, S. Kovács-Domokos (World Scientific, Singapore 1997) p. 39; ‘B Decays and the Heavy Quark Expansion’, in *Heavy Flavours II*, ed. by A.J. Buras, M. Lindner (World Scientific, Singapore 1998) p. 239;

- 'Introduction to B Physics', in *ICTP Summer School in Particle Physics*, ed. G. Senjanovic, A.Yu. Smirnov (World Scientific, Singapore 2000) p. 244
- 15. M.E. Peskin, D.V. Schröder: *Quantum Field Theory* (Perseus, Reading, MA 1995)
  - 16. M.A. Shifman: 'Lectures on Heavy Quarks in Quantum Chromodynamics', in *QCD and Beyond*, ed. by D.E. Soper (World Scientific, Singapore 1996) p. 409
  - 17. N.G. Uraltsev: 'Heavy Quark Expansion in Beauty and its Decays', in *Heavy Flavor Physics – a Probe of Nature's Grand Design*, ed. by I. Bigi, L. Moroni (IOS Press, Amsterdam 1998) p. 329; 'Topics in the Heavy Quark Expansion', in *At the Frontier of Particle Physics: Handbook of QCD*, ed. M. Shifman (World Scientific, Singapore 2001) v. 3, p. 1577
  - 18. M.B. Voloshin: Surv. High Energy Phys. **8**, 27 (1995)
  - 19. M.B. Wise: 'New Symmetries of the Strong Interaction', in *Particle Physics – the Factory Era*, ed. by B.A. Campbell, A.N. Kamel, P. Kitching, F.C. Khanna (World Scientific, Singapore 1991) p. 222; 'Heavy Quark Physics: Course', in *Probing the Standard Model of Particle Interactions*, ed. by R. Gupta, A. Morel, E. Derafael, F. David (Elsevier, Amsterdam 1999) v. 2, p. 1051
  - 20. M.B. Wise: 'Combining Chiral and Heavy Quark Symmetry', in *Particle Physics at the Fermi Scale*, ed. by Y. Pang, J. Qui, Z. Qiu (Gordon and Breach, Amsterdam 1994) p. 71

# Contents

<b>Notation</b>	1
<b>1 Hadrons with a Heavy Quark</b>	3
1.1 Mesons and Baryons with a Heavy Quark	4
1.2 Semileptonic Decays	9
References	17
<b>2 The HQET Lagrangian</b>	19
2.1 The HQET Lagrangian	19
2.2 One-Loop Massless Propagator Diagrams	22
2.3 One-Loop HQET Propagator Diagrams	25
2.4 Two-Loop Massless Propagator Diagrams	27
2.5 Two-Loop HQET Propagator Diagrams	30
References	33
<b>3 Renormalization</b>	35
3.1 Renormalization of QCD	35
3.2 Gluon Propagator	39
3.3 Quark Propagator	45
3.4 Renormalization of HQET	50
3.5 Heavy-Electron Effective Theory	55
References	58
<b>4 The HQET Lagrangian: <math>1/m</math> Corrections</b>	59
4.1 $1/m$ Corrections to the HQET Lagrangian	59
4.2 On-Shell Renormalization of QCD	63
4.3 On-Shell Renormalization of HQET	69
4.4 Scattering in an External Gluonic Field in QCD	71
4.5 Scattering in an External Gluonic Field in HQET	76
4.6 Chromomagnetic Interaction	80
4.7 Decoupling of Heavy-Quark Loops	84
References	89

<b>5</b>	<b>Heavy–Light Currents</b>	91
5.1	Bilinear Quark Currents in QCD	91
5.2	Axial Anomaly	95
5.3	The 't Hooft–Veltman $\gamma_5$ and the Anticommuting $\gamma_5$	98
5.4	Heavy–Light Current in HQET	102
5.5	Decoupling for QCD and HQET Currents	103
5.6	QCD/HQET Matching for Heavy–Light Currents	107
5.7	Meson Matrix Elements	115
	References	119
<b>6</b>	<b>Heavy–Light Currents: <math>1/m</math> Corrections</b>	121
6.1	$1/m$ Corrections to Heavy–Light Currents	121
6.2	Local Dimension-4 Heavy–Light Operators	126
6.3	Bilocal Dimension-4 Heavy–Light Operators	131
6.4	Spin-0 Currents	135
6.5	Spin-1 Currents	140
	References	144
<b>7</b>	<b>Heavy–Heavy Currents</b>	145
7.1	Heavy–Heavy Current in HQET	145
7.2	Flavour-Diagonal Currents at Zero Recoil	152
7.3	Flavour-Changing Currents at Zero Recoil	155
7.4	Flavour-Diagonal Currents at Non-Zero Recoil	161
7.5	Flavour-Changing Currents at Non-Zero Recoil	162
7.6	$1/m$ Corrections	171
	References	173
<b>8</b>	<b>Renormalons in HQET</b>	175
8.1	Large- $\beta_0$ Limit	175
8.2	Renormalons	181
8.3	Light Quarks	183
8.4	HQET Heavy Quark	186
8.5	On-Shell Heavy Quark in QCD	191
8.6	Chromomagnetic Interaction	194
8.7	Heavy–Light Currents	197
8.8	Heavy–Heavy Currents	203
	References	209
<b>Index</b>		211

# Notation

Our notation mainly follows [2]. Covariant and contravariant components of 4-vectors are related by  $a_\mu = g_{\mu\nu}a^\nu$ , where the indices are in the range 0, 1, 2, 3, and the metric tensor is

$$g_{\mu\nu} = \begin{pmatrix} 1 & 0 & 0 & 0 \\ 0 & -1 & 0 & 0 \\ 0 & 0 & -1 & 0 \\ 0 & 0 & 0 & -1 \end{pmatrix}.$$

The velocity 4-vector obeys  $v_\mu v^\mu = 1$ . The unit antisymmetric tensor is normalized by  $\varepsilon^{0123} = -\varepsilon_{0123} = 1$ . The Dirac matrices are defined by

$$\gamma^\mu \gamma^\nu + \gamma^\nu \gamma^\mu = 2g^{\mu\nu}.$$

For any vector  $a$ , we use the notation  $\not{a} = a_\mu \gamma^\mu$ ;  $\sigma^{\mu\nu} = (i/2)[\gamma^\mu, \gamma^\nu]$ . The matrix  $\gamma_5$  is defined by

$$\gamma_5 = \frac{i}{4!} \varepsilon_{\alpha\beta\gamma\delta} \gamma^\alpha \gamma^\beta \gamma^\gamma \gamma^\delta = -i \gamma^0 \gamma^1 \gamma^2 \gamma^3;$$

it satisfies

$$\gamma_5^2 = 1, \quad \gamma_5 \gamma^\mu + \gamma^\mu \gamma_5 = 0.$$

We shall use dimensional regularization for calculating loop diagrams: the space-time dimensionality is

$$d = 4 - 2\varepsilon$$

(dimension 0 is time-like and  $d - 1$  dimensions are space-like). For more details, see the textbook [1].

The number of quark colours is  $N_c = 3$ . We shall write all formulae for the  $SU(N_c)$  gauge group with an arbitrary  $N_c$ . The covariant derivative of the quark field is

$$D_\mu q = (\partial_\mu - iA_\mu) q, \quad A_\mu = g A_\mu^a t^a,$$

where the index  $a$  varies from 1 to the number of gluons  $N_g = N_c^2 - 1$ , and the generators in the fundamental (quark) representation are normalized by the condition

$$\text{Tr } t^a t^b = T_F \delta^{ab}, \quad T_F = \frac{1}{2}.$$

The commutator of the generators is  $[t^a, t^b] = i f^{abc} t^c$ . The covariant derivative in the adjoint representation is

$$D_\mu^{ab} = \partial_\mu \delta^{ab} - i A_\mu^{ab}, \quad A_\mu^{ab} = g A_\mu^c (t^c)^{ab}, \quad (t^c)^{ab} = i f^{acb}.$$

The quadratic Casimir operators in the fundamental (quark) representation and the adjoint (gluon) one are  $t^a t^a = C_F$ ,  $(t^a)^{bc} (t^a)^{cd} = C_A \delta^{bd}$ ,

$$C_A = N_c, \quad C_F = \frac{N_c^2 - 1}{2N_c}$$

(see Sect. 3.3).

## References

1. J.C. Collins: *Renormalization* (Cambridge University Press, Cambridge 1984)
2. M.E. Peskin, D.V. Schröder: *Quantum Field Theory* (Perseus, Reading, MA 1995)

# 1 Hadrons with a Heavy Quark

The  $B$  meson is the hydrogen atom of quantum chromodynamics (QCD), the simplest non-trivial hadron. In the leading approximation, the  $b$  quark in it just sits at rest at the origin and creates a chromoelectric field. Light constituents (gluons, light quarks, and antiquarks) move in this external field. Their motion is relativistic; the number of gluons and light quark–antiquark pairs in this light cloud is undetermined and varying. Therefore, there are no reasons to expect that a non-relativistic potential quark model would describe the  $B$  meson well enough (in contrast to the  $\Upsilon$  meson, where the non-relativistic two-particle picture gives a good starting point).

Similarly, the  $\Lambda_b$  baryon can be called the helium atom of QCD. Unlike in atomic physics, where the hydrogen atom is much simpler than helium, the  $B$  and  $\Lambda_b$  are equally difficult. Both have a light cloud with a variable number of relativistic particles. The size of this cloud is the confinement radius  $1/\Lambda_{\text{QCD}}$ ; its properties are determined by large-distance nonperturbative QCD.

The analogy with atomic physics can tell us a lot about hadrons with a heavy quark. The usual hydrogen and tritium have identical chemical properties, despite the fact that the tritium nucleus is three times heavier than the proton. Both nuclei create identical electric fields, and both stay at rest. Similarly, the  $D$  and  $B$  mesons have identical “hadro-chemical” properties, despite the fact that the  $b$  quark is three times heavier than the  $c$ .

The proton magnetic moment is of the order of the nuclear magneton  $e/(2m_p)$ , and is much smaller than the electron magnetic moment  $e/(2m_e)$ . Therefore, the energy difference between the states of the hydrogen atom with total spins 0 and 1 (hyperfine splitting) is small (of the order  $m_e/m_p$  times the fine structure). Similarly, the  $b$ -quark chromomagnetic moment is proportional to  $1/m_b$  by dimensionality, and the hyperfine splitting between the  $B$  and  $B^*$  mesons is small (proportional to  $1/m_b$ ). Unlike in atomic physics, both “gross”-structure intervals and fine-structure intervals are just some numbers times  $\Lambda_{\text{QCD}}$ , because the light components are relativistic (the practical success of constituent quark models shows that these dimensionless numbers for fine splittings can be rather small, but they contain no small parameter).

In the limit  $m \rightarrow \infty$ , the heavy-quark spin does not interact with the gluon field. Therefore, it may be rotated at will, without changing the physics. Such

rotations can transform the  $B$  and  $B^*$  into each other; they are degenerate and have identical properties in this limit. This heavy-quark spin symmetry yields many useful relations among heavy-hadron form factors [13]. Not only the orientation, but also the magnitude of the heavy-quark spin is irrelevant in the infinite-mass limit. We can switch off the heavy-quark spin, making it spinless, without affecting the physics. This trick considerably simplifies counting independent form factors, and we shall use it often. Or, if we wish, we can make the heavy quark have spin 1; it does not matter.

This leads to a supersymmetry group called the superflavour symmetry [10, 6]. It can be used to predict properties of hadrons containing a scalar or vector heavy quark. Such quarks exist in some extensions of the Standard Model (for example, supersymmetric or composite extensions). This idea can also be applied to baryons with two heavy quarks. They form a small-size bound state (with a radius of order  $1/(m\alpha_s)$ ) which has spin 0 or 1 and is antitriplet in colour. Therefore, these baryons are similar to mesons with a heavy antiquark that has spin 0 or 1. The accuracy of this picture cannot be high, however, because even the radius of the  $bb$  diquark is only a few times smaller than the confinement radius.

## 1.1 Mesons and Baryons with a Heavy Quark

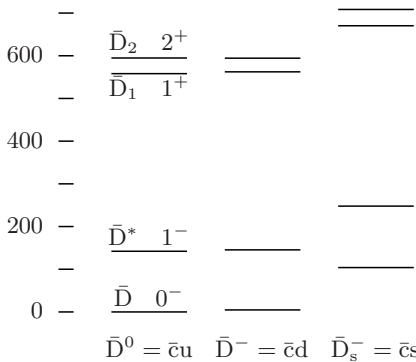
Let us consider mesons with the quark contents  $\bar{Q}q$ , where  $Q$  is a heavy quark with mass  $m$  (c or b), and  $q$  is a light quark (u, d, or s). As discussed above, the heavy-quark spin is inessential in the limit  $m \rightarrow \infty$ , and may be switched off. In a world with a scalar heavy antiquark,  $S$ -wave mesons have angular momentum and parity  $j^P = (1/2)^+$ ;  $P$ -wave mesons have  $j^P = (1/2)^-$  and  $(3/2)^-$ . The energy difference between these two  $P$ -wave states (fine splitting) is a constant times  $\Lambda_{\text{QCD}}$  at  $m \rightarrow \infty$ , just like the splittings between these  $P$ -wave states and the ground state; however, this constant is likely to be small.

In our real world, the heavy antiquark  $\bar{Q}$  has spin and parity  $s_Q^P = (1/2)^-$ . The quantum numbers in the above paragraph are those of the cloud of light fields of a meson. Adding the heavy-antiquark spin, we obtain, in the limit  $m \rightarrow \infty$ , a degenerate doublet of  $S$ -wave mesons with spin and parity  $s^P = 0^-$  and  $1^-$ , and two degenerate doublets of  $P$ -wave mesons, one with  $s^P = 0^+$  and  $1^+$ , and the other with  $s^P = 1^+$  and  $2^+$ . At a large but finite heavy-quark mass  $m$ , these doublets are not exactly degenerate. Hyperfine splittings, equal to some dimensionless numbers times  $\Lambda_{\text{QCD}}^2/m$ , appear. It is natural to expect that hyperfine splittings in  $P$ -wave mesons are less than in the ground-state  $S$ -wave doublet, because the characteristic distance between the quarks is larger in the  $P$ -wave case. Note that the  $1^+$  mesons from the different doublets do not differ from each other by any exactly conserved quantum numbers, and hence can mix. They differ by the angular momenta of the

light fields, which is conserved up to  $1/m$  corrections; therefore, the mixing angle should be of the order of  $\Lambda_{\text{QCD}}/m$ .

Mesons with  $q = u$  and  $d$  form isodoublets; together with isosinglets with  $q = s$ , they form  $SU(3)$  triplets.

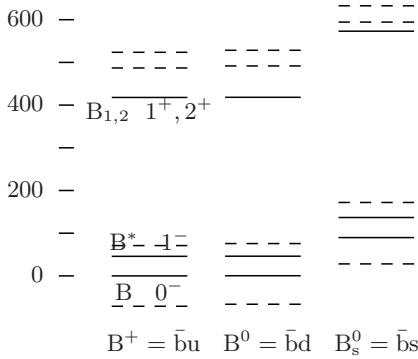
The experimentally observed [18] mesons containing the  $\bar{c}$  antiquark are shown in Fig. 1.1. The energy scale at the left is in MeV, relative to the lowest-mass meson. The mesons  $\bar{D}_1$  and  $\bar{D}_2$  form a doublet, with the quantum numbers of the light fields  $j^P = (3/2)^+$ . The second  $P$ -wave doublet is suspiciously absent. It should be close to the  $(3/2)^+$  one; it is not more difficult to produce these mesons than the  $(3/2)^+$  ones. The problem is that they are too wide, and cannot be cleanly separated from the continuum.



**Fig. 1.1.** Mesons containing  $\bar{c}$

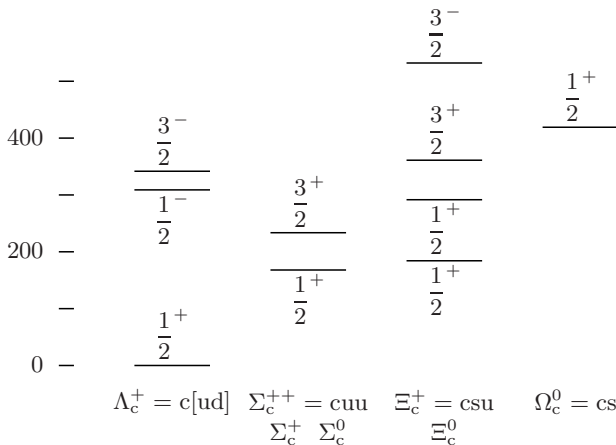
In the leading approximation, the spectrum of  $\bar{b}$ -containing mesons is obtained from the spectrum of  $\bar{c}$ -containing mesons simply by a shift by  $m_b - m_c$ . The experimentally observed mesons containing the  $\bar{b}$  antiquark are shown in Fig. 1.2. The spectrum of  $\bar{c}$ -containing mesons is shown by dashed lines for comparison. It is positioned in such a way that the weighted average energies of the ground-state doublets coincide, where the  $1^-$  meson has weight 3 and the  $0^-$  meson has weight 1. The states  $B_1$  and  $B_2$  are not resolved, and are shown by a single line. Experimentally, it is difficult to measure their masses exactly enough. The hyperfine splitting of the ground-state doublet is smaller for  $B$  mesons than for  $D$  mesons, as expected.

In  $S$ -wave  $Qqq$  baryons, the light-quark spins can add to give  $j^P = 0^+$  or  $1^+$ . In the first case their spin wave function is antisymmetric; the Fermi statistics and the antisymmetry in colour require an antisymmetric flavour wave function. Hence the light quarks must be different; if they are  $u$ ,  $d$ , then their isospin is  $I = 0$ . With the heavy-quark spin switched off, this gives the  $0^+$  baryon  $\Lambda_Q$  with  $I = 0$ . If one of the light quarks is  $s$ , we have the isodoublet  $\Xi_Q$ , which forms an  $SU(3)$  antitriplet together with  $\Lambda_Q$ . With the

**Fig. 1.2.** Mesons containing  $\bar{b}$ 

heavy-quark spin switched on, these baryons have  $s^P = (1/2)^+$ . In the  $1^+$  case, the flavour wave function is symmetric. If the light quarks are  $u, d$ , then their isospin is  $I = 1$ . This gives the  $1^+$  isotriplet  $\Sigma_Q$ ; with one  $s$  quark, we obtain the isodoublet  $\Xi'_Q$ ; and with two  $s$  quarks, the isosinglet  $\Omega_Q$ . Together, they form an  $SU(3)$  sextet. With the heavy-quark spin switched on, we obtain the degenerate doublets with  $s^P = (1/2)^+, (3/2)^+$ :  $\Sigma_Q, \Sigma_Q^*$ ;  $\Xi'_Q, \Xi_Q^*$ ;  $\Omega_Q, \Omega_Q^*$ . The hyperfine splittings in these doublets are of the order of  $\Lambda_{\text{QCD}}^2/m$ . Mixing between  $\Xi_Q$  and  $\Xi'_Q$  is suppressed both by  $1/m$  and by  $SU(3)$ . There is a large number of  $P$ -wave excited states; we shall not discuss them here.

The experimentally observed [18] baryons containing a  $c$  quark are shown in Fig. 1.3. The higher states in the first and the third column are  $P$ -wave. In the third column, the lowest state  $\Xi_c$  is followed by the doublet  $\Xi'_c, \Xi_c^*$ .

**Fig. 1.3.** Baryons containing a  $c$  quark

The  $\Omega_c^*$  baryon has not yet been observed. Only one baryon with a b quark,  $\Lambda_b^0$ , has been discovered so far.

In the leading  $m_b \rightarrow \infty$  approximation, the masses  $m_B$  and  $m_{B^*}$  are both equal to  $m_b + \bar{\Lambda}$ , where  $\bar{\Lambda}$  is the energy of the ground state of the light fields in the chromoelectric field of the  $\bar{b}$  antiquark. This energy  $\bar{\Lambda}$  is of the order of  $\Lambda_{\text{QCD}}$ . The excited states of the light fields have energies  $\bar{\Lambda}_i$ , giving excited degenerate doublets with masses  $m_b + \bar{\Lambda}_i$ .

There are two  $1/m_b$  corrections to the masses. First, the  $\bar{b}$  antiquark has an average momentum squared  $\mu_\pi^2$ , which is of order of  $\Lambda_{\text{QCD}}^2$ . Therefore, it has a kinetic energy  $\mu_\pi^2/(2m_b)$ . Second, the  $\bar{b}$  chromomagnetic moment interacts with the chromomagnetic field created by light constituents at the origin, where the  $\bar{b}$  stays. This chromomagnetic field is proportional to the angular momentum of the light fields  $j_l$ . Therefore, the chromomagnetic interaction energy is proportional to

$$\mathbf{s}_Q \cdot \mathbf{j}_l = \frac{1}{2} [s(s+1) - s_Q(s_Q+1) - j_l(j_l+1)] = \begin{cases} -\frac{3}{4}, & s=0, \\ \frac{1}{4}, & s=1, \end{cases}$$

where  $s = s_Q + j_l$  is the meson spin. If we denote this energy for B by  $-\mu_G^2/(2m_b)$ , then for  $B^*$  it will be  $(1/3)\mu_G^2/(2m_b)$ . Here  $\mu_G^2$  is of order of  $\Lambda_{\text{QCD}}^2$ . The B,  $B^*$  meson masses with  $1/m_b$  corrections taken into account are given by the formulae

$$\begin{aligned} m_B &= m_b + \bar{\Lambda} + \frac{\mu_\pi^2 - \mu_G^2}{2m_b} + \mathcal{O}\left(\frac{\Lambda_{\text{QCD}}^3}{m_b^2}\right), \\ m_{B^*} &= m_b + \bar{\Lambda} + \frac{\mu_\pi^2 + (1/3)\mu_G^2}{2m_b} + \mathcal{O}\left(\frac{\Lambda_{\text{QCD}}^3}{m_b^2}\right). \end{aligned} \quad (1.1)$$

The hyperfine splitting is

$$m_{B^*} - m_B = \frac{2\mu_G^2}{3m_b} + \mathcal{O}\left(\frac{\Lambda_{\text{QCD}}^3}{m_b^2}\right).$$

Taking into account  $m_{B^*} + m_B = 2m_b + \mathcal{O}(\Lambda_{\text{QCD}})$ , we obtain

$$m_{B^*}^2 - m_B^2 = \frac{4}{3}\mu_G^2 + \mathcal{O}\left(\frac{\Lambda_{\text{QCD}}^3}{m_b}\right).$$

The difference  $m_{D^*}^2 - m_D^2$  is given by a similar formula, with  $m_c$  instead of  $m_b$ . Therefore, the ratio

$$\frac{m_{B^*}^2 - m_B^2}{m_{D^*}^2 - m_D^2} = 1 + \mathcal{O}\left(\frac{\Lambda_{\text{QCD}}}{m_{c,b}}\right). \quad (1.2)$$

Experimentally, this ratio is 0.89. This is a spectacular confirmation of the idea that violations of the heavy-quark spin symmetry are proportional to  $1/m$ . As we shall discuss in Chap. 4, the matrix element  $\mu_G^2$  depends on the normalization scale, and hence is not quite the same for D and B; this produces moderate perturbative corrections to (1.2).

$P$ -wave excited states decay into the ground state emitting a pion. In the ideal world with an infinitely heavy scalar  $\bar{c}$ , the  $(1/2)^-$   $P$ -wave meson decays into the  $(1/2)^+$  ground-state meson plus a pion (having  $s^P = 0^-$ ) with an orbital angular momentum  $l = 0$  ( $S$ -wave); the  $(3/2)^-$   $P$ -wave meson decays into the ground-state meson plus a pion with  $l = 2$  ( $D$ -wave). The pion momenta  $p_\pi$  in these decays are rather small, and hence the decay of the  $(3/2)^-$  meson (whose width is proportional to  $p_\pi^5$ ) is strongly suppressed. The decay of the  $(1/2)^-$  meson is not suppressed, its width is proportional to  $p_\pi$ . Therefore, in our real world, the  $0^+$ ,  $1^+$  doublet mesons are very wide, and difficult to observe.

Let us consider decays of  $D_1$  and  $D_2$ , taking the  $\bar{c}$  spin into account, but still in the limit  $m_c \rightarrow \infty$ . The widths of  $D_1$  and  $D_2$  are equal, because the  $\bar{c}$  spin plays no role in the decay.  $D_1$  decays only into  $D^*\pi$ ; the decay into  $D\pi$  is forbidden by angular-momentum conservation.  $D_2$  can decay into both  $D\pi$  and  $D^*\pi$ . In order to find the branching ratio  $B(D_2 \rightarrow D\pi)$ , we shall use a simple device known as the Shmushkevich factory.

Let us take a sample of  $D_{1,2}$  mesons with random polarizations of  $\bar{c}$ . Then  $3/8$  of this sample are  $D_1$ , and  $5/8$  are  $D_2$ . Now let us wait for a small time  $dt$ ; a fraction  $\Gamma dt$  of the sample will decay. The ground-state mesons produced have randomly polarized  $\bar{c}$ . Therefore,  $1/4$  of them are D, and  $3/4$  are  $D^*$ . D mesons are produced only from  $D_2$ :

$$\frac{5}{8}B(D_2 \rightarrow D\pi) = \frac{1}{4},$$

and hence [15]

$$B(D_2 \rightarrow D\pi) = \frac{2}{5}, \quad B(D_2 \rightarrow D^*\pi) = \frac{3}{5}.$$

In the limit  $m_c \rightarrow \infty$ , D and  $D^*$  are degenerate, and so are  $D_1$  and  $D_2$ . In the real world, the pion momenta in these decays differ. The widths are proportional to  $p_\pi^5$ , and even rather small momentum differences produce a drastic effect. It seems natural to suppose that the predictions of heavy-quark spin symmetry hold for the coefficients in front of  $p_\pi^5$ . Then

$$\frac{\Gamma(D_2 \rightarrow D\pi)}{\Gamma(D_2 \rightarrow D^*\pi)} = \frac{2}{3} \left( \frac{p_\pi(D_2 \rightarrow D\pi)}{p_\pi(D_2 \rightarrow D^*\pi)} \right)^5 = 2.5,$$

while the experimental value is  $2.3 \pm 0.6$  [18]. Formally, the difference of  $p_\pi(D_2 \rightarrow D\pi)/p_\pi(D_2 \rightarrow D^*\pi)$  from 1 is a  $1/m_c$  correction. We can only hope that this kinematic  $1/m_c$  effect, included in the above estimate, is dominant.

Let us now discuss the B-meson leptonic decay constant  $f_B$ . It is defined by

$$\langle 0 | \bar{b} \gamma^\mu \gamma^5 u | B(p) \rangle = i f_B p^\mu,$$

where the one-particle state is normalized in the usual Lorentz-invariant way:

$$\langle B(p') | B(p) \rangle = 2p^0(2\pi)^3 \delta(\mathbf{p}' - \mathbf{p}).$$

This relativistic normalization becomes nonsensical in the limit  $m_b \rightarrow \infty$ , and in that case the non-relativistic normalization

$$_{\text{nr}} \langle B(p') | B(p) \rangle_{\text{nr}} = (2\pi)^3 \delta(\mathbf{p}' - \mathbf{p})$$

should be used instead. Then, for the B meson at rest,

$$\langle 0 | \bar{b} \gamma^0 \gamma^5 u | B \rangle_{\text{nr}} = \frac{i m_B f_B}{\sqrt{2m_B}}.$$

Denoting this matrix element (which is mass-independent at  $m_b \rightarrow \infty$ ) by  $iF/\sqrt{2}$ , we obtain

$$f_B = \frac{F}{\sqrt{m_b}} \left[ 1 + \mathcal{O}\left(\frac{\Lambda_{\text{QCD}}}{m_b}\right) \right], \quad (1.3)$$

and hence

$$\frac{f_B}{f_D} = \sqrt{\frac{m_c}{m_b}} \left[ 1 + \mathcal{O}\left(\frac{\Lambda_{\text{QCD}}}{m_{c,b}}\right) \right]. \quad (1.4)$$

As we shall discuss in Chap. 5, the matrix element  $F$  depends on the normalization scale, and hence is not quite the same for D and B; this produces moderate perturbative corrections to (1.4). Lattice simulations and QCD sum rules show that the  $1/m_c$  correction in the formula for  $f_D$  similar to (1.3) is of order 100%, so that the accuracy of (1.4) is not high.

Experimentally [18],

$$f_{D_s^+} = 280 \pm 19 \pm 28 \pm 34 \text{ MeV}, \quad f_{D^+} = 300^{+180+80}_{-150-40} \text{ MeV},$$

from the  $\mu^+ v_\mu$  and  $\tau^+ v_\tau$  decays. The branching  $B(B^+ \rightarrow \tau^+ v_\tau)$  should be of order  $0.5 \times 10^{-4}$ , so that a direct measurement of  $f_{B^+}$  at B-factories seems feasible. Theoretical estimates of  $f_B$  vary by about a factor 2.

## 1.2 Semileptonic Decays

Let us discuss the decay  $B \rightarrow \bar{D} W^*$ , where  $W^*$  is a virtual  $W^+$  which decays into  $l^+ v_l$ . In the limit  $m_b \rightarrow \infty$ ,  $m_c \rightarrow \infty$ , it is enough to consider the case

when  $\bar{b}$ ,  $\bar{c}$ , and  $W^*$  are scalar. We concentrate our attention on decays of  $B$  with 4-velocity  $v$  into  $\bar{D}$  with 4-velocity  $v'$ . Let  $\tilde{J}$  be the scalar current which replaces a scalar  $\bar{b}$  with 4-velocity  $v$  by a scalar  $\bar{c}$  with 4-velocity  $v'$ . With the non-relativistic normalization of the scalar quark wave functions, these wave functions are just 1, and the quark decay matrix element is

$$\langle \bar{c} | \tilde{J} | \bar{b} \rangle = 1. \quad (1.5)$$

The ground-state  $B$  meson has  $s^P = (1/2)^+$ ;  $\bar{D}$  will be used to denote generically a ground-state or excited  $\bar{c}q$  meson. It is convenient to work in the  $B$  rest frame. Let the  $z$  axis be in the direction of the  $\bar{D}$  motion. Angular-momentum conservation gives  $s'_z = s_z$ . Reflection in a plane containing the  $z$  axis transforms a state  $|s, s_z\rangle$  into  $Pi^{2s}|s, -s_z\rangle$ . Therefore, the amplitude of the  $-s_z$  into  $-s_z$  transition is equal to that of the  $s_z$  into  $s_z$  transition, up to a phase factor; an  $s_z = 0$  into  $s'_z = 0$  transition is allowed only when the “naturalness”  $P(-1)^s$  is conserved [19]. For example, the transition  $\Lambda_b \rightarrow \Lambda_c$  is described by a single form factor;  $\Lambda_b \rightarrow \Sigma_c$  is forbidden by “naturalness” (and also suppressed by isospin);  $\Sigma_b \rightarrow \Sigma_c$  is described by two form factors ( $s_z = s'_z = 0$  and  $\pm 1$ ) [16, 9, 17].

The transitions of the ground-state  $(1/2)^+$   $\bar{b}q$  meson into an  $S$ -wave  $(1/2)^+$   $\bar{c}q$  meson, and into a  $P$ -wave  $(1/2)^-$  or  $(3/2)^-$   $\bar{c}q$  meson, are described by one form factor each [13, 8, 14, 7]:

$$\begin{aligned} \langle (1/2)^+ | \tilde{J} | (1/2)^+ \rangle &= \xi(\cosh \vartheta) \bar{u}' u, \\ \langle (1/2)^- | \tilde{J} | (1/2)^+ \rangle &= \tau_{1/2}(\cosh \vartheta) \bar{u}' \gamma_5 u, \\ \langle (3/2)^- | \tilde{J} | (1/2)^+ \rangle &= \tau_{3/2}(\cosh \vartheta) v^\mu \bar{u}'_\mu u, \end{aligned} \quad (1.6)$$

where  $\cosh \vartheta = v \cdot v'$ , and  $\vartheta$  is the Minkowski angle between the 4-velocities of the  $B$  and  $\bar{D}$ .

The Dirac wave function  $u$  of the initial  $(1/2)^+$  meson satisfies  $(\not{v} - 1)u = 0$  and is normalized by the non-relativistic condition  $\bar{u}u = 1$ ; the sum over its two polarizations is

$$\sum u \bar{u} = \frac{1 + \not{v}}{2}.$$

The Dirac wave function  $u'$  of the final  $(1/2)^\pm$  meson has similar properties, with  $v'$  instead of  $v$ . The Rarita–Schwinger wave function  $u'_\mu$  of the spin-(3/2) meson satisfies  $(\not{v}' - 1)u'_\mu = 0$ ,  $\gamma^\mu u'_\mu = 0$ ,  $v'^\mu u'_\mu = 0$ , and is normalized by  $\bar{u}'^\mu u'_\mu = -1$ ; the sum over the four polarizations of the meson is

$$\sum u'_\mu \bar{u}'_\nu = \frac{1 + \not{v}'}{2} \left( -g_{\mu\nu} + \frac{1}{3} \gamma_\mu \gamma_\nu + \frac{2}{3} v_\mu v_\nu \right) \frac{1 + \not{v}'}{2}. \quad (1.7)$$

All the form factors of  $B$  transitions into  $\bar{D}$ ,  $\bar{D}^*$  via the vector and axial  $\bar{bc}$  weak currents are proportional to the Isgur–Wise form factor  $\xi(\cosh \vartheta)$ ,

with trivial kinematic coefficients. When the current  $\tilde{J}$  replaces an infinitely heavy  $\bar{b}$  by an infinitely heavy  $\bar{c}$  with the same 4-velocity and colour, light fields do not notice it:

$$\xi(1) = 1. \quad (1.8)$$

The maximum  $\cosh \vartheta$  accessible in  $B \rightarrow \bar{D}, \bar{D}^*$  decays is about 1.6; a rough sketch of  $\xi(\cosh \vartheta)$  as extracted from experimental data is shown in Fig. 1.4. At  $\cosh \vartheta \gg 1$ , the Isgur–Wise form factor behaves as [12]

$$\xi(\cosh \vartheta) \sim \frac{\alpha_s}{\cosh^2 \vartheta}, \quad (1.9)$$

up to logarithmic factors.

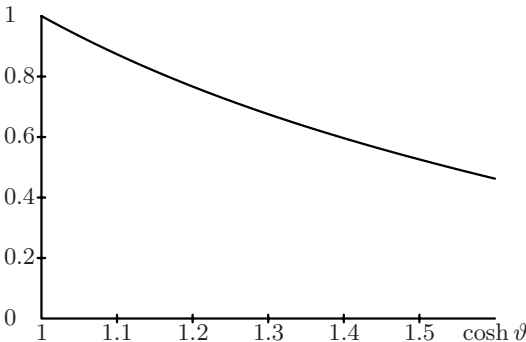


**Fig. 1.4.** The Isgur–Wise form factor

The  $B \rightarrow B$  form factor is also proportional to  $\xi(\cosh \vartheta)$ . In this case,  $q^2 = 2m_B^2(1 - \cosh \vartheta)$ . The form factor has a cut in the annihilation channel from  $q^2 = 4m_B^2$  to  $+\infty$ . Therefore,  $\xi(\cosh \vartheta)$  has a cut from  $\cosh \vartheta = -1$  to  $-\infty$  (Fig. 1.5). Geometrically speaking,  $\cosh \vartheta > 1$  corresponds to Minkowski angles between the world lines of the incoming heavy quark and the outgoing one – this is the scattering (or decay) channel. When  $\cosh \vartheta = 1$ , the world line is straight, and there is no transition at all (see (1.8)). When  $|\cosh \vartheta| < 1$ , the angle is Euclidean. When  $\cosh \vartheta < -1$ , we have a Minkowski angle again, but one of the 4-velocities is directed into the past – this is the annihilation channel. At the point  $\cosh \vartheta = -1$ , the heavy quark returns back along the same world line. In fact, the very concept of the Isgur–Wise form factor is inapplicable near this point. The HQET picture is based on the fact that heavy quarks move along straight world lines. If their relative velocity in the annihilation channel is  $\lesssim \alpha_s$ , they rotate around each other instead. The  $B$  meson form factor has poles below the threshold corresponding to  $\Upsilon$  mesons with binding energies  $\sim m_b \alpha_s^2$ ; its behaviour in this region is not universal. The concept of the Isgur–Wise form factor is only applicable at  $|\cosh \vartheta + 1| \gg \alpha_s^2$  (Fig. 1.5).

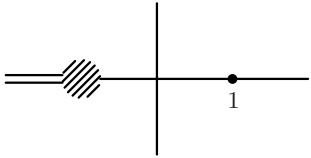


**Fig. 1.5.** The complex  $\cosh \vartheta$  plane

Squaring the matrix elements (1.6), summing over the final meson polarizations (using (1.7) for the spin  $3/2$  meson), averaging over the initial meson polarizations, and normalizing to the quark decay (1.5), we obtain the branching ratios

$$\begin{aligned} B((1/2)^+ \rightarrow (1/2)^+) &= \frac{\cosh \vartheta + 1}{2} \xi^2(\cosh \vartheta), \\ B((1/2)^+ \rightarrow (1/2)^-) &= \frac{\cosh \vartheta - 1}{2} \tau_{1/2}^2(\cosh \vartheta), \\ B((1/2)^+ \rightarrow (3/2)^-) &= \frac{(\cosh \vartheta + 1)^2(\cosh \vartheta - 1)}{3} \tau_{3/2}^2(\cosh \vartheta). \end{aligned} \quad (1.10)$$

They are the fractions of the number of  $B \rightarrow X_{\bar{c}} W^+$  decays with  $X_{\bar{c}}$  velocity  $v'$ , where the hadronic system  $X_{\bar{c}}$  happens to be a single meson. The decay  $(1/2)^+ \rightarrow (1/2)^+$  is  $S$ -wave, and therefore the squared matrix element tends to a constant at  $\vartheta \rightarrow 0$ . The decays  $(1/2)^+ \rightarrow (1/2)^-$  and  $(1/2)^+ \rightarrow (3/2)^-$  are  $P$ -wave, and therefore the squared matrix elements behave as the relative velocity squared,  $\vartheta^2$ . Similarly, decays into  $D$ -wave mesons  $(3/2)^+, (5/2)^+$  are  $D$ -wave, and behave as  $\vartheta^4$  at  $\vartheta \rightarrow 0$ . If we choose the mass of the virtual  $W^*$  larger than  $m_B + m_D$ , we can consider the channel  $W^* \rightarrow BD$ . The squared matrix elements are given by the formulae (1.10) with an extra factor 2, because we sum over the  $B$  polarizations now, not average. The decays of the scalar  $W^*$  into  $(1/2)^+(1/2)^-, (1/2)^+(1/2)^+,$  and  $(1/2)^+(3/2)^+$  are  $P$ -wave,  $S$ -wave, and  $D$ -wave. Therefore, their squared matrix elements behave as the relative velocity to the power 2, 0, and 4, correspondingly. This explains the behaviour of the formulae (1.10) at  $\cosh \vartheta \rightarrow -1$ .

The inclusive decay rate  $B \rightarrow X_{\bar{c}} W^*$  can be written as  $F(\varepsilon, \cosh \vartheta) d\varepsilon$ , where  $p_X = m_X v'$ ,  $v'$  is the  $X_{\bar{c}}$  4-velocity,  $\cosh \vartheta = v \cdot v'$ , and  $\varepsilon = m_X - m_D$  is the excitation energy (we are still in the limit  $m_c \rightarrow \infty$ , where  $m_{D^*} = m_D$ ). The structure function is

$$\begin{aligned} F(\varepsilon, \cosh \vartheta) &= \frac{\cosh \vartheta + 1}{2} \sum_{(1/2)^+} \xi_i^2(\cosh \vartheta) \delta(\varepsilon - \varepsilon_i) \\ &\quad + \frac{\cosh \vartheta - 1}{2} \sum_{(1/2)^-} \tau_{1/2}^2(\cosh \vartheta) \delta(\varepsilon - \varepsilon_i) \end{aligned}$$

$$\begin{aligned}
& + \frac{(\cosh \vartheta + 1)^2 (\cosh \vartheta - 1)}{3} \sum_{(3/2)^-} \tau_{3/2}^2(\cosh \vartheta) \delta(\varepsilon - \varepsilon_i) \\
& + \dots
\end{aligned} \tag{1.11}$$

where the sums run over final states with the quantum numbers indicated,  $\varepsilon_i$  are their excitation energies, the index  $i$  is not explicitly shown in the form factors  $\tau_{1/2}$  and  $\tau_{3/2}$ , and the dots mean the contribution of  $D$ -wave and higher states. At  $\vartheta = 0$ ,  $F(\varepsilon, 1) = \delta(\varepsilon)$ . A qualitative sketch of  $F(\varepsilon, \cosh \vartheta)$  as a function of  $\varepsilon$  at some fixed  $\vartheta > 0$  is shown in Fig. 1.6. It contains a  $\delta$  peak at  $\varepsilon = 0$  due to the transition into the ground state ( $\bar{D}$  and  $\bar{D}^*$ ), then some peaks due to excited states which become wider when  $\varepsilon$  increases, and then the curve becomes smooth. At  $\varepsilon \gg \Lambda_{\text{QCD}}$ , it is given by the perturbative gluon radiation:

$$F(\varepsilon, \cosh \vartheta) = \frac{2C_F \alpha_s(\vartheta \coth \vartheta - 1)}{\pi \varepsilon}. \tag{1.12}$$

Its  $\varepsilon$  dependence is evident from dimensionality, and the  $\vartheta$  dependence is given by the well-known QED soft-photon radiation function. It is also known from classical electrodynamics: this function is the distribution in the radiation energy when a charge suddenly changes its velocity from  $v$  to  $v'$ .

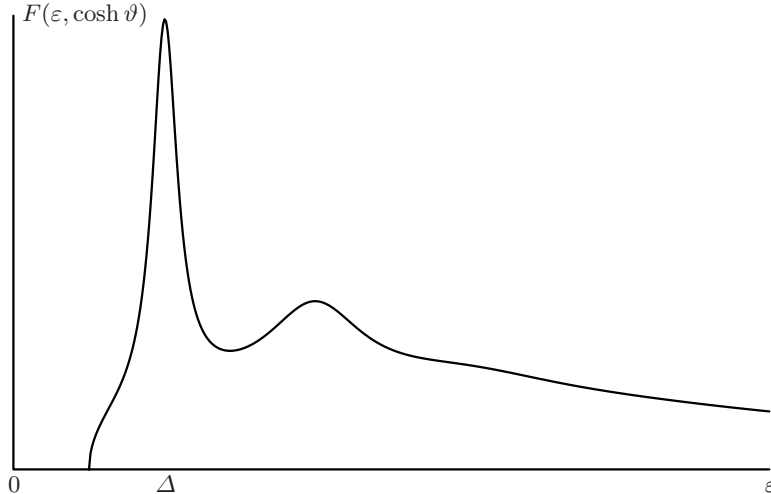


**Fig. 1.6.** A qualitative sketch of the  $B \rightarrow X_{\bar{c}}$  decay structure function

The total decay probability is unity:

$$\int F(\varepsilon, \cosh \vartheta) d\varepsilon = 1. \tag{1.13}$$

This is the Bjorken sum rule [4, 5, 14]. In particular, the decay rate into the ground-state  $(1/2)^+$  meson must not exceed the total rate:

$$\xi(\cosh \vartheta) \leq \sqrt{\frac{2}{\cosh \vartheta + 1}}. \quad (1.14)$$

At  $\cosh \vartheta \gg 1$ , the ground state is rarely produced, and the Isgur–Wise form factor (1.9) is much less than the bound (1.14).

The Bjorken sum rule becomes much simpler in the small- $\vartheta$  limit. The Isgur–Wise form factor of the transition into the ground state behaves as  $\xi(\cosh \vartheta) = 1 - \rho^2(\cosh \vartheta - 1) + \dots$ , and form factors of transitions into higher  $S$ -wave mesons as  $\xi_i(\cosh \vartheta) = \rho_i^2(\cosh \vartheta - 1) + \dots$ . Expanding (1.13) up to linear terms in  $\cosh \vartheta - 1$ , we obtain

$$1 + \left[ \frac{1}{2} - 2\rho^2 + \frac{1}{2} \sum \tau_{1/2}^2(1) + \frac{4}{3} \sum \tau_{3/2}^2(1) \right] (\cosh \vartheta - 1) = 1. \quad (1.15)$$

$D$ -wave final state do not contribute in this order, nor do higher  $S$ -wave final states. Therefore, the slope of the Isgur–Wise form factor  $\rho^2$  can be expressed via the form factors of  $P$ -wave meson production at  $\cosh \vartheta = 1$ :

$$\rho^2 = \frac{1}{4} + \frac{1}{4} \sum \tau_{1/2}^2(1) + \frac{2}{3} \sum \tau_{3/2}^2(1). \quad (1.16)$$

In particular,

$$\rho^2 > \frac{1}{4} \quad (1.17)$$

(this also follows from (1.14)).

We can also consider the inclusive decay of a polarized  $B$ . Its structure function is (we use (1.7) for the spin-(3/2) meson)

$$\begin{aligned} & \bar{u} \frac{\not{v}' + 1}{2} u \sum_{(1/2)^+} \xi_i^2(\cosh \vartheta) \delta(\varepsilon - \varepsilon_i) + \bar{u} \frac{\not{v}' - 1}{2} u \sum_{(1/2)^-} \tau_{1/2}^2(\cosh \vartheta) \delta(\varepsilon - \varepsilon_i) \\ & + \frac{\cosh \vartheta + 1}{3} [2 \cosh \vartheta - 1 - (2 - \cosh \vartheta) \bar{u} \not{v}' u] \sum_{(3/2)^-} \tau_{3/2}^2(\cosh \vartheta) \delta(\varepsilon - \varepsilon_i) \\ & + \dots \end{aligned}$$

Averaging it over polarizations  $\bar{u} \not{v}' u \rightarrow \cosh \vartheta$ , we reproduce (1.11). The decay rate does not depend on the initial meson polarization. This gives the Uraltsev sum rule [22]

$$\begin{aligned} & \sum_{(1/2)^+} \xi_i^2(\cosh \vartheta) + \sum_{(1/2)^-} \tau_{1/2}^2(\cosh \vartheta) \\ & - \frac{2}{3} (\cosh \vartheta + 1)(2 - \cosh \vartheta) \sum_{(3/2)^-} \tau_{3/2}^2(\cosh \vartheta) + \dots = 0. \end{aligned} \quad (1.18)$$

This sum rule becomes much simpler at  $\vartheta \rightarrow 0$ .  $D$ - and higher-wave contributions vanish, and

$$1 + \sum \tau_{1/2}^2(1) - \frac{4}{3} \sum \tau_{3/2}^2(1) = 0. \quad (1.19)$$

Substituting  $\sum \tau_{3/2}^2(1)$  from this sum rule into (1.16), we obtain

$$\rho^2 = \frac{3}{4} \left[ 1 + \sum \tau_{1/2}^2(1) \right]. \quad (1.20)$$

In particular,

$$\rho^2 > \frac{3}{4}. \quad (1.21)$$

This Uraltsev bound is much stronger than the Bjorken bound (1.17). Experimentally,  $\rho^2 \sim 0.8$ .

More sum rules can be obtained from energy conservation. In the  $v$  rest frame, the light fields in the B have a definite energy  $E = \bar{\Lambda}$ . They have no definite momentum, because they are in the external chromoelectric field created by the  $\bar{b}$  antiquark. The average of this momentum is  $\langle \mathbf{p} \rangle = 0$ , and the average of its square is  $\langle \mathbf{p}^2 \rangle = \mu_\pi^2$  (it is the same as the average squared momentum of the heavy antiquark, see (1.1)). The light fields' energy in the  $v'$  rest frame is  $E' = \bar{\Lambda} \cosh \vartheta - p_x \sinh \vartheta$ . When a b with a 4-velocity  $v$  is suddenly transformed into a  $\bar{c}$  with a 4-velocity  $v'$ , the light fields remain in their original state at first. After that, the energy  $E'$  is conserved in the field of the  $\bar{c}$  moving with the 4-velocity  $v'$ . Therefore, the average excitation energy of the  $X_{\bar{c}}$  and the average squared excitation energy are

$$\begin{aligned} \langle E' - \bar{\Lambda} \rangle &= \bar{\Lambda}(\cosh \vartheta - 1), \\ \langle (E' - \bar{\Lambda})^2 \rangle &= \bar{\Lambda}^2(\cosh \vartheta - 1)^2 + \frac{\mu_\pi^2}{3}(\cosh^2 \vartheta - 1) \end{aligned}$$

(because  $\langle p_x^2 \rangle = \langle \mathbf{p}^2 \rangle / 3$ ). This gives the Voloshin sum rule [23] and the BGSUV sum rule [1]:

$$\int F(\varepsilon, \cosh \vartheta) \varepsilon \, d\varepsilon = \bar{\Lambda}(\cosh \vartheta - 1), \quad (1.22)$$

$$\int F(\varepsilon, \cosh \vartheta) \varepsilon^2 \, d\varepsilon = \bar{\Lambda}^2(\cosh \vartheta - 1)^2 + \frac{\mu_\pi^2}{3}(\cosh^2 \vartheta - 1). \quad (1.23)$$

The transition into the ground-state meson with  $\varepsilon = 0$  does not contribute here.

Expanding these sum rules up to linear terms in  $\cosh \vartheta - 1$ , we obtain, similarly to (1.15),

$$\frac{1}{2} \sum \tau_{1/2}^2(1) \varepsilon_i + \frac{4}{3} \sum \tau_{3/2}^2(1) \varepsilon_i = \bar{\Lambda}, \quad (1.24)$$

$$\frac{1}{2} \sum \tau_{1/2}^2(1) \varepsilon_i^2 + \frac{4}{3} \sum \tau_{3/2}^2(1) \varepsilon_i^2 = \frac{2}{3} \mu_\pi^2. \quad (1.25)$$

Let  $\Delta$  be the minimum  $P$ -wave excitation energy. Then, replacing  $\varepsilon_i$  by  $\Delta$  in the left-hand side of (1.24), we decrease it. After singling out this factor  $\Delta$ , the remaining sum is  $2(\rho^2 - 1/4)$  (1.16):

$$\bar{\Lambda} \geq 2\Delta \left( \rho^2 - \frac{1}{4} \right). \quad (1.26)$$

This inequality can also be rewritten as an upper bound on  $\rho^2$  [23]:

$$\rho^2 \leq \frac{1}{4} + \frac{\bar{\Lambda}}{2\Delta}. \quad (1.27)$$

Similarly, replacing  $\varepsilon_i^2$  by  $\Delta \varepsilon_i$  in the left-hand side of (1.25), we decrease it. After singling out the factor  $\Delta$ , the remaining sum is  $\bar{\Lambda}$  (1.24), and [1]

$$\mu_\pi^2 \geq \frac{3}{2} \Delta \bar{\Lambda} \geq 3\Delta^2 \left( \rho^2 - \frac{1}{4} \right) \quad (1.28)$$

(in the second step, the inequality (1.26) has been used). If the lowest resonances in the  $(1/2)^-$  and  $(3/2)^-$  channels with nearly equal energies dominate in (1.24), (1.25), then the inequalities (1.26), (1.28) should be close to equalities. This is probably the case. Strictly speaking, the minimum excitation energy  $\Delta$  is equal to  $m_\pi$ , because the ground-state meson plus a soft pion can have the needed quantum numbers. This  $\Delta$  is small, and the bounds are very weak. However, the coupling of a soft pion with a heavy meson is small, and these states contribute little to the sum rules (1.24), (1.25). The first important contribution comes from the lowest  $P$ -wave resonances.

As you may have noticed, the integral in the Bjorken sum rule (1.13) diverges logarithmically at large  $\varepsilon$ , owing to (1.12). The integrals (1.22), (1.23) diverge even more strongly. Therefore, if we want to take  $\alpha_s$  effects into account, we have to cut these integrals somehow. On the other hand, the form factors  $\xi_i(\cosh \vartheta)$ ,  $\tau_{1/2}(\cosh \vartheta)$ ,  $\tau_{3/2}(\cosh \vartheta)$  depend on the normalization point  $\mu$ , if perturbative effects are taken into consideration. It is natural to expect that the sum rules are valid, up to  $\mathcal{O}(\alpha_s(\mu))$  corrections, when  $\mu$  is of the order of the cut-off energy (this is discussed in [11] in more detail). Therefore, the anomalous dimension of the HQET heavy-heavy quark current (which describes the  $\mu$ -dependence of the form factors) is proportional to the soft-photon radiation function (1.12).

For more information about inclusive sum rules, see [3, 2, 21, 24].

It is also possible to establish a bound on the Isgur–Wise form factor at the cut (Fig. 1.5). The decay rate  $W^* \rightarrow BD$  must be less than the total decay rate  $W^* \rightarrow bc$ :

$$n_l |\xi(\cosh \vartheta)|^2 |\cosh \vartheta + 1| \leq N_c , \quad (1.29)$$

where  $n_l$  is the number of light flavours, and  $N_c$  is the number of colours. The left-hand side should be the sum over light flavours, if  $SU(3)$  breaking is taken into account. The inequality (1.29) is applicable at  $|\cosh \vartheta + 1| \gg \alpha_s^2$  (outside the shaded region in Fig. 1.5), where the Isgur–Wise form factor makes sense, and the decay rate  $W^* \rightarrow \bar{b}c$  is given by the free-quark formula. At  $|\cosh \vartheta| \gg 1$ , production of the pair of ground-state mesons is rare, and the Isgur–Wise form factor (1.9) is much less than the bound (1.29). The inequality (1.29) was proposed in [20], where the factor  $n_l$  was erroneously omitted. It was used, together with analyticity, to obtain bounds on the Isgur–Wise form factor in the physical region.

## References

1. I. Bigi, A.G. Grozin, M. Shifman, N.G. Uraltsev, A. Vainshtein: Phys. Lett. B **339**, 160 (1994) [15, 16](#)
2. I. Bigi, M.A. Shifman, N.G. Uraltsev: Annu. Rev. Nucl. Part. Sci. **47**, 591 (1997) [16](#)
3. I. Bigi, M. Shifman, N.G. Uraltsev, A. Vainshtein: Phys. Rev. D **52**, 196 (1995) [16](#)
4. J.D. Bjorken: ‘New Symmetries in Heavy Flavor Physics’. In *Results and Perspectives in Particle Physics*, ed. by M. Greco (Editions Frontieres, Gif-sur-Yvette 1990) p. 583 [14](#)
5. J.D. Bjorken, I. Dunietz, J. Taron: Nucl. Phys. B **371**, 111 (1992) [14](#)
6. C.D. Carone, Phys. Lett. B **253**, 408 (1991) [4](#)
7. A.F. Falk: Nucl. Phys. B **378**, 79 (1992) [10](#)
8. A.F. Falk, H. Georgi, B. Grinstein, M.B. Wise: Nucl. Phys. B **343**, 1 (1990) [10](#)
9. H. Georgi: Nucl. Phys. B **348**, 293 (1991) [10](#)
10. H. Georgi, M.B. Wise: Phys. Lett. B **243**, 279 (1990) [4](#)
11. A.G. Grozin, G.P. Korchemsky: Phys. Rev. D **53**, 1378 (1996) [16](#)
12. A.G. Grozin, M. Neubert: Phys. Rev. D **55**, 272 (1997) [11](#)
13. N. Isgur, M.B. Wise: Phys. Lett. B **237**, 527 (1990) [4, 10](#)
14. N. Isgur, M.B. Wise: Phys. Rev. D **43**, 819 (1991) [10, 14](#)
15. N. Isgur, M.B. Wise: Phys. Rev. Lett. **66**, 1130 (1991) [8](#)
16. N. Isgur, M.B. Wise: Nucl. Phys. B **348**, 276 (1991) [10](#)
17. T. Mannel, W. Roberts, Z. Ryzak: Nucl. Phys. B **355**, 38 (1991) [10](#)
18. Particle Data Group: Eur. Phys. J. C **15**, 1 (2000) [5, 6, 8, 9](#)
19. H.D. Politzer: Phys. Lett. B **250**, 128 (1990) [10](#)
20. E. de Rafael, J. Taron: Phys. Lett. B **282**, 215 (1992) [17](#)
21. N.G. Uraltsev: ‘Heavy Quark Expansion in Beauty and its Decays’, in *Heavy Flavor Physics – a Probe of Nature’s Grand Design*, ed. by I. Bigi, L. Moroni (IOS Press, Amsterdam 1998) p. 329; ‘Topics in the Heavy Quark Expansion’, in *At the Frontier of Particle Physics: Handbook of QCD*, ed. by M. Shifman (World Scientific, Singapore 2001) v. 3, p. 1577 [16](#)
22. N.G. Uraltsev: Phys. Lett. B **501**, 86 (2001); J. Phys. G **27**, 1081 (2001) [14](#)
23. M.B. Voloshin: Phys. Rev. D **46**, 3062 (1992) [15, 16](#)
24. A. Le Yaouanc, L. Oliver, J.-C. Raynal: Phys. Rev. D **67**, 114009 (2003) [16](#)

## 2 The HQET Lagrangian

In this chapter, we introduce HQET – an effective field theory approximating QCD for problems with a single heavy quark in certain kinematics, to the leading order in  $1/m$  (Sect. 2.1). The rest of the chapter is about methods used for calculation of one- and two-loop Feynman diagrams in HQET. These methods have much in common with the ones used to calculate loop diagrams in massless theories, such as QCD with light quarks. Therefore, for the convenience of readers, we shall recall some well-known facts about massless diagrams, too.

### 2.1 The HQET Lagrangian

Let us consider QCD with a heavy flavour  $Q$  with mass  $m$ , and a number of light flavours. We shall be interested in problems with a single heavy quark that stays approximately at rest. More exactly, let  $\omega \ll m$  be the characteristic momentum scale. We shall assume that the heavy quark has a momentum  $|\mathbf{p}| \lesssim \omega$  and an energy  $|p_0 - m| \lesssim \omega$ ; light quarks and gluons have momenta  $|\mathbf{k}_i| \lesssim \omega$  and energies  $|k_{0i}| \lesssim \omega$ . Heavy quark effective theory (HQET) is an effective field theory constructed to reproduce QCD results for such problems expanded up to some order in  $\omega/m$ . In practice, only the first few orders in the  $1/m$  expansion are considered, because the complexity of the theory grows rapidly with the order.

Let us start from the QCD Lagrangian

$$L = \bar{Q}(i\cancel{D} - m)Q + \dots \quad (2.1)$$

where  $Q$  is the heavy-quark field, and the dots mean all the terms with light quarks and gluons. The free heavy-quark Lagrangian  $\bar{Q}(i\cancel{\partial} - m)Q$  gives the dependence of the energy on the momentum  $p_0 = \sqrt{m^2 + \mathbf{p}^2}$ . If we assume that the characteristic momenta  $|\mathbf{p}| \ll m$ , then we can simplify the dispersion law to  $p_0 = m$ . This law corresponds to the Lagrangian  $\bar{Q}(i\gamma_0\partial_0 - m)Q$ . In our class of problems, the lowest-energy state (“vacuum”) consists of a single particle – the heavy quark at rest. Therefore, it is convenient to use the energy of this state  $m$  as a new zero level. This means that, instead of the true energy  $p_0$  of the heavy quark (or any state containing this quark), we

shall use the residual energy  $\tilde{p}_0 = p_0 - m$ . Then the on-shell heavy quark has an energy  $\tilde{p}_0 = 0$  independently of the momentum. The free Lagrangian giving such a dispersion law is  $\bar{Q} i \gamma_0 \partial_0 Q$ . The spin of the heavy quark at rest can be described by a two-component spinor  $\tilde{Q}$  (we can also consider it as a four-component spinor with vanishing lower components:  $\gamma_0 \tilde{Q} = \tilde{Q}$ ). Reintroducing the interaction with the gluon field by the requirement of gauge invariance, we arrive at the HQET Lagrangian [4]

$$L = \tilde{Q}^+ i D_0 \tilde{Q} + \dots , \quad (2.2)$$

where all light-field parts (denoted by dots) are exactly the same as in QCD. The field theory (2.2) is not Lorentz-invariant, because the heavy quark defines a selected frame – its rest frame.

The Lagrangian (2.2) gives the static-quark propagator

$$\tilde{S}(\tilde{p}) = \frac{1}{\tilde{p}_0 + i0}, \quad \tilde{S}(x) = \tilde{S}(x_0) \delta(\mathbf{x}), \quad \tilde{S}(t) = -i\theta(t). \quad (2.3)$$

In the momentum space it depends only on  $\tilde{p}_0$  and not on  $\mathbf{p}$ , because we have neglected the kinetic energy. Therefore, in the coordinate space, the static quark does not move. The unit  $2 \times 2$  matrix is assumed in the propagator (2.3). It is often convenient to use it as a  $4 \times 4$  matrix; in such a case the projector  $(1 + \gamma_0)/2$  onto the upper components is assumed. The static quark interacts only with  $A_0$ ; the vertex is  $ig\delta_0^\mu t^a$ .

The static-quark propagator in a gluon field is given by the straight Wilson line

$$\tilde{S}(x) = -i\theta(x_0) \delta(\mathbf{x}) P \exp \left( ig \int A_\mu d\mathbf{x}^\mu \right). \quad (2.4)$$

Many properties of HQET were first derived in the course of the investigation of the renormalization of Wilson lines in QCD. In fact, the HQET Lagrangian was used as a technical device for investigation of Wilson lines.

Loops of a static quark vanish, because it propagates only forward in time. In other words, in the momentum space, all poles in the  $\tilde{p}_0$  plane lie in the lower half-plane; closing the integration contours upward, we obtain zero.

The Lagrangian (2.2) can be rewritten in covariant notation [7, 6]:

$$L_v = \overline{\tilde{Q}}_v i v \cdot D \tilde{Q}_v + \dots \quad (2.5)$$

where the static-quark field  $\tilde{Q}_v$  is a four-component spinor obeying the relation  $\not{v} \tilde{Q}_v = \tilde{Q}_v$ , and  $v^\mu$  is the quark velocity. The momentum  $p$  of the heavy quark (or any state containing it) is related to the residual momentum  $\tilde{p}$  by

$$p = mv + \tilde{p}, \quad |\tilde{p}^\mu| \ll m. \quad (2.6)$$

The static-quark propagator is

$$\tilde{S}(\tilde{p}) = \frac{1+\not{v}}{2} \frac{1}{\tilde{p} \cdot v + i0}, \quad (2.7)$$

and the vertex is  $igv^\mu t^a$ .

One can look [7] at how expressions for QCD diagrams tend to the corresponding HQET expressions in the limit  $m \rightarrow \infty$ . The QCD heavy-quark propagator is

$$S(p) = \frac{\not{p} + m}{p^2 - m^2} = \frac{m(1+\not{v}) + \not{p}}{2m\not{p} \cdot v + \not{p}^2} = \frac{1+\not{v}}{2} \frac{1}{\not{p} \cdot v} + \mathcal{O}\left(\frac{\not{p}}{m}\right). \quad (2.8)$$

A vertex  $ig\gamma^\mu t^a$  sandwiched between two projectors  $(1+\not{v})/2$  may be replaced by  $igv^\mu t^a$  (one may insert the projectors at external heavy-quark legs, too). Therefore, any tree QCD diagram equals the corresponding HQET one up to  $\mathcal{O}(\not{p}/m)$  terms. In loops, momenta can be arbitrarily large, and the relation (2.8) can break. Loops with momenta much larger than  $\omega$  yield contributions local in the coordinate space, which can be removed by counterterms. Then loop integrals become convergent, with characteristic loop momenta of order  $\omega$ , and one may use (2.8). Therefore, we can choose a renormalization scheme of HQET (by tuning the coefficients of local counterterms) in such a way as to reproduce renormalized QCD results (see [11] for details).

The renormalization properties (anomalous dimensions, etc.) of HQET differ from those of QCD. The ultraviolet behaviour of an HQET diagram is determined by the region of loop momenta much larger than the characteristic momentum scale of the process  $\omega$ , but much less than the heavy-quark mass  $m$  (which tends to infinity from the very beginning). It has nothing to do with the ultraviolet behaviour of the corresponding QCD diagram with the heavy-quark line, which is determined by the region of loop momenta much larger than  $m$ . In conventional QCD, the first region produces hybrid logarithms which are difficult to sum. In HQET, hybrid logarithms become ultraviolet logarithmic divergences governed by the renormalization group, with corresponding anomalous dimensions.

The HQET Lagrangian (2.2) possesses the  $SU(2)$  heavy-quark spin symmetry [9]. If there are  $n_h$  heavy-quark fields with the same velocity, it has the  $SU(2n_h)$  spin-flavour symmetry. For example, if we consider the  $B \rightarrow \bar{D}, \bar{D}^*$  transitions with  $v' = v$ , to the leading order in  $1/m_{c,b}$ , then the Lagrangian has  $SU(4)$  spin-flavour symmetry, which relates all form factors to the  $B \rightarrow B$  form factor at zero momentum transfer, which is equal to 1. If  $v' \neq v$ , it has only  $SU(2) \times SU(2)$  spin symmetry, which allows one to express all form factors via a single unknown function of  $v \cdot v'$ .

The heavy-quark mass is not uniquely defined. If we shift  $m$  by  $\delta m$  in (2.6), then the HQET Lagrangian (2.5) becomes

$$L_v = \overline{\tilde{Q}}_v i(v \cdot D - \delta m) \tilde{Q}_v + \dots, \quad (2.9)$$

where  $\delta m$  is called the residual mass term. The most convenient definition of the heavy-quark mass  $m$  is the one which gives  $\delta m = 0$  in (2.9). It gives the

HQET propagator having a pole at  $\tilde{p} \cdot v = 0$ , or the QCD propagator having a pole at  $p^2 = m^2$ . This mass is called the pole mass; it is well defined and gauge-invariant at any order of perturbation theory [10], but it is difficult to define it non-perturbatively. However, any mass differing from it by a constant  $\delta m$  (not growing with  $m$ ) is equally good, and produces the same physical results [5].

HQET has great advantages over QCD in lattice simulation of heavy-quark problems. Indeed, the applicability conditions of the lattice approximation for problems with light hadrons require that the lattice spacing is much less than the characteristic hadron size and that the total lattice length is much larger than this size. For simulation of QCD with a heavy quark, the lattice spacing must be much less than the heavy-quark Compton wavelength  $1/m$ . For the b quark, this is technically impossible at present. The HQET Lagrangian does not involve the heavy-quark mass  $m$ , and the applicability conditions of the lattice approximation for HQET are the same as in the case of light hadrons.

## 2.2 One-Loop Massless Propagator Diagrams

In this section, we shall calculate the one-loop massless propagator diagram with arbitrary degrees of the denominators (Fig. 2.1),

$$G = \int \frac{d^d k}{(-(k+p)^2 - i0)^{n_1} (-k^2 - i0)^{n_2}}. \quad (2.10)$$

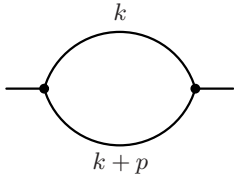


**Fig. 2.1.** One-loop massless propagator diagram

The first step is to combine the denominators together. To this end, we write  $1/a^n$  for  $\text{Re } a > 0$  as

$$\frac{1}{a^n} = \frac{1}{\Gamma(n)} \int_0^\infty e^{-a\alpha} \alpha^{n-1} d\alpha \quad (2.11)$$

( $\alpha$ -representation). Multiplying two such representations, we have

$$\frac{1}{a_1^{n_1} a_2^{n_2}} = \frac{1}{\Gamma(n_1)\Gamma(n_2)} \int e^{-a_1\alpha_1 - a_2\alpha_2} \alpha_1^{n_1-1} \alpha_2^{n_2-1} d\alpha_1 d\alpha_2. \quad (2.12)$$

Now we proceed to the new variables  $\alpha_1 = x\alpha$ ,  $\alpha_2 = (1-x)\alpha$ , and obtain

$$\frac{1}{a_1^{n_1} a_2^{n_2}} = \frac{\Gamma(n_1 + n_2)}{\Gamma(n_1)\Gamma(n_2)} \int_0^1 \frac{x^{n_1-1}(1-x)^{n_2-1} dx}{[a_1 x + a_2(1-x)]^{n_1+n_2}}. \quad (2.13)$$

This Feynman parametrization is valid not only when  $\text{Re } a_{1,2} > 0$ , but also, by analytical continuation, in all cases where the integral in  $x$  is well defined.

Combining the denominators in (2.10) and shifting the integration momentum  $k \rightarrow k - xp$ , we obtain

$$G = \frac{\Gamma(n_1 + n_2)}{\Gamma(n_1)\Gamma(n_2)} \int \frac{x^{n_1-1}(1-x)^{n_2-1} dx d^d k}{[-k^2 + x(1-x)(-p^2) - i0]^{n_1+n_2}}. \quad (2.14)$$

Now we shall calculate the one-loop massive vacuum diagram, which appears as a sub-expression in many calculations. Performing the Wick rotation  $k_0 = ik_{E0}$  and going to the Euclidean space  $k^2 = -k_E^2$ , we have (here  $2\pi^{d/2}/\Gamma(d/2)$  is the  $d$ -dimensional full solid angle)

$$\int \frac{d^d k}{(-k^2 + m^2 - i0)^n} = i \frac{2\pi^{d/2}}{\Gamma(d/2)} \int \frac{k_E^{d-1} dk_E}{(k_E^2 + m^2)^n}. \quad (2.15)$$

At this point, the meaning of the  $d$ -dimensional integral for an arbitrary  $d$  becomes completely well defined. Then we use  $2k_E dk_E \rightarrow dk_E^2$ , and proceed to the dimensionless variable  $z = k_E^2/m^2$  to obtain

$$\frac{i\pi^{d/2}}{\Gamma(d/2)} (m^2)^{d/2-n} \int_0^\infty \frac{z^{d/2-1} dz}{(z+1)^n}.$$

The substitution  $x = 1/(z+1)$  reduces this integral to the Euler  $B$ -function, and we arrive at

$$\int \frac{d^d k}{(-k^2 + m^2 - i0)^n} = i\pi^{d/2} \frac{\Gamma(-d/2 + n)}{\Gamma(n)} (m^2)^{d/2-n}. \quad (2.16)$$

We can now resume the calculation of the integral  $G$  (2.14). We shall assume that  $p^2 < 0$ , so that production of a pair of on-shell massless particles is not possible. Using (2.16) with  $m^2 \rightarrow x(1-x)(-p^2)$  and  $n \rightarrow n_1 + n_2$ , we obtain

$$\begin{aligned} G &= i\pi^{d/2} \frac{\Gamma(-d/2 + n_1 + n_2)}{\Gamma(n_1)\Gamma(n_2)} (-p^2)^{d/2-n_1-n_2} \\ &\times \int_0^1 x^{d/2-n_2-1} (1-x)^{d/2-n_1-1} dx. \end{aligned} \quad (2.17)$$

This integral is a  $B$ -function. Our final result can be written as

$$\begin{aligned} \int \frac{d^d k}{D_1^{n_1} D_2^{n_2}} &= i\pi^{d/2} (-p^2)^{d/2-n_1-n_2} G(n_1, n_2), \\ D_1 &= -(k+p)^2, \quad D_2 = -k^2, \end{aligned}$$

$$G(n_1, n_2) = \frac{\Gamma(-d/2 + n_1 + n_2)\Gamma(d/2 - n_1)\Gamma(d/2 - n_2)}{\Gamma(n_1)\Gamma(n_2)\Gamma(d - n_1 - n_2)}, \quad (2.18)$$

where the correct i0 terms are assumed in  $D_{1,2}$ . If  $n_{1,2}$  are integer,  $G(n_1, n_2)$  is proportional to  $G_1 = \Gamma(1 + \varepsilon)\Gamma^2(1 - \varepsilon)/\Gamma(1 - 2\varepsilon)$ , the coefficient being a rational function of  $d$ .

The ultraviolet (UV) divergences of the original integral (2.10) are reproduced by the loop-momentum integral (2.16), and are given by the poles of  $\Gamma(-d/2 + n_1 + n_2)$  (with a minus sign in front of  $d$ ). The infrared (IR) divergences of the original integral reside in the integral in the Feynman parameter  $x$  (2.17), and are given by the poles of  $\Gamma(d/2 - n_1)$  and  $\Gamma(d/2 - n_2)$  (with a plus sign in front of  $d$ ).

In many cases, calculation of diagrams in the coordinate space can be simpler than in the momentum space. In particular, the one-loop propagator diagram of Fig. 2.1 in the coordinate space is just the product of two propagators. The massless propagators in the  $p$ -space and the  $x$ -space are related to each other by a Fourier transform:

$$\int \frac{e^{-ip \cdot x}}{(-p^2 - i0)^n} \frac{d^d p}{(2\pi)^d} = i2^{-2n} \pi^{-d/2} \frac{\Gamma(d/2 - n)}{\Gamma(n)} \frac{1}{(-x^2 + i0)^{d/2-n}}, \quad (2.19)$$

$$\int \frac{e^{ip \cdot x}}{(-x^2 + i0)^n} d^d x = -i2^{d-2n} \pi^{d/2} \frac{\Gamma(d/2 - n)}{\Gamma(n)} \frac{1}{(-p^2 - i0)^{d/2-n}} \quad (2.20)$$

(sanity checks: transform  $1/(-p^2 - i0)^n$  to  $x$ -space (2.19) and back (2.20), and you get  $1/(-p^2 - i0)^n$ ; take the complex conjugate of (2.19) and rename  $x \leftrightarrow p$ , and you get (2.20)). Multiplying two propagators (2.19) with degrees  $n_1$  and  $n_2$ , we obtain

$$-2^{-2(n_1+n_2)} \pi^{-d} \frac{\Gamma(d/2 - n_1)\Gamma(d/2 - n_2)}{\Gamma(n_1)\Gamma(n_2)} \frac{1}{(-x^2)^{d-n_1-n_2}}.$$

Applying the inverse Fourier transform (2.20), we reproduce the result (2.18).

The one-loop diagram (2.18) is an analytic function in the complex  $p^2$  plane with a cut. The cut at  $p^2 > 0$ , where real pair production is possible, begins at a branch point at the threshold  $p^2 = 0$ . This cut comes from the factor  $(-p^2)^{-\varepsilon}$ , which is equal to  $(p^2)^{-\varepsilon} e^{-i\pi\varepsilon}$  at the upper side of the cut and  $(p^2)^{-\varepsilon} e^{i\pi\varepsilon}$  at the lower side, and hence has a discontinuity  $-2i(p^2)^{-\varepsilon} \sin \pi\varepsilon$ . Therefore, the discontinuity of the one-loop diagram (2.18) at  $\varepsilon \rightarrow 0$  is proportional to the residue of  $G(n_1, n_2)$  at  $\varepsilon = 0$ . The discontinuity of the diagram with  $n_1 = n_2 = 1$  can be calculated directly using the Cutkosky rules: draw a cut across the loop indicating the real intermediate state, and replace the cut propagators by their discontinuities:

$$\frac{1}{-p^2 - i0} \rightarrow 2\pi i \delta(p^2). \quad (2.21)$$

### 2.3 One-Loop HQET Propagator Diagrams

Now we shall calculate the one-loop HQET propagator diagram with arbitrary degrees of the denominators (Fig. 2.2),

$$I = \int \frac{d^d k}{(-(k + \tilde{p})_0 - i0)^{n_1} (-k^2 - i0)^{n_2}}. \quad (2.22)$$

This diagram depends only on  $\omega = \tilde{p}_0$ , and not on  $\mathbf{p}$ .

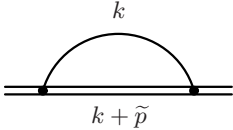


**Fig. 2.2.** One-loop HQET propagator diagram

We cannot use the ordinary Feynman parametrization (2.13), because the denominators have different dimensionalities. Therefore, we make a different change of variables in the double  $\alpha$ -parametric integral (2.12),  $\alpha_1 = y\alpha$ ,  $\alpha_2 = \alpha$ , and obtain the HQET Feynman parametrization

$$\frac{1}{a_1^{n_1} a_2^{n_2}} = \frac{\Gamma(n_1 + n_2)}{\Gamma(n_1)\Gamma(n_2)} \int_0^\infty \frac{y^{n_1-1} dy}{[a_1 y + a_2]^{n_1+n_2}}. \quad (2.23)$$

If the denominator  $a_1$  has the dimensionality of energy, and  $a_2$  has the dimensionality of energy squared, then the Feynman parameter  $y$  has the dimensionality of energy; it runs from 0 to  $\infty$ . When combining the denominators in (2.22), it is slightly more convenient to double the linear denominator; shifting the integration momentum  $k \rightarrow k - yv$ , we obtain

$$I = 2^{n_1} \frac{\Gamma(n_1 + n_2)}{\Gamma(n_1)\Gamma(n_2)} \int \frac{y^{n_1-1} dy d^d k}{[-k^2 + y(y - 2\omega) - i0]^{n_1+n_2}}. \quad (2.24)$$

We must have a definite sign of  $i0$  in the combined denominator, therefore, the  $i0$  terms in both denominators must have the same sign.

We shall assume that  $\omega < 0$ , so that production of a pair of on-shell particles is not possible. Using (2.16) with  $m^2 \rightarrow y(y - 2\omega)$  and  $n \rightarrow n_1 + n_2$ , we obtain

$$I = i\pi^{d/2} 2^{n_1} \frac{\Gamma(-d/2 + n_1 + n_2)}{\Gamma(n_1)\Gamma(n_2)} \int_0^\infty y^{n_1-1} [y(y - 2\omega)]^{d/2 - n_1 - n_2} dy. \quad (2.25)$$

We proceed to the dimensionless variable  $z = y/(-2\omega)$ . Then the substitution  $z + 1 = 1/x$  reduces this integral to the Euler  $B$ -function:

$$\int_0^\infty y^{d/2-n_2-1} (y - 2\omega)^{d/2-n_1-n_2} dy = (-2\omega)^{d-n_1-2n_2} \frac{\Gamma(-d+n_1+2n_2)\Gamma(d/2-n_2)}{\Gamma(-d/2+n_1+n_2)}. \quad (2.26)$$

Our final result can be written as

$$\begin{aligned} \int \frac{d^d k}{D_1^{n_1} D_2^{n_2}} &= i\pi^{d/2} (-2\omega)^{d-2n_2} I(n_1, n_2), \\ D_1 &= (k \cdot v + \omega)/\omega, \quad D_2 = -k^2, \\ I(n_1, n_2) &= \frac{\Gamma(-d+n_1+2n_2)\Gamma(d/2-n_2)}{\Gamma(n_1)\Gamma(n_2)}. \end{aligned} \quad (2.27)$$

If  $n_{1,2}$  are integer,  $I(n_1, n_2)$  is proportional to  $I_1 = \Gamma(1+2\varepsilon)\Gamma(1-\varepsilon)$ , the coefficient being a rational function of  $d$ .

The integral (2.16) in  $d^d k$  can have a UV divergence, and it produces  $\Gamma(-d/2+n_1+n_2)$  in the numerator of (2.25). However, it is too optimistic with respect to UV convergence: for example, at  $n_1 = 2, n_2 = 1$  it has no pole at  $d = 4$ , while the original integral (2.22) is UV divergent. The HQET Feynman parameter  $y$  has the dimensionality of energy and runs up to  $\infty$ . It is natural to expect that this can produce an extra UV divergence. The region  $y \rightarrow \infty$  produces  $\Gamma(-d+n_1+2n_2)$  in the Feynman parametric integral (2.26). The “wrong” UV  $\Gamma$ -function is cancelled by the denominator of (2.26), and  $n_1+2n_2$  determines the correct UV behaviour. The region  $y \rightarrow 0$  produces the IR  $\Gamma(d/2-n_2)$ . The rule about the negative/positive sign of  $d$  in UV/IR  $\Gamma$ -functions remains valid.

The one-loop propagator diagram of Fig. 2.2 in the coordinate space is just the product of two propagators. The HQET propagators in the  $p$ -space and the  $x$ -space are related to each other by a Fourier transform:

$$\int_{-\infty}^{+\infty} \frac{e^{-i\omega t}}{(-\omega - i0)^n} \frac{d\omega}{2\pi} = \frac{i^n}{\Gamma(n)} t^{n-1} \theta(t), \quad (2.28)$$

$$\int_0^\infty e^{i\omega t} t^n dt = \frac{(-i)^{n+1} \Gamma(n+1)}{(-\omega - i0)^{n+1}}. \quad (2.29)$$

The first integral is non-zero only at  $t > 0$ , when we close the integration contour downward; for integer  $n$ , its value is given by the residue at  $\omega = -i0$ . In the second integral, we substitute  $\omega \rightarrow \omega + i0$  for convergence. Multiplying an HQET propagator (2.28) with degree  $n_1$  and a massless propagator (2.19) with degree  $n_2$ , we obtain

$$-2^{-2n_2} \pi^{-d/2} \frac{\Gamma(d/2-n_2)}{\Gamma(n_1)\Gamma(n_2)} (it)^{n_1+2n_2-d-1} \theta(t)$$

(where  $-x^2 = (it)^2$ ). Applying the inverse Fourier transform (2.29), we reproduce the result (2.27).

The one-loop diagram (2.27) is an analytic function in the complex  $\omega$  plane with a cut. The cut at  $\omega > 0$ , where real pair production is possible, begins at a branch point at the threshold  $\omega = 0$ . This cut comes from the factor  $(-\omega)^{-2\varepsilon}$ , which has a discontinuity  $-2i\omega^{-2\varepsilon} \sin 2\pi\varepsilon$ . Therefore, the discontinuity of the one-loop diagram (2.27) at  $\varepsilon \rightarrow 0$  is proportional to the residue of  $I(n_1, n_2)$  at  $\varepsilon = 0$ . The discontinuity of the diagram with  $n_1 = n_2 = 1$  can be directly calculated using the Cutkosky rules (2.21), and

$$\frac{1}{-\tilde{p}_0 - i0} \rightarrow 2\pi i \delta(\tilde{p}_0). \quad (2.30)$$

## 2.4 Two-Loop Massless Propagator Diagrams

There is only one generic topology of two-loop massless propagator diagrams, Fig. 2.3a. If one of the lines is shrunk to a point, the diagrams of Figs. 2.3b,c result. If any two adjacent lines are shrunk to a point, the diagram contains a no-scale vacuum tadpole, and hence vanishes.

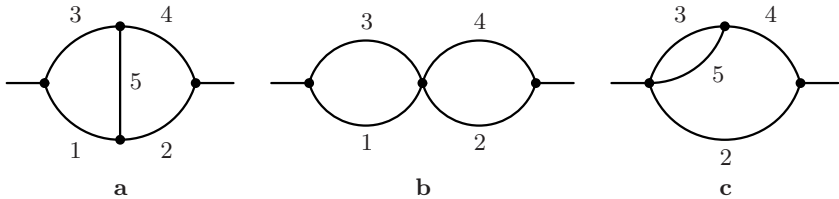


**Fig. 2.3.** Two-loop massless propagator diagram

We write down the diagram of Fig. 2.3a as

$$\begin{aligned} \int \frac{d^d k_1 d^d k_2}{D_1^{n_1} D_2^{n_2} D_3^{n_3} D_4^{n_4} D_5^{n_5}} &= -\pi^d (-p^2)^{d-\sum n_i} G(n_1, n_2, n_3, n_4, n_5), \\ D_1 &= -(k_1 + p)^2, \quad D_2 = -(k_2 + p)^2, \\ D_3 &= -k_1^2, \quad D_4 = -k_2^2, \quad D_5 = -(k_1 - k_2)^2. \end{aligned} \quad (2.31)$$

It is symmetric with respect to  $(1 \leftrightarrow 2, 3 \leftrightarrow 4)$ , and with respect to  $(1 \leftrightarrow 3, 2 \leftrightarrow 4)$ . If the indices of any two adjacent lines are non-positive, the diagram contains a scale-free vacuum subdiagram, and hence vanishes. If  $n_5 = 0$ , this diagram is a product of two one-loop diagrams (Fig. 2.3b):

$$G(n_1, n_2, n_3, n_4, 0) = G(n_1, n_3)G(n_2, n_4). \quad (2.32)$$

If  $n_1 = 0$  (Fig. 2.3c), the  $(3, 5)$  integral (2.18) gives  $G(n_3, n_5)/(-k_2^2)^{n_3+n_5-d/2}$ ; this is combined with the denominator 4, and we obtain

$$G(0, n_2, n_3, n_4, n_5) = G(n_3, n_5)G(n_2, n_4 + n_3 + n_5 - d/2). \quad (2.33)$$

Of course, the cases  $n_2 = 0$ ,  $n_3 = 0$ ,  $n_4 = 0$  follow by symmetry.

When all  $n_i > 0$ , the problem does not immediately reduce to a repeated use of the one-loop formula (2.18). We shall use a powerful method called integration by parts [12, 3]. It is based on the simple observation that any integral of  $\partial/\partial k_1(\dots)$  (or  $\partial/\partial k_2(\dots)$ ) vanishes (in dimensional regularization, no surface terms can appear). From this, we can obtain recurrence relations which involve  $G(n_1, n_2, n_3, n_4, n_5)$  with different sets of indices. By applying these relations in a carefully chosen order, we can reduce any  $G(n_1, n_2, n_3, n_4, n_5)$  to trivial ones, such as (2.32), (2.33).

The differential operator  $\partial/\partial k_2$  applied to the integrand of (2.31) acts as

$$\frac{\partial}{\partial k_2} \rightarrow \frac{n_2}{D_2} 2(k_2 + p) + \frac{n_4}{D_4} 2k_2 + \frac{n_5}{D_5} 2(k_2 - k_1). \quad (2.34)$$

Applying  $(\partial/\partial k_2) \cdot k_2$  to the integrand of (2.31), we obtain a vanishing integral. On the other hand, from (2.34),  $2k_2 \cdot k_2 = -2D_4$ ,  $2(k_2 + p) \cdot k_2 = (-p^2) - D_2 - D_4$ , and  $2(k_2 - k_1) \cdot k_2 = D_3 - D_4 - D_5$ , we see that this differential operator is equivalent to inserting

$$d - n_2 - n_5 - 2n_4 + \frac{n_2}{D_2}((-p^2) - D_4) + \frac{n_5}{D_5}(D_3 - D_4)$$

under the integral sign (here  $(\partial/\partial k_2) \cdot k_2 = d$ ). Taking into account the definition (2.31), we obtain the recurrence relation

$$\begin{aligned} & (d - n_2 - n_5 - 2n_4)G(n_1, n_2, n_3, n_4, n_5) \\ & + n_2 [G(n_1, n_2 + 1, n_3, n_4, n_5) - G(n_1, n_2 + 1, n_3, n_4 - 1, n_5)] \\ & + n_5 [G(n_1, n_2, n_3 - 1, n_4, n_5 + 1) - G(n_1, n_2, n_3, n_4 - 1, n_5 + 1)] = 0. \end{aligned}$$

This relation looks lengthy. When using the integration-by-parts method, one has to work with a large number of relations of this kind. Therefore, special concise notation has been invented. Let us introduce the raising and lowering operators

$$\mathbf{1}^\pm G(n_1, n_2, n_3, n_4, n_5) = G(n_1 \pm 1, n_2, n_3, n_4, n_5), \quad (2.35)$$

and similar ones for the other indices. Then our recurrence relation can be written in a shorter and more easily digestible form,

$$[d - n_2 - n_5 - 2n_4 + n_2 \mathbf{2}^+(1 - \mathbf{4}^-) + n_5 \mathbf{5}^+(\mathbf{3}^- - \mathbf{4}^-)] G = 0. \quad (2.36)$$

This is a particular example of the triangle relation. We differentiate with respect to the loop momentum running along the triangle 254, and insert the momentum of the line 4 in the numerator. The differentiation raises the degree of one of the denominators 2, 5, 4. In the case of the line 4, we

obtain  $-2D_4$  in the numerator, giving just  $-2n_4$ . In the case of the line 5, we obtain the denominator  $D_3$  of the line attached to the vertex 45 of our triangle, minus the denominators  $D_4$  and  $D_5$ . The case of the line 2 is similar; the denominator of the line attached to the vertex 24 of our triangle is just  $-p^2$ , and it does not influence any index of  $G$ . Of course, there are three more relations that can be obtained from (2.36) by symmetry. Another useful triangle relation is derived by applying the operator  $(\partial/\partial k_2) \cdot (k_2 - k_1)$ :

$$[d - n_2 - n_4 - 2n_5 + n_2 \mathbf{2}^+(1^- - \mathbf{5}^-) + n_4 \mathbf{4}^+(\mathbf{3}^- - \mathbf{5}^-)] G = 0. \quad (2.37)$$

One more relation is obtained by symmetry. Relations of this kind can be written for any diagram having a triangle in it, when at least two vertices of the triangle each have only a single line (not belonging to the triangle) attached.

We can obtain a relation from the homogeneity of the integral (2.31) with respect to  $p$ . Applying the operator  $p \cdot (\partial/\partial p)$  to the integral (2.31), we see that it is equivalent to a factor  $2(d - \sum n_i)$ . On the other hand, explicit differentiation of the integrand gives  $-(n_1/D_1)(-p^2 + D_1 - D_3) - (n_2/D_2)(-p^2 + D_2 - D_4)$ . Therefore,

$$[2(d - n_3 - n_4 - n_5) - n_1 - n_2 + n_1 \mathbf{1}^+(1 - \mathbf{3}^-) + n_2 \mathbf{2}^+(1 - \mathbf{4}^-)] G = 0. \quad (2.38)$$

This is nothing but the sum of the  $(\partial/\partial k_2) \cdot k_2$  relation (2.36) and its mirror-symmetric  $(\partial/\partial k_1) \cdot k_1$  relation.

Another interesting relation is obtained by inserting  $(k_1 + p)^\mu$  into the integrand of (2.31) and taking the derivative  $\partial/\partial p^\mu$  of the integral. On the one hand, the vector integral must be proportional to  $p^\mu$ , and we can make the substitution

$$k_1 + p \rightarrow \frac{(k_1 + p) \cdot p}{p^2} p = \left(1 + \frac{D_1 - D_3}{-p^2}\right) \frac{p}{2}$$

in the integrand. Taking  $\partial/\partial p^\mu$  of this vector integral produces (2.31) with

$$\left(\frac{3}{2}d - \sum n_i\right) \left(1 + \frac{D_1 - D_3}{-p^2}\right)$$

inserted into the integrand. On the other hand, explicit differentiation with respect to  $p$  gives

$$\begin{aligned} d + \frac{n_1}{D_1} 2(k_1 + p)^2 + \frac{n_2}{D_2} 2(k_2 + p) \cdot (k_1 + p), \\ 2(k_2 + p) \cdot (k_1 + p) = D_5 - D_1 - D_2. \end{aligned}$$

Therefore, we obtain

$$\left[ \frac{1}{2}d + n_1 - n_3 - n_4 - n_5 + \left( \frac{3}{2}d - \sum n_i \right) (\mathbf{1}^- - \mathbf{3}^-) + n_2 \mathbf{2}^+ (\mathbf{1}^- - \mathbf{5}^-) \right] G = 0. \quad (2.39)$$

Three more relations follow from symmetries.

Expressing  $G(n_1, n_2, n_3, n_4, n_5)$  by use of (2.37),

$$G(n_1, n_2, n_3, n_4, n_5) = \frac{n_2 \mathbf{2}^+ (\mathbf{5}^- - \mathbf{1}^-) + n_4 \mathbf{4}^+ (\mathbf{5}^- - \mathbf{3}^-)}{d - n_2 - n_4 - 2n_5} G, \quad (2.40)$$

we see that the sum  $n_1 + n_3 + n_5$  is reduced by 1. Therefore, by applying (2.40) sufficiently many times, we can reduce an arbitrary  $G$  integral with integer indices to a combination of integrals with  $n_5 = 0$  (Fig. 2.3b, (2.32)),  $n_1 = 0$  (Fig. 2.3c, (2.33)), and  $n_3 = 0$  (mirror-symmetric to the previous case). Of course, if  $\max(n_2, n_4) < \max(n_1, n_3)$ , it may be more efficient to use the relation mirror-symmetric to (2.37). The relation (2.39) can also be used instead of (2.37). Thus, any integral  $G(n_1, n_2, n_3, n_4, n_5)$  with integer  $n_i$  can be expressed as a linear combination of  $G_1^2$  and  $G_2$ , the coefficients being rational functions of  $d$ . Here the combinations of  $\Gamma$ -functions appearing in the  $n$ -loop sunset massless diagram are

$$G_n = \frac{\Gamma(1+n\varepsilon)\Gamma^{n+1}(1-\varepsilon)}{\Gamma(1-(n+1)\varepsilon)} = \frac{\Gamma(2n+1-nd/2)\Gamma^{n+1}(d/2-1)}{\Gamma((n+1)d/2-2n-1)}. \quad (2.41)$$

Methods of calculation of three-loop massless propagator diagrams are considered in [3].

## 2.5 Two-Loop HQET Propagator Diagrams

There are two generic topologies of two-loop HQET propagator diagrams, Figs. 2.4a,b. If one of the lines is shrunk to a point, the diagrams of Figs. 2.4c,d,e result. If any two adjacent lines are shrunk to a point, the diagram contains a no-scale vacuum tadpole, and hence vanishes.

We write down the diagram of Fig. 2.4a as

$$\begin{aligned} \int \frac{d^d k_1 d^d k_2}{D_1^{n_1} D_2^{n_2} D_3^{n_3} D_4^{n_4} D_5^{n_5}} &= -\pi^d (-2\omega)^{2(d-n_3-n_4-n_5)} I(n_1, n_2, n_3, n_4, n_5), \\ D_1 &= (k_1 + \tilde{p}) \cdot v/\omega, \quad D_2 = (k_2 + \tilde{p}) \cdot v/\omega, \\ D_3 &= -k_1^2, \quad D_4 = -k_2^2, \quad D_5 = -(k_1 - k_2)^2. \end{aligned} \quad (2.42)$$

It is symmetric with respect to  $(1 \leftrightarrow 3, 2 \leftrightarrow 4)$ . If the indices of any two adjacent lines are non-positive, the diagram contains a scale-free vacuum subdiagram, and hence vanishes. If  $n_5 = 0$ , this diagram is a product of two one-loop diagrams (Fig. 2.4c):

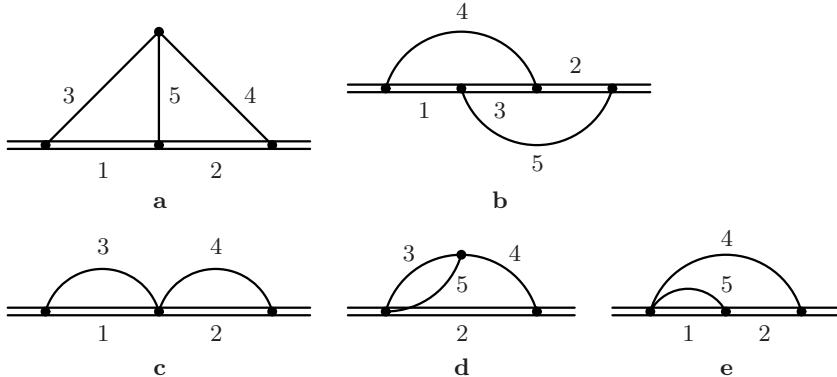


**Fig. 2.4.** Two-loop HQET propagator diagram

$$I(n_1, n_2, n_3, n_4, 0) = I(n_1, n_3)I(n_2, n_4). \quad (2.43)$$

If  $n_1 = 0$  (Fig. 2.4d), the  $(3, 5)$  integral (2.18) gives  $G(n_3, n_5)/(-k_2^2)^{n_3+n_5-d/2}$ ; this is combined with the denominator 4, and we obtain

$$I(0, n_2, n_3, n_4, n_5) = G(n_3, n_5)I(n_2, n_4 + n_3 + n_5 - d/2) \quad (2.44)$$

(and similarly for  $n_2 = 0$ ). If  $n_3 = 0$  (Fig. 2.4e), the  $(1, 5)$  integral (2.27) gives  $I(n_1, n_5)/(-2\omega)^{n_1+2n_5-d}$ ; this is combined with the denominator 2, and we obtain

$$I(n_1, n_2, 0, n_4, n_5) = I(n_1, n_5)I(n_2 + n_1 + 2n_5 - d, n_4) \quad (2.45)$$

(and similarly for  $n_4 = 0$ ).

When all  $n_i > 0$ , we apply integration by parts [1]. The differential operator  $\partial/\partial k_2$  applied to the integrand of (2.42) acts as

$$\frac{\partial}{\partial k_2} \rightarrow -\frac{n_2}{D_2} \frac{v}{\omega} + \frac{n_4}{D_4} 2k_2 + \frac{n_5}{D_5} 2(k_2 - k_1). \quad (2.46)$$

Applying  $(\partial/\partial k_2) \cdot k_2$  and  $(\partial/\partial k_2) \cdot (k_2 - k_1)$  to the integrand of (2.42), we obtain vanishing integrals. On the other hand, from (2.46),  $k_2 v/\omega = D_2 - 1$ , and  $2(k_2 - k_1) \cdot k_2 = D_3 - D_4 - D_5$ , we see that these differential operators are equivalent to inserting

$$d - n_2 - n_5 - 2n_4 + \frac{n_2}{D_2} + \frac{n_5}{D_5} (D_3 - D_4),$$

$$d - n_2 - n_4 - 2n_5 + \frac{n_2}{D_2} D_1 + \frac{n_4}{D_4} (D_3 - D_5)$$

under the integral sign. Therefore, we obtain the triangle relations

$$[d - n_2 - n_5 - 2n_4 + n_2 \mathbf{2}^+ + n_5 \mathbf{5}^+ (\mathbf{3}^- - \mathbf{4}^-)] I = 0, \quad (2.47)$$

$$[d - n_2 - n_4 - 2n_5 + n_2 \mathbf{2}^+ \mathbf{1}^- + n_4 \mathbf{4}^+ (\mathbf{3}^- - \mathbf{5}^-)] I = 0 \quad (2.48)$$

(two more relations are obtained by  $(1 \leftrightarrow 3, 2 \leftrightarrow 4)$ ). Similarly, applying the differential operator  $2\omega(\partial/\partial k_2) \cdot v$  is equivalent to inserting

$$-2\frac{n_2}{D_2} + \frac{n_4}{D_4} 4\omega^2(D_2 - 1) + \frac{n_5}{D_5} 4\omega^2(D_2 - D_1),$$

and we obtain (taking into account the definition (2.42))

$$[-2n_2\mathbf{2}^+ + n_4\mathbf{4}^+(\mathbf{2}^- - 1) + n_5\mathbf{5}^+(\mathbf{2}^- - \mathbf{1}^-)] I = 0 \quad (2.49)$$

(there is also the symmetric relation, of course).

We can obtain a relation from the homogeneity of the integral (2.42) with respect to  $\omega$ . Applying the operator  $\omega(d/d\omega)$  to the integral (2.42) multiplied by  $(-\omega)^{-n_1-n_2}$ , we see that it is equivalent to a factor  $2(d - n_3 - n_4 - n_5) - n_1 - n_2$ . On the other hand, explicit differentiation of  $(-\omega D_1)^{-n_1}(-\omega D_2)^{-n_2}$  gives  $-n_1/D_1 - n_2/D_2$ . Therefore,

$$[2(d - n_3 - n_4 - n_5) - n_1 - n_2 + n_1\mathbf{1}^+ + n_2\mathbf{2}^+] I = 0. \quad (2.50)$$

This is nothing but the sum of the  $(\partial/\partial k_2) \cdot k_2$  relation (2.47) and its mirror-symmetric  $(\partial/\partial k_1) \cdot k_1$  relation.

When trying to find the most useful combinations of recurrence relations, it is convenient to manipulate these relations in an algebraic way. We shall consider the raising and lowering symbols, such as  $\mathbf{1}^\pm$ , as operators not commuting with  $n_i$ , etc. Traditionally, these operators are written to the right of the  $n_i$  factors. Of course, any relation may be multiplied (from the left) by any  $n_i$  factors. We can also apply a shift, say  $n_1 \rightarrow n_1 \pm 1$ , everywhere in the relation. This operation can be represented by multiplication by  $\mathbf{1}^\pm$  from the left followed by commuting this operator to the right, if we assume

$$\mathbf{1}^\pm n_1 = (n_1 \pm 1)\mathbf{1}^\pm. \quad (2.51)$$

The most useful combination of recurrence relations for the integral  $I$  (2.42) is the triangle relation (2.48) minus  $\mathbf{1}^-$  times the homogeneity relation (2.50):

$$[d - n_1 - n_2 - n_4 - 2n_5 + 1 - (2(d - n_3 - n_4 - n_5) - n_1 - n_2 + 1)\mathbf{1}^- + n_4\mathbf{4}^+(\mathbf{3}^- - \mathbf{5}^-)] I = 0. \quad (2.52)$$

Expressing  $I(n_1, n_2, n_3, n_4, n_5)$  by use of this relation,

$$I(n_1, n_2, n_3, n_4, n_5) = \frac{(2(d - n_3 - n_4 - n_5) - n_1 - n_2 + 1)\mathbf{1}^- + n_4\mathbf{4}^+(\mathbf{5}^- - \mathbf{3}^-)}{d - n_1 - n_2 - n_4 - 2n_5 + 1} I, \quad (2.53)$$

we see that the sum  $n_1 + n_3 + n_5$  is reduced by 1. Therefore, by applying (2.53) sufficiently many times, we can reduce an arbitrary  $I$  integral

with integer indices to a combination of integrals with  $n_5 = 0$  (Fig. 2.4c, (2.43)),  $n_1 = 0$  (Fig. 2.4d, (2.44)), and  $n_3 = 0$  (Fig. 2.4e, (2.45)). Of course, if  $\max(n_2, n_4) < \max(n_1, n_3)$ , it may be more efficient to use the relation mirror-symmetric to (2.52). Thus, any integral  $I(n_1, n_2, n_3, n_4, n_5)$  with integer  $n_i$  can be expressed as a linear combination of  $I_1^2$  and  $I_2$ , the coefficients being rational functions of  $d$ . Here the combinations of  $\Gamma$ -functions appearing in the  $n$ -loop sunset HQET diagram are

$$I_n = \Gamma(1 + 2n\varepsilon)\Gamma^n(1 - \varepsilon) = \Gamma(4n + 1 - nd)\Gamma^n(d/2 - 1). \quad (2.54)$$

We write down the diagram of the second topology, Fig. 2.4b, as

$$\begin{aligned} \int \frac{d^d k_1 d^d k_2}{D_1^{n_1} D_2^{n_2} D_3^{n_3} D_4^{n_4} D_5^{n_5}} &= -\pi^d (-2\omega)^{2(d-n_4-n_5)} J(n_1, n_2, n_3, n_4, n_5), \\ D_1 &= (k_1 + \tilde{p}) \cdot v/\omega, \quad D_2 = (k_2 + \tilde{p}) \cdot v/\omega, \quad D_3 = (k_1 + k_2 + \tilde{p}) \cdot v/\omega, \\ D_4 &= -k_1^2, \quad D_5 = -k_2^2. \end{aligned} \quad (2.55)$$

It is symmetric with respect to  $(1 \leftrightarrow 2, 4 \leftrightarrow 5)$ . If  $n_4 \leq 0$ , or  $n_5 \leq 0$ , or two adjacent heavy indices are non-positive, the diagram vanishes. If  $n_3 = 0$ , this diagram is a product of two one-loop diagrams (Fig. 2.4c). If  $n_1 = 0$  or  $n_2 = 0$ , it is a diagram of Fig. 2.4e. When  $n_{1,2,3}$  are all positive, we can insert

$$1 = D_1 + D_2 - D_3$$

into the integrand of (2.55), and obtain

$$J = (\mathbf{1}^- + \mathbf{2}^- - \mathbf{3}^-)J. \quad (2.56)$$

This reduces  $n_1 + n_2 + n_3$  by 1. Therefore, by applying (2.56) sufficiently many times, we can reduce an arbitrary  $J$  integral with integer indices to a combination of integrals with  $n_1 = 0, n_2 = 0, n_3 = 0$ .

Methods of calculation of three-loop HQET propagator diagrams are considered in [8, 2].

## References

1. D.J. Broadhurst, A.G. Grozin: Phys. Lett. B **267**, 105 (1991) **31**
2. K.G. Chetyrkin, A.G. Grozin: Nucl. Phys. B **666**, 289 (2003) **33**
3. K.G. Chetyrkin, F.V. Tkachov: Nucl. Phys. B **192**, 159 (1981) **28, 30**
4. E. Eichten, B. Hill: Phys. Lett. B **234**, 511 (1990) **20**
5. A.F. Falk, M. Neubert, M. Luke: Nucl. Phys. B **388**, 363 (1992) **22**
6. H. Georgi: Phys. Lett. B **240**, 447 (1990) **20**
7. B. Grinstein: Nucl. Phys. B **339**, 253 (1990) **20, 21**
8. A.G. Grozin: JHEP **03**, 013 (2000) **33**
9. N. Isgur, M.B. Wise: Phys. Lett. B **237**, 527 (1990) **21**
10. A.S. Kronfeld: Phys. Rev. D **58**, 051501 (1998) **22**
11. V.A. Smirnov: *Applied Asymptotic Expansions in Momenta and Masses* (Springer, Berlin, Heidelberg 2001) **21**
12. F.V. Tkachov: Phys. Lett. B **100**, 65 (1981) **28**

### 3 Renormalization

In this chapter, we discuss renormalization of HQET at the leading order in  $1/m$ . Most of it is identical to the renormalization of QCD, which is also discussed. The abelian version of HQET (heavy-electron effective theory, Sect. 3.5) has some unique and beautiful features, which are useful for understanding some aspects of renormalization of the real (non-abelian) HQET.

#### 3.1 Renormalization of QCD

The QCD Lagrangian expressed via the bare (unrenormalized) quantities (denoted by the subscript 0) is

$$L = \sum_i \bar{q}_{i0} (\mathrm{i} \not{D}_0 - m_{i0}) q_{i0} - \frac{1}{4} G_{0\mu\nu}^a G_0^{a\mu\nu} - \frac{1}{2a_0} (\partial_\mu A_0^\mu)^2 + (\partial_\mu \bar{c}_0^a)(D_0^\mu c_0^a), \quad (3.1)$$

where  $D_{0\mu} q_0 = (\partial_\mu - \mathrm{i} g_0 A_{0\mu}^a t^a) q_0$ ,  $a_0$  is the gauge-fixing parameter,  $c$  is the ghost field, and  $D_{0\mu} c_0^a = (\partial_\mu \delta^{ab} - g_0 f^{abc} A_\mu^c) c_0^b$ . The renormalized quantities are related to the bare ones by

$$\begin{aligned} q_{i0} &= Z_q^{1/2} q_i, & A_0 &= Z_A^{1/2} A, & c_0 &= Z_c^{1/2} c, \\ g_0 &= Z_\alpha^{1/2} g, & m_{i0} &= Z_m m_i, & a_0 &= Z_A a, \end{aligned} \quad (3.2)$$

where the renormalization factors have the minimal structure

$$Z = 1 + \frac{Z_{11}}{\varepsilon} \frac{\alpha_s}{4\pi} + \left( \frac{Z_{22}}{\varepsilon^2} + \frac{Z_{21}}{\varepsilon} \right) \left( \frac{\alpha_s}{4\pi} \right)^2 + \dots \quad (3.3)$$

It will be explained in Sect. 3.2 why the gauge-fixing parameter  $a$  is renormalized by the same factor  $Z_A$  as the gluon field  $A$ .

The Lagrangian has the dimensionality  $[L] = d$ , because the action  $S = \int L \mathrm{d}^d x$  is exactly dimensionless in a space-time with any  $d$ . The gluon kinetic term, which is the  $g_0^0$  term in  $-(1/4) G_{0\mu\nu}^a G_0^{a\mu\nu}$ , has the structure  $(\partial A_0)^2$ ; hence, the dimensionality of the gluon field is  $[A_0] = d/2 - 1 = 1 - \varepsilon$ . Similarly, from the quark kinetic terms, the dimensionality of the quark fields is  $[q_{i0}] =$

$(d - 1)/2 = 3/2 - \varepsilon$ . The covariant derivative  $D_{0\mu} = \partial_\mu - ig_0 A_{0\mu}^a t^a$  has the dimensionality 1, hence the dimensionality of the coupling constant is  $[g_0] = 2 - d/2 = \varepsilon$ .

We define  $\alpha_s$  to be exactly dimensionless:

$$\frac{\alpha_s(\mu)}{4\pi} = \mu^{-2\varepsilon} \frac{g^2}{(4\pi)^{d/2}} e^{-\gamma\varepsilon} \quad \text{or} \quad \frac{g_0^2}{(4\pi)^{d/2}} = \mu^{2\varepsilon} \frac{\alpha_s(\mu)}{4\pi} Z_\alpha(\alpha_s(\mu)) e^{\gamma\varepsilon}. \quad (3.4)$$

Here  $\mu$  is the renormalization scale, and the factor  $\exp(-\gamma\varepsilon)$  is included for convenience (it allows one to get rid of the Euler constant  $\gamma$  in all equations in the limit  $\varepsilon \rightarrow 0$  when they are written via  $\alpha_s$ ). This renormalization scheme is called  $\overline{\text{MS}}$ . All the bare quantities, including  $g_0$ , are  $\mu$ -independent. By differentiating (3.4), we obtain the renormalization-group equation for  $\alpha_s(\mu)$ :

$$\begin{aligned} \frac{d \log \alpha_s}{d \log \mu} &= -2\varepsilon - 2\beta(\alpha_s), \\ \beta(\alpha_s) &= \frac{1}{2} \frac{d \log Z_\alpha}{d \log \mu} = \beta_0 \frac{\alpha_s}{4\pi} + \beta_1 \left( \frac{\alpha_s}{4\pi} \right)^2 + \dots, \end{aligned} \quad (3.5)$$

where

$$\beta_0 = \frac{11}{3} C_A - \frac{4}{3} T_F n_f, \quad \beta_1 = \frac{34}{3} C_A^2 - 4 C_F T_F n_f - \frac{20}{3} C_A T_F n_f, \quad (3.6)$$

and  $\beta_{2,3}$  are also known [7] (we shall derive  $\beta_0$  in Sect. 4.5). Here  $n_f$  is the number of flavours.

Sometimes it may be convenient to use other definitions of  $\alpha_s(\mu)$  (renormalization schemes). For example, we can define

$$\alpha'_s(\mu) = \alpha_s(\mu f(\varepsilon)) \quad \text{so that} \quad \frac{g_0^2}{(4\pi)^{d/2}} = \mu^{2\varepsilon} \frac{\alpha'_s(\mu)}{4\pi} Z_\alpha(\alpha'_s(\mu)) e^{\gamma\varepsilon} f(\varepsilon)^{2\varepsilon}.$$

This  $\alpha'_s(\mu)$  obeys the same renormalization-group equation (3.5) with the same function  $\beta(\alpha'_s)$ . When a bare physical quantity  $A_0(-p^2)$  is multiplied by the corresponding renormalization constant  $Z^{-1}(\alpha_s(\mu))$ , it becomes finite, with the coefficients of the perturbative series depending on  $L = \log [(-p^2)/\mu^2]$ . If we multiply  $A_0$  by  $Z^{-1}(\alpha'_s(\mu))$ , we obtain the same expression with  $L = \log [(-p^2)/(f(\varepsilon))^2]$ . This expression is also finite at  $\varepsilon \rightarrow 0$ ; hence,  $Z(\alpha'_s)$  is the correct renormalization factor in the new scheme. Therefore, the anomalous dimensions  $\gamma(\alpha_s)$  of  $A$  are the same in both schemes. When a renormalized physical quantity is expressed via  $\alpha_s(\mu)$ , we may take the limit  $\varepsilon \rightarrow 0$  in such expression. Therefore, renormalized results expressed via  $\alpha'_s(\mu)$  coincide with the results expressed via  $\alpha_s(\mu f(0))$ . Such schemes are equivalent to just rescaling  $\mu$ .

We can consider more general redefinitions

$$\frac{\alpha'_s(\mu)}{4\pi} = \frac{\alpha_s(\mu)}{4\pi} \left[ 1 + c_1 \frac{\alpha_s(\mu)}{4\pi} + c_2 \left( \frac{\alpha_s(\mu)}{4\pi} \right)^2 + \dots \right].$$

The term with  $c_1$  can be absorbed by a rescaling of  $\mu$ ; therefore, we shall assume  $c_1 = 0$ . The new  $\alpha'_s(\mu)$  obeys the renormalization-group equation (3.5) with a new  $\beta'(\alpha'_s)$ :

$$\beta'_0 = \beta_0, \quad \beta'_1 = \beta_1, \quad \beta'_2 = \beta_2 + c_2, \dots$$

The first two  $\beta$ -function coefficients  $\beta_{0,1}$  are the same in all mass-independent (or minimal) schemes; the higher coefficients  $\beta_{2,3,\dots}$  can be set to arbitrary values by adjusting the renormalization scheme (i.e., the coefficients  $c_{2,3,\dots}$ ). In this book, we shall always use the  $\overline{\text{MS}}$  scheme.

The information contained in  $Z_\alpha$  is equivalent to that in  $\beta(\alpha_s)$ . Equation (3.5) can be rewritten as

$$\frac{d \log Z_\alpha}{d \log \alpha_s} = -\frac{\beta(\alpha_s)}{\varepsilon + \beta(\alpha_s)} = -\frac{\beta(\alpha_s)}{\varepsilon} + \frac{\beta^2(\alpha_s)}{\varepsilon^2} - \frac{\beta^3(\alpha_s)}{\varepsilon^3} + \dots \quad (3.7)$$

Any minimal renormalization constant (3.3) can be represented as

$$Z = \exp \left( \frac{Z_1}{\varepsilon} + \frac{Z_2}{\varepsilon^2} + \dots \right), \quad (3.8)$$

where  $Z_1$  starts from the order  $\alpha_s$ ,  $Z_2$  starts from  $\alpha_s^2$ , and so on. Then

$$\frac{dZ_{\alpha 1}}{d \log \alpha_s} = -\beta(\alpha_s), \quad \frac{dZ_{\alpha 2}}{d \log \alpha_s} = \beta^2(\alpha_s), \quad \frac{dZ_{\alpha 3}}{d \log \alpha_s} = -\beta^3(\alpha_s), \dots \quad (3.9)$$

and

$$\begin{aligned} Z_{\alpha 1} &= - \int_0^{\alpha_s} \beta(\alpha_s) \frac{d\alpha_s}{\alpha_s} = -\beta_0 \frac{\alpha_s}{4\pi} - \frac{1}{2}\beta_1 \left( \frac{\alpha_s}{4\pi} \right)^2 - \frac{1}{3}\beta_2 \left( \frac{\alpha_s}{4\pi} \right)^3 - \dots, \\ Z_{\alpha 2} &= \int_0^{\alpha_s} \beta^2(\alpha_s) \frac{d\alpha_s}{\alpha_s} = \frac{1}{2}\beta_0^2 \left( \frac{\alpha_s}{4\pi} \right)^2 + \frac{2}{3}\beta_0\beta_1 \left( \frac{\alpha_s}{4\pi} \right)^3 + \dots, \\ Z_{\alpha 3} &= - \int_0^{\alpha_s} \beta^3(\alpha_s) \frac{d\alpha_s}{\alpha_s} = -\frac{1}{3}\beta_0^3 \left( \frac{\alpha_s}{4\pi} \right)^3 - \dots, \\ &\dots \end{aligned} \quad (3.10)$$

Hence, one can obtain  $\beta(\alpha_s)$  from  $Z_1$ , the coefficient of  $1/\varepsilon$  in  $Z_\alpha$ , and vice versa. Higher poles ( $1/\varepsilon^2, 1/\varepsilon^3, \dots$ ) contain no new information; at each order in  $\alpha_s$ , their coefficients ( $Z_2, Z_3, \dots$ ) can be reconstructed from lower-loop results. Up to two loops,

$$Z_\alpha = 1 - \beta_0 \frac{\alpha_s}{4\pi\varepsilon} + \left( \beta_0^2 - \frac{1}{2}\beta_1\varepsilon \right) \left( \frac{\alpha_s}{4\pi\varepsilon} \right)^2 + \dots \quad (3.11)$$

Since  $a_0$  does not depend on  $\mu$ ,  $a(\mu)$  obeys the renormalization-group equation

$$\frac{da(\mu)}{d \log \mu} + \gamma_A(\alpha_s(\mu))a(\mu) = 0, \quad \text{where} \quad \gamma_A = \frac{d \log Z_A}{d \log \mu}. \quad (3.12)$$

For any renormalization constant (3.3), the corresponding anomalous dimension is defined by

$$\gamma(\alpha_s) = \frac{d \log Z}{d \log \mu} = \gamma_0 \frac{\alpha_s}{4\pi} + \gamma_1 \left( \frac{\alpha_s}{4\pi} \right)^2 + \dots \quad (3.13)$$

It is more convenient to present results for anomalous dimensions instead of renormalization constants, because the anomalous dimensions contain the same information but are more compact. If we are considering the renormalization of a gauge-invariant quantity, then  $Z$  does not depend on  $a(\mu)$ , and the only source of its  $\mu$ -dependence is  $\alpha_s(\mu)$ :

$$\frac{d \log Z}{d \log \alpha_s} = -\frac{1}{2} \frac{\gamma(\alpha_s)}{\varepsilon + \beta(\alpha_s)} = -\frac{\gamma(\alpha_s)}{2\varepsilon} + \frac{\beta(\alpha_s)\gamma(\alpha_s)}{2\varepsilon^2} - \frac{\beta^2(\alpha_s)\gamma(\alpha_s)}{2\varepsilon^3} + \dots \quad (3.14)$$

Then

$$\begin{aligned} \frac{dZ_1}{d \log \alpha_s} &= -\frac{1}{2}\gamma(\alpha_s), & \frac{dZ_2}{d \log \alpha_s} &= \frac{1}{2}\beta(\alpha_s)\gamma(\alpha_s), \\ \frac{dZ_3}{d \log \alpha_s} &= -\frac{1}{2}\beta^2(\alpha_s)\gamma(\alpha_s), \dots \end{aligned} \quad (3.15)$$

and

$$\begin{aligned} Z_1 &= -\frac{1}{2} \int_0^{\alpha_s} \gamma(\alpha_s) \frac{d\alpha_s}{\alpha_s} = -\frac{1}{2}\gamma_0 \frac{\alpha_s}{4\pi} - \frac{1}{4}\gamma_1 \left( \frac{\alpha_s}{4\pi} \right)^2 - \frac{1}{6}\gamma_2 \left( \frac{\alpha_s}{4\pi} \right)^3 - \dots, \\ Z_2 &= \frac{1}{2} \int_0^{\alpha_s} \beta(\alpha_s)\gamma(\alpha_s) \frac{d\alpha_s}{\alpha_s} \\ &= \frac{1}{4}\beta_0\gamma_0 \left( \frac{\alpha_s}{4\pi} \right)^2 + \frac{1}{6}(\beta_0\gamma_1 + \beta_1\gamma_0) \left( \frac{\alpha_s}{4\pi} \right)^3 + \dots, \\ Z_3 &= -\frac{1}{2} \int_0^{\alpha_s} \beta^2(\alpha_s)\gamma(\alpha_s) \frac{d\alpha_s}{\alpha_s} = -\frac{1}{6}\beta_0^2\gamma_0 \left( \frac{\alpha_s}{4\pi} \right)^3 - \dots, \\ &\dots \end{aligned} \quad (3.16)$$

When the quantity being considered is gauge-dependent,  $Z$  depends on  $\mu$  via both  $\alpha_s$  and  $a$ :

$$-2(\varepsilon + \beta(\alpha_s)) \frac{\partial \log Z}{\partial \log \alpha_s} - \gamma_A(\alpha_s)a \frac{\partial \log Z}{\partial a} = \gamma(\alpha_s). \quad (3.17)$$

Equating  $\varepsilon^0$  terms, we see that the first equation in (3.15) does not change, and  $Z_1$  is still given by (3.16). Equating  $\varepsilon^{-1}$  terms, we find  $Z_2 = Z_2^{(0)} + \Delta Z_2$ , where  $Z_2^{(0)}$  is given by (3.16) and

$$\Delta Z_2 = -\frac{1}{2} \int_0^{\alpha_s} \gamma_A(\alpha_s) a \frac{\partial Z_1(\alpha_s)}{\partial a} \frac{d\alpha_s}{\alpha_s} = \frac{1}{8} \gamma_{A0} a \frac{d\gamma_0}{da} \left( \frac{\alpha_s}{4\pi} \right)^2 + \dots \quad (3.18)$$

Equating  $\varepsilon^{-2}$  terms, we can find  $\Delta Z_3$ , and so on. Up to two loops, the renormalization constant is

$$Z = 1 - \frac{1}{2} \gamma_0 \frac{\alpha_s}{4\pi\varepsilon} + \frac{1}{8} \left[ \gamma_0 (\gamma_0 + 2\beta_0) + \gamma_{A0} a \frac{d\gamma_0}{da} - 2\gamma_1 \varepsilon \right] \left( \frac{\alpha_s}{4\pi\varepsilon} \right)^2 + \dots \quad (3.19)$$

One can obtain the anomalous dimension  $\gamma(\alpha_s)$  from  $Z_1$ , the coefficient of  $1/\varepsilon$  in  $Z$ , and vice versa. The coefficients  $Z_2, Z_3, \dots$  contain no new information; at each order in  $\alpha_s$ , they can be reconstructed from lower-loop results.

## 3.2 Gluon Propagator

The bare (unrenormalized) gluon propagator  $-iD_{\mu\nu}(p)$  has the structure (Fig. 3.1)

$$\begin{aligned} -iD_{\mu\nu}(p) = & -iD_{\mu\nu}^0(p) + (-i)D_{\mu\alpha}^0(p)i\Pi^{\alpha\beta}(p)(-i)D_{\beta\nu}^0(p) \\ & + (-i)D_{\mu\alpha}^0(p)i\Pi^{\alpha\beta}(p)(-i)D_{\beta\gamma}^0(p)i\Pi^{\gamma\delta}(p)(-i)D_{\gamma\nu}^0(p) \\ & + \dots, \end{aligned} \quad (3.20)$$

where

$$D_{\mu\nu}^0(p) = \frac{1}{p^2} \left[ g_{\mu\nu} - (1 - a_0) \frac{p_\mu p_\nu}{p^2} \right] \quad (3.21)$$

is the free gluon propagator, and the gluon self-energy (polarization operator)  $i\Pi_{\mu\nu}(p)$  is the sum of one-particle-irreducible gluon self-energy diagrams (which cannot be separated into two disconnected parts by cutting a single gluon line). The series (3.20) implies the equation

$$D_{\mu\nu}(p) = D_{\mu\nu}^0(p) + D_{\mu\alpha}^0(p)\Pi^{\alpha\beta}(p)D_{\beta\nu}(p). \quad (3.22)$$

To solve this equation, it is convenient to introduce the inverse tensor  $A_{\mu\nu}^{-1}$  of a symmetric tensor  $A^{\mu\nu}$  satisfying  $A_{\mu\alpha}^{-1} A^{\alpha\nu} = \delta_\mu^\nu$ . If

$$A_{\mu\nu} = A_\perp \left( g_{\mu\nu} - \frac{p_\mu p_\nu}{p^2} \right) + A_{||} \frac{p_\mu p_\nu}{p^2},$$



**Fig. 3.1.** Structure of diagrams for the gluon propagator

then

$$A_{\mu\nu}^{-1} = A_{\perp}^{-1} \left( g_{\mu\nu} - \frac{p_\mu p_\nu}{p^2} \right) + A_{||}^{-1} \frac{p_\mu p_\nu}{p^2}.$$

Using this notation, the equation (3.22) can be rewritten as

$$D_{\mu\nu}^{-1}(p) = (D^0)_{\mu\nu}^{-1}(p) - \Pi_{\mu\nu}(p). \quad (3.23)$$

Owing to the Ward identity  $\Pi_{\mu\nu}(p)p^\nu = 0$ , the gluon self-energy is transverse:

$$\Pi_{\mu\nu}(p) = (p^2 g_{\mu\nu} - p_\mu p_\nu) \Pi(p^2). \quad (3.24)$$

Therefore, the gluon propagator is

$$D_{\mu\nu}(p) = \frac{1}{p^2(1 - \Pi(p^2))} \left( g_{\mu\nu} - \frac{p_\mu p_\nu}{p^2} \right) + a_0 \frac{p_\mu p_\nu}{(p^2)^2}. \quad (3.25)$$

Its longitudinal part acquires no corrections. The renormalized gluon propagator is related to the bare propagator by  $D_{\mu\nu}(p) = Z_A(\mu) D_{\mu\nu}^r(p; \mu)$ . The gluon field renormalization constant  $Z_A$  is constructed to make the transverse part of  $D_{\mu\nu}^r(p; \mu)$  finite in the limit  $\varepsilon \rightarrow 0$ :

$$D_{\mu\nu}^r(p; \mu) = D_{\perp}^r(p^2; \mu) \left( g_{\mu\nu} - \frac{p_\mu p_\nu}{p^2} \right) + a(\mu) \frac{p_\mu p_\nu}{(p^2)^2}. \quad (3.26)$$

At the same time, it converts  $a_0$  to the renormalized gauge parameter  $a(\mu)$ . This is the reason why the gauge parameter is renormalized (3.2) by the same constant  $Z_A$ .

In the one-loop approximation (Fig. 3.2), we can use the methods of Sect. 2.2 to obtain

$$\begin{aligned} \Pi(p^2) &= \frac{g_0^2 (-p^2)^{-\varepsilon}}{(4\pi)^{d/2}} \frac{G_1}{(d-1)(d-3)(d-4)} \\ &\times \left[ \left( -3d + 2 - (d-1)(2d-7)\xi + \frac{1}{4}(d-1)(d-4)\xi^2 \right) C_A \right. \\ &\quad \left. + 4(d-2)T_F n_f \right], \end{aligned} \quad (3.27)$$

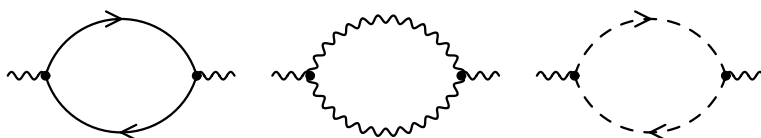


**Fig. 3.2.** One-loop gluon self-energy

where  $G_1$  is defined in (2.41) and  $\xi = 1 - a_0$ . When dealing with higher-loop diagrams, it is often convenient to calculate a diagram with a quark-loop insertion, and then to incorporate the other two insertions in Fig. 3.2 by means of replacing  $T_F n_f$  with

$$P = T_F n_f - \frac{3d - 2 + (d-1)(2d-7)\xi - (1/4)(d-1)(d-4)\xi^2}{4(d-2)} C_A . \quad (3.28)$$

Now we re-express the one-loop propagator

$$p^2 D_\perp(p^2) = \frac{1}{1 - \Pi(p^2)} = 1 + \Pi(p^2)$$

via the renormalized quantities  $\alpha_s(\mu)$ ,  $a(\mu)$  instead of the bare ones  $g_0^2$ ,  $a_0$ . These quantities only appear in the  $\alpha_s$ -correction, and we may omit the  $\alpha_s$  terms in them:

$$\frac{g_0^2}{(4\pi)^{d/2}} = e^{\gamma\varepsilon} \mu^{2\varepsilon} \frac{\alpha_s(\mu)}{4\pi}, \quad a_0 = a(\mu).$$

We expand the result in  $\varepsilon$  using

$$\Gamma(1+\varepsilon) = \exp \left[ -\gamma\varepsilon + \sum_{n=2}^{\infty} \frac{(-1)^n \zeta_n}{n} \varepsilon^n \right], \quad (3.29)$$

where

$$\zeta_n = \sum_{k=1}^{\infty} \frac{1}{k^n}, \quad \zeta_2 = \frac{\pi^2}{6}, \quad \zeta_3 \approx 1.202, \quad \zeta_4 = \frac{\pi^4}{90}, \quad \dots \quad (3.30)$$

is the Riemann  $\zeta$ -function. The Euler constant  $\gamma$  cancels, and we arrive at

$$\begin{aligned} p^2 D_\perp(p^2) &= 1 + \frac{\alpha_s}{4\pi\varepsilon} e^{-L\varepsilon} \left[ -\frac{1}{2} \left( a - \frac{13}{3} \right) C_A - \frac{4}{3} T_F n_f \right. \\ &\quad \left. + \left( \frac{9a^2 + 18a + 97}{36} C_A - \frac{20}{9} T_F n_f \right) \varepsilon + \dots \right], \end{aligned}$$

$$L = \log \frac{-p^2}{\mu^2}.$$

This should be equal to  $Z_A(\alpha_s(\mu), a(\mu)) p^2 D_\perp^r(p^2; \mu)$ , where the renormalization constant  $Z_A(\alpha_s, a)$  has the minimal form (3.3), and the renormalized propagator  $D_\perp^r(p^2; \mu)$  is finite at  $\varepsilon \rightarrow 0$ . We obtain

$$Z_A(\alpha_s, a) = 1 - \frac{\alpha_s}{4\pi\varepsilon} \left[ \frac{1}{2} \left( a - \frac{13}{3} \right) C_A + \frac{4}{3} T_F n_f \right], \quad (3.31)$$

$$\begin{aligned} p^2 D_\perp^r(p^2; \mu) &= 1 + \frac{\alpha_s}{4\pi} \left[ \frac{9a^2 + 18a + 97}{36} C_A - \frac{20}{9} T_F n_f \right. \\ &\quad \left. + \frac{1}{2} \left( \left( a - \frac{13}{3} \right) C_A - \frac{8}{3} T_F n_f \right) L \right]. \end{aligned} \quad (3.32)$$

Using (3.19), we arrive at the anomalous dimension of the gluon field at one loop,

$$\gamma_A = \left[ \left( a - \frac{13}{3} \right) C_A + \frac{8}{3} T_F n_f \right] \frac{\alpha_s}{4\pi} + \dots \quad (3.33)$$

The dependence of the renormalized propagator  $D_\perp^r(p^2; \mu)$  (3.32) on  $\mu$  (or  $L$ ) is determined by the renormalization-group equation

$$\frac{dD_\perp^r(p^2; \mu)}{dL} = \frac{1}{2} \gamma_A(\alpha_s(\mu), a(\mu)) D_\perp^r(p^2; \mu). \quad (3.34)$$

Therefore, the coefficient of  $L$  in (3.32) is just  $\gamma_{A0}/2$ . It is enough to know the initial condition  $D_\perp^r(p^2; \mu^2 = -p^2)$  in order to reconstruct  $D_\perp^r(p^2; \mu)$  from (3.34).

It is straightforward to calculate  $\Pi(p^2)$  at two loops (Fig. 3.3) by the methods of Sect. 2.4 using any suitable computer algebra system. The utmost attention to detail is required: do not forget mirror-symmetric diagrams if needed; include symmetry factors and minus signs for quark and ghost loops; use consistent leg orderings for the colour and Lorentz parts of three-gluon

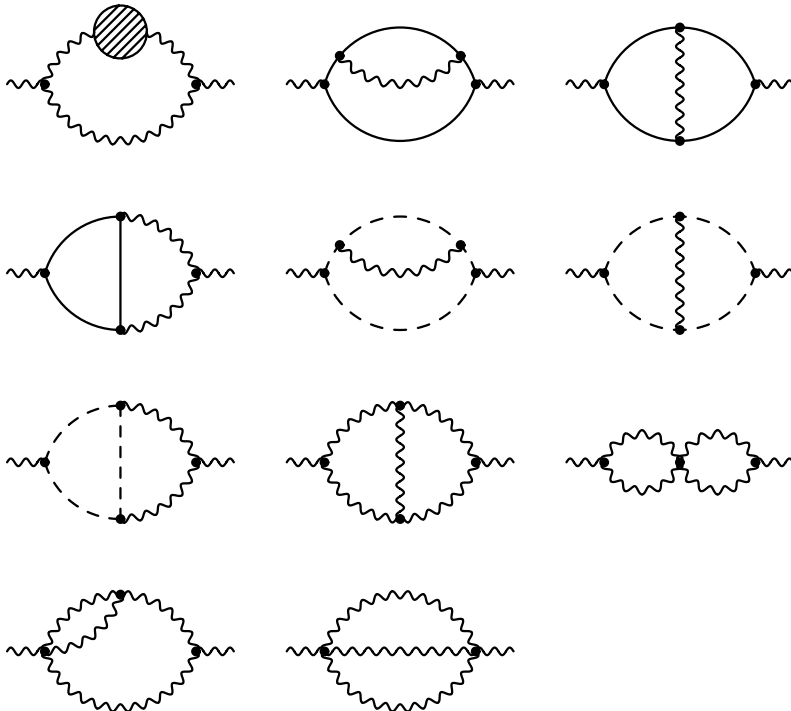


**Fig. 3.3.** Two-loop gluon self-energy

vertices; be careful while decomposing four-gluon vertices into three terms with different colour structures. Every perturbative-QCD practitioner has performed this tedious calculation at least once, because the result is often needed for higher loops. Here is the result, for reference:

$$\begin{aligned}
\Pi_2 = & \frac{g_0^4(-p^2)^{-2\varepsilon}}{(4\pi)^d} \left\{ C_A^2 \left[ \left( -2(d^2 - 4d - 2) - (6d^3 - 51d^2 + 120d - 56)\xi \right. \right. \right. \\
& - 2(d-1)(d-4)(2d^2 - 14d + 25)\xi^2 + \frac{1}{8}(d-1)(d-4)^2(8d-27)\xi^3 \\
& - \frac{1}{16}(d-1)(d-4)^3\xi^4 \Big) J_1 \\
& + \left( 2(3d^5 - 59d^4 + 376d^3 - 1084d^2 + 1648d - 1248) \right. \\
& - 2(43d^4 - 475d^3 + 1764d^2 - 2388d + 656)\xi \\
& + \frac{1}{2}(d-4)(3d-8)(9d^4 - 118d^3 + 547d^2 - 1034d + 608)\xi^2 \\
& \left. \left. \left. - \frac{1}{4}(d-1)(d-4)^2(3d-8)(d^2 - 9d + 22)\xi^3 \right) J_2 \right] \\
& + C_F T_F n_f 8(d-2) [-(d^2 - 7d + 16)J_1 + 4(d-3)(d-6)(d^2 - 4d + 8)J_2] \\
& + C_A T_F n_f 2(d-2) \left[ (2(d^2 - 5d + 8) + 2(d-4)(4d-13)\xi - (d-4)^2\xi^2)J_1 \right. \\
& - 4(d^4 - 5d^3 - 56d^2 + 364d - 528 \\
& \left. \left. \left. + (d-4)(3d-8)(3d^2 - 27d + 56)\xi)J_2 \right] \right\} \tag{3.35}
\end{aligned}$$

where

$$\begin{aligned}
J_1 &= \frac{G_1^2}{(d-1)(d-3)^2(d-4)^3}, \\
J_2 &= \frac{G_2}{(d-1)(d-3)(d-4)^3(d-6)(3d-8)(3d-10)}
\end{aligned}$$

(see (2.41)).

The gluon propagator with two-loop accuracy,

$$p^2 D_\perp(p^2) = \frac{1}{1 - \Pi(p^2)} = 1 + \Pi_1(p^2) + \Pi_1^2(p^2) + \Pi_2(p^2),$$

has the form

$$p^2 D_\perp(p^2) = 1 + \frac{g_0^2(-p^2)^{-\varepsilon}}{(4\pi)^{d/2}} f_1(a_0) + \frac{g_0^4(-p^2)^{-2\varepsilon}}{(4\pi)^d} f_2(a_0).$$

Now we are going to re-express it via the renormalized quantities  $\alpha_s(\mu)$  and  $a(\mu)$ . In the one-loop term, we have to use the expressions including one-loop corrections,

$$\frac{g_0^2}{(4\pi)^{d/2}} = e^{\gamma\varepsilon} \mu^{2\varepsilon} \frac{\alpha_s(\mu)}{4\pi} \left(1 - \beta_0 \frac{\alpha_s}{4\pi\varepsilon}\right), \quad a_0 = a(\mu) \left(1 - \frac{1}{2} \gamma_{A0} \frac{\alpha_s}{4\pi\varepsilon}\right),$$

and we obtain

$$\begin{aligned} p^2 D_\perp(p^2) &= 1 \\ &+ \frac{\alpha_s(\mu)}{4\pi\varepsilon} e^{-L\varepsilon} \left(1 - \beta_0 \frac{\alpha_s}{4\pi\varepsilon}\right) \varepsilon e^{\gamma\varepsilon} \left(f_1(a(\mu)) - \frac{1}{2} \gamma_{A0} \frac{\alpha_s}{4\pi\varepsilon} a \frac{df_1(a)}{da}\right) \\ &+ \left(\frac{\alpha_s}{4\pi\varepsilon}\right)^2 e^{-2L\varepsilon} \varepsilon^2 e^{2\gamma\varepsilon} f_2(a). \end{aligned} \quad (3.36)$$

For simplicity, we set  $\mu^2 = -p^2$ , i.e.,  $L = 0$ :

$$\begin{aligned} p^2 D_\perp(p^2) &= 1 + \frac{\alpha_s(\mu)}{4\pi\varepsilon} (c_{10} + c_{11}\varepsilon + c_{12}\varepsilon^2 + \dots) \\ &+ \left(\frac{\alpha_s}{4\pi\varepsilon}\right)^2 \left[ c_{20} + c_{21}\varepsilon + c_{22}\varepsilon^2 + \dots \right. \\ &\quad \left. - \left(\beta_0 + \frac{1}{2} \gamma_{A0} a \frac{d}{da}\right) (c_{10} + c_{11}\varepsilon + c_{12}\varepsilon^2 + \dots) \right], \end{aligned}$$

where the expansions

$$\begin{aligned} \varepsilon e^{\gamma\varepsilon} f_1(a) &= c_{10} + c_{11}\varepsilon + c_{12}\varepsilon^2 + \dots, \\ \varepsilon^2 e^{2\gamma\varepsilon} f_2(a) &= c_{20} + c_{21}\varepsilon + c_{22}\varepsilon^2 + \dots, \end{aligned} \quad (3.37)$$

can be easily calculated using (3.29). This bare propagator must be equal to  $Z_A(\alpha_s(\mu)) D_\perp^r(p^2; \mu)$  at  $\mu^2 = -p^2$ , where

$$\begin{aligned} Z_A(\alpha_s) &= 1 + \frac{\alpha_s}{4\pi\varepsilon} z_1 + \left(\frac{\alpha_s}{4\pi\varepsilon}\right)^2 (z_{20} + z_{21}\varepsilon), \\ p^2 D_\perp^r(p^2; \mu^2 = -p^2) &= 1 + \frac{\alpha_s(\mu)}{4\pi} (r_1 + r_{11}\varepsilon + \dots) + \left(\frac{\alpha_s}{4\pi}\right)^2 (r_2 + \dots) \end{aligned}$$

(because  $D_\perp^r(p^2; \mu)$  must be finite at  $\varepsilon \rightarrow 0$ ). Equating the coefficients of the powers of  $\varepsilon$  in the  $\alpha_s$  term, we obtain

$$z_1 = c_{10}, \quad r_1 = c_{11}, \quad r_{11} = c_{12}.$$

Using this and equating the coefficients in the  $\alpha_s^2$  term, we obtain

$$\begin{aligned} z_{20} &= c_{20} - \left(\beta_0 + \frac{1}{2} \gamma_{A0} a \frac{d}{da}\right) c_{10}, \\ z_{21} &= c_{21} - \left(c_{10} + \beta_0 + \frac{1}{2} \gamma_{A0} a \frac{d}{da}\right) c_{11}, \\ r_2 &= c_{22} - \left(c_{10} + \beta_0 + \frac{1}{2} \gamma_{A0} a \frac{d}{da}\right) c_{12}. \end{aligned}$$

The renormalization constant should have the structure (3.19). Therefore, the leading coefficient of the two-loop term must satisfy the self-consistency condition

$$c_{20} = \frac{1}{2} \left( c_{10} + \beta_0 + \frac{1}{2} \gamma_{A0} a \frac{d}{da} \right) c_{10}. \quad (3.38)$$

When calculating the expansions (3.37) for the gluon propagator, it is convenient to use

$$\frac{G_2}{G_1^2} = 1 - 6\zeta_3 \varepsilon^3 + \dots \quad (3.39)$$

We see that the condition (3.38) is indeed satisfied; the gluon field anomalous dimension is

$$\begin{aligned} \gamma_A = & \left[ \left( a - \frac{13}{3} \right) C_A + \frac{8}{3} T_F n_f \right] \frac{\alpha_s}{4\pi} \\ & + \left[ \frac{2a^2 + 11a - 59}{4} C_A^2 + 2(4C_F + 5C_A) T_F n_f \right] \left( \frac{\alpha_s}{4\pi} \right)^2 + \dots \end{aligned} \quad (3.40)$$

(see [5] for the three-loop result), and the renormalized propagator at  $\mu^2 = -p^2$  is

$$\begin{aligned} p^2 D_\perp^r(p^2; \mu^2 = -p^2) = & 1 + \left( \frac{9a^2 + 18a + 97}{36} C_A - \frac{20}{9} T_F n_f \right) \frac{\alpha_s(\mu)}{4\pi} \\ & + \left[ \left( (2a - 3)\zeta_3 + \frac{810a^3 + 2430a^2 + 2817a + 83105}{2592} \right) C_A^2 \right. \\ & \left. + \left( 16\zeta_3 - \frac{55}{3} \right) C_F T_F n_f - \left( 8\zeta_3 + \frac{360a + 8659}{324} \right) C_A T_F n_f \right] \left( \frac{\alpha_s}{4\pi} \right)^2. \end{aligned}$$

The propagator for an arbitrary  $\mu$  can be found by solving the renormalization-group equation (3.34) (this will be discussed in Sect. 4.6). Alternatively, we can multiply (3.36) by  $Z_A^{-1}(\mu)$ ; the result is finite for all  $\mu$ , owing to (3.38).

### 3.3 Quark Propagator

The bare (unrenormalized) quark propagator  $iS(p)$  has the structure (Fig. 3.4)

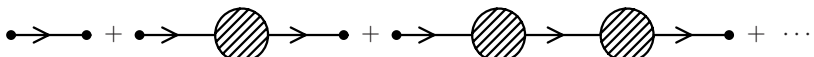


**Fig. 3.4.** Structure of diagrams for the quark propagator

$$\begin{aligned} iS(p) &= iS_0(p) + iS_0(p)(-i)\Sigma(p)iS_0(p) \\ &\quad + iS_0(p)(-i)\Sigma(p)iS_0(p)(-i)\Sigma(p)iS_0(p) + \dots, \end{aligned} \quad (3.41)$$

where

$$S_0(p) = \frac{1}{\not{p} - m_0} = \frac{\not{p} + m_0}{\not{p}^2 - m_0^2} \quad (3.42)$$

is the free quark propagator, and the quark self-energy (mass operator)  $-i\Sigma(p)$  is the sum of one-particle-irreducible quark self-energy diagrams (which cannot be separated into two disconnected parts by cutting a single quark line). The series (3.41) implies the equation

$$S(p) = S_0(p) + S_0(p)\Sigma(p)S(p), \quad (3.43)$$

with the solution

$$S(p) = \frac{1}{S_0^{-1}(p) - \Sigma(p)} = \frac{1}{\not{p} - m_0 - \Sigma(p)}. \quad (3.44)$$

The quark self-energy has the structure

$$\Sigma(p) = \not{p}\Sigma_V(p^2) + m_0\Sigma_S(p^2). \quad (3.45)$$

Therefore, the quark propagator is

$$S(p) = \frac{1}{1 - \Sigma_V(p^2)} \frac{1}{\not{p} - (1 - \Sigma_V(p^2))^{-1}(1 + \Sigma_S(p^2))m_0} = Z_q S_r(p; \mu), \quad (3.46)$$

and the renormalization constants  $Z_q$ ,  $Z_m$  are constructed to make  $Z_q(1 - \Sigma_V)$  and  $Z_m Z_q(1 + \Sigma_S)$  finite.

For a massless quark in the one-loop approximation (Fig. 3.5),

$$\Sigma_V(p^2) = C_F \frac{g_0^2(-p^2)^{-\varepsilon}}{(4\pi)^{d/2}} \frac{d-2}{(d-3)(d-4)} G_1 a_0. \quad (3.47)$$

The one-loop self-energy vanishes in the Landau gauge  $a_0 = 0$ . Now we re-express the one-loop propagator  $\not{p}S(p) = 1/[1 - \Sigma_V(p^2)]$  via the renormalized quantities  $\alpha_s(\mu)$ ,  $a(\mu)$  and expand it in  $\varepsilon$ :

$$\not{p}S(p) = 1 - C_F \frac{\alpha_s}{4\pi\varepsilon} e^{-L\varepsilon} a(1 + \varepsilon + \dots).$$



**Fig. 3.5.** One-loop quark self-energy

Therefore,

$$Z_q(\alpha_s, a) = 1 - C_F a \frac{\alpha_s}{4\pi\varepsilon}, \quad (3.48)$$

$$\not{p} S_r(p; \mu) = 1 + C_F a (L - 1) \frac{\alpha_s}{4\pi}. \quad (3.49)$$

The anomalous dimension of the quark field at one loop is

$$\gamma_q = 2C_F a \frac{\alpha_s}{4\pi} + \dots \quad (3.50)$$

UV divergences do not depend on masses; therefore, this result is also valid for a massive quark. The coefficient of  $L$  in (3.49) is just  $\gamma_{q0}/2$ , as required by the renormalization-group equation.

Let us also rederive this result in the coordinate space. Transforming the gluon propagator (3.21) to  $x$ -space (2.19), we obtain

$$D_{\mu\nu}^0(x) = \frac{i\Gamma(d/2 - 1)}{8\pi^{d/2}} \frac{(1 + a_0)x^2 g_{\mu\nu} + (d - 2)(1 - a_0)x_\mu x_\nu}{(-x^2 + i0)^{d/2}}. \quad (3.51)$$

Similarly, the propagator (3.42) for a massless quark ( $m = 0$ ) becomes

$$S_0(x) = \frac{\Gamma(d/2)}{2\pi^{d/2}} \frac{\not{x}}{(-x^2 + i0)^{d/2}}. \quad (3.52)$$

The one-loop light-quark self-energy (Fig. 3.5) is

$$\Sigma(x) = -iC_F g_0^2 \gamma^\mu S_0(x) \gamma^\nu D_{\mu\nu}^0(x) = C_F g_0^2 a_0 \frac{\Gamma^2(d/2)}{4\pi^d} \frac{\not{x}}{(-x^2 + i0)^{d-1}}. \quad (3.53)$$

Transforming it to  $p$ -space (2.20), we recover (3.47).

Two-loop diagrams for the quark self-energy are shown in Fig. 3.6. The first one contains the one-loop gluon self-energy (3.27); it can be easily calculated using (2.18), and is proportional to  $G_2$  (2.41) and  $P$  (3.28):

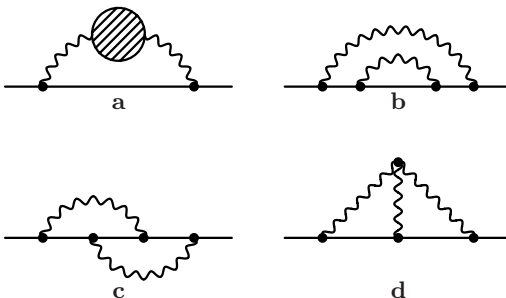


**Fig. 3.6.** Two-loop quark self-energy

$$\Sigma_{V2a}(p^2) = C_F \frac{g_0^4 (-p^2)^{-2\varepsilon}}{(4\pi)^d} \frac{8(d-2)^2 G_2}{(d-3)(d-4)(d-6)(3d-8)(3d-10)} P. \quad (3.54)$$

The second one is also recursively one-loop; it is proportional to  $C_F^2 G_2$ . It is also not difficult to understand its dependence on the gauge parameter  $a_0$ . The quark propagator with the one-loop correction inside the exterior loop is proportional to  $(k+p)/[-(k+p)^2]^n$  with  $n = 1 + \varepsilon$ . The resulting integral is proportional to  $\not{p}$ , and we may take  $(1/4)\text{Tr}$  of the numerator with  $\not{p}/p^2$  to find the coefficient. Substituting the gluon propagator, we see that the exterior loop integral is proportional to

$$\begin{aligned} & (d-3+a_0)[G(1,n)+G(1,n-1)] \\ & + (1-a_0)[G(2,n)-2G(2,n-1)+G(2,n-2)] \\ & = a_0 \frac{(d-2)(d-2n)}{d-n-1} G(1,n). \end{aligned}$$

The same is true for the interior gluon line, with  $n = 1$ , as in the one-loop case (3.47). Therefore, the result contains  $a_0^2$ :

$$\Sigma_{V2b}(\omega) = C_F^2 \frac{g_0^4 (-p^2)^{-2\varepsilon}}{(4\pi)^d} \frac{4(d-2)^2 G_2}{(d-4)^2(3d-8)(3d-10)} a_0^2. \quad (3.55)$$

The colour factor of the third diagram can be easily found using the Cvitanović algorithm [4] (Fig. 3.7). The gluon exchange between two quark lines is replaced by exchange by a quark–antiquark pair, minus a colourless exchange which compensates its colour-singlet part. The correctness of the coefficients in this identity can be checked by closing the upper quark line, and closing it with a gluon attached (Fig. 3.8). Two example applications of this algorithm are shown in Fig. 3.9: the first one is a calculation of  $C_F$ , and the second one shows that the colour factor of the diagram Fig. 3.6c is  $-C_F/(2N_c) = C_F(C_F - C_A/2)$ . The colour factor of the three-gluon vertex  $if^{abc}$  is defined via the commutator  $[t^a, t^b] = if^{abc}t^c$  (Fig. 3.10). Therefore, the colour factor of the diagram Fig. 3.6d is the difference between those of Fig. 3.6b and Fig. 3.6c,  $C_F C_A/2$ .

The diagrams in Fig. 3.6c,d can be calculated using the methods of Sect. 2.4. Collecting all the contributions, we obtain

$$\begin{aligned} \Sigma_{V2} &= C_F \frac{g_0^4 (-p^2)^{-2\varepsilon}}{(4\pi)^d} (d-2) \left\{ C_F \left[ -((d-2)a_0^2 + d-6) J_1 \right. \right. \\ &+ 2(d-3)(d-6)((3d-8)a_0^2 - d-4) J_2 \Big] \\ &+ \frac{C_A}{d-4} \left[ (-2(d-3)a_0 + d^2 - 10d + 22) J_1 \right. \end{aligned}$$

$$= \frac{1}{2} \left[ \text{diagram with gluon loop and gluon line} - \frac{1}{N_c} \text{diagram with gluon line} \right]$$

**Fig. 3.7.** Cvitanović algorithm

$$= \frac{1}{2} \left[ \text{diagram with gluon loop and gluon line} - \frac{1}{N_c} \text{diagram with gluon line} \right] = 0$$

$$= \frac{1}{2} \left[ \text{diagram with gluon loop and gluon line} - \frac{1}{N_c} \text{diagram with gluon line} \right] = \frac{1}{2} \text{diagram with gluon line}$$

**Fig. 3.8.** Checking the coefficients

$$= \frac{1}{2} \left[ \text{diagram with gluon loop and gluon line} - \frac{1}{N_c} \text{diagram with gluon line} \right]$$

$$= \frac{N_c^2 - 1}{2N_c} \text{diagram with gluon line}$$

$$= \frac{1}{2} \left[ \text{diagram with gluon loop and gluon line} - \frac{1}{N_c} \text{diagram with gluon line} \right]$$

$$= -\frac{1}{2N_c} \text{diagram with gluon line}$$

**Fig. 3.9.** Sample applications of Cvitanović algorithm

$$= \text{diagram with gluon loop and gluon line} - \text{diagram with gluon loop and gluon line}$$

**Fig. 3.10.** Three-gluon vertex; the curved arrow shows the order of indices in  $if^{abc}$

$$\begin{aligned}
& + \left. \left( -\frac{1}{2}(d-4)(3d-8)(d^2-9d+16)(1-a_0)^2 \right. \right. \\
& \quad \left. \left. - 2(d-5)(3d-8)^2(1-a_0) + 2(9d^3 - 114d^2 + 440d - 544) \right) J_2 \right] \\
& + T_F n_f 8(d-2)(d-4) J_2 \Big\} , \tag{3.56}
\end{aligned}$$

where

$$\begin{aligned}
J_1 &= \frac{G_1^2}{(d-3)^2(d-4)^2} , \\
J_2 &= \frac{G_2}{(d-3)(d-4)^2(d-6)(3d-8)(3d-10)}
\end{aligned}$$

(see (2.41)). Now we expand the  $\not{p}S(p) = [1 - \Sigma_V]^{-1}$  to  $g_0^4$  and follow the same procedure as in Sect. 3.2. The self-consistency condition (3.38) is satisfied, the quark field anomalous dimension is

$$\gamma_q = 2C_F a \frac{\alpha_s}{4\pi} + C_F \left( -3C_F + \frac{a^2 + 8a + 25}{2} C_A - 4T_F n_f \right) \left( \frac{\alpha_s}{4\pi} \right)^2 + \dots \tag{3.57}$$

(see [3] for the four-loop result), and the renormalized massless-quark propagator at  $\mu^2 = -p^2$  is

$$\begin{aligned}
\not{p}S_r(p; \mu^2 = -p^2) &= 1 - C_F a(\mu) \frac{\alpha_s(\mu)}{4\pi} \\
& + C_F \left[ \left( a^2 + \frac{5}{8} \right) C_F + \left( 3(a+1)\zeta_3 - \frac{9a^2 + 52a + 82}{8} \right) C_A \right. \\
& \quad \left. + \frac{7}{2} T_F n_f \right] \left( \frac{\alpha_s}{4\pi} \right)^2 .
\end{aligned}$$

### 3.4 Renormalization of HQET

The HQET Lagrangian expressed via the bare (unrenormalized) quantities is

$$L = \overline{\tilde{Q}}_0 i v \cdot D_0 \tilde{Q}_0 + L_{\text{QCD}}, \quad \tilde{Q}_0 = \tilde{Z}_Q^{1/2} \tilde{Q}. \tag{3.58}$$

All the renormalization constants in (3.2) are the same as in QCD, where the heavy flavour  $Q$  is not counted in  $n_f$ . In order to find the new constant  $\tilde{Z}_Q$ , we need to calculate the heavy-quark propagator in HQET.

The bare (unrenormalized) static-quark propagator  $i\tilde{S}(\omega)$  has the structure (Fig. 3.11)

$$\begin{aligned} i\tilde{S}(\omega) &= i\tilde{S}_0(\omega) + i\tilde{S}_0(\omega)(-i)\tilde{\Sigma}(\omega)i\tilde{S}_0(\omega) \\ &\quad + i\tilde{S}_0(\omega)(-i)\tilde{\Sigma}(\omega)i\tilde{S}_0(\omega)(-i)\tilde{\Sigma}(\omega)i\tilde{S}_0(\omega) + \dots \end{aligned} \quad (3.59)$$

where  $\tilde{S}_0(\omega) = 1/\omega$  is the free HQET propagator, and the static quark self-energy (mass operator)  $-i\tilde{\Sigma}(\omega)$  is the sum of one-particle-irreducible HQET self-energy diagrams (which cannot be separated into two disconnected parts by cutting a single heavy-quark line). Summing this series, we obtain

$$\tilde{S}(\omega) = \frac{1}{\omega - \tilde{\Sigma}(\omega)}. \quad (3.60)$$

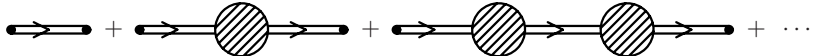


**Fig. 3.11.** Structure of diagrams for the heavy quark propagator in HQET

In the one-loop approximation (Fig. 3.12),

$$\tilde{\Sigma}(\omega) = iC_F \int \frac{d^d k}{(2\pi)^d} ig_0 v^\mu \frac{i}{k \cdot v + \omega} ig_0 v^\nu \frac{-i}{k^2} \left( g_{\mu\nu} - (1 - a_0) \frac{k_\mu k_\nu}{k^2} \right).$$

After contraction over the indices, the second term in the brackets contains  $(k \cdot v)^2 = (k \cdot v + \omega - \omega)^2$ . This factor can be replaced by  $\omega^2$ , because all integrals without  $k \cdot v + \omega$  in the denominator are scale-free and hence vanish. Using the definition (2.27), we obtain

$$\tilde{\Sigma}(\omega) = C_F \frac{g_0^2 (-2\omega)^{1-2\varepsilon}}{(4\pi)^{d/2}} \left[ 2I(1,1) + \frac{1}{2}(1-a_0)I(1,2) \right],$$

and, finally,

$$\tilde{\Sigma}(\omega) = -C_F \frac{g_0^2 (-2\omega)^{1-2\varepsilon}}{(4\pi)^{d/2}} \frac{I_1}{d-4} A, \quad A = a_0 - 1 - \frac{2}{d-3}, \quad (3.61)$$

where  $I_1$  is defined in (2.54).



**Fig. 3.12.** One-loop heavy quark self-energy in HQET

Let us also rederive this result in the coordinate space. Using the heavy-quark propagator (2.3) and the gluon propagator (3.51), we obtain

$$\begin{aligned}\tilde{\Sigma}(x) &= -C_F g_0^2 D_{\mu\nu}^0(vt)v^\mu v^\nu \theta(t) \\ &= -i C_F g_0^2 \frac{\Gamma(d/2-1)}{8\pi^{d/2}}(d-3)A(it)^{2-d}\theta(t).\end{aligned}\quad (3.62)$$

Transforming this to  $p$ -space (2.29), we recover (3.61).

Therefore, with one-loop accuracy, the heavy-quark propagator in HQET is

$$\omega \tilde{S}(\omega) = 1 + C_F \frac{g_0^2 (-2\omega)^{-2\varepsilon}}{(4\pi)^{d/2}} \frac{I_1}{d-4} 2A.\quad (3.63)$$

In the coordinate space,

$$\tilde{S}(t) = \tilde{S}_0(t) \left[ 1 + C_F \frac{g_0^2 (it/2)^{2\varepsilon}}{(4\pi)^{d/2}} \Gamma(-\varepsilon) A + \dots \right], \quad \tilde{S}_0(t) = -i\theta(t). \quad (3.64)$$

Now we re-express  $\tilde{S}$  via the renormalized quantities  $\alpha_s(\mu)$ ,  $a(\mu)$ . Expanding the result in  $\varepsilon$  up to the finite term, we obtain

$$\omega \tilde{S}(\omega) = 1 + C_F \frac{\alpha_s(\mu)}{4\pi\varepsilon} e^{-2L\varepsilon} (3 - a(\mu) + 4\varepsilon), \quad \text{where } L = \log \frac{-2\omega}{\mu}.$$

This should be equal to  $\tilde{Z}_Q(\alpha_s(\mu), a(\mu))\omega \tilde{S}_r(\omega; \mu)$ , where the renormalization constant  $\tilde{Z}_Q(\alpha_s, a)$  has the minimal form (3.3), and the renormalized propagator  $\tilde{S}_r(\omega; \mu)$  is finite at  $\varepsilon \rightarrow 0$ . We obtain

$$\tilde{Z}_Q(\alpha_s, a) = 1 + C_F \frac{\alpha_s}{4\pi\varepsilon} (3 - a), \quad (3.65)$$

$$\omega \tilde{S}_r(\omega; \mu) = 1 + C_F \frac{\alpha_s(\mu)}{4\pi} 2[(a(\mu) - 3)L + 2]. \quad (3.66)$$

Using (3.19), we arrive at the anomalous dimension

$$\tilde{\gamma}_Q = 2C_F(a - 3) \frac{\alpha_s}{4\pi} + \dots \quad (3.67)$$

Note that there is no UV divergence in the Yennie gauge  $a = 3$ . The dependence of the renormalized propagator  $\tilde{S}_r(\omega; \mu)$  (3.66) on  $\mu$  (or  $L$ ) is determined by the renormalization-group equation

$$\frac{d\tilde{S}_r(\omega; \mu)}{dL} = \tilde{\gamma}_Q(\alpha_s(\mu), a(\mu))\tilde{S}_r(\omega; \mu). \quad (3.68)$$

Therefore, the coefficient of  $L$  in (3.66) is just  $\tilde{\gamma}_{Q0}$ . It is enough to know the initial condition  $\tilde{S}_r(\omega; \mu = -2\omega)$  in order to reconstruct  $\tilde{S}_r(\omega; \mu)$  from (3.68).

Two-loop diagrams for the heavy-quark self-energy are shown in Fig. 3.13. The first one contains the one-loop gluon self-energy (3.27); it can be easily calculated using (2.27), and is proportional to  $I_2$  (2.54) and  $P$  (3.28):

$$\tilde{\Sigma}_{2a}(\omega) = -C_F \frac{g_0^4 (-2\omega)^{1-4\varepsilon}}{(4\pi)^d} \frac{(d-2)I_2}{(d-3)(d-4)^2(d-6)(2d-7)} 4P. \quad (3.69)$$

The second diagram is also recursively one-loop; it is proportional to  $C_F^2 I_2$ . It is also not difficult to understand its dependence on the gauge parameter  $a_0$ . The exterior loop contains the heavy-quark line with a non-integer index  $n$  (in fact,  $n = 1 + 2\varepsilon$ ). The propagator (3.21) of the exterior gluon produces, as compared with the Feynman gauge  $a_0 = 1$ , an extra factor

$$\begin{aligned} 1 + \frac{1-a_0}{4} \frac{I(n, 2) - 2I(n-1, 2) + I(n-2, 2)}{I(n, 1)} \\ = 1 + \frac{1}{2}(1-a_0)(d-3) = -\frac{1}{2}(d-3)A. \end{aligned}$$

The same is true for the interior gluon line, with  $n = 1$ , as in the one-loop case (3.61). Therefore, the result contains  $A^2$ :

$$\tilde{\Sigma}_{2b}(\omega) = -C_F^2 \frac{g_0^4 (-2\omega)^{1-4\varepsilon}}{(4\pi)^d} \frac{(d-3)I_2}{(d-4)^2(2d-7)} A^2. \quad (3.70)$$

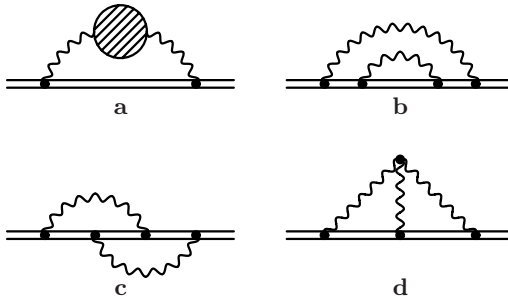


**Fig. 3.13.** Two-loop heavy quark self-energy in HQET

The diagram Fig. 3.13c, after killing one of the heavy-quark lines (2.56), yields  $I_1^2$  or  $I_2$ ; it contains  $A^2$  for the same reason as for Fig. 3.13b:

$$\begin{aligned} \tilde{\Sigma}_{2c}(\omega) &= C_F \left( C_F - \frac{1}{2}C_A \right) \frac{g_0^4 (-2\omega)^{1-4\varepsilon}}{(4\pi)^d} \\ &\times \left[ \frac{2I_1^2}{(d-4)^2} - \frac{I_2}{(d-4)(2d-7)} \right] A^2. \end{aligned} \quad (3.71)$$

The diagram Fig. 3.13d vanishes in the Feynman gauge, because the three-gluon vertex vanishes after contraction with three identical vectors  $v$ . It also vanishes if the longitudinal parts of all three gluon propagators are taken, and hence contains no  $(1 - a_0)^3$  term. The result is

$$\tilde{\Sigma}_{2d}(\omega) = -C_F C_A \frac{g_0^4 (-2\omega)^{1-4\varepsilon}}{(4\pi)^d} \frac{1}{(d-4)^2} \left[ I_1^2 + \frac{I_2}{2(2d-7)} \right] A(1-a_0). \quad (3.72)$$

Collecting these results together, we obtain the bare heavy-quark propagator with two-loop accuracy [1],

$$\begin{aligned} \omega \tilde{S}(\omega) = & 1 + C_F \frac{g_0^2 (-2\omega)^{-2\varepsilon}}{(4\pi)^{d/2}} \frac{I_1}{d-4} 2A + C_F \frac{g_0^4 (-2\omega)^{-4\varepsilon}}{(4\pi)^d} \frac{1}{(d-4)^2} \\ & \times \left[ \frac{8(d-2)}{(d-3)(d-6)(2d-7)} T_F n_f I_2 + 2A^2 C_F I_2 - \frac{4A}{d-3} C_A I_1^2 \right. \\ & + \frac{2}{(d-3)^2(d-6)} \left( \frac{(d-2)^2(d-5)}{(d-3)(2d-7)} + (d^2 - 4d + 5)A \right. \\ & \left. \left. - \frac{1}{4}(d^2 - 9d + 16)(d-3)A^2 \right) C_A I_2 \right]. \end{aligned} \quad (3.73)$$

Now we re-express it via  $\alpha_s$  (3.4) and  $a$  (3.2) and expand it in  $\varepsilon$ . Instead of (3.39), we now have

$$\frac{I_2}{I_1^2} = 1 + 4\zeta_2 \varepsilon^2 - 16\zeta_3 \varepsilon^3 + \dots \quad (3.74)$$

and hence  $\zeta_2$  appears in the results. The self-consistency condition (3.38) is satisfied; the anomalous dimension of the static-quark field is [1]

$$\tilde{\gamma}_Q = 2C_F(a-3) \frac{\alpha_s}{4\pi} + C_F \left( \frac{3a^2 + 24a - 179}{6} C_A + \frac{32}{3} T_F n_f \right) \left( \frac{\alpha_s}{4\pi} \right)^2 + \dots \quad (3.75)$$

Its difference from the QCD quark field anomalous dimension (3.57) is gauge-invariant up to two loops:

$$\tilde{\gamma}_Q - \gamma_q = -6C_F \frac{\alpha_s}{4\pi} - C_F \left( \frac{127}{3} C_A - 3C_F - \frac{44}{3} T_F n_f \right) \left( \frac{\alpha_s}{4\pi} \right)^2 + \dots \quad (3.76)$$

The three-loop anomalous dimension has been calculated recently [6, 2]; the difference (3.76) is not gauge-invariant at three loops. The renormalized static-quark propagator at  $\mu = -2\omega$  is

$$\begin{aligned} \omega \tilde{S}_r(\omega; \mu = -2\omega) &= 1 + 4C_F \frac{\alpha_s(\mu)}{4\pi} \\ &+ C_F \left[ (2(a-3)^2 \zeta_2 + 8) C_F \right. \\ &- \left( (a^2 - a - 10)\zeta_2 + \frac{(3a-29)(3a+53)}{24} \right) C_A \\ &\left. - \left( 8\zeta_2 + \frac{76}{3} \right) T_F n_l \right] \left( \frac{\alpha_s}{4\pi} \right)^2 + \dots \end{aligned}$$

(see [2] for the three-loop result).

### 3.5 Heavy-Electron Effective Theory

Now we make a short digression into the abelian version of HQET – the heavy-electron effective theory, an effective field theory of QED describing the interaction of a single electron with soft photons. It is obtained by setting  $C_F \rightarrow 1$ ,  $C_A \rightarrow 0$ ,  $g_0 \rightarrow e_0$ ,  $\alpha_s \rightarrow \alpha$ . This theory was considered long ago, and is called the Bloch–Nordsieck model.

Suppose we calculate the one-loop correction to the heavy-electron propagator in the coordinate space. Let us multiply this correction by itself (Fig. 3.14). We obtain an integral in  $t_1$ ,  $t_2$ ,  $t'_1$ ,  $t'_2$  with  $0 < t_1 < t_2 < t$ ,  $0 < t'_1 < t'_2 < t$ . The ordering of primed and non-primed integration times can be arbitrary. The integration area is subdivided into six regions, corresponding to the six diagrams in Fig. 3.14. This is twice the two-loop correction to the propagator. Continuing this drawing exercise, we see that the one-loop correction cubed is  $3!$  times the three-loop correction, and so on. Therefore, the exact all-order propagator is the exponential of the one-loop term:

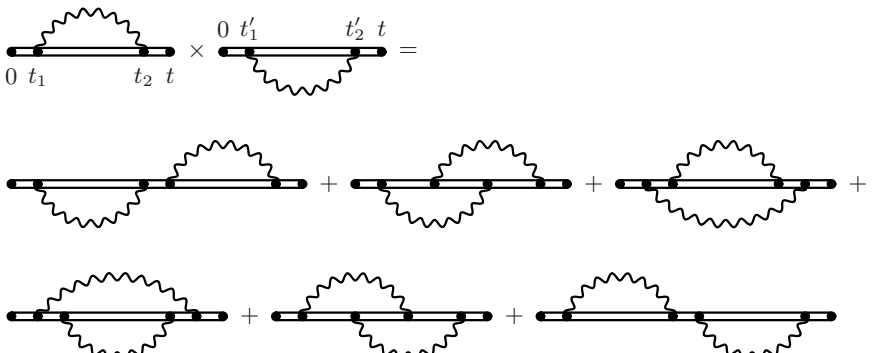


**Fig. 3.14.** Exponentiation theorem

$$\tilde{S}(t) = \tilde{S}_0(t) \exp \left[ \frac{e_0^2 (it/2)^{2\varepsilon}}{(4\pi)^{d/2}} \Gamma(-\varepsilon) A \right]. \quad (3.77)$$

In this theory,  $Z_A = 1$ , because there exist no loops which can be inserted into the photon propagator. Now we are going to show that  $Z_\alpha = 1$ , too. To this end, let us consider the sum of all one-particle-irreducible vertex diagrams, not including the external leg propagators – the electron–photon proper vertex. It has the same structure as the tree-level term:  $i e_0 v^\mu \tilde{\Gamma}$ ,  $\tilde{\Gamma} = 1 + \tilde{\Lambda}$ , where  $\tilde{\Lambda}$  is the sum of all unrenormalized diagrams starting from one loop. Let us multiply the vertex by the incoming photon momentum  $q_\mu$ . This product can be simplified by the Ward identity for the electron propagator (Fig. 3.15):

$$\begin{aligned} i\tilde{S}_0(\tilde{p}') i e_0 v \cdot q i\tilde{S}_0(\tilde{p}) &= i e_0 \frac{i}{\tilde{p}' \cdot v} [\tilde{p}' \cdot v - \tilde{p} \cdot v] \frac{i}{\tilde{p} \cdot v} \\ &= i e_0 \left[ \tilde{S}_0(\tilde{p}') - \tilde{S}_0(\tilde{p}) \right]. \end{aligned} \quad (3.78)$$

In the figure, the photon line with the black triangle at the end means that the vertex is contracted with the incoming photon momentum  $q$  (it includes no photon propagator!); a dot near an electron propagator means that its momentum is shifted by  $q$ .

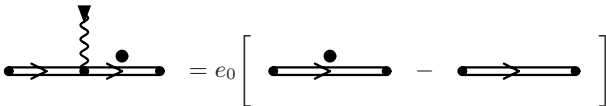


**Fig. 3.15.** Ward identity for the free electron propagator

Starting from each diagram for  $\tilde{\Sigma}$ , we can obtain a set of diagrams for  $\tilde{\Lambda}$  by inserting the external photon vertex into each electron propagator. After multiplying by  $q_\mu$ , each diagram in this set becomes a difference. All terms cancel each other, except the extreme ones (Fig. 3.16), and we obtain the Ward identity

$$\tilde{\Lambda}(\omega, \omega') = -\frac{\tilde{\Sigma}(\omega') - \tilde{\Sigma}(\omega)}{\omega' - \omega} \quad \text{or} \quad \tilde{\Gamma}(\omega', \omega) = \frac{\tilde{S}^{-1}(\omega') - \tilde{S}^{-1}(\omega)}{\omega' - \omega}. \quad (3.79)$$

The vertex function is thus also known to all orders. The charge renormalization constant  $Z_\alpha$  is obtained from the requirement that the renormalized vertex function  $g_0 \tilde{\Gamma} Z_A^{1/2} \tilde{Z}_Q$  is finite. The factor  $\tilde{Z}_Q$  transforms  $\tilde{S}^{-1}$  in (3.79) into  $\tilde{S}_r^{-1}$  and hence makes  $\tilde{\Gamma}$  finite. Therefore, the remaining factor  $(Z_\alpha Z_A)^{1/2} = 1$  (this is also true in QED). In the Bloch–Nordsieck model,  $Z_A = 1$  and hence  $Z_\alpha = 1$ .

Owing to the absence of charge and photon-field renormalization, we may replace  $e_0 \rightarrow e$ ,  $a_0 \rightarrow a$  in the bare propagator (3.77). This propagator is

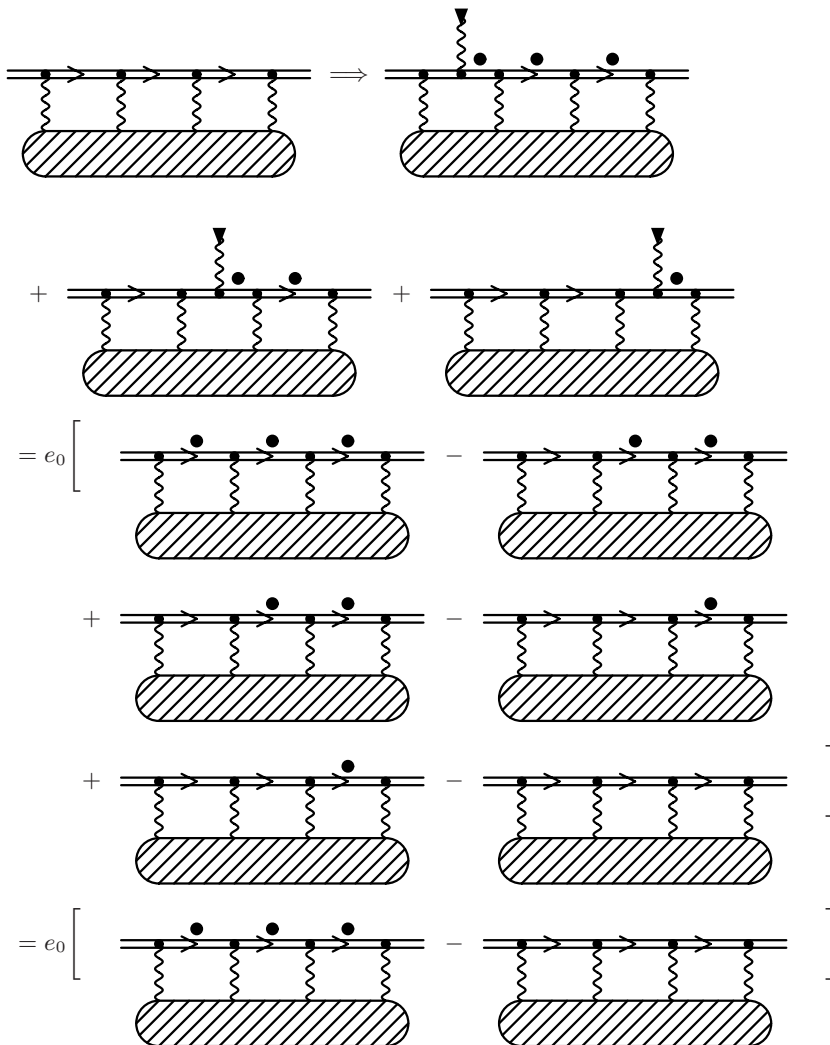


**Fig. 3.16.** Ward identity for the electron–photon vertex

made finite by the minimal (in the sense of (3.3)) renormalization constant, which is just the exponential of the one-loop term

$$\tilde{Z}_Q = \exp \left[ -(a - 3) \frac{\alpha}{4\pi\varepsilon} \right], \quad (3.80)$$

and the anomalous dimension is exactly equal to the one-loop contribution

$$\tilde{\gamma}_Q = 2(a - 3) \frac{\alpha}{4\pi}. \quad (3.81)$$

Note that the electron propagator is finite to all orders in the Yennie gauge.

What information useful for the real HQET can be extracted from this simple abelian model? We can obtain the  $C_F^2$  term in (3.73) by Fourier transformation, without explicit calculation. There should be no  $C_F^2$  term in the two-loop anomalous dimension of the field (3.75).

## References

1. D.J. Broadhurst, A.G. Grozin: Phys. Lett. B **267**, 105 (1991) [54](#)
2. K.G. Chetyrkin, A.G. Grozin: Nucl. Phys. B **666**, 289 (2003) [54, 55](#)
3. K.G. Chetyrkin, A. Retey: Nucl. Phys. B **583**, 3 (2000) [50](#)
4. P. Cvitanović: Phys. Rev. D **14**, 1536 (1979); *Group Theory, Part I* (Nordita, Copenhagen 1984) [48](#)
5. S.A. Larin, J.A.M. Vermaasen: Phys. Lett. B **303**, 334 (1993) [45](#)
6. K. Melnikov, T. van Ritbergen: Nucl. Phys. B **591**, 515 (2000) [54](#)
7. T. van Ritbergen, J.A.M. Vermaasen, S.A. Larin: Phys. Lett. B **400**, 379 (1997) [36](#)

## 4 The HQET Lagrangian: $1/m$ Corrections

This chapter is about the first  $1/m$  correction to the HQET Lagrangian. It contains two terms: the heavy-quark kinetic energy and the chromomagnetic interaction. The coefficient of the kinetic term is known exactly owing to the reparametrization invariance. The chromomagnetic interaction coefficient is obtained by matching the on-shell quark scattering amplitudes in an external chromomagnetic field in QCD and HQET. To this end, methods for on-shell calculations in QCD and HQET, in particular in external fields, are discussed. The dependence of the chromomagnetic interaction coefficient on the renormalization scale  $\mu$  is discussed, both within intervals between heavy-flavour masses and when crossing a threshold.

### 4.1 $1/m$ Corrections to the HQET Lagrangian

As discussed in Sect. 2.1, we are interested in processes with characteristic momenta and energies  $\omega \ll m$ . The heavy quark effective theory is constructed to reproduce QCD  $S$ -matrix elements expanded up to some order in  $\omega/m$ . There is a ‘folk theorem’ that any  $S$ -matrix having all the required properties follows from some Lagrangian. Therefore, the HQET Lagrangian is constructed as a series in  $1/m$  containing all operators having the necessary symmetries, with arbitrary coefficients. These coefficients are tuned to reproduce several QCD  $S$ -matrix elements expanded to some degree in  $\omega/m$ . We must perform this matching for a sufficient number of amplitudes to fix all the coefficients in the Lagrangian. After that, we can use this HQET Lagrangian instead of the QCD one for calculating other amplitudes.

The HQET Lagrangian is not unique, because the heavy-quark field  $\tilde{Q}$  can be redefined. Such field transformations can be used to eliminate all time derivatives  $D_0$  acting on  $\tilde{Q}$ , except in the leading term (2.2) [26].

The velocity  $v$  can be varied by a small amount  $\delta v \lesssim \omega/m$  without violating the applicability of HQET or changing its predictions. This reparametrization invariance [31] (see also [14, 21]) relates terms of different orders in  $1/m$ .

At the level of  $1/m$  terms, the heavy-quark spin symmetry and the superflavour symmetry are violated by interaction of the heavy-quark chromomagnetic moment with the magnetic component of the gluon field. This leads

to hyperfine splittings between states which were degenerate in the infinite-mass limit (such as  $B$  and  $B^*$ ), as well as to violation of leading-order relations among form factors. First, we are going to discuss the simpler case of a scalar heavy quark. We shall return to the realistic spin-(1/2) case at the end of this Section.

The only dimension-5 operator in scalar HQET that does not contain  $D_0$  acting on  $\tilde{Q}$  is  $\tilde{Q}^+ \mathbf{D}^2 \tilde{Q}$ . Therefore, the Lagrangian is

$$L = \tilde{Q}^+ i D_0 \tilde{Q} + \frac{C_k}{2m} \tilde{Q}^+ \mathbf{D}^2 \tilde{Q} + \dots \quad (4.1)$$

The additional term is the heavy-quark kinetic energy. This Lagrangian leads to the dispersion law of a free quark  $\tilde{p}_0 = p_0 - m = C_k \mathbf{p}^2 / (2m)$ . Therefore, at tree level,  $C_k = 1$ . The Lagrangian (4.1) can be rewritten in a covariant form:

$$L_v = \tilde{Q}_v^+ i v \cdot D \tilde{Q}_v - \frac{C_k}{2m} \tilde{Q}_v^+ D_\perp^2 \tilde{Q}_v + \dots, \quad (4.2)$$

where  $D_\perp = D - v(v \cdot D)$ . More accurately, this term should be written as  $(C_k^0 / (2m)) \mathcal{O}_k^0$ , where  $\mathcal{O}_k^0 = -\tilde{Q}_{v0}^+ D_{\perp 0}^2 \tilde{Q}_{v0}$  is the bare kinetic-energy operator. This operator is related to the renormalized operator by  $\mathcal{O}_k^0 = \tilde{Z}_k(\mu) \mathcal{O}_k(\mu)$ , and hence the term in the Lagrangian is  $(C_k(\mu) / (2m)) \mathcal{O}_k(\mu)$ , where  $C_k(\mu) = \tilde{Z}_k(\mu) C_k^0$ .

The kinetic-energy term gives the new vertices (Fig. 4.1)

$$i \frac{C_k^0}{2m} \tilde{p}_\perp^2, \quad i \frac{C_k^0}{2m} g_0 t^\alpha (p + p')^\mu_\perp, \quad i \frac{C_k^0}{2m} g_0^2 (t^a t^b + t^b t^a) g_\perp^{\mu\nu},$$

where  $g_\perp^{\mu\nu} = g^{\mu\nu} - v^\mu v^\nu$ .

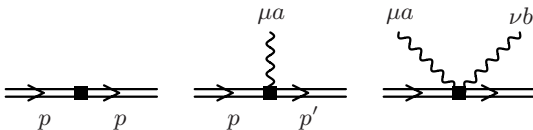


**Fig. 4.1.** Kinetic-energy vertices

In Sect. 3.4, we considered the sum of all one-particle-irreducible heavy-quark self-energy diagrams  $-i\tilde{\Sigma}(\omega)$  in the infinite-mass limit. Let us denote by  $-i(C_k^0 / (2m)) \tilde{\Sigma}_k(\omega, p_\perp^2)$  the sum of all bare one-particle-irreducible self-energy diagrams at the order  $1/m$ . Each of these diagrams contains a single kinetic-energy vertex (Fig. 4.1). Let us consider the variation of  $\tilde{\Sigma}$  for  $v \rightarrow v + \delta v$  with an infinitesimal  $\delta v$  ( $v \cdot \delta v = 0$ ). There are two sources of this variation. The expansion of the heavy-quark propagators  $1/(\tilde{p} \cdot v + i0)$  produces insertions  $i\tilde{p}_i \cdot \delta v$  into each propagator in turn. Variations of the

quark-gluon vertices produce  $i g_0 t^a \delta v^\mu$  for each vertex in turn. Now let us consider the variation of  $\tilde{\Sigma}_k$  for  $p_\perp \rightarrow p_\perp + \delta p_\perp$  with an infinitesimal  $\delta p_\perp$ . No-gluon kinetic vertices (Fig. 4.1) produce  $i(C_k^0/m)\tilde{p}_i \cdot \delta p_\perp$ ; single-gluon kinetic vertices (Fig. 4.1) produce  $i(C_k^0/m)g_0 t^a \delta p_\perp^\mu$ ; two-gluon kinetic vertices do not change. Therefore,

$$\frac{\partial \tilde{\Sigma}_k}{\partial p_\perp^\mu} = 2 \frac{\partial \tilde{\Sigma}}{\partial v^\mu}. \quad (4.3)$$

This is the Ward identity of reparametrization invariance. Taking into account  $\partial \tilde{\Sigma}_k / \partial p_\perp^\mu = 2(\partial \tilde{\Sigma}_k / \partial p_\perp^2)p_\perp^\mu$  and  $\partial \tilde{\Sigma} / \partial v^\mu = (d\tilde{\Sigma}/d\omega)p_\perp^\mu$ , we obtain

$$\frac{\partial \tilde{\Sigma}_k}{\partial p_\perp^2} = \frac{d\tilde{\Sigma}}{d\omega}. \quad (4.4)$$

The right-hand side does not depend on  $p_\perp^2$ , and hence

$$\tilde{\Sigma}_k(\omega, p_\perp^2) = \frac{d\tilde{\Sigma}(\omega)}{d\omega} p_\perp^2 + \tilde{\Sigma}_{k0}(\omega). \quad (4.5)$$

This result can also be understood in a more direct way. The momentum  $p_\perp$  flows through the heavy-quark line. No-gluon kinetic vertices are quadratic in it; one-gluon vertices are linear; two-gluon vertices are independent of  $p_\perp$ . The  $p_\perp^2$  term comes from diagrams with a no-gluon kinetic vertex. Terms linear in  $p_\perp$  vanish owing to the rotational symmetry. The coefficient of  $p_\perp^2$  in a no-gluon kinetic vertex is  $iC_k/(2m)$ . Therefore, the coefficient of  $p_\perp^2$  in the sum of all diagrams is the sum of the leading-order HQET diagrams with a unit operator insertion into each heavy-quark propagator in turn. This sum is just  $-id\tilde{\Sigma}/d\omega$ , and hence we arrive at (4.5) again.

At one loop (Fig. 4.2),

$$\begin{aligned} \tilde{\Sigma}_{k0}(\omega) &= iC_F g_0^2 \int \frac{d^d k}{(2\pi)^d} \frac{v^\mu [2(k \cdot v + \omega)k_\perp^\nu - k_\perp^2 v^\nu]}{(-k^2)(k \cdot v + \omega)^2} \\ &\times \left[ g_{\mu\nu} + (1 - a_0) \frac{k_\mu k_\nu}{-k^2} \right] \\ &= -2C_F \frac{g_0^2 (-2\omega)^{-2\varepsilon}}{(4\pi)^{d/2}} \frac{d-1}{d-4} I_1 A \omega^2 \end{aligned} \quad (4.6)$$

(see (2.54), (3.61)).



**Fig. 4.2.** One-loop diagrams for  $\tilde{\Sigma}_{k0}$

As we discussed at the beginning of this section, the coefficients in the HQET Lagrangian are obtained by equating on-shell scattering amplitudes in full QCD and in HQET with the required accuracy in  $1/m$ . A prerequisite for this matching is the requirement that the mass shell itself is the same in both theories, to the accuracy considered. The mass shell is defined as the position of the pole of the full quark propagator. In QCD it is  $p_0 = \sqrt{m^2 + \mathbf{p}^2}$ , where  $m$  is the on-shell mass (see Sect. 4.2 for more details). To the first order in  $1/m$ , this means  $\omega = \mathbf{p}^2/(2m)$ . In HQET, the mass shell is the zero of the denominator of the bare heavy-quark propagator

$$\tilde{S}(p) = \frac{1}{\omega - \tilde{\Sigma}(\omega) - \frac{C_k^0}{2m} \left[ \mathbf{p}^2 - \frac{d\tilde{\Sigma}(\omega)}{d\omega} \mathbf{p}^2 + \tilde{\Sigma}_{k0}(\omega) \right]}. \quad (4.7)$$

In Sect. 4.3, we shall obtain  $\tilde{\Sigma}(0) = 0$  and  $\tilde{\Sigma}_{k0}(0) = 0$  at the two-loop level. I do not know if this is true at higher orders or not. If not, these equalities can be restored by adding a residual-mass counterterm to the Lagrangian (2.9); this does not contradict any general requirements. The mass shell is

$$\left[ 1 - \frac{d\tilde{\Sigma}(\omega)}{d\omega} \right]_{\omega=0} \omega = \frac{C_k^0}{2m} \left[ 1 - \frac{d\tilde{\Sigma}(\omega)}{d\omega} \right]_{\omega=0} \mathbf{p}^2. \quad (4.8)$$

This is correct if  $C_k^0 = \tilde{Z}_k^{-1}(\mu)C_k(\mu) = 1$ . The minimal (3.3) renormalization constant  $\tilde{Z}_k$  has to make  $C_k(\mu)$  finite; here this means  $\tilde{Z}_k = 1$ . The kinetic-energy operator is not renormalized; its anomalous dimension is zero to all orders. The coefficient of the kinetic-energy operator in the HQET Lagrangian is exactly unity,

$$C_k(\mu) = 1, \quad (4.9)$$

to all orders in perturbation theory, owing to the reparametrization invariance!

In the case of a spin-(1/2) heavy quark, there is one more dimension-5 operator, in addition to the kinetic energy – the chromomagnetic interaction [19, 20]

$$L = \tilde{Q}^+ i D_0 \tilde{Q} + \frac{C_k}{2m} \tilde{Q}^+ \mathbf{D}^2 \tilde{Q} - \frac{C_m}{2m} \tilde{Q}^+ \mathbf{B} \cdot \boldsymbol{\sigma} \tilde{Q} + \dots \quad (4.10)$$

or, in covariant notation,

$$L_v = \overline{\tilde{Q}}_v i v \cdot D \tilde{Q}_v - \frac{C_k}{2m} \overline{\tilde{Q}}_v D_\perp^2 \tilde{Q}_v + \frac{C_m}{4m} \overline{\tilde{Q}}_v G_{\mu\nu} \sigma^{\mu\nu} \tilde{Q}_v + \dots, \quad (4.11)$$

where  $G_{\mu\nu} = g G_{\mu\nu}^a t^a$ . In the  $v$  rest frame, only chromomagnetic components of  $G_{\mu\nu}$  contribute, because  $\sigma^{0i}$  sandwiched between  $\overline{\tilde{Q}}$  and  $\tilde{Q}$  yields zero.

Again, it is more accurate to write this term as  $C_m^0 \mathcal{O}_m^0 = C_m(\mu) \mathcal{O}_m(\mu)$ , where  $\mathcal{O}_m^0 = \tilde{Z}_m(\mu) \mathcal{O}_m(\mu)$  is the bare chromomagnetic operator, and  $C_m^0 = \tilde{Z}_m^{-1}(\mu) C_m(\mu)$ . The kinetic term in (4.10) does not violate the heavy-quark spin symmetry (because it contains no spin matrix between  $\tilde{Q}^+$  and  $\tilde{Q}$ ), while the chromomagnetic term violates it, producing hyperfine splittings. The chromomagnetic interaction gives the new vertices (Fig. 4.3)

$$\frac{C_m^0}{2m} g_0 t^a \sigma^{\nu\mu} q_\nu, \quad \frac{C_m^0}{2m} g_0^2 [t^a, t^b] \sigma^{\mu\nu}.$$

The arguments leading to (4.9) remain valid in the spin-(1/2) case. The coefficient of the chromomagnetic interaction  $C_m(\mu)$  is not related to the lower-order term in  $1/m$  by the reparametrization invariance, and can only be calculated by QCD/HQET matching (Sect. 4.6).

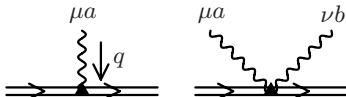


**Fig. 4.3.** Chromomagnetic-interaction vertices

The HQET Lagrangian at the  $1/m^2$  level was discussed in [30, 5, 22, 8, 6], and at the  $1/m^3$  level in [33, 4]. At the tree level, one can easily find as many terms in  $1/m$  as one wishes, without QCD/HQET matching. This can be done by the Foldy–Wouthuysen transformation [26, 3]. Alternatively, one can substitute the lower components of the heavy-quark field from the equation of motion into the QCD Lagrangian [30], or integrate them out in the functional integral [32]. These two methods produce the same Lagrangian, which contains  $D_0$  acting on  $\tilde{Q}$  in correction terms. Such terms can be eliminated by a suitable field redefinition, and the result of the first method is reproduced.

## 4.2 On-Shell Renormalization of QCD

Now we are going to discuss the calculation of on-shell propagator diagrams of a massive quark in QCD. Let us write the one-loop diagram with arbitrary degrees of the denominators (Fig. 4.4) as

$$\int \frac{d^d k}{D_1^{n_1} D_2^{n_2}} = i\pi^{d/2} m^{d-2(n_1+n_2)} M(n_1, n_2),$$

$$D_1 = m^2 - (k + mv)^2 - i0, \quad D_2 = -k^2 - i0. \quad (4.12)$$

After the Wick rotation  $k_0 = ik_{E0}$ ,  $k^2 = -k_E^2$  and transformation to the dimensionless integration momentum  $K = k_E/m$ , the diagram becomes

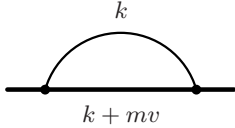


**Fig. 4.4.** One-loop on-shell propagator diagram

$$\int \frac{d^d K}{(K^2 - 2iK_0)^{n_1} (K^2)^{n_2}} = \pi^{d/2} M(n_1, n_2). \quad (4.13)$$

Now let us compare this diagram with the one-loop HQET diagram  $I(n_1, n_2)$  (2.27). In terms of the dimensionless Euclidean integration momentum  $K = k_E/(-2\omega)$ , it has the form

$$\int \frac{d^d K}{(1 - 2iK_0)^{n_1} (K^2)^{n_2}} = \pi^{d/2} I(n_1, n_2). \quad (4.14)$$

The on-shell integral (4.13) can be cast into the HQET form (4.14) using the inversion [13]  $K = K'/K'^2$ . The on-shell denominator  $K^2 - 2iK_0 = (1 - 2iK'_0)/K'^2$  produces the HQET denominator. The integration measure becomes  $d^d K = K^{d-1} dK d\Omega = (K')^{-d-1} dK' d\Omega = d^d K' / (K'^2)^d$ . The final result is

$$\begin{aligned} M(n_1, n_2) &= I(n_1, d - n_1 - n_2) \\ &= \frac{\Gamma(d - n_1 - 2n_2)\Gamma(-d/2 + n_1 + n_2)}{\Gamma(n_1)\Gamma(d - n_1 - n_2)}. \end{aligned} \quad (4.15)$$

This result can also be obtained using the Feynman parametrization (2.13). If  $n_{1,2}$  are integer,  $M(n_1, n_2)$  is proportional to  $M_1 = \Gamma(1 + \varepsilon)$ , the coefficient being a rational function of  $d$ .

The inversion interchanges the UV and IR behaviours of an integral. Therefore, the poles of  $\Gamma(d - n_1 - 2n_2)$  are IR divergences (sometimes called on-shell divergences in this case), and the poles of  $\Gamma(-d/2 + n_1 + n_2)$  are UV divergences. The usual rule about the sign of  $d$  in  $\Gamma$ -functions applies.

There are two generic topologies of two-loop on-shell propagator diagrams, shown in Figs. 4.5a,b. We shall start from the simpler type  $M$ , Fig. 4.5a:

$$\begin{aligned} \int \frac{d^d k_1 d^d k_2}{D_1^{n_1} D_2^{n_2} D_3^{n_3} D_4^{n_4} D_5^{n_5}} &= -\pi^d m^{2(d - \sum n_i)} M(n_1, n_2, n_3, n_4, n_5), \\ D_1 &= m^2 - (k_1 + mv)^2, \quad D_2 = m^2 - (k_2 + mv)^2, \\ D_3 &= -k_1^2, \quad D_4 = -k_2^2, \quad D_5 = -(k_1 - k_2)^2. \end{aligned} \quad (4.16)$$

Using inversion, we can relate this diagram to the HQET two-loop propagator diagram. The on-shell denominators  $D_{1,2}$  produce the HQET denominators,

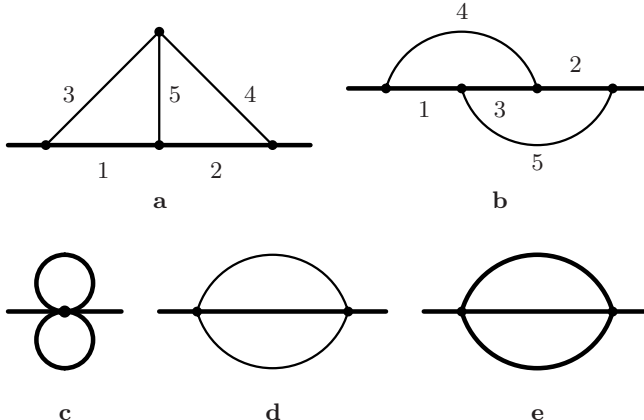


**Fig. 4.5.** Two-loop on-shell propagator diagrams

just as in the one-loop case. The denominator  $D_5$  becomes  $(K_1 - K_2)^2 = (K'_1 - K'_2)^2 / (K'^2_1 K'^2_2)$ . We obtain [13]

$$M(n_1, n_2, n_3, n_4, n_5) = I(n_1, n_2, d - n_1 - n_3 - n_5, d - n_2 - n_4 - n_5, n_5). \quad (4.17)$$

However, this relation is not particularly useful for calculation of  $M(n_1, n_2, n_3, n_4, n_5)$ , because this HQET integral contains two non-integer indices. The integrals  $M$  can be calculated using integration by parts recurrence relations. This is not so easy as in the massless case (Sect. 2.4) and the HQET case (Sect. 2.5). We shall not discuss the algorithm here; it can be found in the original literature [24, 11, 10, 23]. The conclusion is that any integral  $M(n_1, n_2, n_3, n_4, n_5)$  with integer indices  $n_i$  can be expressed as a linear combination of  $M_1^2$  (Fig. 4.5c) and  $M_2$  (Fig. 4.5d), the coefficients being rational functions of  $d$ . Here the combinations of  $\Gamma$ -functions appearing in  $n$ -loop on-shell sunset diagrams with a single massive line are

$$M_n = \frac{\Gamma(1 + (n-1)\varepsilon)\Gamma(1+n\varepsilon)\Gamma(1-2n\varepsilon)\Gamma^n(1-\varepsilon)}{\Gamma(1-n\varepsilon)\Gamma(1-(n+1)\varepsilon)}. \quad (4.18)$$

The type  $N$  (Fig. 4.5b),

$$\begin{aligned} \int \frac{d^d k_1 d^d k_2}{D_1^{n_1} D_2^{n_2} D_3^{n_3} D_4^{n_4} D_5^{n_5}} &= -\pi^d m^{2(d-\sum n_i)} N(n_1, n_2, n_3, n_4, n_5), \\ D_1 &= m^2 - (k_1 + mv)^2, \quad D_2 = m^2 - (k_2 + mv)^2, \\ D_3 &= m^2 - (k_1 + k_2 + mv)^2, \quad D_4 = -k_1^2, \quad D_5 = -k_2^2, \end{aligned} \quad (4.19)$$

is more difficult. The integrals  $N$  can be expressed [24, 11, 10, 23], using integration by parts, as linear combinations of  $M_1^2$  (Fig. 4.5c),  $M_2$  (Fig. 4.5d), and

a single difficult integral  $N(1, 1, 1, 0, 0)$  (Fig. 4.5e), with rational coefficients. Instead of using  $N(1, 1, 1, 0, 0)$  as a basis integral, it is more convenient to use the convergent integral  $N(1, 1, 1, 1, 1)$ . This integral can be expressed via the  ${}_3F_2$  hypergeometric functions with a unit argument and indices depending on  $\varepsilon$ . Several terms of the expansion in  $\varepsilon$  are known [9, 10]:

$$N(1, 1, 1, 1, 1) = I + \mathcal{O}(\varepsilon), \quad I = \pi^2 \log 2 - \frac{3}{2} \zeta(3). \quad (4.20)$$

Until now, we have discussed on-shell propagator diagrams with a single non-zero mass. Starting from two loops, there are also diagrams with loops of a quark with a different mass  $m'$  (say, c-quark loops in the b-quark self-energy, or vice versa) (Fig. 4.6). Such diagrams can be reduced [17], using integration by parts, to two trivial integrals (Figs. 4.7a,b) and two non-trivial ones (Figs. 4.7c,d). These non-trivial integrals are

$$\begin{aligned} \frac{I_0}{\Gamma^2(1+\varepsilon)} &= -m^{2-4\varepsilon} \left[ \frac{1}{2\varepsilon^2} + \frac{5}{4\varepsilon} + 2(1-r^2)^2(L_+ + L_-) - 2\log^2 r + \frac{11}{8} \right] \\ &\quad - m'^{2-4\varepsilon} \left[ \frac{1}{\varepsilon^2} + \frac{3}{\varepsilon} - 2\log r + 6 \right] + \mathcal{O}(\varepsilon), \\ \frac{I_1}{\Gamma^2(1+\varepsilon)} &= m^{-4\varepsilon} \left[ \frac{1}{2\varepsilon^2} + \frac{5}{2\varepsilon} + 2(1+r)^2L_+ + 2(1-r)^2L_- \right. \\ &\quad \left. - 2\log^2 r + \frac{19}{2} \right] + \mathcal{O}(\varepsilon), \end{aligned} \quad (4.21)$$

where  $r = m'/m$ ,

$$\begin{aligned} L_+ &= -\text{Li}_2(-r) + \frac{1}{2}\log^2 r - \log r \log(1+r) - \frac{1}{6}\pi^2 \\ &= \text{Li}_2(-r^{-1}) + \log r^{-1} \log(1+r^{-1}), \end{aligned}$$

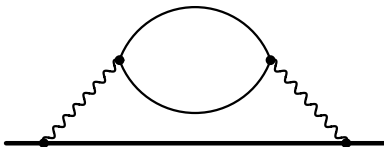


**Fig. 4.6.** Two-loop on-shell propagator diagram with two masses

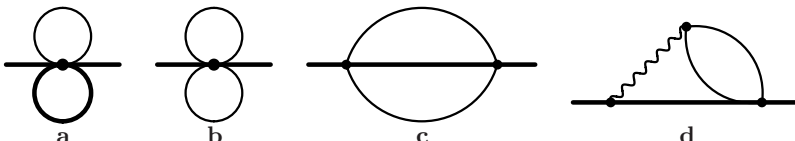


**Fig. 4.7.** Basis on-shell integrals with two masses

$$\begin{aligned}
L_- &= \text{Li}_2(1-r) + \frac{1}{2} \log^2 r + \frac{1}{6} \pi^2 \\
&= -\text{Li}_2(1-r^{-1}) + \frac{1}{6} \pi^2 \\
&= -\text{Li}_2(r) + \frac{1}{2} \log^2 r - \log r \log(1-r) + \frac{1}{3} \pi^2 \quad (r < 1) \\
&= \text{Li}_2(r^{-1}) + \log r^{-1} \log(1-r^{-1}) \quad (r > 1), \\
L_+ + L_- &= \frac{1}{2} \text{Li}_2(1-r^2) + \log^2 r + \frac{1}{12} \pi^2 \\
&= -\frac{1}{2} \text{Li}_2(1-r^{-2}) + \frac{1}{12} \pi^2.
\end{aligned} \tag{4.22}$$

The first three-loop on-shell calculation, that of the electron anomalous magnetic moment in QED, has been completed recently [28]. A systematic algorithm for calculation of three-loop on-shell propagator diagrams in QCD, using integration by parts, was constructed and implemented in [34].

The on-shell renormalization scheme is most convenient for calculation of on-shell scattering amplitudes. The heavy-quark part of the QCD Lagrangian (3.1) can be rewritten as

$$L = \bar{Q}_0(iD_0 - m)Q_0 + \delta m \bar{Q}_0 Q_0 + \dots, \tag{4.23}$$

where  $m$  is the on-shell mass (defined as the position of the pole of the full quark propagator), and  $\delta m = m - m_0$  is the mass counterterm ( $m_0 = Z_m^{\text{os}} m$ ). We shall consider it not as a part of the unperturbed Lagrangian, but as a perturbation. It produces the counterterm vertex (Fig. 4.8)  $i\delta m$ .



**Fig. 4.8.** Mass counterterm vertex

The heavy-quark self-energy can be decomposed as

$$\Sigma(p) = m\Sigma_1(p^2) + (\not{p} - m)\Sigma_2(p^2). \tag{4.24}$$

The bare heavy-quark propagator is then

$$S(p) = \frac{1}{(1 - \Sigma_2(p^2))(\not{p} - m) + \delta m - m\Sigma_1(p^2)}. \tag{4.25}$$

It has a pole at  $p^2 = m^2$  if

$$\delta m = m\Sigma_1(m^2). \tag{4.26}$$

The mass counterterm  $\delta m$  is determined by this equation, order by order in perturbation theory;  $Z_m^{\text{os}} = 1 - \delta m/m = 1 - \Sigma_1(m^2)$ . Then, near the mass

shell,  $\Sigma_1(p^2) - \delta m/m = \Sigma'_1(m^2)(p^2 - m^2) + \dots$ , where  $\Sigma'_1(p^2) = d\Sigma_1(p^2)/dp^2$ . The bare quark propagator (4.25) becomes

$$S(p) = \frac{1}{1 - \Sigma_2(m^2) - 2m^2\Sigma'_1(m^2)} \frac{\not{p} + m}{p^2 - m^2} + \dots, \quad (4.27)$$

where the dots mean terms which are non-singular at  $p^2 \rightarrow m^2$ . We define the heavy-quark field renormalization constant in the on-shell scheme  $Z_Q^{\text{os}}$  by the requirement that the renormalized quark propagator  $S_{\text{os}}(p)$  (which is related to  $S(p)$  by  $S(p) = Z_Q^{\text{os}}S_{\text{os}}(p)$ ) behaves as the free one (3.42) near the mass shell. Therefore,  $Z_Q^{\text{os}} = [1 - \Sigma_2(m^2) - 2m^2\Sigma'_1(m^2)]^{-1}$ .

Now let us explicitly calculate  $Z_m^{\text{os}}$  and  $Z_Q^{\text{os}}$  at the one-loop order. It is convenient [34] to introduce the function

$$\begin{aligned} T(t) &= \frac{1}{4m} \text{Tr}(\not{p} + 1)\Sigma(mv(1+t)) \\ &= \Sigma_1(m^2) + [\Sigma_2(m^2) + 2m^2\Sigma'_1(m^2)]t + \mathcal{O}(t^2); \end{aligned} \quad (4.28)$$

then  $Z_m^{\text{os}} = 1 - T(0)$  and  $Z_Q^{\text{os}} = [1 - T'(0)]^{-1}$ . We have

$$\begin{aligned} T(t) &= -iC_F g_0^2 \int \frac{d^d k}{(2\pi)^d} \frac{1}{D_1(t)D_2} \frac{1}{4m} \text{Tr}(\not{p} + 1)\gamma^\mu(\not{p} + \not{k} + m)\gamma^\nu \\ &\quad \times \left[ g_{\mu\nu} + (1 - a_0) \frac{k_\mu k_\nu}{D_2} \right], \end{aligned}$$

where  $D_1(t) = m^2 - (p+k)^2$ . In calculating the numerator, we can express  $p \cdot k$  via  $D_1(t)$  and  $D_2$ , and omit terms with  $D_1(t)$ , because the resulting integrals contain no scale. Omitting also  $t^2$  and higher terms, we obtain

$$T(t) = -iC_F g_0^2 \int \frac{d^d k}{(2\pi)^d} \frac{1}{D_1(t)} \left[ \frac{2}{D_2} - \frac{d-2}{2m^2}(1-t) \right].$$

Note that this result is gauge-independent. Now, taking into account  $D_1(t) = D_1 + (D_1 - D_2 - 2m^2)t + \mathcal{O}(t^2)$ , we arrive at

$$T(t) = C_F \frac{g_0^2 m^{-2\varepsilon}}{(4\pi)^{d/2}} \Gamma(\varepsilon) \frac{d-1}{d-3} (1-t) + \mathcal{O}(t^2).$$

Therefore,

$$Z_m^{\text{os}} = Z_Q^{\text{os}} = 1 - C_F \frac{g_0^2 m^{-2\varepsilon}}{(4\pi)^{d/2}} \Gamma(\varepsilon) \frac{d-1}{d-3}. \quad (4.29)$$

The equality  $Z_m^{\text{os}} = Z_Q^{\text{os}}$  is accidental, and does not hold at higher orders.

On-shell renormalization of QCD at two loops has been performed in [24, 11, 10] (see also [17] for the exact  $d$ -dimensional contributions of the loops

of another massive quark). The  $\mathcal{O}(g_0^2)$  term in  $\delta m = -m(Z_m^{\text{os}} - 1)$ , found in (4.29), is necessary when calculating  $\mathcal{O}(g_0^4)$  diagrams containing the counterterm vertex (Fig. 4.8). Three-loop results have been obtained recently [34]. The on-shell mass is gauge-invariant to all orders [27]; the quark field renormalization  $Z_Q^{\text{os}}$  is gauge-invariant at two loops [11] but not at three [34].

### 4.3 On-Shell Renormalization of HQET

Now we shall consider the on-shell renormalization of the HQET Lagrangian (3.58). The HQET mass shell is  $\omega = 0$ . All loop diagrams without massive particles are no-scale and hence vanish. Only diagrams with loops of massive quarks (of other flavours) can contribute. Such diagrams first appear at two loops (Fig. 4.9).

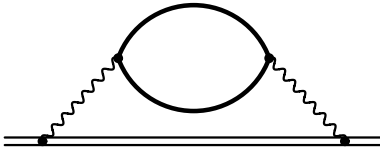


**Fig. 4.9.** Two-loop on-shell HQET propagator diagram

The following method is used for calculation of such diagrams [12, 16]. For two vectors  $a$  and  $b$  in  $d$ -dimensional Euclidean space, the following average over the directions of  $a$  (or  $b$ ) is given by

$$\begin{aligned} \overline{(a \cdot b)^n} &= (a^2 b^2)^{n/2} \frac{\int_0^\pi \cos^n \theta \sin^{d-2} \theta d\theta}{\int_0^\pi \sin^{d-2} \theta d\theta} \\ &= \frac{\Gamma((n+1)/2)}{\Gamma(1/2)} \frac{\Gamma(d/2)}{\Gamma((d+n)/2)} (a^2 b^2)^{n/2} \end{aligned} \quad (4.30)$$

for even  $n$  (positive or negative), and 0 for odd  $n$ . In particular, in a ( $d = 1$ )-dimensional space the right-hand side is just  $(a^2 b^2)^{n/2}$ , as expected. We can use this formula for  $\overline{(k \cdot v)^n}$  in Minkowski scalar integrals, because they are calculated via Wick rotation. The HQET propagator in Fig. 4.9 produces just an additional power of  $k^2$ , and we are left with the vacuum diagram of Fig. 4.10. This diagram has been calculated in [35]:

$$\begin{aligned} &\int \frac{d^d k_1 d^d k_2}{(m^2 - k_1^2 - i0)^{n_1} (m^2 - k_2^2 - i0)^{n_2} [-(k_1 - k_2)^2 - i0]^{n_3}} \\ &= -\pi^d m^{2(d-n_1-n_2-n_3)} \end{aligned}$$

$$\times \frac{\Gamma(-d/2 + n_1 + n_3)\Gamma(-d/2 + n_2 + n_3)\Gamma(d/2 - n_3)\Gamma(-d + n_1 + n_2 + n_3)}{\Gamma(n_1)\Gamma(n_2)\Gamma(d/2)\Gamma(-d + n_1 + n_2 + 2n_3)}. \quad (4.31)$$

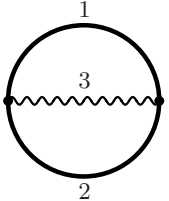


**Fig. 4.10.** Two-loop vacuum diagram

Using this method, we see that  $\tilde{\Sigma}(0) = 0$ , and

$$\begin{aligned} \left. \frac{d\tilde{\Sigma}(\omega)}{d\omega} \right|_{\omega=0} &= -iC_F g_0^2 \int \frac{d^d k}{(2\pi)^d} \frac{v^\mu v^\nu}{(k \cdot v)^2} \frac{\Pi_{\mu\nu}(k)}{(k^2)^2} \\ &= -iC_F g_0^2 \int \frac{d^d k}{(2\pi)^d} \left( \frac{k^2}{(k \cdot v)^2} - 1 \right) \frac{\Pi(k^2)}{(k^2)^2} \\ &= -C_F T_F \frac{g_0^4 \sum m_i^{-4\varepsilon}}{(4\pi)^d} \Gamma^2(\varepsilon) \frac{2(d-1)(d-6)}{(d-2)(d-5)(d-7)}, \end{aligned} \quad (4.32)$$

where  $\Pi_{\mu\nu}(k) = (k^2 g_{\mu\nu} - k_\mu k_\nu) \Pi(k^2)$  is the massive-quark contribution to the gluon self-energy,  $k^2/(k \cdot v)^2 = -(d-2)$ , and the sum is over all massive flavours. Here, from (4.31),

$$iC_F g_0^2 \int \frac{d^d k}{(2\pi)^d} \frac{\Pi(k^2)}{(k^2)^2} = C_F T_F \frac{g_0^4 \sum m_i^{-4\varepsilon}}{(4\pi)^d} \Gamma^2(\varepsilon) \frac{2(d-6)}{(d-2)(d-5)(d-7)}. \quad (4.33)$$

We find the on-shell HQET quark field renormalization constant  $\tilde{Z}_Q^{\text{os}} = [1 - (d\tilde{\Sigma}(\omega)/d\omega)_{\omega=0}]^{-1}$  from the requirement that the renormalized propagator  $\tilde{S}_{\text{os}} = \tilde{S}/\tilde{Z}_Q^{\text{os}}$  (see (4.7)) behaves as the free propagator  $\tilde{S}_0$  near the mass shell:

$$\tilde{Z}_Q^{\text{os}} = 1 - C_F T_F \frac{g_0^4 \sum m_i^{-4\varepsilon}}{(4\pi)^d} \Gamma^2(\varepsilon) \frac{2(d-1)(d-6)}{(d-2)(d-5)(d-7)}. \quad (4.34)$$

The on-shell HQET propagator  $\tilde{S} = \tilde{Z}_Q^{\text{os}} \tilde{S}_{\text{os}}$  contains both UV and IR divergences. The UV divergences can be eliminated by dividing it by the  $\overline{\text{MS}}$  renormalization constant  $\tilde{Z}_Q(\mu)$ , so that  $\tilde{Z}_Q^{\text{os}}/\tilde{Z}_Q(\mu)$  contains only IR

divergences. The same is true for the QCD ratio  $Z_Q^{\text{os}}/Z_Q(\mu)$ . By construction, HQET does not differ from QCD in the IR region. Therefore,

$$\frac{\tilde{Z}_Q^{\text{os}}/\tilde{Z}_Q(\mu)}{Z_Q^{\text{os}}/Z_Q(\mu)} = \text{finite}. \quad (4.35)$$

This fact was used for obtaining  $\tilde{Z}_Q(\mu)$  from on-shell QCD results at two [11] and three [34] loops.

The renormalization constant (4.34) is not smooth at  $m_i \rightarrow 0$ . This discontinuity comes from IR gluon momenta, where HQET does not differ from QCD. Therefore, the QCD on-shell quark field renormalization constant has the same non-smooth behaviour at  $m_i \rightarrow 0$  [11, 17]:

$$\begin{aligned} \frac{Z_Q^{\text{os}}(m_i)}{Z_Q^{\text{os}}(m_i = 0)} &= \frac{\tilde{Z}_Q^{\text{os}}(m_i)}{\tilde{Z}_Q^{\text{os}}(m_i = 0)} \\ &= 1 - C_F T_F \frac{g_0^4 m_i^{-4\varepsilon}}{(4\pi)^d} \Gamma^2(\varepsilon) \frac{2(d-1)(d-6)}{(d-2)(d-5)(d-7)}. \end{aligned} \quad (4.36)$$

Now we are going to calculate  $\tilde{\Sigma}_{k0}(0)$  (see (4.5)). At the two-loop level, it is given by the diagrams of Fig. 4.11 (where the second diagram also implies the mirror symmetric one), with zero external residual momentum ( $\omega = 0$ ,  $p_\perp = 0$ ). We obtain

$$\tilde{\Sigma}_{k0}(0) = iC_F g_0^2 \int \frac{d^d k}{(2\pi)^d} \frac{\Pi(k^2)}{k^2} \left[ d - 2 + \frac{k^2}{(k \cdot v)^2} \right] = 0. \quad (4.37)$$

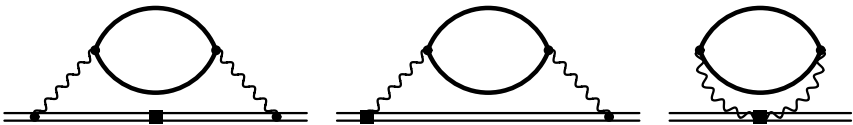


**Fig. 4.11.** Two-loop diagrams for  $\tilde{\Sigma}_{k0}(0)$

## 4.4 Scattering in an External Gluonic Field in QCD

Now we are going to perform matching for the scattering amplitudes of an on-shell heavy quark in an external chromomagnetic field in QCD and in HQET, with linear accuracy in  $q/m$ , where  $q$  is the momentum transfer.

It is most convenient to calculate scattering amplitudes in an external field using the background field method [1]. In the QCD Lagrangian (3.1),

we substitute  $A_0^\mu \rightarrow \bar{A}_0^\mu + A_0^\mu$ , where  $\bar{A}_0^\mu$  is the external field, and choose the gauge-fixing term  $(\bar{D}_\mu A_0^\mu)^2 / (2a_0)$ , where  $\bar{D}_\mu = \partial_\mu - ig_0 \bar{A}_{0\mu}^a t^a$ . The ghost term is changed correspondingly:

$$\begin{aligned} L = & \sum_i \bar{q}_{i0} (i\cancel{D}_0 - m_{i0}) q_{i0} - \frac{1}{4} G_{0\mu\nu}^a G_0^{a\mu\nu} \\ & - \frac{1}{2a_0} (\bar{D}_\mu A_0^\mu)^2 + (\bar{D}_\mu \bar{c}_0^a) (D_0^\mu c_0^a). \end{aligned} \quad (4.38)$$

Some vertices containing the background field  $\bar{A}_0$  differ from the ordinary vertices. In particular, the gauge-fixing term contains an  $\bar{A}_0 A_0^2$  contribution, altering the three-gluon vertex (Fig. 4.12a) to

$$\begin{aligned} g_0 f^{a_1 a_2 a_3} \left[ & (k_2 - k_3)^{\mu_1} g^{\mu_2 \mu_3} + \left( k_3 - k_1 + \frac{1}{a_0} k_2 \right)^{\mu_2} g^{\mu_3 \mu_1} \right. \\ & \left. + \left( k_1 - k_2 - \frac{1}{a_0} k_3 \right)^{\mu_3} g^{\mu_1 \mu_2} \right]. \end{aligned} \quad (4.39)$$

This term contains no  $\bar{A}_0 A_0^3$  contribution, so that the four-gluon vertex does not change. The ghost term in (4.38) gives the vertices (Figs. 4.12b,c)

$$-g_0 f^{ab_1 b_2} (k_1 + k_2)^\mu, \quad ig_0^2 f^{a_1 b_1 c} f^{a_2 b_2 c} g^{\mu_1 \mu_2}.$$

The terms with  $1/a_0$  in the three-gluon vertex contain  $k_1^{\mu_1}$  or  $k_2^{\mu_2}$ ; when they are multiplied by the propagator  $D_{\mu_1 \nu}^0(k_1)$  or  $D_{\mu_2 \nu}^0(k_2)$ , respectively, they extract the term with  $a_0$  from the propagator (3.21), and no terms with negative powers of the gauge parameter  $a_0$  appear.

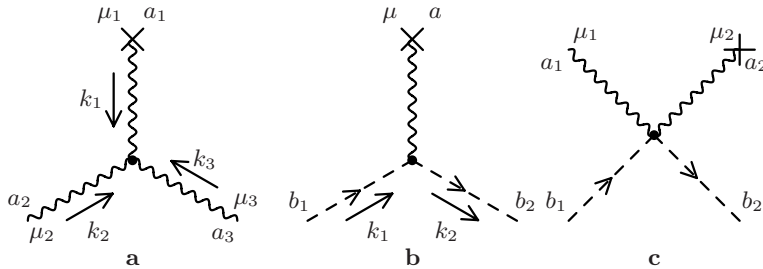


**Fig. 4.12.** Vertices of the interaction with the background field

The sum of one-particle-irreducible background-field vertex diagrams not including the external propagators is the proper vertex  $ig_0 t^a \Gamma_{bf}^\mu(p, q)$ , where  $p$  is the incoming quark momentum,  $p' = p + q$  is the outgoing quark momentum, and  $\mu$  and  $a$  are the background-field gluon polarization and colour

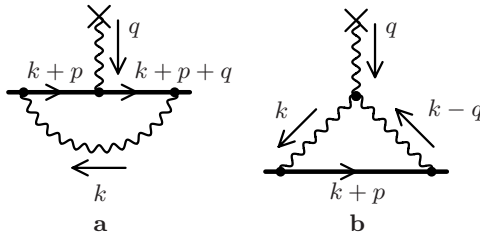


**Fig. 4.13.** One-loop proper vertex

indices. The vertex function is  $\Gamma_{\text{bf}}^\mu(p, q) = \gamma^\mu + \Lambda_{\text{bf}}^\mu(p, q)$ , where  $\Lambda_{\text{bf}}^\mu(p, q)$  contains one-loop (Fig. 4.13) and higher-loop corrections.

Now we are going to derive the Ward identity for  $\Lambda_{\text{bf}}^\mu(p, q)q_\mu$ . Background-field vertices obey the simple identities shown in Fig. 4.14. Here a gluon line with a black triangle at the end means the contraction of the vertex with the incoming gluon momentum (as in Fig. 3.15); the colour structures are singled out as the prefactors. Starting from each diagram for  $\Sigma(p)$ , we can obtain a set of diagrams for  $\Lambda_{\text{bf}}^\mu$  by attaching the background-field gluon to each possible place. For example, starting from the one-loop diagram Fig. 3.5 for  $\Sigma(p)$ , we can attach the external gluon either to the quark line or to the gluon line, obtaining the diagrams in Fig. 4.13. The results of their contraction with  $q_\mu$  are shown in Figs. 4.15a,b. The differences in the square brackets are equal to each other. The colour factors combine to give the colour factor of Fig. 3.5 times  $t^a$  (Fig. 4.15c), owing to the definition of the colour factor of the three-gluon vertex (Fig. 3.10). Therefore, we have the Ward identity

$$\begin{aligned} \Lambda_{\text{bf}}^\mu(p, q)q_\nu &= \Sigma(p) - \Sigma(p + q) \\ \text{or } \quad \Gamma_{\text{bf}}^\mu(p, q)q_\mu &= S^{-1}(p + q) - S^{-1}(p). \end{aligned} \quad (4.40)$$

This identity also holds at higher orders of perturbation theory. To verify this, one has to derive identities similar to Fig. 4.14 for other background-field vertices. For an infinitesimal  $q$ , we obtain

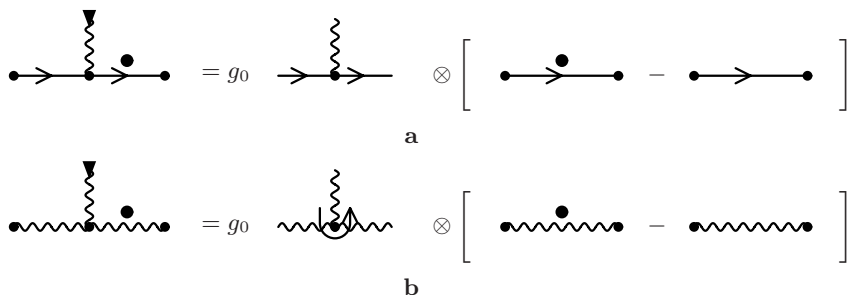


**Fig. 4.14.** Ward identities for the background-field vertices

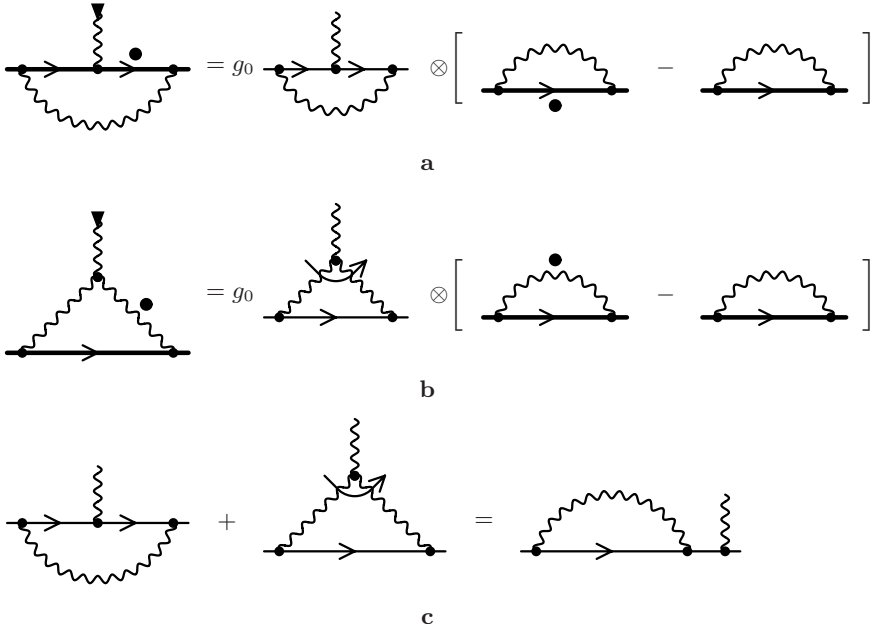


**Fig. 4.15.** Ward identity for the background-field vertex function

$$\Lambda_{\text{bf}}^\mu(p, 0) = -\frac{\partial \Sigma(p)}{\partial p_\mu} \quad \text{or} \quad \Gamma_{\text{bf}}^\mu(p, 0) = \frac{\partial S^{-1}(p)}{\partial p_\mu}. \quad (4.41)$$

The Ward identities (4.40), (4.41) for the background-field vertex are very simple, and are exactly the same as in QED (or in the heavy-electron effective theory, Sect. 3.5). Multiplying the ordinary three-gluon vertex by  $q_\mu$  gives an identity which, in addition to the simple difference shown in Fig. 4.14b, has additional ghost terms (see, e.g., Fig. 3 in [18]). Therefore, the Ward identities for the ordinary quark–gluon vertex function are more complicated than (4.40), (4.41).

The renormalized background field is related to the bare field by  $\bar{A}_0 = \bar{Z}_A^{1/2} \bar{A}$ . The renormalized matrix element is the proper vertex  $g_0 t^a \Gamma_{\text{bf}}^\mu(p, q)$  times  $Z_q \bar{Z}_A^{1/2}$ :  $Z_q \bar{Z}_A^{1/2} Z_\alpha^{1/2} g t^a \Gamma_{\text{bf}}^\mu(p, q)$ . At  $q = 0$ , the factor  $Z_q$  converts  $S^{-1}$  in (4.41) into  $S_r^{-1}$ , making it finite. Therefore,  $Z_\alpha \bar{Z}_A = 1$ , just as in QED (or in heavy-electron effective theory, Sect. 3.5). In other words,  $g_0 \bar{A}_0 = g \bar{A}$ .

The scattering amplitude of the on-shell quark in an external field is  $g Z_Q^{\text{os}} \bar{u}(p') \Gamma_{\text{bf}}^\mu t^a u(p)$ , where  $p^2 = p'^2 = m^2$ ,  $(\not{p} - m)u(p) = 0$ ,  $(\not{p}' - m)u(p') = 0$ . It is UV finite, but may contain IR divergences. It can be expressed via two scalar form factors. For comparison with HQET, it is most convenient to use the Dirac and chromomagnetic form factors:

$$\bar{u}(p') \Gamma_{\text{bf}}^\mu t^a u(p) = \bar{u}(p') \left( F_1^0(q^2) \frac{(p + p')^\mu}{2m} + G_m^0(q^2) \frac{[\not{q}, \gamma^\mu]}{4m} \right) t^a u(p), \quad (4.42)$$

where the renormalized form factors are  $F_1(q^2) = Z_Q^{\text{os}} F_1^0(q^2)$ ,  $G_m(q^2) = Z_Q^{\text{os}} G_m^0(q^2)$ . The form factors can be singled out by the appropriate projectors. Let us rewrite (4.42) as

$$\bar{u}(p') \Gamma_{\text{bf}}^\mu t^a u(p) = \bar{u}(p') \sum F_i T_i^\mu t^a u(p),$$

$$F_1 = F_1^0(q^2), \quad F_2 = G_m^0(q^2), \quad T_1^\mu = \frac{(p + p')^\mu}{2m}, \quad T_2^\mu = \frac{[\not{q}, \gamma^\mu]}{4m},$$

and calculate the traces

$$\frac{1}{4} \text{Tr } \Gamma_{\text{bf}\mu} (\not{p} + 1) T_i^\mu (\not{p} + \not{q}/m + 1).$$

Solving the linear system for  $F_i$ , we obtain

$$F_1^0(q^2) = \frac{1}{2(d-2)(1-q^2/(4m^2))} \frac{1}{4} \text{Tr } \Gamma_{\text{bf}\mu} (\not{p} + 1) \\ \times \left( \frac{d-2+q^2/(4m^2)}{1-q^2/(4m^2)} \left( v + \frac{q}{2m} \right)^\mu + \frac{[\not{q}, \gamma^\mu]}{4m} \right) \left( \not{p} + \frac{\not{q}}{m} + 1 \right),$$

$$G_m^0(q^2) = -\frac{1}{2(d-2)} \frac{1}{4} \text{Tr } \Gamma_{\text{bf}\mu} (\not{p} + 1) \\ \times \left( \frac{1}{1-q^2/(4m^2)} \left( v + \frac{q}{2m} \right)^\mu + \frac{[\not{q}, \gamma^\mu]}{q^2} \right) \left( \not{p} + \frac{\not{q}}{m} + 1 \right). \quad (4.43)$$

There is no singularity in  $G_m^0(q^2)$  at  $q^2 \rightarrow 0$ . We can expand the form factors in  $q^2$  by expanding

$$\Gamma_{\text{bf}}^\mu = \Gamma_0^\mu + \Gamma_1^{\mu\nu} \frac{q_\nu}{m} + \dots,$$

splitting  $q = (q \cdot v)v + q_\perp$  (where  $q \cdot v = -q^2/(2m)$ ), and averaging over the directions of  $q_\perp$  in the  $(d-1)$ -dimensional subspace orthogonal to  $v$ :

$$\overline{q^\alpha} = -\frac{q^2}{2m} v^\alpha, \quad \overline{q^\alpha q^\beta} = \frac{q^2}{d-1} \left[ \left( 1 - \frac{q^2}{4m^2} \right) g^{\alpha\beta} - \left( 1 - d \frac{q^2}{4m^2} \right) v^\alpha v^\beta \right].$$

Thus we obtain

$$F_1^0(q^2) = \frac{1}{4} \text{Tr } \Gamma_0^\mu (\not{p} + 1) v_\mu + \mathcal{O}(q^2/m^2),$$

$$G_m^0(q^2) = \frac{1}{d-1} \frac{1}{4} \text{Tr } \Gamma_0^\mu (\not{p} + 1) (\gamma_\mu - v_\mu) \\ + \frac{2}{(d-1)(d-2)} \frac{1}{4} \text{Tr } \Gamma_1^{\mu\nu} (\not{p} + 1) (\gamma_\mu \gamma_\nu - g_{\mu\nu} + \gamma_\mu v_\nu - \gamma_\nu v_\mu) \\ + \mathcal{O}(q^2/m^2). \quad (4.44)$$

The Dirac form factor at  $q = 0$  is unity, owing to the Ward identity (4.41):

$$\begin{aligned} F_1(0) &= Z_Q^{\text{os}} \left[ 1 + \frac{1}{4} \text{Tr } A_{\text{bf}\mu}(mv, 0)(\not{p} + 1)v^\mu \right] \\ &= Z_Q^{\text{os}} \left[ 1 - v^\mu \frac{\partial}{\partial p^\mu} \frac{1}{4} \text{Tr } \Sigma(p)(\not{p} + 1) \Big|_{p=mv} \right] \\ &= Z_Q^{\text{os}} [1 - T'(0)] = 1 \end{aligned} \quad (4.45)$$

(see (4.28)). The total colour charge of the heavy quark is not changed by renormalization.

The heavy-quark chromomagnetic moment  $\mu_g = G_m(0)$  (4.44) can be calculated as follows. First, we apply the projector in (4.44) to the integrand of each diagram, differentiating all  $q$ -dependent propagators and vertices (Fig. 4.13), and obtain the bare  $\mu_g^0$  via scalar integrals (4.15). Then we multiply  $\mu_g^0$  by  $Z_Q^{\text{os}}$  (4.29). The one-loop result is [19]

$$\mu_g = 1 + \frac{g_0^2 m^{-2\varepsilon}}{(4\pi)^{d/2}} \frac{\Gamma(\varepsilon)}{2(d-3)} [2(d-4)(d-5)C_F - (d^2 - 8d + 14)C_A] + \dots \quad (4.46)$$

Setting  $g_0 \rightarrow e_0$ ,  $C_F \rightarrow 1$ ,  $C_A \rightarrow 0$ , we reproduce the electron magnetic moment  $\mu = 1 + \alpha/(2\pi) + \dots$  in QED. It is convergent. The heavy-quark chromomagnetic moment in QCD (4.46) contains an IR divergence associated with the colour factor  $C_A$ . The two-loop correction to (4.46) was calculated in [16], and the effect of another massive flavour (say, the c-loop correction to the b-quark chromomagnetic moment) was considered in [17].

## 4.5 Scattering in an External Gluonic Field in HQET

First, let us consider the leading (zeroth) order in  $1/m$ . Let the sum of one-particle-irreducible bare vertex diagrams in the background-field method be  $i g_0 t^a \tilde{\Gamma}_{\text{bf}}^\mu(\omega, q)$ , where  $\omega$  and  $\omega' = \omega + q \cdot v$  are the residual energies of the initial and the final quark;  $\tilde{\Gamma}_{\text{bf}}^\mu(\omega, q) = v^\mu + \tilde{A}_{\text{bf}}^\mu(\omega, q)$ . There are two vectors in the problem,  $v^\mu$  and  $q^\mu$ , and hence the vertex function has the structure

$$\begin{aligned} \tilde{A}_{\text{bf}}^\mu &= \tilde{A}_s(\omega, \omega', q^2)v^\mu + \tilde{A}_a(\omega, \omega', q^2)q^\mu, \\ \tilde{A}_s(\omega, \omega', q^2) &= \tilde{A}_s(\omega', \omega, q^2), \quad \tilde{A}_a(\omega, \omega', q^2) = -\tilde{A}_a(\omega', \omega, q^2). \end{aligned} \quad (4.47)$$

This function has been calculated, at one loop, in [18]. It obeys the Ward identity

$$\begin{aligned} \tilde{A}_{\text{bf}}^\mu(\omega, q)q_\nu &= \tilde{A}_s(\omega' - \omega) + \tilde{A}_a q^2 = \tilde{\Sigma}(\omega) - \tilde{\Sigma}(\omega') \\ \text{or} \quad \tilde{\Gamma}_{\text{bf}}^\mu(\omega, q)q_\mu &= \tilde{S}^{-1}(\omega') - \tilde{S}^{-1}(\omega), \end{aligned} \quad (4.48)$$

or, for  $q \rightarrow 0$ ,

$$\tilde{A}_s(\omega, \omega, 0) = -\frac{d\tilde{\Sigma}(\omega)}{d\omega}. \quad (4.49)$$

On the mass shell  $\omega = 0$ ,  $\omega' = 0$ , the renormalized scattering amplitude with linear accuracy in  $q$  is

$$\begin{aligned} \tilde{Z}_Q^{\text{os}}(1 + A_s(0, 0, 0))\bar{u}_v(q)v^\mu u_v(0) &= \tilde{Z}_Q^{\text{os}} \left( 1 - \frac{d\tilde{\Sigma}(\omega)}{d\omega} \right)_{\omega=0} \bar{u}_v(q)v^\mu u_v(0) \\ &= \bar{u}_v(q)v^\mu u_v(0). \end{aligned} \quad (4.50)$$

The total colour charge of the static quark is not changed by renormalization.

Now we shall make a short digression, and derive the one-loop renormalization of the QCD coupling constant (3.6) from the ordinary HQET quark-gluon vertex  $\tilde{\Gamma}^\mu(\omega, q)$ . When the bare vertex  $\tilde{\Gamma}^\mu$  is expressed via the renormalized quantities  $\alpha_s$  and  $a$ , it should become  $\tilde{Z}_\Gamma \tilde{\Gamma}_r^\mu$ , where  $\tilde{Z}_\Gamma$  is a minimal (3.3) renormalization constant, and the renormalized vertex  $\tilde{\Gamma}_r^\mu$  is finite at  $\varepsilon \rightarrow 0$ . When  $g_0 \tilde{\Gamma}^\mu = g \tilde{\Gamma}_r^\mu Z_\alpha^{1/2} \tilde{Z}_\Gamma$  is multiplied by the external-leg renormalization factors  $\tilde{Z}_Q Z_A^{1/2}$ , it should give a finite matrix element. Therefore,  $Z_\alpha = (\tilde{Z}_\Gamma \tilde{Z}_Q)^{-2} Z_A^{-1}$ . At one loop (Fig. 4.16), the HQET vertex  $\tilde{\Gamma}^\mu$  has been calculated in [18]. It obeys a more complicated Ward identity than does the background-field vertex  $\tilde{\Gamma}_{\text{bf}}^\mu(\omega, q)$ . If we write the vertex as  $\tilde{\Gamma}^\mu = \tilde{\Gamma}_{\text{bf}}^\mu + \Delta \tilde{\Lambda}^\mu$ , then  $-\Delta \tilde{\Lambda}^\mu$  is given by Fig. 4.16b, where only the  $1/a_0$  terms in (4.39) are substituted for the three-gluon vertex. Multiplying  $\tilde{\Gamma}^\mu$  by  $\tilde{Z}_Q$ , we obtain at one loop

$$v^\mu + (\text{finite}) + \Delta \tilde{\Lambda}^\mu = \tilde{Z}_Q \tilde{Z}_\Gamma \tilde{\Gamma}_r^\mu,$$

because  $\tilde{Z}_Q \tilde{\Gamma}_{\text{bf}}^\mu$  is finite. Therefore, we need only the UV divergence of  $\Delta \tilde{\Lambda}^\mu$ . This divergence does not depend on the external momenta, and therefore, we may set them to zero. An IR cut-off is then necessary in order to avoid IR  $1/\varepsilon$  terms. We have

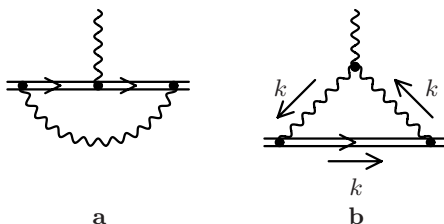


**Fig. 4.16.** One-loop HQET proper vertex

$$\begin{aligned} \Delta\tilde{\Lambda}^\mu v_\mu = & -i\frac{C_A}{2g_0} \int \frac{d^d k}{(2\pi)^d} i g_0 v^{\alpha'} \frac{i}{k \cdot v} i g_0 v^{\beta'} \frac{-i}{k^2} \left[ g_{\alpha'\alpha} - (1-a_0) \frac{k_{\alpha'} k_\alpha}{k^2} \right] \\ & \times \left[ g_{\beta'\beta} - (1-a_0) \frac{k_{\beta'} k_\beta}{k^2} \right] (-i) g_0 \frac{k^\alpha g^{\beta\mu} + k^\beta g^{\alpha\mu}}{a_0} v_\mu . \end{aligned}$$

Here  $1/a_0$  cancels, as explained after (4.39):

$$\Delta\tilde{\Lambda}^\mu v_\mu = -ig_0^2 C_A \int \frac{d^d k}{(2\pi)^d} \frac{1}{(k^2)^2} \left[ 1 - (1-a_0) \frac{(k \cdot v)^2}{k^2} \right].$$

Averaging over the directions of  $v$ , we can replace  $(k \cdot v)^2$  by  $k^2/d$ . The UV  $1/\varepsilon$  pole of the resulting integral is

$$\int \frac{d^d k}{(2\pi)^d} \frac{1}{(k^2)^2} \Big|_{\text{UV}} = \frac{i}{8\pi^2} \int_\lambda^\infty k_E^{-1-2\varepsilon} dk_E = \frac{i}{(4\pi)^2 \varepsilon} \lambda^{-2\varepsilon} = \frac{i}{(4\pi)^2 \varepsilon}, \quad (4.51)$$

where  $\lambda$  is the IR cut-off, and terms regular at  $\varepsilon \rightarrow 0$  are omitted. Therefore,

$$\tilde{Z}_Q \tilde{Z}_\Gamma = 1 + C_A \frac{a+3}{4} \frac{\alpha_s}{4\pi\varepsilon} + \dots$$

The  $C_F$  terms cancel here because  $\tilde{Z}_\Gamma \tilde{Z}_Q = 1$  in the abelian case (Sect. 3.5). Using (3.31), we derive  $Z_\alpha$  (see (3.10) and (3.6)); the gauge dependence cancels, as expected.

There are two kinds of  $1/m$  corrections to the scattering amplitude: diagrams with a single kinetic vertex, and those with a single chromomagnetic vertex. Let us forget for a while that we have obtained the result  $C_k = 1$  (4.9), and denote the sum of one-particle-irreducible bare vertex diagrams in the background-field method containing a single kinetic-energy vertex by  $i g_0 t^a [C_k^0/(2m)] \tilde{\Gamma}_k^\mu(\tilde{p}, q)$ , where  $\tilde{p} = \omega v + p_\perp$  and  $\tilde{p}' = \tilde{p} + q = \omega' v + p'_\perp$  are the initial and final residual momenta of the heavy quark;  $\tilde{\Gamma}_k = (p + p')_\perp^\mu + \Lambda_k^\mu(\tilde{p}, q)$ . The dependence on  $p_\perp$  and  $p'_\perp$  comes only from the kinetic-energy vertex (Sect. 4.1), which is at most quadratic in them. Therefore, the vertex function has the structure

$$\begin{aligned} \tilde{\Lambda}_k^\mu(\tilde{p}, q) = & \tilde{\Lambda}_{ks}(\omega, \omega', q^2) (p + p')_\perp^\mu \\ & + \left[ \tilde{\Lambda}_{k1}(\omega, \omega', q^2) p_\perp^2 + \tilde{\Lambda}_{k1}(\omega', \omega, q^2) p'_\perp^2 + \tilde{\Lambda}_{k0}(\omega, \omega', q^2) \right] v^\mu \\ & + \left[ \tilde{\Lambda}_{k3}(\omega, \omega', q^2) p_\perp^2 - \tilde{\Lambda}_{k3}(\omega', \omega, q^2) p'_\perp^2 + \tilde{\Lambda}_{k2}(\omega, \omega', q^2) \right] q^\mu , \end{aligned}$$

$$\tilde{\Lambda}_{ks}(\omega, \omega', q^2) = \tilde{\Lambda}_{ks}(\omega', \omega, q^2),$$

$$\tilde{\Lambda}_{k0}(\omega, \omega', q^2) = \tilde{\Lambda}_{k0}(\omega', \omega, q^2),$$

$$\tilde{\Lambda}_{k2}(\omega, \omega', q^2) = -\tilde{\Lambda}_{k2}(\omega', \omega, q^2). \quad (4.52)$$

Similarly to Sect. 4.1, the variation of the diagrams for  $\tilde{\Lambda}_{\text{bf}}(\tilde{p}, q)$  for  $v \rightarrow v + \delta v$  is equal to that of the diagrams for  $\tilde{\Lambda}_k(\tilde{p}, q)$  for  $p_\perp \rightarrow p_\perp + \delta p_\perp$ , if  $\delta v = (C_k/m)\delta p_\perp$ . Therefore, the reparametrization invariance ensures that

$$\begin{aligned}\tilde{\Lambda}_{\text{ks}}(\omega, \omega', q^2) &= \tilde{\Lambda}_s(\omega, \omega', q^2), \\ \tilde{\Lambda}_{k1}(\omega, \omega', q^2) &= \frac{\partial \tilde{\Lambda}_s(\omega, \omega', q^2)}{\partial \omega}, \\ \tilde{\Lambda}_{k3}(\omega, \omega', q^2) &= \frac{\partial \tilde{\Lambda}_a(\omega, \omega', q^2)}{\partial \omega}.\end{aligned}\quad (4.53)$$

The Ward identity

$$\tilde{\Lambda}_k^\mu(\tilde{p}, q)q_\mu = \tilde{\Sigma}_k(\tilde{p}) - \tilde{\Sigma}_k(\tilde{p}') \quad (4.54)$$

ensures, owing to (4.5), that

$$\begin{aligned}-\tilde{\Lambda}_{\text{ks}}(\omega, \omega', q^2) + \tilde{\Lambda}_{k1}(\omega, \omega', q^2)(\omega' - \omega) + \tilde{\Lambda}_{k3}(\omega, \omega', q^2)q^2 &= \frac{d\tilde{\Sigma}(\omega)}{d\omega}, \\ \tilde{\Lambda}_{k0}(\omega, \omega', q^2)(\omega' - \omega) + \tilde{\Lambda}_{k2}(\omega, \omega', q^2)q^2 &= \tilde{\Sigma}_{k0}(\omega) - \tilde{\Sigma}_{k0}(\omega').\end{aligned}\quad (4.55)$$

The first relation here is, owing to (4.53), just the derivative of (4.48) with respect to  $\omega$ .

On the mass shell  $\omega = 0$ ,  $\omega' = 0$ , the kinetic-energy correction to the renormalized scattering amplitude with linear accuracy in  $q$  is

$$\frac{C_k^0}{2m} \tilde{Z}_Q^{\text{os}}(1 + \Lambda_s(0, 0, 0))\bar{u}_v(q)(p + p')_\perp^\mu u_v(0) = \frac{C_k^0}{2m} \bar{u}_v(q)(p + p')_\perp^\mu u_v(0). \quad (4.56)$$

Let the sum of one-particle-irreducible bare vertex diagrams in the background-field method containing a single chromomagnetic vertex be

$$ig_0 t^a \frac{C_m^0}{4m} \frac{1 + \not{p}}{2} [\not{q}, \gamma^\mu] \frac{1 + \not{p}}{2} \tilde{\Gamma}_m(\omega, \omega', q^2), \quad (4.57)$$

where  $\tilde{\Gamma}_m(\omega, \omega', q^2) = 1 + \tilde{\Lambda}_m(\omega, \omega', q^2)$ . Reparametrization invariance does not relate  $\tilde{\Lambda}_m$  to any vertex function of zeroth order in  $1/m$ . We have no better alternative than a direct calculation. In order to obtain the on-shell scattering amplitude with linear accuracy in  $q$ , we need only the static-quark chromomagnetic moment  $\tilde{\mu}_g^0 = \tilde{\Gamma}_m(0, 0, 0)$ . All loop diagrams for  $\tilde{\Lambda}_m$  vanish, except those with loops of some massive quark. Such diagrams first appear at two loops. They can be calculated using the method of Sect. 4.3. The renormalized matrix element  $\tilde{\mu}_g = \tilde{Z}_Q^{\text{os}} \tilde{\mu}_g^0$  of the chromomagnetic operator  $\mathcal{O}_m^0$  is [16]

$$\tilde{\mu}_g = 1 + C_A T_F \frac{g_0^4 \sum m_i^{-4\varepsilon}}{(4\pi)^d} F^2(\varepsilon) \frac{d^2 - 9d + 16}{(d-2)(d-5)(d-7)}, \quad (4.58)$$

where the sum is over all massive flavours (except the heavy flavour of our HQET, of course).

## 4.6 Chromomagnetic Interaction

Now we are ready to compare the on-shell scattering amplitudes in full QCD and in HQET. The HQET spinors  $u_v(\tilde{p})$  are two-component in the  $v$  rest frame:  $\not{p}u_v(\tilde{p}) = 0$ . The corresponding QCD spinors  $u(mv + \tilde{p})$  are related to them by the Foldy–Wouthuysen transformation (see, e.g., [7])

$$u(mv + \tilde{p}) = \left( 1 + \frac{\not{p}}{2m} + \mathcal{O}(\not{p}^2/m^2) \right) u_v(\tilde{p}). \quad (4.59)$$

A quick check:

$$(m\not{p} + \not{\tilde{p}} - m)u(mv + \tilde{p}) = m \left[ \not{p} - 1 + (\not{p} + 1)\frac{\not{p}}{2m} \right] u_v(\tilde{p}) = 0,$$

because we may set  $\tilde{p} \cdot v = 0$  in the  $1/m$  term;

$$\bar{u}(mv + \tilde{p})\gamma^\mu u(mv + \tilde{p}) = \frac{(mv + \tilde{p})^\mu}{m} \bar{u}_v(\tilde{p})u_v(\tilde{p}).$$

Expanding the QCD scattering amplitude up to linear terms in  $q/m$  and re-expressing it via HQET spinors, we obtain

$$\bar{u}_v(q) \left( v^\mu + \frac{q^\mu}{2m} + \mu_g \frac{[\not{q}, \gamma^\mu]}{4m} \right) t^a u_v(0). \quad (4.60)$$

The HQET scattering amplitude with  $1/m$  accuracy is

$$\bar{u}_v(q) \left( v^\mu + C_k(\mu) \tilde{Z}_k^{-1}(\mu) \frac{q^\mu}{2m} + C_m(\mu) \tilde{Z}_m^{-1}(\mu) \mu_g \frac{[\not{q}, \gamma^\mu]}{4m} \right) t^a u_v(0). \quad (4.61)$$

Both scattering amplitudes (4.60) and (4.61) are renormalized and hence UV finite. Both may contain IR divergences. By construction, HQET is identical to QCD in the IR region, so that these IR divergences are the same. For example, if there are no other massive flavours in the theory, all loop corrections to  $\tilde{\mu}_g^0$  vanish because they contain no scale. These zero integrals contain UV and IR divergences which cancel. The UV divergences are removed by  $\tilde{Z}_m^{-1}(\mu)$ , and the IR ones match those in  $\mu_g$ .

Comparing the coefficients of  $q^\mu/m$ , we again see that  $\tilde{Z}_k = 1$  and  $C_k(\mu) = 1$  (4.9). Comparing the coefficients of  $[\not{q}, \gamma^\mu]/m$ , we obtain

$$\tilde{Z}_m^{-1}(\mu)C_m(\mu) = \frac{\mu_g}{\tilde{\mu}_g}. \quad (4.62)$$

In the one-loop approximation, re-expressing (4.46) via  $\alpha_s(\mu)$  (3.4) and expanding in  $\varepsilon$ , we obtain

$$\begin{aligned}\tilde{Z}_m^{-1}(\mu)C_m(\mu) &= 1 + \frac{\alpha_s(\mu)}{4\pi}e^{-2L\varepsilon} \left[ 2C_F + \left( \frac{1}{\varepsilon} + 2 \right) C_A \right], \\ L &= \log \frac{m}{\mu}.\end{aligned}\tag{4.63}$$

The minimal (3.3) renormalization constant  $\tilde{Z}_m$  that makes  $C_m$  finite is

$$\tilde{Z}_m = 1 - C_A \frac{\alpha_s}{4\pi\varepsilon} + \dots,\tag{4.64}$$

and the chromomagnetic interaction constant is

$$C_m(\mu) = 1 + 2(-C_A L + C_F + C_A) \frac{\alpha_s(m)}{4\pi} + \dots\tag{4.65}$$

Therefore, the anomalous dimension of the chromomagnetic operator and  $C_m(m)$  are [19]

$$\tilde{\gamma}_m = 2C_A \frac{\alpha_s}{4\pi} + \dots, \quad C_m(m) = 1 + 2(C_F + C_A) \frac{\alpha_s(m)}{4\pi} + \dots\tag{4.66}$$

The two-loop anomalous dimension was calculated in [2] within HQET, and (a week later) in [16] by QCD/HQET matching:

$$\tilde{\gamma}_m = 2C_A \frac{\alpha_s}{4\pi} + \frac{4}{9} C_A (17C_A - 13T_F n_f) \left( \frac{\alpha_s}{4\pi} \right)^2 + \dots\tag{4.67}$$

The anomalous dimension vanishes in QED, where  $C_A = 0$ . It is most convenient to calculate

$$C_m(m) = 1 + C_1 \frac{\alpha_s(m)}{4\pi} + C_2 \left( \frac{\alpha_s(m)}{4\pi} \right)^2 + \dots,$$

because it contains no large logarithms. Then we can use the renormalization-group equation to find  $C_m(\mu)$  at  $\mu \ll m$ . The two-loop term in  $C_m(m)$  was found in [16].

The scattering amplitude (4.61) does not depend on the arbitrary renormalization scale  $\mu$ ; the matrix element  $\tilde{\mu}_g^0$  of the bare chromomagnetic operator is also  $\mu$ -independent. Therefore,

$$\tilde{Z}_m^{-1}(\mu)C_m(\mu) = \text{const.}$$

Differentiating this equality with respect to  $\log \mu$ , we obtain the renormalization-group equation

$$\frac{dC_m(\mu)}{d \log \mu} = \tilde{\gamma}_m(\alpha_s(\mu))C_m(\mu).\tag{4.68}$$

If  $L = \log(m/\mu)$  is not very large, it is reasonable to find the solution as a series in  $\alpha_s(m)$ . Re-expressing  $\alpha_s(\mu)$  via  $\alpha_s(m)$  as

$$\frac{\alpha_s(\mu)}{4\pi} = \frac{\alpha_s(m)}{4\pi} \left[ 1 + 2\beta_0 L \frac{\alpha_s(m)}{4\pi} + \dots \right]$$

in

$$\tilde{\gamma}_m(\alpha_s(\mu)) = \gamma_0 \frac{\alpha_s(\mu)}{4\pi} + \gamma_1 \left( \frac{\alpha_s(\mu)}{4\pi} \right)^2 + \dots,$$

we obtain the equation

$$\frac{dC_m(\mu)}{dL} + \left[ \gamma_0 \frac{\alpha_s(m)}{4\pi} \left( 1 + 2\beta_0 L \frac{\alpha_s(m)}{4\pi} \right) + \gamma_1 \left( \frac{\alpha_s(m)}{4\pi} \right)^2 + \dots \right] C_m(\mu),$$

which can be solved order by order in  $\alpha_s(m)$ :

$$\begin{aligned} C_m(\mu) &= 1 + (-\gamma_0 L + C_1) \frac{\alpha_s(m)}{4\pi} \\ &+ \left[ \gamma_0 \left( \frac{\gamma_0}{2} - \beta_0 \right) L^2 - (\gamma_1 + C_1 \gamma_0) L + C_2 \right] \left( \frac{\alpha_s(m)}{4\pi} \right)^2 + \dots \end{aligned} \quad (4.69)$$

If  $[\alpha_s/(4\pi)]L \sim 1$ , we have to solve the renormalization-group equation (4.68) in another way. Dividing this equation by  $d \log \alpha_s(\mu)/d \log \mu$  (3.5) (at  $\varepsilon = 0$ ), we obtain

$$\frac{d \log C_m(\mu)}{d \log \alpha_s} + \frac{\tilde{\gamma}_m(\alpha_s)}{2\beta(\alpha_s)} = 0.$$

The solution of this equation is

$$C_m(\mu) = C_m(m) \exp \left[ - \int_{\alpha_s(m)}^{\alpha_s(\mu)} \frac{\tilde{\gamma}_m(\alpha_s)}{2\beta(\alpha_s)} \frac{d\alpha_s}{\alpha_s} \right]. \quad (4.70)$$

Subtracting and adding  $\tilde{\gamma}_{m0}/(2\beta_0)$  in the integrand, we can rewrite the solution as

$$C_m(\mu) = C_m(m) \left( \frac{\alpha_s(\mu)}{\alpha_s(m)} \right)^{-\tilde{\gamma}_{m0}/(2\beta_0)} K_{-\tilde{\gamma}_m}(\alpha_s(\mu)) K_{\tilde{\gamma}_m}(\alpha_s(m)). \quad (4.71)$$

Here we have introduced a useful notation: for any anomalous dimension  $\gamma(\alpha_s)$ , we define

$$K_\gamma(\alpha_s) = \exp \int_0^{\alpha_s} \left( \frac{\gamma(\alpha_s)}{2\beta(\alpha_s)} - \frac{\gamma_0}{2\beta_0} \right) \frac{d\alpha_s}{\alpha_s} = 1 + \frac{\gamma_0}{2\beta_0} \left( \frac{\gamma_1}{\gamma_0} - \frac{\beta_1}{\beta_0} \right) \frac{\alpha_s}{4\pi} + \dots \quad (4.72)$$

This function has the obvious properties

$$K_0(\alpha_s) = 1, \quad K_{-\gamma}(\alpha_s) = K_\gamma^{-1}(\alpha_s), \quad K_{\gamma_1+\gamma_2}(\alpha_s) = K_{\gamma_1}(\alpha_s)K_{\gamma_2}(\alpha_s).$$

The solution (4.71) can also be written as

$$\begin{aligned} C_m(\mu) &= \hat{C}_m(m) \left( \frac{\alpha_s(\mu)}{\alpha_s(m)} \right)^{-\tilde{\gamma}_{m0}/(2\beta_0)} K_{-\tilde{\gamma}_m}(\alpha_s(\mu)) \\ &= \left( \frac{\alpha_s(\mu)}{\alpha_s(m)} \right)^{-\tilde{\gamma}_{m0}/(2\beta_0)} \\ &\quad \times \left[ 1 + C_1 \frac{\alpha_s(m)}{4\pi} - \frac{\tilde{\gamma}_{m0}}{2\beta_0} \left( \frac{\tilde{\gamma}_{m1}}{\tilde{\gamma}_{m0}} - \frac{\beta_1}{\beta_0} \right) \frac{\alpha_s(\mu) - \alpha_s(m)}{4\pi} + \dots \right], \end{aligned} \quad (4.73)$$

where

$$\begin{aligned} \hat{C}_m(m) &= C_m(m) K_{\tilde{\gamma}_m}(\alpha_s(m)) \\ &= 1 + \left[ C_1 + \frac{\tilde{\gamma}_{m0}}{2\beta_0} \left( \frac{\tilde{\gamma}_{m1}}{\tilde{\gamma}_{m0}} - \frac{\beta_1}{\beta_0} \right) \right] \frac{\alpha_s(m)}{4\pi} + \dots \end{aligned}$$

Note that this function of  $\mu$  and  $m$  can be presented as a product of a function of  $m$ ,

$$\hat{C}_m(m) \alpha_s(m)^{\tilde{\gamma}_{m0}/(2\beta_0)},$$

and a function of  $\mu$ ,

$$K_{-\tilde{\gamma}_m}(\alpha_s(\mu)) \alpha_s(\mu)^{-\tilde{\gamma}_{m0}/(2\beta_0)}.$$

The fractional power of  $\alpha_s(\mu)/\alpha_s(m)$  in (4.73) contains all leading logarithms  $(\alpha_s L)^n$  in the perturbative series (4.69); the correction inside the brackets contains the subleading logarithms. We cannot use the  $C_2$  term here until we know  $\tilde{\gamma}_{m2}$ .

The largest term missing in (4.69) is  $[\alpha_s/(4\pi)]^3 L^3$ . The largest term missing in (4.71) is  $C_2[\alpha_s/(4\pi)]^2$ . Comparing these errors, we can estimate the value of  $L$  at which (4.71) becomes a better approximation than (4.69).

The most obvious effect of the chromomagnetic interaction is the hyperfine B–B\* splitting:

$$m_{B^*} - m_B = \frac{2}{3m_B} C_m(\mu) \mu_G^2(\mu) + \mathcal{O}\left(\frac{1}{m_B^2}\right), \quad (4.74)$$

where  $\mu_G^2(\mu)$  is the matrix element of the chromomagnetic interaction operator. The product  $C_m(\mu) \mu_G^2(\mu)$  is, of course,  $\mu$ -independent, and hence

$$\mu_G^2(\mu) = \hat{\mu}_G^2 \left( \frac{\alpha_s(\mu)}{4\pi} \right)^{\tilde{\gamma}_{m0}/(2\beta_0)} K_{\tilde{\gamma}_m}(\alpha_s(\mu)). \quad (4.75)$$

The quantity  $\hat{\mu}_G^2$  is  $\mu$ -independent, and hence is equal to  $\Lambda_{\overline{\text{MS}}}^2$  times some number; we obtain

$$m_{B^*} - m_B = \frac{2}{3m_b} \left( \frac{\alpha_s(m_b)}{4\pi} \right)^{\tilde{\gamma}_{m0}/(2\beta_0)} \hat{C}_m(m_b) \hat{\mu}_G^2 + \mathcal{O}\left(\frac{1}{m_b^2}\right). \quad (4.76)$$

We can write a similar equation for  $m_{D^*} - m_D$ . The quantities  $\hat{\mu}_G^2$  in the b-quark and the c-quark HQETs differ by an amount of order  $[\alpha_s(m_c)/\pi]^2$  due to decoupling of c-quark loops (Sect. 4.7). Multiplying (4.76) by  $m_{B^*} + m_B = 2m_b [1 + \mathcal{O}(1/m_b)]$  and dividing by a similar D-meson equation, we obtain [2]

$$\begin{aligned} \frac{m_{B^*}^2 - m_B^2}{m_{D^*}^2 - m_D^2} &= \left( \frac{\alpha_s(m_b)}{\alpha_s(m_c)} \right)^{\tilde{\gamma}_{m0}/(2\beta_0)} \\ &\times \left[ 1 - \left( C_1 + \frac{\tilde{\gamma}_{m0}}{2\beta_0} \left( \frac{\tilde{\gamma}_{m1}}{\tilde{\gamma}_{m0}} - \frac{\beta_1}{\beta_0} \right) \right) \frac{\alpha_s(m_c) - \alpha_s(m_b)}{4\pi} + \mathcal{O}\left(\left(\frac{\alpha_s}{\pi}\right)^2\right) \right] \\ &+ \mathcal{O}\left(\frac{\Lambda_{\overline{\text{MS}}}}{m_{c,b}}\right). \end{aligned} \quad (4.77)$$

In the interval between  $m_c$  and  $m_b$ , the relevant number of flavours is  $n_f = 4$ :

$$\frac{m_{B^*}^2 - m_B^2}{m_{D^*}^2 - m_D^2} = \left( \frac{\alpha_s(m_b)}{\alpha_s(m_c)} \right)^{9/25} \left[ 1 - \frac{7921}{3750} \frac{\alpha_s(m_c) - \alpha_s(m_b)}{\pi} \right] + \dots$$

The experimental value of this ratio is 0.89. The leading logarithmic approximation gives 0.84; the next-to-leading correction reduces this result by 9%, giving 0.76. The agreement is quite good, taking into account the fact that the  $1/m_c$  correction may be rather large.

## 4.7 Decoupling of Heavy-Quark Loops

Let us consider QCD with  $n_l$  light flavours and a single heavy one, say, c. Processes involving only light fields with momenta  $p_i \ll m_c$  can be described by an effective field theory – QCD with  $n_l$  flavours. There are  $1/m_c^n$ -suppressed local operators in the Lagrangian, which are the remnants of heavy-quark loops shrunk to a point. This low-energy effective theory is constructed to reproduce the  $S$ -matrix elements of full QCD expanded to some order in  $p_i/m_c$ . Operators of full QCD can be expanded in operators of the effective theory; higher-dimensional operators are divided by the appropriate powers of  $m_c$ . The coefficients of these  $1/m_c$  expansions are fixed by matching – equating on-shell matrix elements, up to some order in  $p_i/m_c$ . Matching full QCD with the low-energy QCD is called decoupling; it is clearly presented in [15], where references to earlier papers can be found. All quantities in the low-energy theory will be distinguished from those in full QCD by primes.

In particular, the renormalized light fields of full QCD are related to those of the low-energy theory by

$$\begin{aligned} q_i(\mu) &= \zeta_q^{1/2}(\mu, \mu') q'_i(\mu') , \\ A_\alpha(\mu) &= \zeta_A^{1/2}(\mu, \mu') A'_\alpha(\mu') , \quad c(\mu) = \zeta_c^{1/2}(\mu, \mu') c'(\mu') , \end{aligned} \quad (4.78)$$

up to  $1/m_c$ -suppressed terms. The coupling constant and gauge-fixing parameter in the two theories are related by

$$g(\mu) = \zeta_\alpha^{1/2}(\mu, \mu') g'(\mu') , \quad a(\mu) = \zeta_A(\mu, \mu') a'(\mu') \quad (4.79)$$

(we shall see in a moment why the last coefficient is  $\zeta_A$ ). It is more convenient to calculate the coefficients  $\zeta_i^0$  which relate the bare fields and parameters in the two theories. After that, it is easy to find the renormalized coefficients:

$$\begin{aligned} \zeta_q(\mu, \mu') &= \frac{Z'_q(\mu')}{Z_q(\mu)} \zeta_q^0 , \quad \zeta_A(\mu, \mu') = \frac{Z'_A(\mu')}{Z_A(\mu)} \zeta_A^0 , \\ \zeta_c(\mu, \mu') &= \frac{Z'_c(\mu')}{Z_c(\mu)} \zeta_c^0 , \quad \zeta_\alpha(\mu, \mu') = \frac{Z'_\alpha(\mu')}{Z_\alpha(\mu)} \zeta_\alpha^0 . \end{aligned} \quad (4.80)$$

The transverse part of the bare gluon propagator (3.25) near the mass shell in full QCD is

$$D_\perp(p^2) = \frac{Z_A^{\text{os}}}{p^2} , \quad Z_A^{\text{os}} = \frac{1}{1 - \Pi(0)} . \quad (4.81)$$

In the low-energy theory,  $Z_A'^{\text{os}} = 1$ , because all loop diagrams for  $\Pi'(0)$  contain no scale. Therefore, the matching coefficient  $\zeta_A^0$  in the relation  $A_0 = \zeta_A^0 A'_0$  is

$$\zeta_A^0 = \frac{Z_A^{\text{os}}}{Z_A'^{\text{os}}} = \frac{1}{1 - \Pi(0)} . \quad (4.82)$$

Multiplying by this coefficient also converts  $a'_0$  into  $a_0$  in the longitudinal part of the propagator.

In the full theory, only diagrams with c-quark loops (Fig. 4.17) contribute. It is convenient to extract  $\Pi(0)$  using

$$\Pi(0) = \frac{1}{2d(d-1)} \left. \frac{\partial}{\partial p^\nu} \frac{\partial}{\partial p_\nu} \Pi^\mu(p) \right|_{p=0} .$$

In the one-loop approximation (Fig. 4.17a),  $\Pi(0)$  is a combination of one-loop vacuum integrals (2.16); we obtain

$$\Pi(0) = -\frac{4}{3} T_F \frac{g_0^2 m_c^{-2\varepsilon}}{(4\pi)^{d/2}} \Gamma(\varepsilon) + \dots \quad (4.83)$$

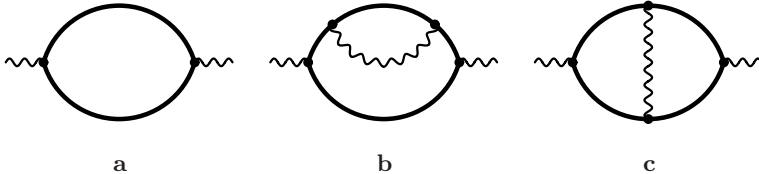


**Fig. 4.17.** Massive loops in gluon self-energy

Therefore,

$$\zeta_A^0 = 1 - \frac{4}{3} T_F \frac{g_0^2 m_c^{-2\epsilon}}{(4\pi)^{d/2}} \Gamma(\epsilon) + \dots$$

It is most natural to calculate  $\zeta_i(m_c, m_c)$ , which contain no large logarithms. The ratio of the renormalization constants for the gluon field is

$$\frac{Z_A(m_c)}{Z'_A(m_c)} = 1 - \frac{1}{2} \Delta \gamma_{A0} \frac{\alpha_s(m_c)}{4\pi\epsilon} + \dots = 1 - \frac{4}{3} T_F \frac{\alpha_s(m_c)}{4\pi\epsilon} + \dots ,$$

where  $\Delta \gamma_{A0} = (8/3)T_F$  is the contribution of a single flavour to the one-loop anomalous dimension (3.33) of the gluon field. Finally, we obtain the renormalized decoupling constant

$$\zeta_A(m_c, m_c) = 1 + \mathcal{O}(\alpha_s^2) .$$

The dependence on  $\mu, \mu'$  can be easily restored using the renormalization-group. It is not too difficult to calculate the two-loop diagrams (Figs. 4.17b,c). They reduce to combinations of two-loop massive vacuum integrals (4.31), and are proportional to  $\Gamma^2(\epsilon)$ . Using also the two-loop anomalous dimension of the gluon field, one can obtain [29]

$$\zeta_A(m_c, m_c) = 1 - \frac{13}{12} (4C_F - C_A) T_F \left( \frac{\alpha_s(m_c)}{4\pi} \right)^2 + \dots \quad (4.84)$$

Similarly, for the light-quark field (see (3.46)),

$$\zeta_q^0 = \frac{Z_q^{os}}{Z_q'^{os}} = \frac{1}{1 - \Sigma_V(0)} . \quad (4.85)$$

The only two-loop diagram contributing is Fig. 4.18. Expanding the quark self-energy (3.45) at  $m_0 = 0$  in  $p$  up to linear terms, we reduce it to the integral (4.33), similarly to (4.32) [15, 25]:

$$\begin{aligned} \Sigma_V(0) &= -i C_F g_0^2 \frac{(d-1)(d-4)}{d} \int \frac{d^d k}{(2\pi)^d} \frac{\Pi(k^2)}{(k^2)^2} , \\ \zeta_q^0 &= [1 - \Sigma_V(0)]^{-1} = 1 + C_F T_F \frac{g_0^4 m_c^{-4\epsilon}}{(4\pi)^d} \Gamma^2(\epsilon) \frac{2(d-1)(d-4)(d-6)}{d(d-2)(d-5)(d-7)} . \end{aligned} \quad (4.86)$$

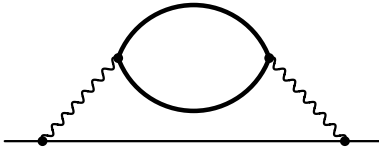


**Fig. 4.18.** Two-loop on-shell massless-quark self-energy

The ratio of the renormalization constants for the quark field is

$$\begin{aligned} \frac{Z_q(m_c)}{Z'_q(m_c)} &= 1 + \frac{1}{4} \left( \gamma_{q0} \Delta\beta_0 + \frac{1}{2} \Delta\gamma_{A0} \frac{d\gamma_{q0}}{da} a - \Delta\gamma_{q1} \varepsilon \right) \left( \frac{\alpha_s(m_c)}{4\pi\varepsilon} \right)^2 + \dots \\ &= 1 + C_F T_F \frac{1}{\varepsilon} \left( \frac{\alpha_s(m_c)}{4\pi} \right)^2 + \dots, \end{aligned}$$

where  $\Delta\beta_0 = -(4/3)T_F$ ,  $\Delta\gamma_{A0} = (8/3)T_F$ , and  $\Delta\gamma_{q1} = -4C_F T_F$  are the single-flavour contributions. Finally, we obtain [15]

$$\zeta_q(m_c, m_c) = 1 - \frac{5}{6} C_F T_F \left( \frac{\alpha_s(m_c)}{4\pi} \right)^2 + \dots \quad (4.87)$$

If we consider b-quark HQET instead of QCD, nothing changes. When all characteristic (residual) momenta become much less than  $m_c$ , c-quark loops shrink to a point. From (4.34), we obtain

$$\tilde{\zeta}_Q^0 = \frac{\tilde{Z}_Q^{os}}{\tilde{Z}_Q'^{os}} = 1 - C_F T_F \frac{g_0^4 m_c^{-4\varepsilon}}{(4\pi)^d} \Gamma^2(\varepsilon) \frac{2(d-1)(d-6)}{(d-2)(d-5)(d-7)}. \quad (4.88)$$

The ratio of renormalization constants is, from (3.75),

$$\frac{\tilde{Z}_Q(m_c)}{\tilde{Z}_Q'(m_c)} = 1 + 2C_F T_F \left( 1 - \frac{4}{3}\varepsilon \right) \left( \frac{\alpha_s(m_c)}{4\pi\varepsilon} \right)^2,$$

and we arrive at [25]

$$\tilde{\zeta}_Q(m_c, m_c) = 1 + \frac{52}{9} C_F T_F \left( \frac{\alpha_s(m_c)}{4\pi} \right)^2 + \dots \quad (4.89)$$

The decoupling relation for the coupling constant can be derived by considering any vertex in the theory. We shall use the HQET heavy-quark-gluon vertex. Let  $g_0 t^\mu \tilde{\Gamma}^\mu(\omega, q)$  be the sum of bare one-particle-irreducible heavy-quark-heavy-quark-gluon vertex diagrams, not including the external propagators. For this vertex,

$$g_0 \tilde{\Gamma}^\mu = \left( \tilde{\zeta}_Q^0 \right)^{-1} \left( \zeta_A^0 \right)^{-1/2} g_0' \tilde{\Gamma}'^\mu,$$

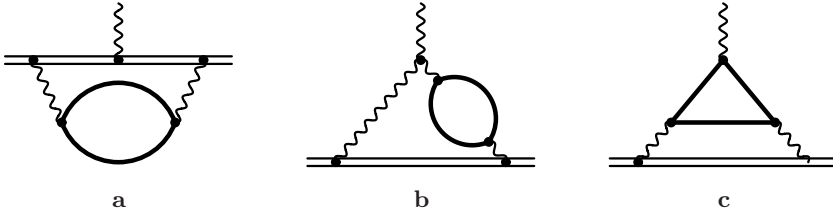


**Fig. 4.19.** Two-loop on-shell HQET quark–gluon vertex (the diagram **b** implies also the mirror-symmetric one; the diagram **c** has two orientations of the quark loop)

because after multiplication by the three propagators it becomes the Green function of  $\tilde{Q}_0$ ,  $\bar{\tilde{Q}}_0$ , and  $A_0$ . It is most convenient to set all the external momenta to zero. In the low-energy theory,  $\tilde{\Gamma}'^\mu = v^\mu$ . In full HQET, only diagrams with c-quark loops contribute, and  $\tilde{\Gamma}^\mu(0, 0) = \tilde{\Gamma}v^\mu$ . They first appear at two loops (Fig. 4.19). We have

$$\zeta_\alpha^0 = \frac{1}{(\tilde{\zeta}_Q^0 \tilde{\Gamma})^2 \zeta_A^0}, \quad \zeta_\alpha = \frac{Z'_\alpha}{Z_\alpha} \zeta_\alpha^0 = \frac{Z'_\alpha}{Z_\alpha} \frac{Z'_A}{Z_A} \frac{1}{\zeta_A} \frac{1}{(\tilde{\zeta}_Q^0 \tilde{\Gamma})^2}.$$

It is convenient to write  $\tilde{\Gamma}^\mu(\omega, q) = \tilde{\Gamma}_{\text{bf}}^\mu + \Delta\tilde{\Lambda}^\mu$ , where  $\tilde{\Gamma}_{\text{bf}}^\mu(\omega, q) = v^\mu + \tilde{\Lambda}_{\text{bf}}^\mu(\omega, q)$  is the background-field vertex (see Sect. 4.5). Using the identities of Fig. 4.14, it is easy to demonstrate that  $\tilde{\Lambda}_{\text{bf}}^\mu(\omega, q)q_\mu = \tilde{\Sigma}(\omega) - \tilde{\Sigma}(\omega + q \cdot v)$  and, in particular,

$$\tilde{\Lambda}_{\text{bf}}^\mu(\omega, 0) = -\frac{d\tilde{\Sigma}(\omega)}{d\omega} v^\mu.$$

At  $\omega = 0$ , only the diagram of Fig. 4.9 with a c-quark loop contributes to the heavy-quark self-energy  $\tilde{\Sigma}(\omega)$ . Therefore,  $\tilde{\zeta}_Q^0 \tilde{\Gamma} = 1 + \Delta\tilde{\Lambda}$ , and  $\tilde{\Lambda}_{\text{bf}}(0, 0)$  cancels (here  $\Delta\tilde{\Lambda}^\mu(0, 0) = \Delta\tilde{\Lambda}v^\mu$ ). The term  $-\Delta\tilde{\Lambda}^\mu$  is given by the diagrams of Fig. 4.19b, where only the  $1/a_0$  terms in (4.39) are substituted for the three-gluon vertex; the two diagrams contribute equally. This diagram can be easily reduced to (4.33) by averaging over the directions of  $k$ :

$$\Delta\tilde{\Lambda} = -C_A T_F \frac{g_0^4 m_c^{-4\varepsilon}}{(4\pi)^d} \Gamma^2(\varepsilon) \frac{2(d-1)(d-6)}{d(d-2)(d-5)(d-7)}. \quad (4.90)$$

Taking into account (4.84) and

$$\frac{Z'_\alpha(m_c)}{Z_\alpha(m_c)} \frac{Z'_A(m_c)}{Z_A(m_c)} = 1 + C_A T_F \left(1 - \frac{5}{6}\varepsilon\right) \left(\frac{\alpha_s(m_c)}{4\pi\varepsilon}\right)^2,$$

we arrive at the well-known result [29]

$$\zeta_\alpha(m_c, m_c) = 1 + \frac{1}{9} (39C_F - 32C_A) T_F \left( \frac{\alpha_s(m_c)}{4\pi} \right)^2 + \dots \quad (4.91)$$

This means that at  $\mu > m_c$ , we have  $\alpha_s(\mu)$ , whose running is given by the  $\beta(\alpha_s)$  function with  $n_f = n_l + 1$  flavours; at  $\mu < m_c$ , we have  $\alpha'_s(\mu)$ , whose running is given by  $\beta'(\alpha'_s)$  with  $n_l$  flavours; at  $\mu = m_c$ ,

$$\alpha_s(m_c) = \zeta_\alpha(m_c, m_c) \alpha'_s(m_c).$$

Finally, we shall discuss the decoupling of c-quark loops in the b-quark chromomagnetic-interaction constant. Both HQET with c-loops and the effective low-energy theory must give identical on-shell scattering amplitudes, up to corrections suppressed by powers of  $1/m_c$ . Therefore, from (4.62) we have

$$C_m(\mu) = \frac{\tilde{Z}_m(\mu)}{\tilde{Z}'_m(\mu)} \frac{\tilde{\mu}'_g}{\tilde{\mu}_g} C'_m(\mu). \quad (4.92)$$

Here  $\tilde{\mu}'_g = 1$ , and  $\tilde{\mu}_g$  is given by (4.58), with just the c-quark contribution. The ratio of the renormalization constants  $\tilde{Z}_m$  is

$$\begin{aligned} \frac{\tilde{Z}_m(m_c)}{\tilde{Z}'_m(m_c)} &= 1 + \frac{1}{4} (\gamma_0 \Delta \beta_0 - \Delta \gamma_1 \varepsilon) \left( \frac{\alpha_s(m_c)}{4\pi\varepsilon} \right)^2 + \dots \\ &= 1 - C_A T_F \left( \frac{2}{3} - \frac{13}{8} \varepsilon \right) \left( \frac{\alpha_s(m_c)}{4\pi\varepsilon} \right)^2 + \dots, \end{aligned} \quad (4.93)$$

where  $\Delta \beta_0 = -(4/3)T_F$  and  $\Delta \gamma_1 = -(4/9) \times 13C_A T_F$  are the single-flavour contributions. Re-expressing (4.58) via  $\alpha_s(m_c)$  and expanding in  $\varepsilon$ , we see that singular terms cancel, and

$$C_m(m_c) = \left[ 1 + \frac{71}{27} C_A T_F \left( \frac{\alpha_s(m_c)}{4\pi} \right)^2 + \dots \right] C'_m(m_c). \quad (4.94)$$

Therefore, when crossing  $\mu = m_c$ , we have to adjust  $C_m(\mu)$  according to (4.94), and at  $\mu < m_c$  the renormalization-group running is driven by the  $\beta$  function and the anomalous dimension for  $n_f = 3$ .

## References

1. L.F. Abbot: Nucl. Phys. B **185**, 189 (1981); Acta Phys. Pol. B **13**, 33 (1982)  
[71](#)
2. G. Amorós, M. Beneke, M. Neubert: Phys. Lett. B **401**, 81 (1997) [81](#), [84](#)
3. S. Balk, J.G. Körner, D. Pirjol: Nucl. Phys. B **428**, 499 (1994) [63](#)

4. C. Balzereit: Phys. Rev. D **59**, 034006 (1999); Phys. Rev. D **59**, 094015 (1999) **63**
5. C. Balzereit, T. Ohl: Phys. Lett. B **386**, 335 (1996) **63**
6. C. Bauer, A.V. Manohar: Phys. Rev. D **57**, 337 (1998) **63**
7. J.D. Bjorken, S.D. Drell: *Relativistic Quantum Mechanics* (McGraw Hill, New York 1964) **80**
8. B. Blok, J.G. Körner, D. Pirjol, J.C. Rojas: Nucl. Phys. B **496**, 358 (1997) **63**
9. D.J. Broadhurst: Z. Phys. C **47**, 115 (1990) **66**
10. D.J. Broadhurst: Z. Phys. C **54**, 599 (1992) **65, 66, 68**
11. D.J. Broadhurst, N. Gray, K. Schilcher: Z. Phys. C **52**, 111 (1991) **65, 68, 69, 71**
12. D.J. Broadhurst, A.G. Grozin: Phys. Rev. D **52**, 4082 (1995) **69**
13. D.J. Broadhurst, A.G. Grozin: ‘Multiloop Calculations in Heavy Quark Effective Theory’, in *New Computing Techniques in Physics Research IV*, ed. by B. Denby, D. Perret-Gallix (World Scientific, Singapore 1995) p. 217 **64, 65**
14. Y.-Q. Chen: Phys. Lett. B **317**, 421 (1993) **59**
15. K.G. Chetyrkin, B.A. Kniehl, M. Steinhauser: Nucl. Phys. B **510**, 61 (1998) **84, 86, 87**
16. A. Czarnecki, A.G. Grozin: Phys. Lett. B **405**, 142 (1997) **69, 76, 79, 81**
17. A.I. Davydychev, A.G. Grozin: Phys. Rev. D **59**, 054023 (1999) **66, 68, 71, 76**
18. A.I. Davydychev, A.G. Grozin: Eur. Phys. J. C **20**, 333 (2001) **74, 76, 77**
19. E. Eichten, B. Hill: Phys. Lett. B **243**, 427 (1990) **62, 76, 81**
20. A.F. Falk, B. Grinstein, M.E. Luke: Nucl. Phys. B **357**, 185 (1991) **62**
21. M. Finkemeier, H. Georgi, M. McIrvin: Phys. Rev. D **55**, 6933 (1997) **59**
22. M. Finkemeier, M. McIrvin: Phys. Rev. D **55**, 377 (1997) **63**
23. J. Fleischer, O.V. Tarasov: Phys. Lett. B **283**, 129 (1992); Comput. Phys. Commun. **71**, 193 (1992) **65**
24. N. Gray, D.J. Broadhurst, W. Grafe, K. Schilcher: Z. Phys. C **48**, 673 (1990) **65, 68**
25. A.G. Grozin: Phys. Lett. B **445**, 165 (1998) **86, 87**
26. J.G. Körner, G. Thompson: Phys. Lett. B **264**, 185 (1991) **59, 63**
27. A.S. Kronfeld: Phys. Rev. D **58**, 051501 (1998) **69**
28. S. Laporta, E. Remiddi: Phys. Lett. B **379**, 283 (1996) **67**
29. S.A. Larin, T. van Ritbergen, J.A.M. Vermaseren: Nucl. Phys. B **438**, 278 (1995) **86, 88**
30. C.L.Y. Lee: *Aspects of the Heavy Quark Effective Field Theory at Subleading Order*, Preprint CALT-68-1663 (CalTech, Pasadena 1991); revised (1997) **63**
31. M.E. Luke, A.V. Manohar: Phys. Lett. B **286**, 348 (1992) **59**
32. T. Mannel, W. Roberts, Z. Ryzak: Nucl. Phys. B **368**, 204 (1992) **63**
33. A.V. Manohar: Phys. Rev. D **56**, 230 (1997) **63**
34. K. Melnikov, T. van Ritbergen: Phys. Lett. B **482**, 99 (2000); Nucl. Phys. B **591**, 515 (2000) **67, 68, 69, 71**
35. A.A. Vladimirov: Theor. Math. Phys. **43**, 417 (1980) **69**

## 5 Heavy–Light Currents

Until now, we have considered the Lagrangian, its Feynman rules, and the Green functions and scattering amplitudes following from them. It is often also important to consider composite operators which do not appear in the Lagrangian – products of fields at coincident points. This division is not strict. Some operators, such as the electromagnetic and weak currents, are interesting precisely because they appear (multiplied by electroweak gauge fields) in the Lagrangian of a wider theory incorporating QCD – the Standard Model. Other composite operators are interesting in their own right, e.g., their space integrals can be generators of exact or approximate symmetries, or they appear in operator product expansions, etc.

In this chapter, as well as in the following two, we shall discuss bilinear quark currents in QCD and HQET, which have numerous applications.

### 5.1 Bilinear Quark Currents in QCD

Now we are going to consider the bilinear quark currents

$$j_{n0} = \bar{q}'_0 \Gamma q_0, \quad \Gamma = \gamma^{[\mu_1} \cdots \gamma^{\mu_n]} \quad (5.1)$$

in QCD. Here  $\Gamma$  is the antisymmetrized product of  $n$   $\gamma$ -matrices, and  $q_0$  and  $\bar{q}'_0$  are bare quark fields of different flavours. Currents with  $q' = q$  have some peculiarities, because the quark line emerging from the current vertex can return to the same current again. We shall not discuss such currents here. All properties that we shall derive for (5.1) are also valid for flavour-non-singlet currents  $\bar{q}_{i0} \Gamma \tau_{ij} q_{j0}$ , where  $\tau$  is a flavour matrix with  $\text{Tr } \tau = 0$ , and all  $q_i$  have equal masses.

The renormalized currents are related to the bare ones by

$$j_n(\mu) = Z_{jn}^{-1}(\mu) j_{n0}, \quad (5.2)$$

where the  $Z_{jn}$  are minimal (3.3) renormalization constants. The  $\mu$  dependence of  $j_n(\mu)$  is determined by the renormalization-group equation

$$\left( \frac{d}{d \log \mu} + \gamma_{jn}(\alpha_s(\mu)) \right) j_n(\mu) = 0, \quad (5.3)$$

where

$$\gamma_{jn}(\alpha_s) = \frac{d \log Z_{jn}}{d \log \mu} \quad (5.4)$$

is the anomalous dimension.

Let the sum of one-particle-irreducible bare diagrams with a current vertex  $\Gamma$ , an incoming quark  $q$  with momentum  $p$ , and an outgoing quark  $q'$  with momentum  $p'$ , not including the external quark propagators, be the proper vertex  $\Gamma_n(p, p') = \Gamma + \Lambda_n(p, p')$  (Fig. 5.1; here  $\Gamma$  in the right-hand side is the Dirac matrix). When the vertex is expressed via the renormalized quantities  $\alpha_s(\mu)$ ,  $a(\mu)$ , it should become  $Z_{\Gamma n} \Gamma_{nr}(p, p')$ , where the renormalized vertex  $\Gamma_{nr}(p, p')$  is finite in the limit  $\varepsilon \rightarrow 0$ . When the proper vertex of the renormalized current  $Z_{jn}^{-1} \Gamma_n(p, p')$  is multiplied by the two external-leg renormalization factors  $Z_q^{1/2}$ , it should give a finite matrix element. Therefore,  $Z_{jn} = Z_q Z_{\Gamma n}$ . The UV divergences of  $\Lambda_n(p, p')$  do not depend on the quark masses and the external momenta. Therefore, we may assume that all quarks are massless, and set  $p = p' = 0$ . An IR cut-off is then necessary in order to avoid IR  $1/\varepsilon$  terms.

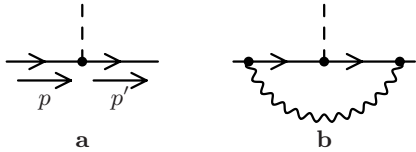


**Fig. 5.1.** Proper vertex of a bilinear quark QCD current

In the one-loop approximation (Fig. 5.1b),

$$\begin{aligned} A_n(0, 0) &= C_F \int \frac{d^d k}{(2\pi)^d} i g_0 \gamma^\mu \frac{i k}{k^2} \Gamma \frac{i k}{k^2} i g_0 \gamma^\nu \frac{-i}{k^2} \left[ g_{\mu\nu} - (1 - a_0) \frac{k_\mu k_\nu}{k^2} \right] \\ &= -i C_F g_0^2 \int \frac{d^d k}{(2\pi)^d} \frac{1}{(k^2)^3} \left[ \frac{\gamma^\mu \gamma^\nu \Gamma \gamma_\nu \gamma_\mu}{d} - (1 - a_0) \Gamma \right], \end{aligned}$$

where the averaging  $\langle k \Gamma k \rangle \rightarrow k^2 \gamma^\alpha \Gamma \gamma_\alpha / d$  has been used. In  $d = 4 - 2\varepsilon$  dimensions,

$$\gamma^\mu \Gamma \gamma_\mu = 2h(d)\Gamma, \quad (5.5)$$

where, for the antisymmetrized product (5.1),

$$h(d) = (-1)^n \left( \frac{d}{2} - n \right). \quad (5.6)$$

Using the UV divergence of the integral (4.51), we obtain

$$Z_{\Gamma n} = 1 + C_F \frac{\alpha_s}{4\pi\varepsilon} [(n-2)^2 - 1 + a] . \quad (5.7)$$

The gauge dependence is cancelled by  $Z_q$  (3.48), and we arrive at

$$\gamma_{jn} = -2(n-1)(n-3)C_F \frac{\alpha_s}{4\pi} + \dots \quad (5.8)$$

The two-loop anomalous dimension for generic  $n$  can be derived by calculating  $\Gamma_n(p, 0)$  or  $\Gamma_n(p, p)$  at two loops, using the methods of Sect. 2.4. Historically, it was first obtained as a by-product of a more difficult QCD/HQET matching calculation [4] (see Sect. 5.6):

$$\begin{aligned} \gamma_{jn} = & -2(n-1)(n-3)C_F \frac{\alpha_s}{4\pi} \\ & \times \left\{ 1 + \left[ \frac{1}{2} (5(n-2)^2 - 19) C_F - \frac{1}{3} (3(n-2)^2 - 19) C_A \right] \frac{\alpha_s}{4\pi} \right\} \\ & - \frac{1}{3}(n-1)(n-15)C_F \beta_0 \left( \frac{\alpha_s}{4\pi} \right)^2 + \dots \end{aligned} \quad (5.9)$$

The corresponding three-loop result has been derived recently [10].

It is not an accident that our results contain a factor  $n-1$ . The vector current has  $\gamma_{j1} = 0$  to all orders. The integral of  $\bar{q}\gamma^0 q$  over all space is the number of quarks minus the number of antiquarks of the flavour being considered. It is an integer, and cannot depend on  $\mu$ . The same argument holds for vector currents with diagonal flavour matrices  $\tau$  having  $\text{Tr } \tau = 0$ , and hence also for  $\bar{q}'\gamma^\mu q$  (the integral of the 0th component of this current is the generator of the flavour symmetry group which replaces  $q$  by  $q'$ ; its normalization is fixed by the commutation relations of this group, and thus cannot depend on  $\mu$ ).

We can understand how this happens using the Ward identity for  $\Gamma_1^\mu(p, p')$ . Starting from each diagram for  $\Sigma(p)$ , we can obtain a set of diagrams for  $\Lambda_1^\mu(p, p')$  by inserting the current vertex into each possible place. This vertex must be on the open quark line going through the diagram, because the current changes the quark flavour. After contracting with  $q_\mu$ , we have exactly the same situation as in Fig. 3.16, and

$$\begin{aligned} \Lambda_1^\mu(p, p+q)q_\mu &= \Sigma(p) - \Sigma(p+q) , \\ \Gamma_1^\mu(p, p+q)q_\mu &= S^{-1}(p+q) - S^{-1}(p) . \end{aligned} \quad (5.10)$$

In particular, at  $q \rightarrow 0$

$$\Lambda_1^\mu(p, p) = -\frac{\partial \Sigma(p)}{\partial p_\mu} \quad \text{or} \quad \Gamma_1^\mu(p, p) = \frac{\partial S^{-1}(p)}{\partial p_\mu} . \quad (5.11)$$

Multiplying the last equation by  $Z_q$  transforms  $S^{-1}$  into  $S_r^{-1}$ , and hence makes the left-hand side finite. Therefore,  $Z_{j1} = Z_q Z_{\Gamma 1} = 1$ .

The renormalization of the scalar current  $\bar{q}'q$  is closely related to that of the quark mass  $m$ . The  $\overline{\text{MS}}$  renormalized mass

$$m(\mu) = Z_m^{-1}(\mu)m_0 \quad (5.12)$$

(with a minimal renormalization constant  $Z_m$ ) is defined in such a way that the bare quark propagator  $S(p)$ , when expressed via the renormalized quantities  $\alpha_s(\mu)$ ,  $a(\mu)$ ,  $m(\mu)$ , is equal to  $Z_q S_r(p)$ , where the renormalized propagator  $S_r(p)$  is finite in the limit  $\varepsilon \rightarrow 0$  (Sect. 3.1). In order to find  $Z_m$ , it is sufficient to consider  $|p^2| \gg m^2$  and retain only terms linear in  $m$ . We can calculate  $[\partial\Sigma(p)/\partial m_0]_{m_0=0}$  using the identity

$$\left. \frac{\partial S_0(p)}{\partial m_0} \right|_{m_0=0} = [S_0(p)]^2. \quad (5.13)$$

Starting from each diagram for  $\Sigma(p)$ , we obtain a set of diagrams for  $[\partial\Sigma(p)/\partial m_0]_{m_0=0}$  by differentiating each quark propagator of the considered flavour in turn. After differentiating a propagator in a quark loop, we obtain a trace with an odd number of  $\gamma$ -matrices, which is zero. Therefore, only the propagators along the open quark line going through the diagram need to be differentiated. The resulting diagrams are exactly those for  $\Lambda_0(p, p)$ . We arrive at

$$1 + \Sigma_S(p^2)|_{m_0=0} = \Gamma_0(p, p). \quad (5.14)$$

As explained after (3.46), the renormalization constant  $Z_m$  is defined by the condition that  $Z_q Z_m(1 + \Sigma_S)$  is finite. Therefore,

$$Z_m = Z_{j0}^{-1}. \quad (5.15)$$

In other words,  $m(\mu)[\bar{q}'q]_\mu = m_0 \bar{q}_0' q_0$  is not renormalized. The anomalous dimension of the mass is

$$\gamma_m = -\gamma_{j0} = 6C_F \frac{\alpha_s}{4\pi} + C_F \left( 3C_F + \frac{97}{3}C_A - \frac{20}{3}T_F n_f \right) \left( \frac{\alpha_s}{4\pi} \right)^2 + \dots \quad (5.16)$$

The four-loop result has been obtained recently [5, 18].

The  $\overline{\text{MS}}$  mass  $m(\mu) = Z_m^{-1}(\mu)m_0$  is related to the on-shell mass  $m = [Z_m^{\text{os}}]^{-1}m_0$  by

$$m(\mu) = \frac{Z_m^{\text{os}}}{Z_m(\mu)}m. \quad (5.17)$$

The UV divergences in  $Z_m^{\text{os}}$  and  $Z_m(\mu)$  cancel;  $Z_m^{\text{os}}$  is IR finite (unlike  $Z_q^{\text{os}}$ ). Substituting (4.29), we find at one loop

$$\frac{m(\mu)}{m} = 1 - 6C_F \frac{\alpha_s}{4\pi} \left( \log \frac{\mu}{m} + \frac{2}{3} \right) + \dots \quad (5.18)$$

It is most natural to use  $\mu = m$ , because the relation between  $m(m)$  and  $m$  contains no large logarithms. The two-loop relation between the  $\overline{\text{MS}}$  mass and the pole mass was derived in [11], and the three-loop relation in [15]. Note that the on-shell mass has a meaning only for heavy quarks, because for light quarks perturbative calculations at  $p^2 = m^2$  are not possible; the  $\overline{\text{MS}}$  mass has a meaning for both heavy and light quarks.

If we need  $m(\mu)$  for  $\mu$  widely separated from  $m$ , we need to solve the renormalization-group equation

$$\left[ \frac{d}{d \log \mu} + \gamma_m(\alpha_s(\mu)) \right] m(\mu) = 0. \quad (5.19)$$

Its solution is (see (4.72))

$$m(\mu) = \hat{m} \left( \frac{\alpha_s(\mu)}{4\pi} \right)^{\gamma_{m0}/(2\beta_0)} K_{\gamma_m}(\alpha_s(\mu)). \quad (5.20)$$

Currents (5.1) with  $n > 4$  do not exist in four-dimensional space. Any matrix element involving such a current contains a  $\gamma$ -matrix trace that vanishes at  $\varepsilon \rightarrow 0$ . However, if it is multiplied by an integral containing  $1/\varepsilon$ , a finite contribution may result. Such operators are called evanescent; we shall not discuss them here. There are five non-evanescent currents with  $0 \leq n \leq 4$ . The currents with  $n = 4, 3$  can be obtained from those with  $n = 0, 1$  by multiplying them by the 't Hooft–Veltman  $\gamma_5$ , discussed in the next section.

## 5.2 Axial Anomaly

It is not possible to define a  $\gamma_5$  satisfying

$$\gamma_5 \gamma^\mu + \gamma^\mu \gamma_5 = 0 \quad (5.21)$$

in  $d$ -dimensional space. Let us consider the following chain of equalities:

$$\begin{aligned} \text{Tr } \gamma_5 \gamma_\mu \gamma^\mu &= d \text{Tr } \gamma_5 = - \text{Tr } \gamma_\mu \gamma_5 \gamma^\mu = - \text{Tr } \gamma_5 \gamma^\mu \gamma_\mu = -d \text{Tr } \gamma_5 \\ &\Rightarrow d \text{Tr } \gamma_5 = 0 \end{aligned}$$

(the anticommutativity of  $\gamma_5$  was used in the second step, and the trace cyclicity in the third one). We have learned that if  $d \neq 0$  then  $\text{Tr } \gamma_5 = 0$ . We assume that  $d \neq 0$  and continue:

$$\begin{aligned} \text{Tr } \gamma_5 \gamma_\mu \gamma^\mu \gamma^\alpha \gamma^\beta &= d \text{Tr } \gamma_5 \gamma^\alpha \gamma^\beta = - \text{Tr } \gamma_5 \gamma_\mu \gamma^\alpha \gamma^\beta \gamma^\mu = -(d-4) \text{Tr } \gamma_5 \gamma^\alpha \gamma^\beta \\ &\Rightarrow (d-2) \text{Tr } \gamma_5 \gamma^\alpha \gamma^\beta = 0. \end{aligned}$$

We have learned that if  $d \neq 2$  then  $\text{Tr } \gamma_5 \gamma^\alpha \gamma^\beta = 0$ . We assume that  $d \neq 2$  and continue:

$$\begin{aligned} \text{Tr } \gamma_5 \gamma_\mu \gamma^\mu \gamma^\alpha \gamma^\beta \gamma^\gamma \gamma^\delta &= d \text{Tr } \gamma_5 \gamma^\alpha \gamma^\beta \gamma^\gamma \gamma^\delta = - \text{Tr } \gamma_5 \gamma_\mu \gamma^\alpha \gamma^\beta \gamma^\gamma \gamma^\delta \gamma^\mu \\ &= -(d-8) \text{Tr } \gamma_5 \gamma^\alpha \gamma^\beta \gamma^\gamma \gamma^\delta \Rightarrow (d-4) \text{Tr } \gamma_5 \gamma^\alpha \gamma^\beta \gamma^\gamma \gamma^\delta = 0, \end{aligned}$$

where we have used  $\gamma_\mu \gamma^\alpha \gamma^\beta \gamma^\gamma \gamma^\delta \gamma^\mu = (d-8) \gamma^\alpha \gamma^\beta \gamma^\gamma \gamma^\delta + \text{terms with fewer } \gamma\text{-matrices}$ . We have learned that if  $d \neq 4$  then  $\text{Tr } \gamma_5 \gamma^\alpha \gamma^\beta \gamma^\gamma \gamma^\delta = 0$ . Assuming  $d \neq 4$ , we can show that  $(d-6) \text{Tr } \gamma_5 \gamma^\alpha \gamma^\beta \gamma^\gamma \gamma^\delta \gamma^\varepsilon \gamma^\zeta = 0$ , and so on. All traces vanish if  $d$  is not an even integer. Therefore, an anticommuting  $\gamma_5$  is not usable in dimensional regularization.

A way out was proposed by 't Hooft and Veltman. Let us split our  $d$ -dimensional space–time into a four-dimensional subspace and the orthogonal  $(d-4)$ -dimensional subspace, and define

$$\begin{aligned} \gamma_5^{\text{HV}} &= \frac{i}{4!} \varepsilon_{\alpha\beta\gamma\delta} \gamma^\alpha \gamma^\beta \gamma^\gamma \gamma^\delta = -i \gamma^0 \gamma^1 \gamma^2 \gamma^3, \\ \gamma_5^{\text{HV}} \underline{\gamma}^\mu + \underline{\gamma}^\mu \gamma_5^{\text{HV}} &= 0, \quad \gamma_5^{\text{HV}} \underline{\underline{\gamma}}^\mu - \underline{\underline{\gamma}}^\mu \gamma_5^{\text{HV}} = 0, \end{aligned} \tag{5.22}$$

where the tensor  $\varepsilon_{\alpha\beta\gamma\delta}$  lives in the four-dimensional subspace. Here  $\underline{\gamma}^\mu$  lives in the physical 4-dimensional subspace, and  $\underline{\underline{\gamma}}^\mu$  in the non-physical  $(d-4)$ -dimensional one. This prescription spoils  $d$ -dimensional Lorentz invariance.

The inconsistency of the naively anticommuting  $\gamma_5$  (5.21) is strikingly demonstrated by the anomaly in the flavour-singlet axial current  $j^\mu = \bar{q} \gamma^\mu \gamma_5 q$  (see, e.g., [7]). Let us consider its matrix element  $M^{\lambda\mu\nu}(p, p')$  between an incoming gluon with momentum  $p$  and an outgoing gluon with momentum  $p'$  (Fig. 5.2). The Ward identities yield

$$M^{\lambda\mu\nu}(p, p') p_\mu = 0, \quad M^{\lambda\mu\nu}(p, p') p'_\nu = 0.$$

Using the equality

$$S_0(p') \not{q} \gamma_5 S_0(p) = \gamma_5 S_0(p) + S_0(p') \gamma_5 + 2m S_0(p') \gamma_5 S_0(p), \quad q = p' - p, \tag{5.23}$$

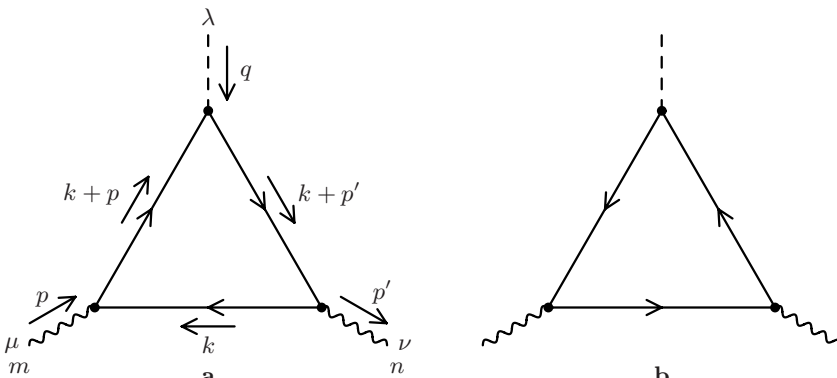


**Fig. 5.2.** Gluon matrix element of the axial current

one can, it seems, prove that for a massless quark,

$$M^{\lambda\mu\nu}(p, p')q_\lambda = 0. \quad (5.24)$$

But this axial Ward identity is wrong!

Let us define  $j_{\text{HV}}^\mu = (1/2)\bar{q}(\gamma^\mu\gamma_5^{\text{HV}} - \gamma_5^{\text{HV}}\gamma^\mu)q$ , and calculate (5.24) for the diagrams of Fig. 5.2 carefully:

$$\begin{aligned} M^{\lambda\mu\nu}(p, p')q_\lambda &= -iT_F g_0^2 \int \frac{d^d k}{(2\pi)^d} \text{Tr } S_0(k + p') \not{p} \gamma_5^{\text{HV}} S_0(k + p) \gamma^\mu S_0(k) \gamma^\nu \\ &\quad + (p \leftrightarrow -p', \mu \leftrightarrow \nu). \end{aligned}$$

Taking into account

$$\begin{aligned} S_0(k + p') \not{p} \gamma_5^{\text{HV}} S_0(k + p) \\ = \gamma_5^{\text{HV}} S_0(k + p) + S_0(k + p') \gamma_5^{\text{HV}} - 2S_0(k + p') \underline{k} \gamma_5^{\text{HV}} S_0(k + p) \end{aligned}$$

at  $m = 0$ , where  $\underline{k}$  and  $\underline{\underline{k}}$  are the components of  $k$  in the physical and non-physical subspaces, we obtain

$$\begin{aligned} M^{\lambda\mu\nu}(p, p')q_\lambda &= iT_F g_0^2 \int \frac{d^d k}{(2\pi)^d} \text{Tr} \left[ \gamma_5^{\text{HV}} S_0(k + p) + S_0(k + p') \gamma_5^{\text{HV}} \right. \\ &\quad \left. - 2S_0(k + p') \underline{k} \gamma_5^{\text{HV}} S_0(k + p) \right] \gamma^\mu S_0(k) \gamma^\nu + (p \leftrightarrow -p', \mu \leftrightarrow \nu). \end{aligned}$$

The first two traces vanish, because they contain only one of the two vectors  $p, p'$  (this is the basis of the naive proof of (5.24)). The last term contains  $\underline{k}$ , and its numerator should vanish at  $\varepsilon \rightarrow 0$ . But the UV divergence of the integral can give  $1/\varepsilon$ , producing a finite result. The trace in the numerator of the last term is

$$\text{Tr}(\underline{k} + \not{p}') \underline{k} \gamma_5^{\text{HV}} (\underline{k} + \not{p}) \gamma^\mu \underline{k} \gamma^\mu = \text{Tr} \not{p}' \underline{k} \gamma_5^{\text{HV}} \not{p} \gamma^\mu \underline{k} \gamma^\nu = 4ik^2 \varepsilon^{\alpha\beta\mu\nu} p_\alpha p'_\beta,$$

because we have to retain both  $p$  and  $p'$ , and  $\underline{k}$  anticommutes with the physical-subspace matrices  $\not{p}, \not{p}', \gamma^\mu, \gamma^\nu$ . Averaging over orientations of the physical subspace, we may make the replacement

$$\underline{k}^2 \rightarrow \frac{d-4}{d} k^2.$$

We need only the UV  $1/\varepsilon$  pole of the integral, so we may set the external momenta to zero and use (4.51). The two diagrams contribute equally, and we arrive at the anomaly in the axial Ward identity,

$$M^{\lambda\mu\nu}(p, p')q_\lambda = 8T_F \frac{\alpha_s}{4\pi} i\varepsilon^{\alpha\beta\mu\nu} p_\alpha p'_\beta. \quad (5.25)$$

If the quark is massive, the normal contribution from (5.23) should be added.

### 5.3 The 't Hooft–Veltman $\gamma_5$ and the Anticommuting $\gamma_5$

The quark line cannot be closed in matrix elements of flavour-nonsinglet currents. Therefore, traces with a single  $\gamma_5$ , which can lead to an anomaly, never appear. There is a general belief that one may use a naively anticommutating  $\gamma_5^{\text{AC}}$  satisfying (5.21), without encountering contradictions. The pseudoscalar currents  $j_{\text{AC}}(\mu) = Z_{\text{P,AC}}^{-1}(\mu)\bar{q}'_0\gamma_5^{\text{AC}}q$  and  $j_{\text{HV}}(\mu) = Z_{\text{P,HV}}^{-1}(\mu)\bar{q}'_0\gamma_5^{\text{HV}}q$  are related to each other by a finite renormalization:

$$\begin{aligned} j_{\text{AC}}(\mu) &= Z_{\text{P}}(\alpha_s(\mu))j_{\text{HV}}(\mu), \\ Z_{\text{P}}(\alpha_s) &= 1 + z_{\text{P1}} \frac{\alpha_s}{4\pi} + z_{\text{P2}} \left( \frac{\alpha_s}{4\pi} \right)^2 + \dots \end{aligned} \quad (5.26)$$

Similarly, the axial currents are related by

$$j_{\text{AC}}^\mu(\mu) = Z_{\text{A}}(\alpha_s(\mu))j_{\text{HV}}^\mu(\mu). \quad (5.27)$$

This is clearly discussed in [14], where references to earlier papers can be found.

If the operator equalities (5.26), (5.27) are valid, they must hold for all matrix elements. We can only calculate a few of them, and check the supposed universality. The vertex functions  $\Gamma(p, p)$  and  $\Gamma(p, 0)$  reduce to propagator integrals. For massless quarks, they were discussed in Sect. 2.2 at one loop and in Sect. 2.4 at two loops. We shall discuss these two examples here; more matrix elements will be discussed in Sects. 5.6, and 7.2–7.5.

Initially, we make no assumptions about the properties of the matrix  $\Gamma$ , and note that the one-loop diagram of Fig. 5.1b for  $\Gamma(p, p)$  or  $\Gamma(p, 0)$  can be written as

$$A = \gamma_{\mu_1}\gamma_{\mu_2}\Gamma\gamma_{\nu_1}\gamma_{\nu_2} \cdot I^{\mu_1\mu_2;\nu_1\nu_2},$$

where  $I^{\mu_1\mu_2;\nu_1\nu_2}$  is an integral with respect to the loop momentum  $k$ . After integration, it can contain only  $g^{\mu\nu}$  and  $p^\alpha$ . Anticommuting the  $\gamma$ -matrices, we can rewrite the diagram as

$$\begin{aligned} A &= x_1\Gamma + x_2\cancel{p}\gamma^\mu\Gamma\gamma_\mu\cancel{p}/p^2 + x_3\gamma^\mu\gamma^\nu\Gamma\gamma_\nu\gamma_\mu = \sum_i x_i L_i \Gamma R_i, \\ L_i \times R_i &= 1 \times 1, \quad \cancel{p}\gamma^\mu \times \gamma_\mu\cancel{p}/p^2, \quad \gamma^\mu\gamma^\nu \times \gamma_\nu\gamma_\mu. \end{aligned} \quad (5.28)$$

The coefficients  $x_i$  can be found by calculating the traces of  $\gamma$ -matrices to the left of  $\Gamma$  and to the right of it, separately. For any term  $L\Gamma R$ , let us define

$$\langle \bar{L} \times \bar{R}, L\Gamma R \rangle = \frac{1}{4} \text{Tr } \bar{L}L \cdot \frac{1}{4} \text{Tr } \bar{R}R. \quad (5.29)$$

Then

$$y_i = \langle \bar{L}_i \times \bar{R}_i, \Lambda \rangle = \sum_j M_{ij} x_j, \quad M_{ij} = \frac{1}{4} \text{Tr } \bar{L}_i L_j \cdot \frac{1}{4} \text{Tr } \bar{R}_i R_j,$$

$$\bar{L}_i \times \bar{R}_i = 1 \times 1, \quad \gamma^\alpha \not{p} \times \not{p} \gamma_\alpha / p^2, \quad \gamma^\alpha \gamma^\beta \times \gamma_\beta \gamma_\alpha.$$

Solving the linear system, we can express the coefficients  $x_i$  via the double traces  $y_i$ :

$$\begin{pmatrix} x_1 \\ x_2 \\ x_3 \end{pmatrix} = \frac{1}{2(d-1)(d-2)} \begin{pmatrix} (d-2)(3d-2) & 0 & -(d-2) \\ 0 & 2d & -2 \\ -(d-2) & -2 & 1 \end{pmatrix} \begin{pmatrix} y_1 \\ y_2 \\ y_3 \end{pmatrix}. \quad (5.30)$$

Now we assume that the matrix  $\Gamma$  either commutes or anticommutes with  $\not{p}$ :

$$\not{p}\Gamma = \sigma\Gamma\not{p}, \quad \sigma = \pm 1. \quad (5.31)$$

This means that the components of  $\gamma^\mu$  parallel and orthogonal to  $p$  have to be treated separately. We also assume that  $\gamma^\mu \Gamma \gamma_\mu$  is proportional to  $\Gamma$ . It is convenient to modify the definition of  $h(d)$  slightly, and to use

$$\gamma^\mu \Gamma \gamma_\mu = 2\sigma h(d)\Gamma, \quad h(d) = (-1)^n \sigma \left( \frac{d}{2} - n \right) \quad (5.32)$$

instead of (5.5). Under these conditions, the correction (5.28) is proportional to  $\Gamma$ :

$$\Lambda = \Gamma [x_1 + x_2(2h) + x_3(2h)^2].$$

Substituting the solution (5.30) for  $x_i$ , we obtain

$$\Lambda = \Gamma \langle P, \Lambda \rangle,$$

$$P = \frac{1}{2(d-1)(d-2)} [(d-2)(3d-2-4h^2)1 \times 1$$

$$+ 4h(d-2h)\gamma^\alpha \not{p} \times \not{p} \gamma_\alpha / p^2 + (-d+2-4h+4h^2)\gamma^\alpha \gamma^\beta \times \gamma_\beta \gamma_\alpha].$$

Now we can apply the projector  $P$  to the integrand of the one-loop diagram of Fig. 5.1b, and reduce it to a scalar expression quadratic in  $h$ . Then the integral can be easily calculated (Sect. 2.2), once, and for all currents.

For any current (5.1) with  $\Gamma$  satisfying (5.31) and (5.32),  $\Gamma(p,p) = \Gamma\Gamma_a(p^2)$  and  $\Gamma(p,0) = \Gamma\Gamma_b(p^2)$ , where  $\Gamma_{a,b}(p^2) = 1 + \Lambda_{a,b}(p^2)$ . At one loop,

$$\Lambda_a = C_F \frac{g_0^2(-p^2)^{-\varepsilon}}{(4\pi)^{d/2}} \frac{G_1}{d-3} \left[ 2 \frac{1-a_0-h^2}{d-4} + \frac{d}{2}(1-a_0) + a_0 h \right], \quad (5.33)$$

$$\Lambda_b = C_F \frac{g_0^2(-p^2)^{-\varepsilon}}{(4\pi)^{d/2}} \frac{G_1}{d-3} \left[ 2 \frac{1-a_0-h^2}{d-4} + 1 - a_0 - h \right], \quad (5.34)$$

where  $G_1$  is defined in (2.41). Both matrix elements are IR finite; their UV divergences are given by (5.7).

A strong check of these results is provided by the Ward identities. From (5.11), we obtain

$$\Lambda_1^\mu(p, p) = -\frac{\partial}{\partial p_\mu} [\not{p}\Sigma_V(p^2)] = -\gamma^\mu\Sigma_V(p^2) - 2\not{p}p^\mu \frac{d\Sigma_V(p^2)}{dp^2}.$$

Therefore, for the longitudinal component of the vector current ( $\Gamma = \not{p}$ ,  $\sigma = +1$ ,  $h = 1 - d/2$ ), we have

$$\Lambda_a(p^2) = -\Sigma_V(p^2) - 2(-p^2) \frac{d\Sigma_V(p^2)}{d(-p^2)} = -(d-3)\Sigma_V(p^2),$$

and for its transverse component ( $\Gamma = \gamma_\perp^\mu = \gamma^\mu - \not{p}p^\mu/p^2$ ,  $\sigma = -1$ ,  $h = d/2 - 1$ ),  $\Lambda_a(p^2) = -\Sigma_V(p^2)$ . Substituting  $\Sigma_V(p^2)$  (3.47), we obtain two checks of (5.33). From (5.10), we obtain  $p_\mu\Lambda_1^\mu(p, 0) = -\not{p}\Sigma_V(p^2)$ , and hence, for the longitudinal component of the vector current ( $h = 1 - d/2$ ),  $\Lambda_b(p^2) = -\Sigma_V(p^2)$ . This provides a check of (5.34).

Now we can resume our investigation of the relation between matrix elements of currents containing  $\gamma_5^{HV}$  and  $\gamma_5^{AC}$ . Multiplying  $\Gamma$  by  $\gamma_5^{AC}$  does not change  $h$  (5.32), and hence cannot change the matrix element. On the other hand, multiplying the antisymmetrized product  $\Gamma$  of  $n$   $\gamma$ -matrices by  $\gamma_5^{HV}$  means  $n \rightarrow 4 - n$  and  $\sigma \rightarrow -\sigma$ . This is equivalent to the substitution  $d \rightarrow 8 - d$ , or  $\varepsilon \rightarrow -\varepsilon$  in  $h$ .

The matrix elements of the bare pseudoscalar currents  $j_{0AC}$  ( $h = 2 - \varepsilon$ ) and  $j_{0HV}$  ( $h = 2 + \varepsilon$ ) are related by (5.26)

$$Z_P(\alpha_s(\mu)) = \frac{Z_{P,AC}(\mu)}{Z_{P,HV}(\mu)} \frac{\Gamma_{a,b}(h = 2 - \varepsilon)}{\Gamma_{a,b}(h = 2 + \varepsilon)}. \quad (5.35)$$

At one loop (but not beyond),  $Z_{P,AC}(\mu) = Z_{j0}(\mu)$  and  $Z_{P,HV}(\mu) = Z_{j4}(\mu)$  coincide (see (5.8)). Therefore,  $Z_P = 1 + \Lambda_{a,b}(h = 2 - \varepsilon) - \Lambda_{a,b}(h = 2 + \varepsilon)$ . Only the  $1/\varepsilon$  term contributes, and we obtain, either from (5.33) or from (5.34),

$$Z_P(\alpha_s) = 1 - 8C_F \frac{\alpha_s}{4\pi} + \dots \quad (5.36)$$

The result for  $Z_A(\alpha_s)$  can be derived either from the longitudinal components of the axial currents or from the transverse components (see (5.27)):

$$Z_A(\alpha_s(\mu)) = \frac{Z_{A,AC}(\mu)}{Z_{A,HV}(\mu)} \frac{\Gamma_{a,b}(h = -1 + \varepsilon)}{\Gamma_{a,b}(h = -1 - \varepsilon)} = \frac{Z_{A,AC}(\mu)}{Z_{A,HV}(\mu)} \frac{\Gamma_{a,b}(h = 1 - \varepsilon)}{\Gamma_{a,b}(h = 1 + \varepsilon)}, \quad (5.37)$$

where  $Z_{A,AC}(\mu) = Z_{j1}(\mu) = 1$  and  $Z_{A,HV}(\mu) = Z_{j4}(\mu)$  coincide at one loop. The  $1/\varepsilon$  term in (5.33) and (5.34) does not change when  $h \rightarrow -h$ , and

$$Z_A(\alpha_s) = 1 - 4C_F \frac{\alpha_s}{4\pi} + \dots \quad (5.38)$$

The finite renormalization constants  $Z_{P,A}(\alpha_s)$  can also be obtained from the anomalous dimensions of the currents. Differentiating (5.26) and (5.27), we have

$$\begin{aligned} \frac{d \log Z_P(\alpha_s)}{d \log \alpha_s} &= \frac{\gamma_{j0}(\alpha_s) - \gamma_{j4}(\alpha_s)}{2\beta(\alpha_s)}, \\ \frac{d \log Z_A(\alpha_s)}{d \log \alpha_s} &= \frac{\gamma_{j1}(\alpha_s) - \gamma_{j3}(\alpha_s)}{2\beta(\alpha_s)}, \quad \text{where } \gamma_{j1} = 0. \end{aligned} \quad (5.39)$$

Therefore,

$$Z_P(\alpha_s) = K_{\gamma_{j0}-\gamma_{j4}}(\alpha_s), \quad Z_A(\alpha_s) = K_{\gamma_{j1}-\gamma_{j3}}(\alpha_s) \quad (5.40)$$

(see (4.72)). The one-loop results (5.36) and (5.38) can be reproduced using the two-loop anomalous dimensions (5.9). Now we see the reason why the last term in (5.9), which is not symmetric with respect to  $n \rightarrow 4 - n$ , is proportional to  $\beta_0$ . As  $Z_{P,A}(\alpha_s)$  can be obtained solely from the anomalous dimensions, they are determined by the UV behaviour of the matrix elements, and cannot depend on masses and external momenta.

The two-loop results

$$Z_P(\alpha_s) = 1 - 8C_F \frac{\alpha_s}{4\pi} + \frac{2}{9} C_F (C_A + 4T_F n_f) \left( \frac{\alpha_s}{4\pi} \right)^2 + \dots, \quad (5.41)$$

$$Z_A(\alpha_s) = 1 - 4C_F \frac{\alpha_s}{4\pi} + \frac{1}{9} C_F (198C_F - 107C_A + 4T_F n_f) \left( \frac{\alpha_s}{4\pi} \right)^2 + \dots \quad (5.42)$$

can be obtained either from the two-loop matrix elements  $\Gamma(p, p)$  (or  $\Gamma(p, 0)$ ), which can be calculated by the methods of Sect. 2.4, or from the three-loop anomalous dimensions. The three-loop results have been calculated [14] from the matrix elements only.

Why have we not discussed a similar relation  $j_{AC}^{\mu\nu}(\mu) = Z_T(\alpha_s(\mu)) j_{HV}^{\mu\nu}(\mu)$  between the tensor currents  $j_{0AC}^{\mu\nu} = \bar{q}_0' \gamma_5^{AC} \sigma^{\mu\nu} q_0$  and  $j_{0HV}^{\mu\nu} = \bar{q}_0' \gamma_5^{HV} \sigma^{\mu\nu} q_0$ ? The reason is the following. The current  $j_{AC}^{\mu\nu}$  has the same anomalous dimension as the current  $j_2^{\mu\nu}$  without  $\gamma_5^{AC}$ . Multiplication of  $\sigma^{\mu\nu}$  by  $\gamma_5^{HV}$  is merely a space–time transformation, e.g.,  $\gamma_5^{HV} \sigma^{01} = -i\sigma^{23}$ , and hence  $j_{HV}^{\mu\nu}$  has the same anomalous dimension, too. Therefore,  $Z_T(\alpha_s(\mu))$  cannot depend on  $\mu$ , and we conclude that  $Z_T(\alpha_s) = 1$ . This result can also be obtained by the following argument. Let us choose the axis 3 along  $p$ . Then  $\Gamma = \gamma_5^{AC} \sigma^{01}$  has  $h = -\varepsilon$ ,  $\Gamma = \gamma_5^{HV} \sigma^{01}$  has  $h = \varepsilon$ , and  $Z_T = \Gamma_{a,b}(h = -\varepsilon)/\Gamma_{a,b}(h = \varepsilon)$ . On the other hand,  $\Gamma = \gamma_5^{AC} \sigma^{23}$  has  $h = \varepsilon$ ,  $\Gamma = \gamma_5^{HV} \sigma^{23}$  has  $h = -\varepsilon$ , and  $Z_T = \Gamma_{a,b}(h = \varepsilon)/\Gamma_{a,b}(h = -\varepsilon)$ . Therefore,  $Z_T = 1$ .

## 5.4 Heavy–Light Current in HQET

Now we are going to consider the current

$$\tilde{j}(\mu) = \tilde{Z}_j^{-1}(\mu)\tilde{j}_0, \quad \tilde{j}_0 = \bar{q}_0\tilde{Q}_0 \quad (5.43)$$

in HQET with a scalar heavy quark  $\tilde{Q}$ . The proper vertex  $\tilde{\Gamma}(\omega, p) = 1 + \tilde{\Lambda}(\omega, p)$  (Fig. 5.3) can contain  $\gamma_0$  and  $\not{p}$ . When the vertex is expressed via the renormalized quantities  $\alpha_s(\mu)$ ,  $a(\mu)$ , it should become  $\tilde{Z}_\Gamma \tilde{\Gamma}_r(\omega, p)$ , where the renormalized vertex  $\tilde{\Gamma}_r(\omega, p)$  is finite at  $\varepsilon \rightarrow 0$ . When the proper vertex of the renormalized current  $\tilde{Z}_j^{-1}\tilde{\Gamma}(\omega, p)$  is multiplied by the external-leg renormalization factors  $Z_q^{1/2}\tilde{Z}_Q^{1/2}$ , it should give a finite matrix element. Therefore,  $\tilde{Z}_j = Z_q^{1/2}\tilde{Z}_Q^{1/2}\tilde{Z}_\Gamma$ . The UV divergences of  $\tilde{\Lambda}(\omega, p)$  do not depend on the masses and external momenta, and we may set these masses and momenta to zero. An IR cut-off is then necessary to avoid IR  $1/\varepsilon$  terms.

In the one-loop approximation (Fig. 5.3b),

$$\begin{aligned} \tilde{\Lambda}(0, 0) &= -iC_F g_0^2 \int \frac{d^d k}{(2\pi)^d} \frac{\gamma^\mu \not{k} v^\nu [g_{\mu\nu} - (1 - a_0)k_\mu k_\nu / k^2]}{(k^2)^2 k_0} \\ &= -iC_F g_0^2 \int \frac{d^d k}{(2\pi)^d} \frac{\gamma_0 \not{k} - (1 - a_0)k_0}{(k^2)^2 k_0}. \end{aligned}$$

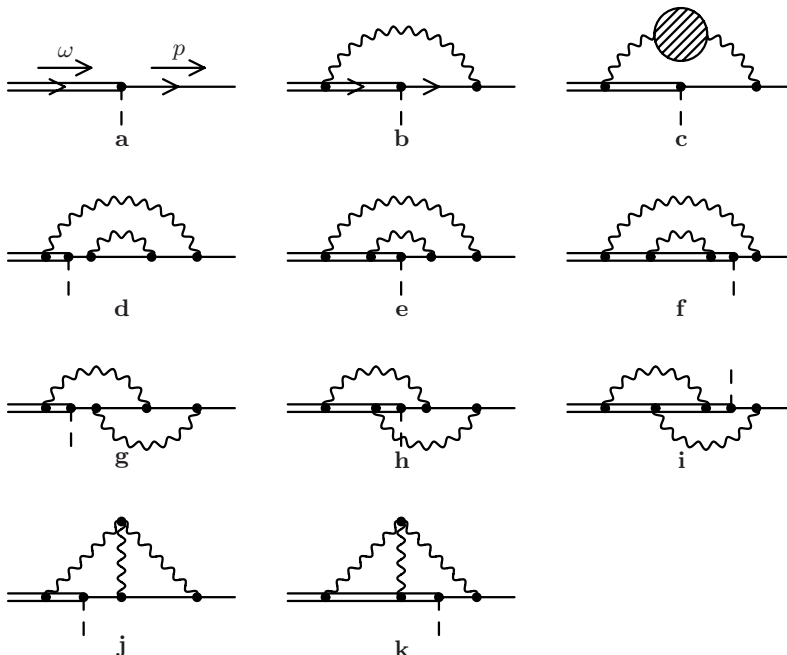


**Fig. 5.3.** Proper vertex of the heavy–light HQET current

Here  $\not{k} = k_0 \gamma_0 - \mathbf{k} \cdot \boldsymbol{\gamma}$ ; the term containing  $\mathbf{k}$  yields 0 after integration:

$$\tilde{A}(0,0) = -i C_F g_0^2 a_0 \int \frac{d^d k}{(2\pi)^d} \frac{1}{(k^2)^2}.$$

This integral contains no HQET denominator; its UV divergence is given by (4.51). We obtain

$$\tilde{Z}_F = 1 + C_F a \frac{\alpha_s}{4\pi\varepsilon}.$$

The gauge dependence is cancelled by  $Z_q^{1/2}$  (3.48) and  $\tilde{Z}_Q^{1/2}$  (3.65), and we arrive at

$$\tilde{\gamma}_j = -3C_F \frac{\alpha_s}{4\pi}. \quad (5.44)$$

Two-loop vertex diagrams (Figs. 5.3c–k) can be obtained by inserting the heavy–light quark vertex in all possible places along the quark line in the quark self-energy diagrams (see Fig. 3.13; the blob in Fig. 5.3c means the one-loop gluon self-energy shown in Fig. 3.2). To find the anomalous dimension, it is enough to calculate  $\tilde{A}(\omega, 0)$  (with a massless light quark), which is IR finite. This quantity contains an even number of  $\gamma$ -matrices, and can depend only on  $\gamma_0$ ; hence, it is just a scalar function of  $\omega$ , and we may take  $(1/4) \text{Tr}$  of the integrand. The two-loop result for  $\tilde{A}(\omega, 0)$  (Figs. 5.3c–k) can be calculated using the methods of Sect. 2.5. This has been done in [3]; the result leads to

$$\begin{aligned} \tilde{\gamma}_j = & -3C_F \frac{\alpha_s}{4\pi} \\ & + C_F \left[ \left( -\frac{8}{3}\pi^2 + \frac{5}{2} \right) C_F + \left( \frac{2}{3}\pi^2 - \frac{49}{6} \right) C_A + \frac{10}{3} T_F n_l \right] \left( \frac{\alpha_s}{4\pi} \right)^2. \end{aligned} \quad (5.45)$$

This anomalous dimension was calculated independently in [13, 9], by more cumbersome methods. The three-loop term has been calculated recently [6].

The vertex of the current  $\tilde{j}_0 = \bar{q}_0 \Gamma \tilde{Q}_0$  with a spin-(1/2) heavy quark is  $[(1 + \gamma_0)/2] \Gamma \tilde{\Gamma}(\omega, p)$ . Its anomalous dimension does not depend on the Dirac matrix  $\Gamma$ . Therefore, the factors relating the currents containing  $\gamma_5^{\text{AC}}$  and  $\gamma_5^{\text{HV}}$  are equal to 1. This is also evident from the fact that *any* renormalized matrix element of  $\tilde{j}(\mu)$  is equal to  $[(1 + \gamma_0)/2] \Gamma \tilde{M}(\mu)$ , where  $\tilde{M}(\mu)$  is the corresponding renormalized matrix element for a spin-0 heavy quark; it is finite, and hence we may take the limit  $\varepsilon \rightarrow 0$ , where  $\gamma_5^{\text{HV}}$  and  $\gamma_5^{\text{AC}}$  are the same thing.

## 5.5 Decoupling for QCD and HQET Currents

Now we are going to discuss the relation between light-quark currents in QCD with a heavy flavour (say, c) and in the effective low-energy theory

without this flavour. This section continues the discussion of decoupling given in Sect. 4.7. The currents in the full theory can be expanded in  $1/m_c$ , where the coefficients are operators of the effective theory with the appropriate quantum numbers and dimensionalities:

$$j_n(\mu) = \zeta_{jn}(\mu, \mu') j'_n(\mu') + \mathcal{O}(1/m_c). \quad (5.46)$$

The meaning of the operator expansion (5.46) is that on-shell matrix elements of  $j_n(\mu)$  with external momenta  $p_i \ll m_c$ , after expansion in  $p_i/m_c$  to some order, coincide with the corresponding matrix elements of the right-hand side. It is natural to match the currents at  $\mu = \mu' = m_c$ , because  $\zeta_{jn}(m_c, m_c)$  contains no large logarithms. Currents at arbitrary normalization scales are related by

$$\begin{aligned} \zeta_{jn}(\mu, \mu') &= \hat{\zeta}_{jn} \left( \frac{\alpha_s(\mu)}{\alpha_s(m_c)} \right)^{\gamma_{jn0}/(2\beta_0)} K_{\gamma_{jn}}(\alpha_s(\mu)) \\ &\times \left( \frac{\alpha'_s(\mu')}{\alpha'_s(m_c)} \right)^{-\gamma'_{jn0}/(2\beta'_0)} K'_{-\gamma'_{jn}}(\alpha'_s(\mu')), \end{aligned} \quad (5.47)$$

where

$$\hat{\zeta}_{jn} = \zeta_{jn}(m_c, m_c) K_{-\gamma_{jn}}(\alpha_s(m_c)) K'_{\gamma'_{jn}}(\alpha'_s(m_c)),$$

$K$  is defined by (4.72), and  $K'$  involves the  $n_l$ -flavour  $\beta$ -function  $\beta'(\alpha_s)$ .

The on-shell matrix element of  $j_n(\mu)$  is  $M_n(p, p', \mu) = Z_q^{\text{os}} Z_{jn}^{-1}(\mu) \Gamma_n(p, p')$ . It should be equal to  $\zeta_{jn}(\mu, \mu') M'_n(p, p', \mu') + \mathcal{O}((p, p')/m_c)$ , where  $M'_n(p, p', \mu') = Z_q^{\text{los}} Z_{jn}'^{-1}(\mu') \Gamma'_n(p, p')$ . Both matrix elements are UV-finite; their IR divergences coincide, because both theories are identical in the IR region. Therefore,

$$\zeta_{jn}(\mu, \mu') = \frac{Z_q^{\text{os}}}{Z_q^{\text{los}}} \frac{Z'_{jn}(\mu')}{Z_{jn}(\mu)} \frac{\Gamma_n(p, p')}{\Gamma'_n(p, p')} + \mathcal{O}\left(\frac{p, p'}{m_c}\right). \quad (5.48)$$

Any on-shell momenta  $p, p'$  can be used; it is easiest to set  $p = p' = 0$ , thus excluding power-suppressed terms in (5.48).

All loop diagrams for  $\Gamma'_n(0, 0)$  contain no scale, and  $\Gamma'_n(0, 0) = \Gamma$ , the antisymmetrized product of  $n$   $\gamma$ -matrices. Only diagrams with c-quark loops contribute to  $\Lambda_n(0, 0)$ ; the only relevant two-loop diagram is shown in Fig. 5.4. It is equal to

$$\begin{aligned} \Lambda_n(0, 0) &= -iC_F g_0^2 \int \frac{d^d k}{(2\pi)^d} \frac{\gamma^\mu \not{k} \Gamma \not{k} \gamma^\nu (k^2 g_{\mu\nu} - k_\mu k_\nu) \Pi(k^2)}{(k^2)^4} \\ &= -iC_F g_0^2 \int \frac{d^d k}{(2\pi)^d} \frac{(\gamma^\mu \not{k} \Gamma \not{k} \gamma_\mu - k^2 \Gamma) \Pi(k^2)}{(k^2)^3}, \end{aligned}$$

where  $\Pi(k^2)$  is the c-quark loop contribution to the gluon self-energy. Averaging over the directions of  $k$  and using the definition (5.5) of  $h$ , we obtain

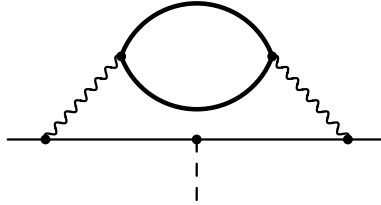


**Fig. 5.4.** Two-loop on-shell matrix element of a QCD bilinear quark current

$$\Lambda_n(0, 0) = -iC_F g_0^2 \Gamma \left( \frac{(2h)^2}{d} - 1 \right) \int \frac{d^d k}{(2\pi)^d} \frac{\Pi(k^2)}{(k^2)^2},$$

and using (4.33),

$$\begin{aligned} \Gamma_n(0, 0) &= \Gamma \left[ 1 - C_F T_F \frac{g_0^4 m_c^{-4\varepsilon}}{(4\pi)^d} \Gamma^2(\varepsilon) \frac{2(d-6)}{(d-2)(d-5)(d-7)} \right. \\ &\quad \times \left. \left( \frac{(d-2n)^2}{d} - 1 \right) \right]. \end{aligned} \quad (5.49)$$

From (5.9), we derive the ratio

$$\begin{aligned} \frac{Z_{jn}(m_c)}{Z'_{jn}(m_c)} &= 1 + \frac{1}{4} (\gamma_{jn0} \Delta\beta_0 - \Delta\gamma_{jn1} \varepsilon) \left( \frac{\alpha_s(m_c)}{4\pi\varepsilon} \right)^2 \\ &= 1 + \frac{1}{9} C_F T_F (n-1) [6(n-3) - (n-15)\varepsilon] \left( \frac{\alpha_s(m_c)}{4\pi\varepsilon} \right)^2, \end{aligned}$$

where  $\Delta\beta_0$  and  $\Delta\gamma_{jn1}$  are the single-flavour contributions. Using also (4.86), we arrive at the final result [12]

$$\zeta_{jn}(m_c, m_c) = 1 + \frac{1}{54} C_F T_F (n-1) (85n - 267) \left( \frac{\alpha_s(m_c)}{4\pi} \right)^2 + \dots \quad (5.50)$$

The vector current has  $\zeta_{j1} = 1$  to all orders. For the vector current with a diagonal flavour matrix  $\tau$ , the integral of its 0th component is an integer – the difference between the numbers of quarks and antiquarks weighted by the diagonal elements of  $\tau$ . This difference is the same in full QCD and in the low-energy effective theory. The same holds for non-diagonal  $\tau$  by flavour symmetry. We can also see this explicitly. Multiplying the Ward identity

$$\Gamma_1^\mu(0, 0) = \gamma^\mu - \left. \frac{\partial \Sigma(p)}{\partial p_\mu} \right|_{p=0} = \gamma^\mu (1 - \Sigma_V(0))$$

by  $Z_q^{os} = [1 - \Sigma_V(0)]^{-1}$ , we obtain just  $\Gamma = \gamma^\mu$ . Taking account of the fact that  $Z_{j1} = 1$ , (5.48) yields  $\zeta_{j1} = 1$ .

The decoupling for the scalar current  $\bar{q}'q$  is closely related to that for the  $\overline{\text{MS}}$  light-quark mass. The quark propagators (3.46) in full QCD and the low-energy effective theory should be related by  $S(p) = \zeta_q^0 S'(p)$ . Therefore,

$$\frac{1 + \Sigma_S(p^2)}{1 - \Sigma_V(p^2)} m_0 = \frac{1 + \Sigma'_S(p^2)}{1 - \Sigma'_V(p^2)} m'_0.$$

Let us define

$$\zeta_m^0 = \frac{m_0}{m'_0}, \quad \zeta_m(\mu, \mu') = \frac{m(\mu)}{m'(\mu')} = \zeta_m^0 \frac{Z'_m(\mu')}{Z_m(\mu)};$$

then

$$\zeta_m^0 = \frac{1 - \Sigma_V(p^2)}{1 - \Sigma'_V(p^2)} \frac{1 + \Sigma'_S(p^2)}{1 + \Sigma_S(p^2)}.$$

This equation should hold for all  $m \ll m_c$ ,  $p \ll m_c$ . It is easiest to set  $m = 0$ , and use (5.14). Then, setting  $p = 0$  and using  $Z_q^{\text{os}} = [1 - \Sigma_V(0)]^{-1}$ , we obtain

$$\zeta_m^0 = \frac{Z'_q^{\text{os}}}{Z_q^{\text{os}}} \frac{\Gamma'_0(0, 0)}{\Gamma_0(0, 0)}.$$

Recalling (5.48) and (5.15), we finally arrive at

$$\zeta_m(\mu, \mu') = \zeta_{j0}^{-1}(\mu, \mu'). \quad (5.51)$$

In other words,  $m(\mu)[\bar{q}'q]_\mu = m'(\mu')[\bar{q}'q]_{\mu'}$  does not vary with  $\mu$  and  $\mu'$ , and does not change when one goes from the full theory to the low-energy one. The  $\overline{\text{MS}}$  mass decoupling constant is

$$\zeta_m(m_c, m_c) = 1 - \frac{89}{18} C_F T_F \left( \frac{\alpha_s(m_c)}{4\pi} \right)^2 + \dots \quad (5.52)$$

This means that at  $\mu > m_c$ , the running of the light-quark  $\overline{\text{MS}}$  masses  $m(\mu)$  is governed by the anomalous dimension  $\gamma_m(\alpha_s)$  (5.16) and  $\beta(\alpha_s)$ , with  $n_f = n_l + 1$  flavours; at  $\mu < m_c$ , the running of  $m'(\mu)$  is governed by  $\gamma'_m(\alpha'_s)$  and  $\beta'(\alpha'_s)$ , with  $n_l$  flavours; and at  $\mu = m_c$

$$m(m_c) = \zeta_m(m_c, m_c) m'(m_c).$$

The currents  $j_4$  and  $j_3$  differ from  $j_0$  and  $j_1$  by insertion of  $\gamma_5^{\text{HV}}$ . They are related to those containing  $\gamma_5^{\text{AC}}$  by (5.26) and (5.27). Inserting  $\gamma_5^{\text{AC}}$  does not change the decoupling coefficient. Therefore,

$$\zeta_{j4} = \zeta_{j0} \frac{Z'_P}{Z_P}, \quad \zeta_{j3} = \zeta_{j1} \frac{Z'_A}{Z_A}, \quad (5.53)$$

where  $Z_{P,A}$  are given by (5.41) and (5.42) at two loops, and  $Z'_{P,A}$  contain  $n_l$  instead of  $n_f = n_l + 1$ .

The heavy–light current  $\tilde{j}$  in b-quark HQET can be considered similarly. Instead of (5.48), we now have

$$\tilde{\zeta}_j(\mu, \mu') = \left( \frac{Z_q^{\text{os}}}{Z_q'^{\text{os}}} \right)^{1/2} \left( \frac{\tilde{Z}_Q^{\text{os}}}{\tilde{Z}_Q'^{\text{os}}} \right)^{1/2} \frac{\tilde{Z}_j(\mu)}{\tilde{Z}'_j(\mu')} \frac{\tilde{\Gamma}(0, 0)}{\tilde{\Gamma}'(0, 0)}, \quad (5.54)$$

where  $\tilde{\Gamma}(\omega, p)$  is the proper vertex of the current. Only diagrams with c-quark loops can contribute to  $\tilde{\Gamma}(0, 0)$ . For a massless light quark,  $\tilde{\Gamma}(0, 0)$  contains an even number of  $\gamma$ -matrices, and can depend only on  $\gamma_0$ . Therefore, it is scalar, and we may take  $(1/4) \text{Tr}$  of an integrand. The only relevant two-loop diagram is shown in Fig. 5.5:

$$\tilde{\Lambda}(0, 0) = -iC_F g_0^2 \int \frac{d^d k}{(2\pi)^d} \frac{(1/4) \text{Tr} \gamma^\mu \not{k} \cdot v^\nu (k^2 g_{\mu\nu} - k_\mu k_\nu) \Pi(k^2)}{(k^2)^3 k_0} = 0. \quad (5.55)$$

From (5.45), we derive the ratio

$$\frac{\tilde{Z}_j(m_c)}{\tilde{Z}'_j(m_c)} = 1 + C_F T_F \left( 1 - \frac{5}{6}\varepsilon \right) \left( \frac{\alpha_s(m_c)}{4\pi\varepsilon} \right)^2 + \dots$$

Using also (4.86) and (4.88), we arrive at [12]

$$\tilde{\zeta}_j(m_c, m_c) = 1 + \frac{89}{36} C_F T_F \left( \frac{\alpha_s(m_c)}{4\pi} \right)^2 + \dots \quad (5.56)$$

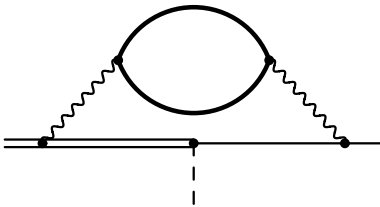


**Fig. 5.5.** Two-loop on-shell matrix element of the HQET heavy–light current

## 5.6 QCD/HQET Matching for Heavy–Light Currents

In physical applications, we are interested in matrix elements of QCD operators. However, we want to utilize the simplifications introduced by HQET.

Therefore, we expand the QCD operators in  $1/m$ ; the coefficients of these expansions are HQET operators with the appropriate quantum numbers and dimensionalities:

$$j(\mu) = C_\Gamma(\mu, \mu') \tilde{j}(\mu') + \frac{1}{2m} \sum_i B_i^\Gamma(\mu, \mu') \mathcal{O}_i(\mu') + \mathcal{O}\left(\frac{1}{m^2}\right). \quad (5.57)$$

The meaning of the operator expansion (5.57) is that matrix elements of  $j(\mu)$ , in situations amenable to HQET treatment, after expansion to a given order in  $1/m$ , coincide with the corresponding matrix elements of the right-hand side of this equation. Here we shall discuss the leading order;  $1/m$  terms are discussed in Chap. 6, and  $1/m^2$  terms in [1].

For example, let us consider the decay of a heavy quark into a light quark with energy  $\omega \ll m$  via a heavy–light weak current. The matrix element in QCD depends on two widely separated large scales  $m \gg \omega$  and the renormalization scale  $\mu$  (if the current has a non-zero anomalous dimension). For no choice of  $\mu$  can we get rid of large logarithmic corrections. When we go to HQET, all  $m$ -dependence is isolated in the matching coefficient of the heavy–light current  $C_\Gamma$ . The HQET matrix element knows nothing about  $m$ , and depends only on  $\omega$  and  $\mu'$ , where the  $\mu'$ -dependence is determined by the anomalous dimension of the HQET heavy–light current. If  $\mu'$  is chosen to be of the order of  $\omega$ , then there are no large logarithmic corrections.

It is natural to perform the matching at  $\mu = \mu' = m$ , where the matching coefficients  $C_\Gamma$  contain no large logarithms. Currents at arbitrary normalization scales are related by

$$\begin{aligned} C_\Gamma(\mu, \mu') &= \hat{C}_\Gamma \left( \frac{\alpha_s(\mu)}{\alpha_s(m)} \right)^{\gamma_{jn0}/(2\beta_0)} K_{\gamma_{jn}}(\alpha_s(\mu)) \\ &\times \left( \frac{\alpha'_s(\mu')}{\alpha'_s(m)} \right)^{-\tilde{\gamma}_{j0}/(2\beta'_0)} K'_{-\tilde{\gamma}_j}(\alpha'_s(\mu')), \end{aligned} \quad (5.58)$$

where

$$\hat{C}_\Gamma = C_\Gamma(m, m) K_{-\gamma_{jn}}(\alpha_s(m)) K'_{\tilde{\gamma}_j}(\alpha'_s(m))$$

(see (4.72)). If the heavy flavour considered in HQET is, say, b, then there are no b-quark loops in HQET; its  $\alpha'_s(\mu')$  is the same as in  $n_l$ -flavour QCD (Sect. 4.7), and its running is governed by the  $n_l$ -flavour  $\beta'(\alpha'_s)$ .

The on-shell matrix element of  $j(\mu)$  is  $M(p, p', \mu) = (Z_q^{\text{os}})^{1/2} (Z_Q^{\text{os}})^{1/2} Z_j^{-1}(\mu) \Gamma(p, p')$ . It should be equal to  $C_\Gamma(\mu, \mu') \tilde{M}(\tilde{p}, p', \mu') + \mathcal{O}((\tilde{p}, p')/m)$ , where  $p = mv + \tilde{p}$  and  $\tilde{M}(\tilde{p}, p', \mu') = (Z_q'^{\text{os}})^{1/2} (\tilde{Z}_Q^{\text{os}})^{1/2} \tilde{Z}_j^{-1}(\mu') \tilde{\Gamma}(\tilde{p}, p')$  (here  $Z_q'^{\text{os}}$  contains no b-quark loops, see Sect. 4.7). Both matrix elements are UV-finite; their IR divergences coincide, because HQET coincides with QCD in the IR region. Therefore,

$$C_\Gamma(\mu, \mu') = \left( \frac{Z_q^{\text{os}}}{Z_q'^{\text{os}}} \right)^{1/2} \left( \frac{Z_Q^{\text{os}}}{\tilde{Z}_Q^{\text{os}}} \right)^{1/2} \frac{\tilde{Z}_j(\mu')}{Z_j(\mu)} \frac{\Gamma(p, p')}{\tilde{\Gamma}(\tilde{p}, p')} + \mathcal{O}\left(\frac{\tilde{p}, p'}{m}\right). \quad (5.59)$$

Any on-shell momenta  $p, p'$  can be used; it is easiest to set  $\tilde{p} = p' = 0$ , thus excluding power-suppressed terms in (5.59).

The ratio  $\zeta_q^0 = Z_q^{\text{os}}/Z_q'^{\text{os}}$  (4.85) was considered in Sect. 4.7. At one loop, it is just 1; at two loops, it contains the b-loop contribution (4.86) (with  $m = m_b$  instead of  $m_c$ ). The on-shell renormalization constant of the HQET quark field  $\tilde{Z}_Q^{\text{os}}$  was considered in Sect. 4.3. It is just 1 if all quarks lighter than b are considered massless; the two-loop  $m_c$  correction is given by (4.34). The on-shell renormalization constant of a massive-quark field in QCD,  $Z_Q^{\text{os}}$ , was considered in Sect. 4.2. The one-loop result is given by (4.29); the two-loop result has been obtained in [2]. The  $\overline{\text{MS}}$  renormalization constant of the HQET heavy–light current  $\tilde{Z}_j(\mu)$  was considered in Sect. 5.4. It is the same for all  $\gamma$ -matrix structures  $\Gamma$ ; the two-loop result is given by (5.45). The  $\overline{\text{MS}}$  renormalization constant of QCD quark currents was considered in Sect. 5.1. For the antisymmetrized product of  $n$   $\gamma$ -matrices, the two-loop result is given by (5.9). The HQET proper vertex  $\tilde{\Gamma}(0, 0) = 1$  if all light quarks are considered massless. At two loops, only the diagram of Fig. 5.5 with a c-quark loop can contribute. However, it vanishes; see (5.55).

We have only to calculate  $\Gamma(mv, 0)$  (Fig. 5.6). The tree diagram (Fig. 5.6a) just gives

$$\Gamma_0 = \bar{u}_q \Gamma u_Q ,$$

where  $\Gamma$  is the Dirac matrix in the current. Initially, we make no assumptions about its properties. The one-loop diagram (Fig. 5.6b) can be written as a sum of terms of the form

$$\bar{u}_q \gamma_{\mu_1} \dots \gamma_{\mu_l} \Gamma \gamma_{\nu_1} \dots \gamma_{\nu_r} u_Q \cdot I^{\mu_1 \dots \mu_l; \nu_1 \dots \nu_r} , \quad (5.60)$$

where  $I$  is some integral over the loop momentum,  $l$  is even, and  $l + r \leq 4$ . After the integration,  $I^{\mu_1 \dots \mu_l; \nu_1 \dots \nu_r}$  can contain only  $g^{\mu\nu}$  and  $v^\alpha$ . The resulting contractions of pairs of  $\gamma$ -matrices on the left, and of pairs on the right, merely produce additional terms of the form (5.60), with smaller values of  $l + r$ . Before performing the remaining contractions, one may anticommutate  $\gamma$ -matrices, so as to arrange things such that  $\not{p}$  occurs only on the extreme left or on the extreme right, with the contracted indices in between occurring in opposite orders on the left and right of  $\Gamma$ . The additional terms arising from the anticommutations have fewer  $\gamma$ -matrices, with  $l$  remaining even. Repeating this procedure for all values of  $l + r$ , from 4 down to 0, we may cast the diagram of Fig. 5.6b in the form

$$\begin{aligned} A &= \bar{u}_q [\Gamma(x'_1 + x'_2 \not{p}) + \not{p} \gamma_\mu \Gamma \gamma^\mu (x'_3 + x'_4 \not{p}) + \gamma_\mu \gamma_\nu \Gamma \gamma^\nu \gamma^\mu x'_5] u_Q \\ &= \bar{u}_q \left( \sum_i x_i L_i \Gamma R_i \right) u_Q , \end{aligned}$$

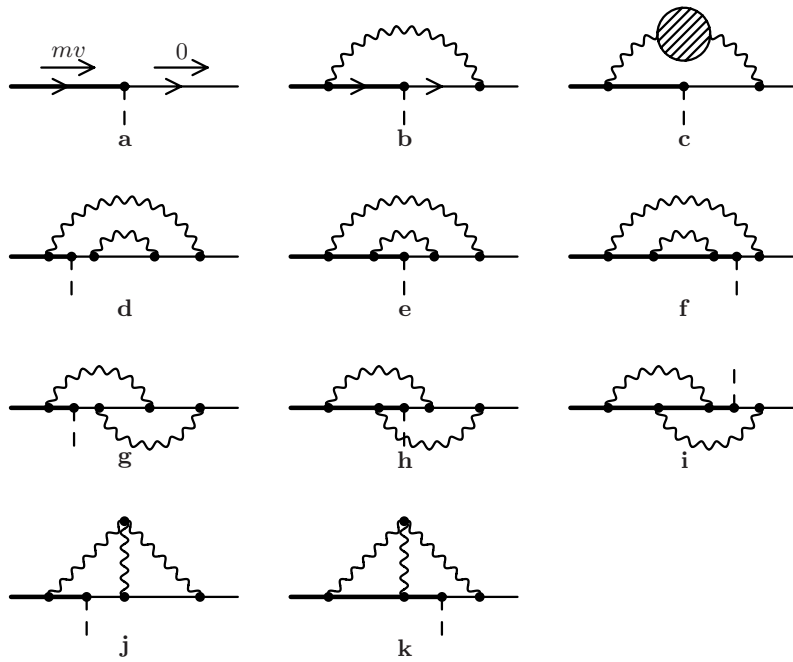


**Fig. 5.6.** Proper vertex of the heavy–light QCD current

where

$$x_1 = x'_1 + x'_2, \quad x_2 = x'_3 + x'_4, \quad x_3 = x'_5, \\ L_i \times R_i = 1 \times 1, \not{p} \gamma^\mu \times \gamma_\mu, \gamma^\mu \gamma^\nu \times \gamma_\nu \gamma_\mu$$

(because  $\not{p} u_Q = u_Q$ ). The coefficients  $x_i$  can be found by calculating the double traces (5.29)

$$y_i = \langle \bar{L}_i \times \bar{R}_i, \Lambda \rangle, \\ \bar{L}_i \times \bar{R}_i = 1 \times (\not{p} + 1), \gamma^\alpha \not{p} \times (\not{p} + 1) \gamma_\alpha, \gamma^\alpha \gamma^\beta \times (\not{p} + 1) \gamma_\beta \gamma_\alpha.$$

Solving the linear system, we obtain (5.30).

Now we assume, similarly to (5.31) and (5.32),

$$\not{p} \Gamma = \sigma \Gamma \not{p}, \quad \sigma = \pm 1, \quad \gamma^\mu \Gamma \gamma_\mu = 2\sigma h(d) \Gamma, \quad (5.61)$$

where

$$h(d) = \eta \left( n - \frac{d}{2} \right), \quad \eta = (-1)^{n+1} \sigma \quad (5.62)$$

for the antisymmetrized product of  $n$   $\gamma$ -matrices. The effect of each contraction is then to produce a factor  $2\sigma h$ . Terms with an odd number of contractions necessarily contain  $\not{p}$  on the left, which yields an extra  $\sigma$  when moved

to the right, where it merely gives  $\not{p} u_Q = u_Q$ . Thus the result involves only powers of  $h$ :

$$\Lambda = \bar{u}_q [x_1 + x_2 \cdot 2h + x_3(2h)^2] u_Q .$$

Substituting the solution (5.30) for  $x_i$ , we obtain

$$\begin{aligned} \Lambda &= \Gamma_0 \langle P, \Lambda \rangle , \\ P &= \frac{1}{2(d-1)(d-2)} \left[ (d-2)(3d^2 - 2 - 4h^2)1 \times (\not{p} + 1) \right. \\ &\quad + 4h(d-2h)\gamma^\alpha\not{p} \times (\not{p} + 1)\gamma_\alpha \\ &\quad \left. - (d-2-4h(1-h))\gamma^\alpha\gamma^\beta \times (\not{p} + 1)\gamma_\beta\gamma_\alpha \right] . \end{aligned}$$

Now we can apply the projector  $P$  to the integrand of the one-loop diagram of Fig. 5.6b and reduce it to a scalar expression quadratic in  $h$ :

$$\Lambda = \frac{iC_F g_0^2}{2(d-1)} \int \frac{d^d k}{(2\pi)^d} \frac{2(d-1) + (dD_2/m^2 + 4)h - 2(D_2/m^2 + 4)h^2}{D_1 D_2}, \quad (5.63)$$

where terms with  $D_1$  in the numerator have been omitted as they yield 0. The integral can be easily calculated (Sect. 2.2), once, and for all currents. We obtain the one-loop result [4]

$$\Lambda = -C_F \frac{g_0^2 m^{-2\varepsilon}}{(4\pi)^{d/2}} \Gamma(\varepsilon) \frac{(1-h)(d-2+2h)}{(d-2)(d-3)} . \quad (5.64)$$

This on-shell vertex is gauge-invariant. The two-loop contribution (Figs. 5.6c–k) has been calculated in [4]. It is a sum of terms of the form (5.60) with  $l+r \leq 8$ . Repeating the above discussion, we see that the integrand of each diagram can be reduced to a scalar expression quartic in  $h$ . Only the diagrams of Figs. 5.6e and 5.6h contain enough  $\gamma$ -matrices on each side of  $\Gamma$  to generate  $h^3$  and  $h^4$ . Scalar integrals are calculated by the method discussed in Sect. 4.2. The diagram of Fig. 5.6i and the heavy-quark loop contribution in Fig. 5.6c are of type  $N$  (4.19); they contain the non-trivial basis integral of Fig. 4.5e. The other diagrams are of type  $M$  (4.16), and can be expressed via  $\Gamma$ -functions (Figs. 4.5c,d). If there is an additional massive flavour ( $c$  in b-quark HQET), its loop in Fig. 5.6c yields a contribution which depends on  $m_c/m$ . This contribution is quadratic in  $h$ . It has been taken into account in [4].

In Sect. 5.3, we discussed the relation between quark currents containing  $\gamma_5^{AC}$  and  $\gamma_5^{HV}$ . The operator relations (5.26) and (5.27) were supposed to be universal. We have checked them for massless quarks by calculating two off-shell matrix elements. Now we are in a position to check them in the a

situation: one of the quarks is massive, and the momenta are on-shell ( $mv$  and 0). From (5.35) and (5.64) we recover (5.36); from (5.37) and (5.64) we have two new ways to derive (5.38). The two-loop results presented in [4] confirm (5.36) and (5.38).

At the time when the paper [4] was written, the two-loop anomalous dimension (5.9) of the generic quark current was not yet known (though all specific results except the one for  $n = 2$  were known). Therefore, the matching condition (5.59) was used to find both the minimal renormalization constant  $Z_j(\mu)$  and the finite matching coefficient  $C_\Gamma(\mu)$ . Of course,  $Z_j(\mu)$  could have been obtained from an easier massless calculation, but actually it was a by-product of a more difficult massive on-shell calculation.

At last, we can combine all pieces of (5.59). With two-loop accuracy,

$$C_\Gamma(m, m) = 1 + C_F \frac{\alpha_s(m)}{4\pi} [3(n-2)^2 + (2-\eta)(n-2) - 4] + C_F \left( \frac{\alpha_s}{4\pi} \right)^2 \left[ C_F a_F + C_A a_A + T_F a_h + T_F \sum_{i=1}^{n_1} \left( a_i + \Delta \left( \frac{m_i}{m} \right) \right) \right]. \quad (5.65)$$

The one-loop result (following from (5.64)) was first obtained in [8]. The two-loop calculation was done in [4]. There, a slightly different (and less useful) quantity was obtained. The proper matching coefficient (given by (5.59)) was considered in [12], where an additional term to be added to the results of [4] was derived. Here, for convenience, the complete result is presented:

$$\begin{aligned} a_F &= \left( \frac{317}{24} - \frac{10}{3}\zeta_2 \right) (n-2)^4 + 11(n-2)^3 - \frac{11}{2}\eta(n-2)^3 \\ &\quad + \left( -\frac{253}{6} + 48\zeta_2 - \frac{16}{3}I \right) (n-2)^2 - 2\eta(n-2)^2 - 20(n-2) \\ &\quad + \left( \frac{32}{3} - \frac{64}{3}\zeta_2 + \frac{8}{3}I \right) \eta(n-2) + \frac{689}{16} - 81\zeta_2 - 8\zeta_3 + 12I, \\ a_A &= \left( -\frac{43}{12} + \frac{4}{3}\zeta_2 \right) (n-2)^4 - 2(n-2)^3 + \eta(n-2)^3 \\ &\quad + \left( \frac{9491}{216} - \frac{52}{3}\zeta_2 + \frac{8}{3}I \right) (n-2)^2 + \frac{143}{18}(n-2) \\ &\quad + \left( -\frac{281}{18} + 8\zeta_2 - \frac{4}{3}I \right) \eta(n-2) - \frac{29017}{432} + 29\zeta_2 + 2\zeta_3 - 6I, \\ a_h &= \frac{59}{54}(n-2)^2 - \frac{2}{9}(n-2) + \left( -\frac{82}{9} + \frac{16}{3}\zeta_2 \right) \eta(n-2) + \frac{809}{27} - \frac{56}{3}\zeta_2, \\ a_l &= \left( -\frac{445}{54} - \frac{8}{3}\zeta_2 \right) (n-2)^2 - \frac{2}{9}(n-2) + \frac{38}{9}\eta(n-2) + \frac{1745}{108} + \frac{20}{3}\zeta_2, \end{aligned} \quad (5.66)$$

(see (4.20)). The mass correction

$$\begin{aligned} \Delta(r) = & \frac{2}{3} \left[ 4(\Delta_1(r) + \Delta_2(r) - \Delta_3(r))(n-2)^2 \right. \\ & \left. - 4(\Delta_2(r) - 2\Delta_3(r))\eta(n-2) - 10\Delta_1(r) - 5\Delta_2(r) - 18\Delta_3(r) \right] \end{aligned} \quad (5.67)$$

is the difference between the contribution of diagrams with a quark loop with mass  $m_i$  and the corresponding massless contribution ( $\Delta(0) = 0$ ). This difference is finite at  $\varepsilon = 0$ , and hence depends only on  $h|_{\varepsilon=0} = \eta(n-2)$ . It can be expressed via dilogarithms:

$$\begin{aligned} \Delta_1(r) &= -(1+r)L_+(r) - (1-r)L_-(r) + \log^2 r + \zeta_2, \\ \Delta_2(r) &= -r(1-r^2)L_+(r) + r(1-r^2)L_-(r) + 2r^2(\log r + 1), \\ \Delta_3(r) &= -r^3(1+r)L_+(r) + r^3(1-r)L_-(r) - r^2 \left( \log r + \frac{3}{2} \right), \end{aligned} \quad (5.68)$$

where  $L_{\pm}(r)$  are defined in (4.22).

There are eight distinct kinds of  $\Gamma$  in four-dimensional space–time. In the  $v$  rest frame, they are antisymmetrized products of zero to three matrices  $\gamma^i$ , and the same products times  $\gamma^0$ . For each current, we obtain the matching coefficient  $C_\Gamma(m)$  by choosing the appropriate values of  $n$  and  $\eta$  (defined in (5.62)) in (5.66) and (5.68), see Table 5.1. Typical matrices  $\Gamma$  are presented in the first column; the results are, of course, the same for other spatial components.

Multiplying  $\Gamma$  by  $\gamma_5^{\text{AC}}$  does not change  $h$  (5.61), and hence cannot change  $C_\Gamma(\mu)$ . On the other hand, multiplying  $\Gamma$  by  $\gamma_5^{\text{HV}}$  leads to  $n \rightarrow 4-n$  and  $\eta \rightarrow -\eta$ , and thus affects  $C_\Gamma(\mu)$ . The renormalized HQET currents containing  $\gamma_5^{\text{HV}}$  and  $\gamma_5^{\text{AC}}$  coincide with each other (Sect. 5.4). The renormalized QCD currents are related to each other by (5.26) and (5.27). Therefore,

$$\begin{aligned} Z_P(\alpha_s(\mu)) &= \frac{C_{\gamma_5^{\text{AC}}}(\mu, \mu')}{C_{\gamma_5^{\text{HV}}}(\mu, \mu')} = \frac{C_1(\mu, \mu')}{C_{\gamma^0\gamma^1\gamma^2\gamma^3}(\mu, \mu')}, \\ Z_A(\alpha_s(\mu)) &= \frac{C_{\gamma_5^{\text{AC}}\gamma^0}(\mu, \mu')}{C_{\gamma_5^{\text{HV}}\gamma^0}(\mu, \mu')} = \frac{C_{\gamma^0}(\mu, \mu')}{C_{\gamma^1\gamma^2\gamma^3}(\mu, \mu')} \\ &= \frac{C_{\gamma_5^{\text{AC}}\gamma^3}(\mu, \mu')}{C_{\gamma_5^{\text{HV}}\gamma^3}(\mu, \mu')} = \frac{C_{\gamma^3}(\mu, \mu')}{C_{\gamma^0\gamma^1\gamma^2}(\mu, \mu')}, \\ Z_T(\alpha_s(\mu)) &= \frac{C_{\gamma_5^{\text{AC}}\gamma^0\gamma^1}(\mu, \mu')}{C_{\gamma_5^{\text{HV}}\gamma^0\gamma^1}(\mu, \mu')} = \frac{C_{\gamma^0\gamma^1}(\mu, \mu')}{C_{\gamma^1\gamma^2}(\mu, \mu')} \\ &= \frac{C_{\gamma_5^{\text{AC}}\gamma^2\gamma^3}(\mu, \mu')}{C_{\gamma_5^{\text{HV}}\gamma^2\gamma^3}(\mu, \mu')} = \frac{C_{\gamma^2\gamma^3}(\mu, \mu')}{C_{\gamma^0\gamma^1}(\mu, \mu')} = 1. \end{aligned} \quad (5.69)$$

Two matching coefficients are equal:  $C_{\gamma^0\gamma^1}(\mu, \mu') = C_{\gamma^2\gamma^3}(\mu, \mu')$ ; indeed, for  $n = 2$  the results (5.66) and (5.68) do not depend on  $\eta$ . From (5.66), we can

**Table 5.1.** Matching coefficients  $C_\Gamma(m)$ 

$\Gamma$	$n$	$\eta$	$C_\Gamma(m, m)$
1	0	-1	$1 + 2C_F \frac{\alpha_s(m)}{4\pi} + C_F \left[ C_F \left( \frac{369}{16} + 15\zeta_2 - 8\zeta_3 - 4I \right) \right.$ $+ C_A \left( \frac{1351}{48} - 3\zeta_2 + 2\zeta_3 + 2I \right) + T_F \left( \frac{149}{9} - 8\zeta_2 \right)$ $\left. + T_F \sum_{i=1}^{n_1} \left( -\frac{95}{12} - 4\zeta_2 + 4\Delta_1 + 2\Delta_2 - 12\Delta_3 \right) \right] \left( \frac{\alpha_s}{4\pi} \right)^2$
$\gamma^0$	1	+1	$1 - 2C_F \frac{\alpha_s(m)}{4\pi} + C_F \left[ C_F \left( \frac{255}{16} - 15\zeta_2 - 8\zeta_3 + 4I \right) \right.$ $+ C_A \left( -\frac{871}{48} + 5\zeta_2 + 2\zeta_3 - 2I \right) + T_F \left( \frac{727}{18} - 24\zeta_2 \right)$ $\left. + T_F \sum_{i=1}^{n_1} \left( \frac{47}{12} + 4\zeta_2 - 4\Delta_1 + 2\Delta_2 - 20\Delta_3 \right) \right] \left( \frac{\alpha_s}{4\pi} \right)^2$
$\gamma^1$	1	-1	$1 - 4C_F \frac{\alpha_s(m)}{4\pi} + C_F \left[ C_F \left( -\frac{1453}{48} - \frac{173}{3}\zeta_2 - 8\zeta_3 + \frac{28}{3}I \right) \right.$ $+ C_A \left( -\frac{6821}{144} + 21\zeta_2 + 2\zeta_3 - \frac{14}{3}I \right) + T_F \left( \frac{133}{6} - \frac{40}{3}\zeta_2 \right)$ $\left. + T_F \sum_{i=1}^{n_1} \left( \frac{445}{36} + 4\zeta_2 - 4\Delta_1 - \frac{10}{3}\Delta_2 - \frac{28}{3}\Delta_3 \right) \right] \left( \frac{\alpha_s}{4\pi} \right)^2$
$\gamma^0\gamma^1$	2	+1	$1 - 4C_F \frac{\alpha_s(m)}{4\pi} + C_F \left[ C_F \left( \frac{689}{16} - 81\zeta_2 - 8\zeta_3 + 12I \right) \right.$ $+ C_A \left( -\frac{29017}{432} + 29\zeta_2 + 2\zeta_3 - 6I \right) + T_F \left( \frac{809}{27} - \frac{56}{3}\zeta_2 \right)$
$\gamma^1\gamma^2$	-1		$\left. + T_F \sum_{i=1}^{n_1} \left( \frac{1745}{108} + \frac{20}{3}\zeta_2 - \frac{20}{3}\Delta_1 - \frac{10}{3}\Delta_2 - 12\Delta_3 \right) \right] \left( \frac{\alpha_s}{4\pi} \right)^2$
$\gamma^0\gamma^1\gamma^2$	3	+1	$1 + C_F \left[ C_F \left( \frac{397}{48} - \frac{173}{3}\zeta_2 - 8\zeta_3 + \frac{28}{3}I \right) \right.$ $+ C_A \left( -\frac{1703}{48} + 21\zeta_2 + 2\zeta_3 - \frac{14}{3}I \right) + T_F \left( \frac{391}{18} - \frac{40}{3}\zeta_2 \right)$ $\left. + T_F \sum_{i=1}^{n_1} \left( \frac{143}{12} + 4\zeta_2 - 4\Delta_1 - \frac{10}{3}\Delta_2 - \frac{28}{3}\Delta_3 \right) \right] \left( \frac{\alpha_s}{4\pi} \right)^2$
$\gamma^1\gamma^2\gamma^3$	3	-1	$1 + 2C_F \frac{\alpha_s(m)}{4\pi} + C_F \left[ C_F \left( \frac{31}{16} - 15\zeta_2 - 8\zeta_3 + 4I \right) \right.$ $+ C_A \left( -\frac{901}{144} + 5\zeta_2 + 2\zeta_3 - 2I \right) + T_F \left( \frac{719}{18} - 24\zeta_2 \right)$ $\left. + T_F \sum_{i=1}^{n_1} \left( \frac{125}{36} + 4\zeta_2 - 4\Delta_1 + 2\Delta_2 - 20\Delta_3 \right) \right] \left( \frac{\alpha_s}{4\pi} \right)^2$
$\gamma^0\gamma^1\gamma^2\gamma^3$	4	+1	$1 + 10C_F \frac{\alpha_s(m)}{4\pi} + C_F \left[ C_F \left( \frac{1649}{16} + 15\zeta_2 - 8\zeta_3 - 4I \right) \right.$ $+ C_A \left( \frac{4021}{144} - 3\zeta_2 + 2\zeta_3 + 2I \right) + T_F \left( \frac{47}{3} - 8\zeta_2 \right)$ $\left. + T_F \sum_{i=1}^{n_1} \left( -\frac{317}{36} - 4\zeta_2 + 4\Delta_1 + 2\Delta_2 - 12\Delta_3 \right) \right] \left( \frac{\alpha_s}{4\pi} \right)^2$

reconstruct the two-loop results for  $Z_P$  (5.41) and  $Z_A$  (5.42) (in two ways). The finite-mass corrections depend only on  $\eta(n-2)$ , and are not affected when  $\Gamma$  is multiplied by  $\gamma_5^{\text{HV}}$ ; therefore, they cancel in the ratios giving  $Z_P$  and  $Z_A$ , as expected for results obtainable from anomalous dimensions (Sect. 5.3) which are mass-independent.

## 5.7 Meson Matrix Elements

Weak currents contain  $\gamma_5^{\text{AC}}$ . After eliminating the currents containing  $\gamma_5^{\text{HV}}$ , we are left with four essentially different currents, having  $\Gamma = 1, \gamma^0, \gamma, \gamma\gamma^0$ , and another four currents with an extra  $\gamma_5^{\text{AC}}$ . When  $\Gamma$  anticommutes with  $\gamma^0 (\sigma = -1)$ , the current has a non-zero matrix element between the vacuum and a ground-state ( $0^-$  or  $1^-$ ) meson:

$$\begin{aligned} \langle 0 | (\bar{q}\gamma_5^{\text{AC}} Q)_\mu | B \rangle &= -im_B f_B^P(\mu), \\ \langle 0 | \bar{q}\gamma^\alpha \gamma_5^{\text{AC}} Q | B \rangle &= if_B p^\alpha, \\ \langle 0 | \bar{q}\gamma^\alpha Q | B^* \rangle &= im_{B^*} f_{B^*} e^\alpha, \\ \langle 0 | (\bar{q}\sigma^{\alpha\beta} Q)_\mu | B^* \rangle &= f_{B^*}^T(\mu)(p^\alpha e^\beta - p^\beta e^\alpha), \end{aligned} \quad (5.70)$$

where  $e$  is the  $B^*$  polarization vector. When  $\Gamma$  commutes with  $\gamma^0 (\sigma = +1)$ , the current has a non-zero matrix element between the vacuum and a  $P$ -wave  $0^+$  or  $1^+$  meson. These matrix elements are given by similar formulae with  $\bar{q} \rightarrow \bar{q}\gamma_5^{\text{AC}}$ .

The matrix elements (in the relativistic normalization) of the corresponding HQET currents are compactly represented by the trace formula [16]:

$$\langle 0 | (\bar{q}\Gamma\tilde{Q})_\mu | M \rangle = \frac{F(\mu)}{2} \text{Tr } \Gamma \mathcal{M}, \quad (5.71)$$

where the spin wave function  $\mathcal{M}$  of the meson  $M$  is, for the ground-state mesons,

$$\mathcal{M} = i\sqrt{m_M} \frac{1+\not{v}}{2} \begin{cases} -\gamma_5 \\ \not{v} \end{cases} \quad (5.72)$$

(for  $0^+$  and  $1^+$  mesons  $\mathcal{M}$  should be right-multiplied by  $\gamma_5$ ; of course, their  $F(\mu)$  differs from the ground-state value). This wave function has the obvious property

$$\not{v}\mathcal{M} = \sigma\mathcal{M}\not{v} = \mathcal{M} \quad (5.73)$$

( $\sigma = -1$  for ground-state mesons and  $+1$  for  $P$ -wave ones). The trace formula (5.71) shows that the HQET quantities corresponding to those in (5.70) coincide:

$$\tilde{f}_B^P(\mu) = \tilde{f}_B(\mu) = \tilde{f}_{B^*}(\mu) = \tilde{f}_{B^*}^T(\mu) = \frac{F(\mu)}{\sqrt{m_B}}$$

(see (1.3)), as a consequence of the heavy-quark spin symmetry. Hence, ratios of QCD matrix elements are equal to ratios of matching coefficients. These ratios do not depend on the three-loop HQET anomalous dimension.

From the equations of motion,

$$i\partial_\alpha (\bar{q}\gamma_5^{AC}\gamma^\alpha Q) = m(\mu) (\bar{q}\gamma_5^{AC}Q)_\mu .$$

Taking the matrix element, we obtain [4]

$$\frac{f_B^P(\mu)}{f_B} = \frac{\langle 0 | (\bar{q}\gamma_5^{AC}Q)_\mu | B \rangle}{\langle 0 | \bar{q}\gamma_5^{AC}\gamma^0 Q | B \rangle} = \frac{m_B}{m(\mu)}, \quad (5.74)$$

where  $m(\mu)$  is the  $\overline{\text{MS}}$  running mass of the b-quark. To the leading order in  $1/m$ , we may replace  $m_B$  by the on-shell b-quark mass  $m$ , obtaining

$$\begin{aligned} \frac{f_B^P(m)}{f_B} &= \frac{m}{m(m)} = \frac{C_1(m, m)}{C_{\gamma^0}(m, m)} \\ &= 1 + 4C_F \frac{\alpha_s(m)}{4\pi} \\ &+ C_F \left[ C_F \left( \frac{121}{8} + 30\zeta_2 - 8I \right) + C_A \left( \frac{1111}{24} - 8\zeta_2 + 4I \right) \right. \\ &\quad \left. + T_F \left( -\frac{143}{6} + 16\zeta_2 \right) \right. \\ &\quad \left. + T_F \sum_{i=1}^{n_1} \left( -\frac{71}{6} - 8\zeta_2 + 8\Delta_1(r_i) + 8\Delta_3(r_i) \right) \right] \left( \frac{\alpha_s}{4\pi} \right)^2 . \end{aligned} \quad (5.75)$$

The one-loop result was derived in Sect. 5.1 (see (5.18)); the two-loop result was obtained in [11] (a typographical error was corrected in [4]).

The ratio of two observable matrix elements,

$$\frac{\langle 0 | \bar{q}\gamma Q | B^* \rangle}{\langle 0 | \bar{q}\gamma^0 \gamma_5^{AC} Q | B \rangle} = \frac{m_{B^*} f_{B^*} e}{m_B f_B}, \quad (5.76)$$

is independent of the renormalization scale. At the leading order in  $1/m$ , we obtain [4]

$$\begin{aligned} \frac{f_{B^*}}{f_B} &= \frac{C_{\gamma^1}(m, m)}{C_{\gamma^0}(m, m)} \\ &= 1 - 2C_F \frac{\alpha_s(m)}{4\pi} \end{aligned}$$

$$\begin{aligned}
& + C_F \left[ \frac{1}{3} C_F (31 - 128\zeta_2 + 16I) + C_A \left( -\frac{263}{9} + 16\zeta_2 - \frac{8}{3}I \right) \right. \\
& \quad + \frac{4}{3} T_F \left( -\frac{41}{3} + 8\zeta_2 \right) \\
& \quad \left. + \frac{4}{3} T_F \sum_{i=1}^{n_1} \left( \frac{19}{3} - 4\Delta_2(r_i) + 8\Delta_3(r_i) \right) \right] \left( \frac{\alpha_s}{4\pi} \right)^2 . \tag{5.77}
\end{aligned}$$

Numerically,

$$\begin{aligned}
\frac{f_B^*}{f_B} & = 1 - \frac{2}{3} \frac{\alpha_s(m_b)}{\pi} - (6.37 + \Delta_c) \left( \frac{\alpha_s}{\pi} \right)^2 + \mathcal{O} \left( \alpha_s^3, \frac{\Lambda_{\overline{\text{MS}}}}{m_b} \right) \\
& = 1 - 0.046 - 0.031 + \dots ,
\end{aligned}$$

where  $\Delta_c \approx 0.18$  is the correction due to  $m_c \neq 0$ . The convergence of the perturbation series is very slow.

Let us now consider the ratio  $f_B/f_D$  (1.4). We have

$$f_B = \frac{1}{\sqrt{m_b}} \left[ C_{\gamma^0}(m_b, m_b) F(m_b) + \mathcal{O} \left( \frac{\Lambda_{\overline{\text{MS}}}}{m_b} \right) \right],$$

where (5.66)

$$C_{\gamma^0}(m_b, m_b) = 1 + C_1 \frac{\alpha_s(m_b)}{4\pi} + \mathcal{O}(\alpha_s^2), \quad C_1 = -2C_F.$$

The HQET matrix element  $F(\mu)$  has the anomalous dimension  $\tilde{\gamma}_j$  (5.45); its  $\mu$ -dependence is given by the solution of the renormalization-group equation,

$$F(\mu) = \hat{F} \left( \frac{\alpha_s(\mu)}{4\pi} \right)^{\tilde{\gamma}_{j0}/(2\beta_0)} \left[ 1 + \frac{\tilde{\gamma}_{j0}}{2\beta_0} \left( \frac{\tilde{\gamma}_{j1}}{\tilde{\gamma}_{j0}} - \frac{\beta_1}{\beta_0} \right) \frac{\alpha_s(\mu)}{4\pi} + \mathcal{O}(\alpha_s^2) \right],$$

where  $\hat{F}$  is  $\mu$ -independent, and hence is just a number times  $\Lambda_{\overline{\text{MS}}}^{3/2}$ . Similar formulae hold for  $f_D$ . Therefore,

$$\begin{aligned}
\frac{f_B}{f_D} & = \sqrt{\frac{m_c}{m_b}} \left\{ \left( \frac{\alpha_s(m_b)}{\alpha_s(m_c)} \right)^{\tilde{\gamma}_{j0}/(2\beta_0)} \left[ 1 \right. \right. \\
& \quad \left. \left. + \left( C_1 + \frac{\tilde{\gamma}_{j0}}{2\beta_0} \left( \frac{\tilde{\gamma}_{j1}}{\tilde{\gamma}_{j0}} - \frac{\beta_1}{\beta_0} \right) \right) \frac{\alpha_s(m_b) - \alpha_s(m_c)}{4\pi} + \mathcal{O}(\alpha_s^2) \right] + \mathcal{O} \left( \frac{\Lambda_{\overline{\text{MS}}}}{m_{c,b}} \right) \right\} \\
& \tag{5.78}
\end{aligned}$$

(cf. (4.77)). Substituting  $\tilde{\gamma}_{j0}$ ,  $\tilde{\gamma}_{j1}$  (5.45) and  $\beta_0$ ,  $\beta_1$  (3.6) at  $n_f = 4$ , we obtain

$$\begin{aligned}
\frac{f_B}{f_D} & = \sqrt{\frac{m_c}{m_b}} \left\{ \left( \frac{\alpha_s(m_c)}{\alpha_s(m_b)} \right)^{6/25} \left[ 1 \right. \right. \\
& \quad \left. \left. + \frac{7}{225} \left( \pi^2 + \frac{1887}{100} \right) \frac{\alpha_s(m_c) - \alpha_s(m_b)}{\pi} + \mathcal{O}(\alpha_s^2) \right] + \mathcal{O} \left( \frac{\Lambda_{\overline{\text{MS}}}}{m_{c,b}} \right) \right\}.
\end{aligned}$$

The next-to-next-to-leading-order correction has been calculated recently [6].

For the last ratio,

$$\frac{\langle 0 | (\bar{q} \gamma^i \gamma^0 Q)_\mu | B^* \rangle}{\langle 0 | \bar{q} \gamma^i Q | B^* \rangle} = \frac{f_{B^*}^T(\mu)}{f_{B^*}}, \quad (5.79)$$

we have [4]

$$\begin{aligned} \frac{f_{B^*}^T(m)}{f_{B^*}} &= \frac{C_{\gamma^0 \gamma^1}(m, m)}{C_{\gamma^1}(m, m)} \\ &= 1 + C_F \left[ \frac{1}{3} C_F \left( \frac{307}{8} - 70\zeta_2 + 8I \right) + C_A \left( -\frac{4277}{216} + 8\zeta_2 - \frac{4}{3}I \right) \right. \\ &\quad + \frac{1}{3} T_F \left( \frac{421}{18} - 16\zeta_2 \right) \\ &\quad \left. + \frac{8}{3} T_F \sum_{i=1}^{n_1} \left( \frac{205}{144} + \zeta_2 - \Delta_1(r_i) - \Delta_3(r_i) \right) \right] \left( \frac{\alpha_s}{4\pi} \right)^2. \end{aligned} \quad (5.80)$$

The one-loop term vanishes at  $\mu = \mu' = m$ , but will of course appear at any other  $\mu, \mu'$ . If one wants  $f_{B^*}^T(\mu)$  at a scale  $\mu$  widely separated from  $m$ , one needs to use the three-loop anomalous dimension [10] of the QCD current  $\bar{q}\sigma^{\alpha\beta}q$  in conjunction with (5.80).

We can look at the calculation of QCD matrix elements via matching with HQET from a slightly different point of view. Let us return to the example of a heavy quark with mass  $m$  decaying into a light quark with energy  $\omega = k \cdot v \ll m$  (Figs. 5.7a,b). The one-loop QCD correction to this process (Fig. 5.7b) is a complicated diagram with two widely separated large scales. The decay amplitude (Figs. 5.7a,b) can be written as a matching coefficient times an HQET amplitude. The matching coefficient depends only on  $m$ , and is given by the QCD diagrams (Figs. 5.7a,b) at the threshold  $\omega = 0$ . The HQET matrix element (Figs. 5.7c,d) depends only on  $\omega$ . Therefore, the one-loop QCD diagram of Fig. 5.7b at  $\omega \ll m$  is just the sum of its value

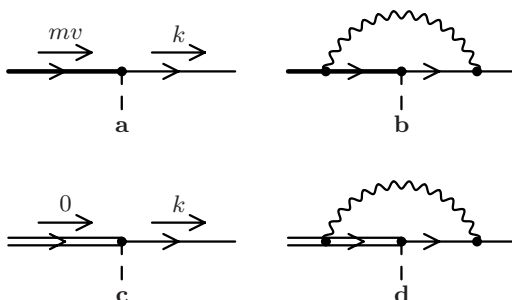


**Fig. 5.7.** The decay  $Q \rightarrow q$  in QCD and HQET

at the threshold ( $\omega = 0$ ) and the HQET contribution (Fig. 5.7d). This is a simple case of the threshold expansion, which is discussed in the book [17].

## References

1. C. Balzereit, T. Ohl: Phys. Lett. B **398**, 365 (1997) [108](#)
2. D.J. Broadhurst, N. Gray, K. Schilcher: Z. Phys. C **52**, 111 (1991) [109](#)
3. D.J. Broadhurst, A.G. Grozin: Phys. Lett. B **267**, 105 (1991) [103](#)
4. D.J. Broadhurst, A.G. Grozin: Phys. Rev. D **52**, 4082 (1995) [93, 111, 112, 116, 118](#)
5. K.G. Chetyrkin: Phys. Lett. B **404**, 161 (1997) [94](#)
6. K.G. Chetyrkin, A.G. Grozin: Nucl. Phys. B **666**, 289 (2003) [103, 118](#)
7. J.C. Collins: *Renormalization* (Cambridge University Press, Cambridge 1984) [96](#)
8. E. Eichten, B. Hill: Phys. Lett. B **234**, 511 (1990) [112](#)
9. V. Giménez: Nucl. Phys. B **375**, 582 (1992) [103](#)
10. J.A. Gracey: Phys. Lett. B **488**, 175 (2000) [93, 118](#)
11. N. Gray, D.J. Broadhurst, W. Grafe, K. Schilcher: Z. Phys. C **48**, 673 (1990) [95, 116](#)
12. A.G. Grozin: Phys. Lett. B **445**, 165 (1998) [105, 107, 112](#)
13. X.-D. Ji, M.J. Musolf: Phys. Lett. B **257**, 409 (1991) [103](#)
14. S.A. Larin: ‘The Renormalization of the Axial Anomaly in Dimensional Regularization’, in *Quarks-92*, ed. by D.Yu. Grigoriev, V.A. Matveev, V.A. Rubakov, P.G. Tinyakov (World Scientific, Singapore 1993), p. 201; Phys. Lett. B **303**, 113 (1993) [98, 101](#)
15. K. Melnikov, T. van Ritbergen: Phys. Lett. B **482**, 99 (2000); Nucl. Phys. B **591**, 515 (2000) [95](#)
16. M. Neubert: Phys. Rev. D **45**, 2451 (1992) [115](#)
17. V.A. Smirnov: *Applied Asymptotic Expansions in Momenta and Masses* (Springer, Berlin, Heidelberg 2001) [119](#)
18. J.A.M. Vermaasen, S.A. Larin, T. van Ritbergen: Phys. Lett. B **405**, 327 (1997) [94](#)

# 6 Heavy–Light Currents: $1/m$ Corrections

In this chapter, we continue the discussion of heavy–light bilinear quark currents, and consider  $1/m$  corrections in the expansion of QCD currents in HQET, as well as dimension-4 HQET operators which appear in these corrections. The  $1/m$  term in the expansion (5.57) for the vector current (and the axial current containing  $\gamma_5^{\text{AC}}$ ) was first investigated in [4], where the one-loop anomalous dimension matrix of dimension-4 operators  $\mathcal{O}_i$  was found. The full one-loop corrections to  $B_i$  were obtained in [5, 7]. Some general properties of the matching coefficients  $B_i$  and the anomalous dimension matrix of  $\mathcal{O}_i$  following from reparametrization invariance and the equations of motion were established in [7], and the two-loop anomalous-dimension matrix was calculated in [1, 2].

## 6.1 $1/m$ Corrections to Heavy–Light Currents

In the right-hand side of the  $1/m$  expansion (5.57), the  $\mathcal{O}_i$  are all local dimension-4 HQET operators with the appropriate quantum numbers. Matrix elements of this right-hand side are calculated according to the Feynman rules of the HQET Lagrangian (4.11) with  $1/m$  corrections. To the first order in  $1/m$ , we can either take a  $1/m$ -suppressed operator in (5.57) and use only vertices of the leading-order HQET Lagrangian (2.5), or take the leading HQET current in (5.57) and use a single vertex from the  $1/m$  terms in the Lagrangian (4.11). Alternatively, we can include the bilocal operators – integrals of time-ordered products

$$\mathcal{O}_{jk} = i \int dx T \{ \tilde{j}(0), \mathcal{O}_k(x) \}, \quad \mathcal{O}_{jm} = i \int dx T \{ \tilde{j}(0), \mathcal{O}_m(x) \} \quad (6.1)$$

with the coefficients

$$B_{jk}(\mu, \mu') = C_T(\mu, \mu'), \quad B_{jm}(\mu, \mu') = C_T(\mu, \mu')C_m(\mu') \quad (6.2)$$

in the sum in the right-hand side of the expansion (5.57), and use the leading-order Lagrangian (2.5) to calculate its matrix elements. Renormalization of the bilocal operators (6.1) requires both bilocal counterterms of the same structure and local counterterms proportional to the local operators  $\mathcal{O}_i$  in

this sum. Therefore, renormalization-group equations should be written for the full set of local and bilocal operators.

The local dimension-4 operators  $\mathcal{O}_i$  have the structure  $\bar{q}D\tilde{Q}$  or  $\bar{q}\overleftrightarrow{D}\tilde{Q}$ . If the light-quark mass cannot be neglected, there is also  $m_q\bar{q}\tilde{Q}$ ; this is important if the light quark is  $c$  in the b-quark HQET (see Sects. 7.3 and 7.5). To find their coefficients, we need to match matrix elements of the QCD current and its HQET expansion (5.57) from an on-shell heavy quark to an on-shell light quark, where either the heavy-quark residual momentum  $\tilde{p}$  or the light-quark momentum  $p'$  is non-zero, with linear accuracy in  $\tilde{p}/m$ ,  $p'/m$ , and  $m_q/m$ . There is no need to calculate the QCD vertex  $\Gamma(p, 0)$  with an on-shell  $p = mv + \tilde{p}$ , because it can be obtained from  $\Gamma(mv, 0)$  by a Lorentz transformation. Therefore, the coefficients  $B_i$  of the operators  $\mathcal{O}_i$  with  $D_\mu$  acting on  $\tilde{Q}$  can be obtained [7] from the leading-order matching coefficients  $C_\Gamma$  (reparametrization invariance).

Let  $\Gamma$  be a combination of  $\gamma$  matrices not depending on  $v$ . This Dirac matrix can be decomposed as

$$\Gamma = \Gamma_+ + \Gamma_- , \quad \Gamma_\pm = \frac{1}{2} (\Gamma \pm \not{v} \Gamma \not{v}) , \quad (6.3)$$

where  $\Gamma_+$  commutes with  $\not{v}$ , and  $\Gamma_-$  anticommutes. The matrix element of the renormalized QCD current  $\bar{q}\Gamma Q$  from the heavy-quark state with momentum  $mv$  to the light-quark state with momentum 0 is (see (5.59))

$$\frac{1}{2} (C_{\Gamma_+} + C_{\Gamma_-}) \bar{u}_q \Gamma u(mv) + \frac{1}{2} (C_{\Gamma_+} - C_{\Gamma_-}) \bar{u}_q \not{v} \Gamma u(mv) . \quad (6.4)$$

In this equation, we may substitute  $v \rightarrow v + \tilde{p}/m$ :

$$\begin{aligned} & \frac{1}{2} (C_{\Gamma_+} + C_{\Gamma_-}) \bar{u}_q \Gamma u(mv + \tilde{p}) \\ & + \frac{1}{2} (C_{\Gamma_+} - C_{\Gamma_-}) \bar{u}_q (\not{v} + \not{\tilde{p}}/m) \Gamma u(mv + \tilde{p}) . \end{aligned}$$

Using the Foldy–Wouthuysen transformation (4.59), we obtain the leading term (6.4) plus

$$\frac{1}{4m} [(C_{\Gamma_+} + C_{\Gamma_-}) \bar{u}_q \Gamma \not{p} u_v + (C_{\Gamma_+} - C_{\Gamma_-}) \bar{u}_q (\not{v} \Gamma \not{p} + 2\not{p} \Gamma) u_v] .$$

Therefore, the  $\bar{q}D\tilde{Q}$  terms in the sum in (5.57) are

$$\frac{1}{2} (C_{\Gamma_+} + C_{\Gamma_-}) \bar{q} \Gamma i\not{D} \tilde{Q}_v + \frac{1}{2} (C_{\Gamma_+} - C_{\Gamma_-}) \bar{q} (\not{v} \Gamma i\not{D} + 2i\not{D} \Gamma) \tilde{Q}_v . \quad (6.5)$$

This derivation can be reformulated in an operator form. In order to construct reparametrization-invariant objects, one should use not  $v$  but

$$\mathcal{V} = v + \frac{iD}{m} , \quad (6.6)$$

which is the gauge-covariant extension of  $p/m$  (2.6). One should also use  $\tilde{Q}_V$  instead of  $\tilde{Q}_v$ . This field is obtained by a Lorentz transformation which rotates  $v$  into  $V$ . With linear accuracy in  $1/m$ ,

$$\tilde{Q}_V = \frac{1 + \gamma}{2} \tilde{Q}_v = \left( 1 + \frac{iP}{2m} \right) \tilde{Q}_v. \quad (6.7)$$

The leading-order expression

$$\bar{q}\Gamma Q = \frac{1}{2} (C_{\Gamma_+} + C_{\Gamma_-}) \bar{q}\Gamma \tilde{Q}_v + \frac{1}{2} (C_{\Gamma_+} - C_{\Gamma_-}) \bar{q}\not{\psi}\Gamma \tilde{Q}_v$$

is not reparametrization-invariant. It should be replaced by the invariant combination

$$\begin{aligned} & \frac{1}{2} (C_{\Gamma_+} + C_{\Gamma_-}) \bar{q}\Gamma \left( 1 + \frac{iP}{2m} \right) \tilde{Q}_v \\ & + \frac{1}{2} (C_{\Gamma_+} - C_{\Gamma_-}) \bar{q} \left( \not{\psi} + \frac{iP}{m} \right) \Gamma \left( 1 + \frac{iP}{2m} \right) \tilde{Q}_v. \end{aligned}$$

Operators of the form  $\bar{q}D\tilde{Q}_v$  are not reparametrization-invariant separately, and can appear only in this combination. Therefore, we arrive at (6.5).

The coefficients of the operators  $\bar{q}\overleftrightarrow{D}\tilde{Q}$  and  $m_q\bar{q}\tilde{Q}$  are not determined by general considerations. These coefficients appear first at the one-loop level. We shall consider only  $\mathcal{O}(\alpha_s)$  corrections at  $m_q = 0$  here, because some anomalous dimensions for mixing with  $m_q\bar{q}\tilde{Q}$  operators are not yet known at the next-to-leading order (Sect. 6.3). We calculate the matrix element of the QCD current from a heavy quark with momentum  $mv$  to a massless quark with momentum  $p$  (with  $p^2 = 0$ ), expanded in  $p/m$  to the linear term, and equate it to the corresponding HQET matrix element. In HQET, loop corrections contain no scale, and hence vanish (except, possibly, massive-quark loops, which first appear at the two-loop level). The QCD matrix element is proportional to  $\bar{u}(p)\Gamma(p, mv)u(mv)$ , where  $\Gamma(p, mv)$  is the bare proper-vertex function. At one loop, it is given by Fig. 6.1.

If we assume nothing about the properties of  $\Gamma$ , then the term linear in  $p$  has the structure

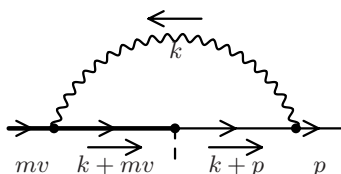


**Fig. 6.1.** Proper vertex of the heavy–light QCD current

$$\bar{u}(p) \left[ \sum_i x_i L_i \Gamma R_i \right] u(mv), \quad (6.8)$$

with  $L_i \times R_i = p \cdot v 1 \times 1, p \cdot v \not{p} \gamma_\mu \times \gamma^\mu, p \cdot v \gamma_\mu \gamma_\nu \times \gamma^\nu \gamma^\mu, 1 \times \not{p}, \not{p} \gamma_\mu \times \gamma^\mu \not{p}$ . The coefficients  $x_i$  can be obtained, by solving a linear system, from the double traces of  $\gamma$ -matrices to the left of  $\Gamma$  with  $\bar{L}_j$  and of  $\gamma$ -matrices to the right of  $\Gamma$  with  $\bar{R}_j$ , where  $\bar{L}_j \times \bar{R}_j = \not{p} \not{p} \times (1 + \not{p}), \gamma_\rho \not{p} \times (1 + \not{p}) \gamma^\rho, \gamma_\rho \gamma_\sigma \not{p} \not{p} \times (1 + \not{p}) \gamma^\sigma \gamma^\rho, \not{p} \not{p} \times (1 + \not{p}) \not{p}, \gamma_\rho \not{p} \times (1 + \not{p}) \not{p} \gamma^\rho$ . Now we can take these double traces of the *integrand* of Fig. 6.1, and express  $x_i$  via scalar integrals. Their numerators involve  $(k \cdot p)^n$ ; putting  $k = (k \cdot v)v + k_\perp$  and averaging over the directions of  $k_\perp$  in the  $(d - 1)$ -dimensional subspace, we can express them via the factors in the denominator.

Now we assume that  $\Gamma$  satisfies (5.61). Then (6.8) becomes

$$\begin{aligned} & [x_1 + (x_2 + 2x_5) \cdot 2h + x_3(2h)^2] p \cdot v \bar{u}(p) \Gamma u(mv) \\ & + [x_4 - x_5 \cdot 2h] \bar{u}(p) \Gamma \not{p} u(mv). \end{aligned} \quad (6.9)$$

Performing a simple calculation, we obtain

$$\Gamma(p, mv) = \Gamma(0, mv) + \frac{1}{2m} C_F \frac{g_0^2 m^{-2\varepsilon}}{(4\pi)^{d/2}} \Gamma(\varepsilon) \Gamma(b_1^\Gamma p \cdot v + b_2^\Gamma \not{p}) \quad (6.10)$$

(see (5.64)), where

$$\begin{aligned} b_1^\Gamma &= -2 \frac{(d-2)(d-8) - (d-5)(d-4+2h)h}{(d-2)(d-3)(d-5)}, \\ b_2^\Gamma &= 2 \frac{d-2-h}{(d-2)(d-3)}. \end{aligned}$$

The first-order coefficients for the components of the vector current were calculated in [5, 7].

For  $\Gamma = 1, \gamma^0$ , the bracket in (6.10) becomes  $b_\Gamma p \cdot v$ , with  $b_1 = b_1^1$  and  $b_{\gamma^0} = b_1^{\gamma^0} + 2b_2^{\gamma^0}$ . For  $\Gamma = \gamma^i, \gamma^i \gamma^0$ , it becomes  $b_1 p \cdot v \gamma^i + b_2 p^i$ , where  $b_1 = b_1^{\gamma^i}$  and  $b_2 = 2b_2^{\gamma^i}$  for  $\Gamma = \gamma^i$ ,  $b_1 = b_1^{\gamma^i \gamma^0} + 2b_2^{\gamma^i \gamma^0}$  and  $b_2 = -2b_2^{\gamma^i \gamma^0}$  for  $\Gamma = \gamma^i \gamma^0$ . A strong check is provided by the Ward identity: contracting the vertex function  $\Gamma^\alpha(p, mv)$  (for  $\Gamma = \gamma^\alpha$ ) with the momentum transfer  $(mv - p)_\alpha$ , we obtain

$$\Gamma^\alpha(p, mv)(mv - p)_\alpha = m\Gamma(p, mv) + \Sigma(mv),$$

where  $\Gamma(p, mv)$  is the scalar vertex (for  $\Gamma = 1$ ), and  $\Sigma$  is the heavy-quark self-energy (Sect. 4.2). At the first order in  $p$ , this leads to

$$b_1 - b_{\gamma^0} = 2(c_{\gamma^i} - c_{\gamma^0}), \quad (6.11)$$

where  $c_\Gamma$  is the coefficient in (5.64).

HQET matrix elements of dimension-4 operators between the vacuum and ground-state  $0^-$  and  $1^-$  mesons (or  $P$ -wave  $0^+$  and  $1^+$  mesons) can be compactly represented in the trace formalism [6], similarly to (5.71). The most general form of the matrix element of an operator with  $D$  acting on  $\tilde{Q}$  is

$$\langle 0 | \mathcal{O}_1^\Gamma(\mu) | M \rangle = \frac{F_2(\mu)}{2} \text{Tr} \gamma_\perp^\alpha \Gamma \mathcal{M}, \quad \mathcal{O}_1^\Gamma = \bar{q} i D^\alpha \Gamma \tilde{Q} \quad (6.12)$$

(see (6.23)). If we now take  $\Gamma = \gamma_\alpha \Gamma'$ , this operator becomes

$$\bar{q} i \not{D} \Gamma' \tilde{Q} = i \partial_\alpha \left( \bar{q} \gamma^\alpha \Gamma' \tilde{Q} \right)$$

(we shall see in Sect. 6.2 that this is no longer true at the  $\alpha_s$  level), and its matrix element is

$$\bar{\Lambda} \frac{F(\mu)}{2} \text{Tr} \not{p} \Gamma' \mathcal{M} = \sigma \bar{\Lambda} \frac{F(\mu)}{2} \text{Tr} \Gamma' \mathcal{M}$$

( $\sigma = -1$  for ground-state mesons and  $+1$  for  $P$ -wave  $0^+$  and  $1^+$  ones). On the other hand, this matrix element is, from (6.12),

$$\frac{3}{2} F_2(\mu) \text{Tr} \Gamma' \mathcal{M}.$$

Therefore,

$$F_2(\mu) = \frac{\sigma}{3} \bar{\Lambda} F(\mu), \quad (6.13)$$

up to an  $\alpha_s$  correction, which will be obtained in Sect. 6.2.

The matrix elements of the bilocal operators (6.1) are [6]

$$\begin{aligned} \langle 0 | \mathcal{O}_{jk}(\mu) | M \rangle &= \frac{F(\mu) G_k(\mu)}{2} \text{Tr} \Gamma \mathcal{M}, \\ \langle 0 | \mathcal{O}_{jm}(\mu) | M \rangle &= \frac{F(\mu) G_m(\mu)}{12} \text{Tr} \Gamma \frac{1 + \not{p}}{2} \sigma_{\mu\nu} \mathcal{M} \sigma^{\mu\nu}. \end{aligned} \quad (6.14)$$

The last formula requires some explanation. The chromomagnetic vertex always has the structure  $\sigma_{\mu\nu}$  (Sect. 4.1), and there is always a heavy-quark propagator containing  $(1 + \not{p})/2$  between  $\Gamma$  and this vertex. We can always insert the projector  $(1 + \not{p})/2$  to the left of  $\mathcal{M}$ ; therefore, the indices  $\mu, \nu$  live in the subspace orthogonal to  $v$ .

Let us consider the  $1/m$  correction to the QCD current matrix element  $\langle 0 | j | M \rangle$ , neglecting all  $\alpha_s$  corrections. We may omit all  $\bar{q} \not{D} \tilde{Q}$  and  $m_q \bar{q} \not{Q}$  operators in the sum in (5.57), because their matching coefficients start at the order  $\alpha_s$ . Reparametrization invariance (6.5) tells us that the  $\bar{q} D \tilde{Q}$  part of this sum is just  $\bar{q} \Gamma i \not{D} \tilde{Q}$ . Its matrix element is, from (6.12),

$$\langle 0 | \bar{q} \Gamma i \not{D} \tilde{Q} | M \rangle = -\frac{1}{3} \bar{d}_\Gamma \bar{\Lambda} \langle 0 | \tilde{j} | M \rangle,$$

where  $\bar{d}_\Gamma$  is defined by

$$\sigma \gamma_\perp^\alpha \Gamma \gamma_\alpha = -\bar{d}_\Gamma \Gamma, \quad \bar{d}_\Gamma = 1 - 2h(d=4) = 1 - 2\eta(n-2) \quad (6.15)$$

(the properties (5.61) of  $\Gamma$  have been used). The matrix elements of the bilocal operators (6.1) are

$$\langle 0 | \mathcal{O}_{jk} | M \rangle = G_k \langle 0 | \tilde{j} | M \rangle, \quad \langle 0 | \mathcal{O}_{jk} | M \rangle = \frac{1}{3} d_\Gamma G_m \langle 0 | \tilde{j} | M \rangle,$$

where  $d_\Gamma$  is defined by

$$\sigma_{\mu\nu} \Gamma \frac{1+\not{\psi}}{2} \sigma^{\mu\nu} \frac{1+\not{\psi}}{2} = 2d_\Gamma \Gamma \frac{1+\not{\psi}}{2}, \quad d_\Gamma = \frac{1}{2} (\bar{d}_\Gamma^2 - 3). \quad (6.16)$$

Collecting all contributions, we arrive at

$$\frac{\langle 0 | j(\mu) | M \rangle}{\langle 0 | \tilde{j}(\mu) | M \rangle} = C_\Gamma(\mu) + \frac{1}{2m} \left( -\frac{1}{3} \bar{d}_\Gamma \bar{\Lambda} + G_k + \frac{1}{3} d_\Gamma G_m \right). \quad (6.17)$$

The numbers  $\bar{d}_\Gamma$  (6.15) and  $d_\Gamma$  (6.16) have some interesting properties. Multiplying  $\Gamma$  by  $\gamma_5$  does not change them. Multiplying  $\Gamma$  by  $\not{\psi} = \gamma^0$  changes the sign of  $\bar{d}_\Gamma$  (6.15), leaving  $d_\Gamma$  (6.16) unchanged. For all eight antisymmetrized products (Sect. 5.6),  $\bar{d}_\Gamma = (-1)^{n+1} d_\Gamma$ ;  $d_\Gamma = 3$  for the four currents that couple to  $0^\pm$  mesons, and  $d_\Gamma = -1$  for those four that couple to  $1^\pm$  mesons.

In the rest of this chapter, we shall consider perturbative corrections to the  $1/m$  term of the expansion (5.57). It is sufficient to consider two spin-0 currents with  $\Gamma = 1$ ,  $\gamma^0$  (Sect. 6.4) and two spin-1 currents with  $\Gamma = \gamma^i$ ,  $\gamma^i \gamma^0$  (Sect. 6.5). Replacing  $\bar{q}$  by  $\bar{q} \gamma_5^{\text{AC}}$  and  $m_q$  by  $-m_q$  does not change the matching. All the other QCD currents can be obtained by  $\gamma_5^{\text{AC}} \rightarrow \gamma_5^{\text{HV}}$ , i.e., by dividing the current by  $Z_P$ ,  $Z_A$ , or  $Z_T = 1$  (Sect. 5.3). Before considering  $1/m$  corrections to these four currents in detail, we shall discuss renormalization of the local (Sect. 6.2) and bilocal (Sect. 6.3) dimension-4 heavy–light operators which appear in these corrections.

## 6.2 Local Dimension-4 Heavy–Light Operators

Let us consider a set of operators  $O_i$  closed under renormalization, and write them as a column matrix. Then the renormalized operators  $O(\mu)$  and the bare ones  $O_0$  are related by

$$O_0 = Z(\mu) O(\mu), \quad O(\mu) = Z^{-1}(\mu) O_0, \quad (6.18)$$

where  $Z$  is a matrix of renormalization constants. Its  $\alpha_s^0$  term is the unit matrix, and the corrections have the minimal structure (3.3). The operators  $O(\mu)$  obey the renormalization-group equation

$$\frac{dO(\mu)}{d \log \mu} + \gamma(\alpha_s(\mu))O(\mu) = 0, \quad (6.19)$$

where

$$\gamma = Z^{-1}(\mu) \frac{dZ(\mu)}{d \log \mu} = -\frac{dZ^{-1}(\mu)}{d \log \mu} Z(\mu) \quad (6.20)$$

is the anomalous-dimension matrix. The matrix of renormalization constants can be written as

$$Z = 1 + \frac{Z_1}{\varepsilon} + \frac{Z_2}{\varepsilon^2} + \dots,$$

where  $Z_1$  starts from the order  $\alpha_s$ ,  $Z_2$  from  $\alpha_s^2$ , and so on. The anomalous-dimension matrix must be finite at  $\varepsilon \rightarrow 0$ , and hence

$$\gamma = -2 \frac{dZ_1}{d \log \alpha_s}, \quad \frac{dZ_2}{d \log \alpha_s} = (Z_1 - \beta(\alpha_s)) \frac{dZ_1}{d \log \alpha_s} \quad (6.21)$$

(we consider only gauge-invariant operators here). One can obtain the anomalous-dimension matrix  $\gamma$  from  $Z_1$ , the coefficient of  $1/\varepsilon$  in the matrix  $Z$ , and vice versa. The coefficients  $Z_2, Z_3, \dots$  contain no new information; at each order in  $\alpha_s$ , they can be reconstructed from lower-loop results. With two-loop accuracy, the matrix of renormalization constants  $Z$  can be expressed via the matrix of anomalous dimensions  $\gamma$  as

$$\begin{aligned} Z &= 1 - \frac{1}{2} \gamma_0 \frac{\alpha_s}{4\pi\varepsilon} + \frac{1}{8} [(\gamma_0 + 2\beta_0)\gamma_0 - 2\gamma_1\varepsilon] \left( \frac{\alpha_s}{4\pi\varepsilon} \right)^2 + \dots, \\ Z^{-1} &= 1 + \frac{1}{2} \gamma_0 \frac{\alpha_s}{4\pi\varepsilon} + \frac{1}{8} [(\gamma_0 - 2\beta_0)\gamma_0 + 2\gamma_1\varepsilon] \left( \frac{\alpha_s}{4\pi\varepsilon} \right)^2 + \dots \end{aligned} \quad (6.22)$$

First, let us discuss the renormalization of the local dimension-4 operators [1]

$$\begin{aligned} \mathcal{O}_1^\Gamma &= \bar{q} \Gamma i D^\alpha \tilde{Q} = \bar{q} \Gamma i D_\perp^\alpha \tilde{Q}, \quad \mathcal{O}_2^\Gamma = \bar{q} \left( -i \overleftrightarrow{D}_\perp^\alpha \right) \Gamma \tilde{Q}, \\ \mathcal{O}_3^\Gamma &= \bar{q} \left( -i v \cdot \overleftrightarrow{D} \right) \gamma_\perp^\alpha \not{p} \Gamma \tilde{Q} = -i v \cdot \partial \left( \bar{q} \gamma_\perp^\alpha \not{p} \Gamma \tilde{Q} \right), \quad \mathcal{O}_4^\Gamma = m_q \bar{q} \gamma_\perp^\alpha \Gamma \tilde{Q}, \end{aligned} \quad (6.23)$$

for any Dirac matrix  $\Gamma$ . Note that  $\mathcal{O}_1^\Gamma - \mathcal{O}_2^\Gamma = i \partial_\perp^\alpha (\bar{q} \Gamma \tilde{Q})$ . When radiative corrections to matrix elements of these operators are calculated, the HQET quark line contains no Dirac matrices, just scalar propagators (2.3) and vertices  $v^\mu$ . Therefore, no  $\gamma$ -matrices can appear to the right of  $\Gamma$ . If the light quark is massless, the number of  $\gamma$ -matrices to the left of  $\Gamma$  remains even, if it was even initially; in the terms proportional to  $m_q$ , it becomes odd. The full set of dimension-4 operators satisfying these conditions is listed in (6.23). Therefore, they are closed under renormalization.

Two of the operators are full derivatives of dimension-3 currents which are renormalized by  $\tilde{Z}_j$  (5.45):  $\mathcal{O}_{30}^\Gamma = \tilde{Z}_j \mathcal{O}_3^\Gamma$ ,  $\mathcal{O}_{10}^\Gamma - \mathcal{O}_{20}^\Gamma = \tilde{Z}_j (\mathcal{O}_1^\Gamma - \mathcal{O}_2^\Gamma)$ . The operator  $\mathcal{O}_4^\Gamma$  with the  $\overline{\text{MS}}$  light-quark mass  $m_q$  is renormalized as  $\mathcal{O}_{40}^\Gamma = Z_m \tilde{Z}_j \mathcal{O}_4^\Gamma$ , where  $Z_m$  is the mass renormalization factor (Sect. 5.1). The operator  $\mathcal{O}_1^\Gamma$  is renormalized as

$$\mathcal{O}_{10}^\Gamma = \tilde{Z}_j \mathcal{O}_1^\Gamma + \tilde{Z}_a \mathcal{O}_2^\Gamma + \tilde{Z}_b \mathcal{O}_3^\Gamma + \tilde{Z}_c \mathcal{O}_4^\Gamma \quad (6.24)$$

(we shall see in Sect. 6.5 that the first coefficient is indeed  $\tilde{Z}_j$ ). Therefore,

$$Z = \begin{pmatrix} \tilde{Z}_j & \tilde{Z}_a & \tilde{Z}_b & \tilde{Z}_c \\ 0 & \tilde{Z}_j + \tilde{Z}_a & \tilde{Z}_b & \tilde{Z}_c \\ 0 & 0 & \tilde{Z}_j & 0 \\ 0 & 0 & 0 & \tilde{Z}_j Z_m \end{pmatrix}, \quad (6.25)$$

and

$$Z^{-1} = \begin{pmatrix} \tilde{Z}_j^{-1} & \bar{Z}_a & \bar{Z}_b & \bar{Z}_c \\ 0 & \tilde{Z}_j^{-1} + \bar{Z}_a & \bar{Z}_b & \bar{Z}_c \\ 0 & 0 & \tilde{Z}_j^{-1} & 0 \\ 0 & 0 & 0 & \tilde{Z}_j^{-1} Z_m^{-1} \end{pmatrix},$$

where  $\bar{Z}_{a,b,c}$  can be easily expressed via  $\tilde{Z}_{a,b,c}$ ,  $\tilde{Z}_j$ ,  $Z_m$ . The anomalous-dimension matrix (6.20) is

$$\gamma = \tilde{\gamma}_j + \begin{pmatrix} 0 & \tilde{\gamma}_a & \tilde{\gamma}_b & \tilde{\gamma}_c \\ 0 & \tilde{\gamma}_a & \tilde{\gamma}_b & \tilde{\gamma}_c \\ 0 & 0 & 0 & 0 \\ 0 & 0 & 0 & \gamma_m \end{pmatrix}. \quad (6.26)$$

The renormalization constants  $\tilde{Z}_j$ ,  $\tilde{Z}_{a,b,c}$ ,  $\bar{Z}_{a,b,c}$ ,  $Z_m$  can be easily expressed via the anomalous dimensions  $\tilde{\gamma}_j$ ,  $\tilde{\gamma}_{a,b,c}$ ,  $\gamma_m$  using (6.22).

Now let us take  $\Gamma = \gamma_\alpha \Gamma'$ . Then

$$\begin{aligned} \mathcal{O}_{10}^\Gamma &= \mathcal{O}'_{10} + \mathcal{O}'_{30}, & \mathcal{O}_{20}^\Gamma &= \mathcal{O}'_{20} + \mathcal{O}'_{30}, \\ \mathcal{O}_{30}^\Gamma &= (3 - 2\varepsilon) \mathcal{O}'_{20}, & \mathcal{O}_{40}^\Gamma &= (3 - 2\varepsilon) \mathcal{O}'_{30}, \end{aligned} \quad (6.27)$$

where

$$\mathcal{O}'_1 = i\partial_\alpha \left( \bar{q} \gamma^\alpha \Gamma' \tilde{Q} \right), \quad \mathcal{O}'_2 = iv \cdot \partial \left( \bar{q} \not{v} \Gamma' \tilde{Q} \right), \quad \mathcal{O}'_3 = m_q \bar{q} \Gamma' \tilde{Q}. \quad (6.28)$$

Of course, these operators are renormalized as  $\mathcal{O}'_{10} = \tilde{Z}_j(\mu) \mathcal{O}'_1(\mu)$ ,  $\mathcal{O}'_{20} = \tilde{Z}_j(\mu) \mathcal{O}'_2(\mu)$ ,  $\mathcal{O}'_{30} = \tilde{Z}_j(\mu) Z_m(\mu) \mathcal{O}'_3(\mu)$ . We obtain

$$\begin{aligned}
\mathcal{O}_1^\Gamma(\mu) &= \mathcal{O}'_1(\mu) + \tilde{Z}_j (\bar{Z}_a + (3 - 2\varepsilon)\bar{Z}_b) \mathcal{O}'_2(\mu) \\
&\quad + Z_m \left[ 1 + \tilde{Z}_j (\bar{Z}_a + (3 - 2\varepsilon)\bar{Z}_c) \right] \mathcal{O}'_3(\mu), \\
\mathcal{O}_2^\Gamma(\mu) &= \left[ 1 + \tilde{Z}_j (\bar{Z}_a + (3 - 2\varepsilon)\bar{Z}_b) \right] \mathcal{O}'_2(\mu) \\
&\quad + Z_m \left[ 1 + \tilde{Z}_j (\bar{Z}_a + (3 - 2\varepsilon)\bar{Z}_c) \right] \mathcal{O}'_3(\mu), \\
\mathcal{O}_3^\Gamma(\mu) &= 3\mathcal{O}'_2(\mu), \quad \mathcal{O}_4^\Gamma(\mu) = 3\mathcal{O}'_3(\mu).
\end{aligned} \tag{6.29}$$

Therefore,

$$\tilde{Z}_j (\bar{Z}_a + (3 - 2\varepsilon)\bar{Z}_b) \quad \text{and} \quad Z_m \left[ 1 + \tilde{Z}_j (\bar{Z}_a + (3 - 2\varepsilon)\bar{Z}_c) \right]$$

must be finite at  $\varepsilon \rightarrow 0$ . This allows one to reconstruct  $\tilde{\gamma}_{b,c}$  from  $\tilde{\gamma}_a$ :

$$\begin{aligned}
\tilde{\gamma}_b &= -\frac{1}{3} (\tilde{\gamma}_a + \Delta\tilde{\gamma}_b), \quad \tilde{\gamma}_c = -\frac{1}{3} (\tilde{\gamma}_a - \gamma_m + \Delta\tilde{\gamma}_c), \\
\Delta\tilde{\gamma}_b &= \frac{1}{3} \tilde{\gamma}_{a0} (\tilde{\gamma}_{a0} - 2\beta_0) \left( \frac{\alpha_s}{4\pi} \right)^2 + \mathcal{O}(\alpha_s^3), \\
\Delta\tilde{\gamma}_c &= \frac{1}{3} (\tilde{\gamma}_{a0} - \gamma_{m0}) (\tilde{\gamma}_{a0} - \gamma_{m0} - 2\beta_0) \left( \frac{\alpha_s}{4\pi} \right)^2 + \mathcal{O}(\alpha_s^3).
\end{aligned} \tag{6.30}$$

The finite parts, at the next-to-leading order, are

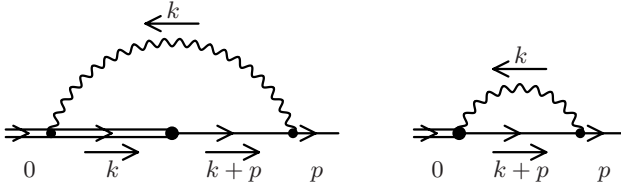
$$\begin{aligned}
\mathcal{O}_1^\Gamma(\mu) &= \mathcal{O}'_1(\mu) + \frac{1}{3} \tilde{\gamma}_{a0} \frac{\alpha_s(\mu)}{4\pi} \mathcal{O}'_2(\mu) + \frac{1}{3} (\tilde{\gamma}_{a0} - \gamma_{m0}) \frac{\alpha_s(\mu)}{4\pi} \mathcal{O}'_3(\mu), \\
\mathcal{O}_2^\Gamma(\mu) &= \left[ 1 + \frac{1}{3} \tilde{\gamma}_{a0} \frac{\alpha_s(\mu)}{4\pi} \right] \mathcal{O}'_2(\mu) + \frac{1}{3} (\tilde{\gamma}_{a0} - \gamma_{m0}) \frac{\alpha_s(\mu)}{4\pi} \mathcal{O}'_3(\mu), \\
\mathcal{O}_3^\Gamma(\mu) &= 3\mathcal{O}'_2(\mu), \quad \mathcal{O}_4^\Gamma(\mu) = 3\mathcal{O}'_3(\mu).
\end{aligned} \tag{6.31}$$

Note a fact which seems to contradict our intuition: at  $m_q = 0$ , the bare operators are equal,  $\mathcal{O}_{10}^\Gamma = \mathcal{O}'_{10}$ , but the renormalized ones are not,  $\mathcal{O}_1^\Gamma(\mu) \neq \mathcal{O}'_1(\mu)$ ! A renormalized operator is defined not only by the corresponding bare operator, but also by the set of operators being renormalized together. In our case, additional counterterms in (6.29) yield a finite contribution, because of the  $\mathcal{O}(\varepsilon)$  term in (6.27).

Let us calculate the anomalous dimensions  $\tilde{\gamma}_{a,b,c}$  at one loop. To this end, we take the on-shell matrix element  $\bar{u}\Gamma^\alpha(p, 0) \cdot \Gamma u$  of  $\mathcal{O}_{10}^\Gamma$  from  $\tilde{Q}$  with  $\tilde{p} = 0$  to  $q$  with a small on-shell momentum  $p$ , and expand it in  $p$  and  $m_q$  up to the linear term:

$$\Gamma^\alpha(p, 0) = \Gamma_0^\alpha + \Gamma_1^\alpha m_q + \Gamma_1^{\alpha\mu} p_\mu + \dots$$

The tree matrix element does not depend on  $p$  or  $m_q$ . The first contribution to the linear term is one-loop (Fig. 6.2; the third diagram, not shown here, does not depend on  $p$  or  $m_q$ ). The linear terms  $\Gamma_1^\alpha m_q + \Gamma_1^{\alpha\mu} p_\mu$  have a logarithmic

**Fig. 6.2.** Matrix element of  $O_{10}^F$ 

UV divergence, and we may retain only UV  $1/\varepsilon$  poles (it also is IR-divergent, and we need an IR cut-off). According to (6.24), the result should be equal to

$$\tilde{Z}_a p_\perp^\alpha + \tilde{Z}_b p \cdot v \gamma_\perp^\alpha \not{p} + \tilde{Z}_c m_q \gamma_\perp^\alpha.$$

From Fig. 6.2,

$$\begin{aligned} \Gamma^\alpha(p, 0) &= iC_F g_0^2 \int \frac{d^d k}{(2\pi)^d} \gamma^\mu \left( \frac{\not{k} + m_q}{k^2} - \frac{\not{k}}{k^2} \not{p} \frac{\not{k}}{k^2} + \dots \right) \left( g_\perp^{\alpha\nu} - \frac{k_\perp^\alpha v^\nu}{k \cdot v} \right) \\ &\quad \times \frac{1}{k^2} \left[ g_{\mu\nu} - (1 - a_0) \frac{k_\mu k_\nu}{k^2} \right]. \end{aligned}$$

The longitudinal part of the gluon propagator vanishes when multiplied by the second bracket, and the result is gauge-invariant. The term linear in  $p$  and  $m_q$  is

$$-iC_F g_0^2 \int \frac{d^d k}{(2\pi)^d} \left( \gamma_\perp^\alpha - \frac{k_\perp^\alpha \not{p}}{k \cdot v} \right) \frac{\not{k} \not{p} \not{k} - k^2 m_q}{(k^2)^3}.$$

In the numerator, we decompose  $k = (k \cdot v)v + k_\perp$ . Terms with an odd number of  $k_\perp$ s vanish; we average over the directions of  $k_\perp$  using  $\overline{k_\perp^\mu k_\perp^\nu} = [k_\perp^2/(d-1)]g_\perp^{\mu\nu}$ . The HQET denominator cancels. We may use four-dimensional Dirac algebra, and anticommute  $\not{p}$  to the left, where it gives  $m_q$  in the on-shell matrix element. Using the UV divergence of the resulting integral given by (4.51), we obtain

$$\begin{aligned} Z_a p_\perp^\alpha + Z_b p \cdot v \gamma_\perp^\alpha \not{p} + \tilde{Z}_c m_q \gamma_\perp^\alpha \\ = \frac{1}{4} C_F \frac{\alpha_s}{4\pi\varepsilon} (-6p_\perp^\alpha + 2p \cdot v \gamma_\perp^\alpha \not{p} - 2m_q \gamma_\perp^\alpha). \end{aligned}$$

Finally, we arrive at

$$\tilde{Z}_a = 3C_F \frac{\alpha_s}{4\pi} + \dots, \quad \tilde{Z}_b = -C_F \frac{\alpha_s}{4\pi} + \dots, \quad \tilde{Z}_c = C_F \frac{\alpha_s}{4\pi} + \dots,$$

in accord with (6.30). The two-loop calculation was performed in [1]:

$$\begin{aligned} \tilde{\gamma}_a &= 3C_F \frac{\alpha_s}{4\pi} \\ &+ C_F \left[ \left( \frac{4}{3}\pi^2 - 5 \right) C_F + \left( -\frac{1}{3}\pi^2 + \frac{41}{3} \right) C_A - \frac{10}{3}T_F n_l \right] \left( \frac{\alpha_s}{4\pi} \right)^2 + \dots \end{aligned} \quad (6.32)$$

### 6.3 Bilocal Dimension-4 Heavy–Light Operators

Next we shall discuss bilocal operators with a kinetic-energy insertion  $\mathcal{O}_k$  (4.11), following [2]. The three operators

$$\begin{aligned} \mathcal{O}_1^k &= \bar{q} \left( -iv \cdot \overleftrightarrow{D} \right) \Gamma \tilde{Q} = -iv \cdot \partial \tilde{j}, \quad \mathcal{O}_2^k = m_q \bar{q} \not{p} \Gamma \tilde{Q}, \\ \mathcal{O}_3^k &= i \int dx T \{ \tilde{j}(0), \mathcal{O}_k(x) \} \end{aligned} \quad (6.33)$$

(where  $\tilde{j} = \bar{q} \Gamma \tilde{Q}$ ) are closed under renormalization for any Dirac matrix  $\Gamma$ . Of course,  $\mathcal{O}_{10}^k = \tilde{Z}_j(\mu) \mathcal{O}_1^k(\mu)$  and  $\mathcal{O}_{20}^k = \tilde{Z}_j(\mu) Z_m(\mu) \mathcal{O}_2^k(\mu)$ . To renormalize  $\mathcal{O}_{30}^k$ , we need to renormalize  $\tilde{j}_0$  and  $\mathcal{O}_{k0}$  (the later is trivial:  $\tilde{Z}_k = 1$ , Sect. 4.1). However, this is not enough. The product of the renormalized operators is singular at  $x = 0$ , and the bilocal operator needs additional local counter-terms:

$$\mathcal{O}_{30}^k = \tilde{Z}_j(\mu) \mathcal{O}_3^k(\mu) + \tilde{Z}_a^k(\mu) \mathcal{O}_1^k(\mu) + \tilde{Z}_b^k(\mu) \mathcal{O}_2^k(\mu). \quad (6.34)$$

Therefore,

$$Z = \begin{pmatrix} \tilde{Z}_j & 0 & 0 \\ 0 & \tilde{Z}_j Z_m & 0 \\ \tilde{Z}_a^k & \tilde{Z}_b^k & \tilde{Z}_j \end{pmatrix}, \quad Z^{-1} = \begin{pmatrix} \tilde{Z}_j^{-1} & 0 & 0 \\ 0 & \tilde{Z}_j^{-1} Z_m^{-1} & 0 \\ \tilde{Z}_a^k & \tilde{Z}_b^k & \tilde{Z}_j^{-1} \end{pmatrix}, \quad (6.35)$$

and

$$\gamma = \tilde{\gamma}_j + \begin{pmatrix} 0 & 0 & 0 \\ 0 & \gamma_m & 0 \\ \tilde{\gamma}_a^k & \tilde{\gamma}_b^k & 0 \end{pmatrix}. \quad (6.36)$$

The renormalization-group equations for these operators are

$$\begin{aligned} \frac{d\mathcal{O}_1^k(\mu)}{d \log \mu} + \tilde{\gamma}_j(\alpha_s(\mu)) \mathcal{O}_1^k(\mu) &= 0, \\ \frac{d\mathcal{O}_2^k(\mu)}{d \log \mu} + (\tilde{\gamma}_j(\alpha_s(\mu)) + \gamma_m(\alpha_s(\mu))) \mathcal{O}_2^k(\mu) &= 0, \\ \frac{d\mathcal{O}_3^k(\mu)}{d \log \mu} + \tilde{\gamma}_j(\alpha_s(\mu)) \mathcal{O}_3^k(\mu) + \tilde{\gamma}_a^k(\alpha_s(\mu)) \mathcal{O}_1^k(\mu) + \tilde{\gamma}_b^k(\alpha_s(\mu)) \mathcal{O}_2^k(\mu) &= 0. \end{aligned} \quad (6.37)$$

The running of the local operators, of course, does not depend on the bilocal ones. The renormalized bilocal operator contains an (infinite) admixture of the local operators which compensates its singularity at  $x = 0$ . The “amount” of the local operators “contained” in the renormalized bilocal operator varies with  $\mu$ , as shown by the last equation.

Let us calculate  $\tilde{\gamma}_{a,b}^k$  at one loop. To this end, we take the on-shell matrix element  $\bar{u}\Gamma(p, 0) \cdot \Gamma u$  of  $\mathcal{O}_{30}^k$  from  $\tilde{Q}$  with  $\tilde{p} = 0$  to  $q$  with a small on-shell momentum  $p$ , and expand it in  $p$  and  $m_q$  up to the linear term:

$$\Gamma(p, 0) = \Gamma_0 + \Gamma_1 m_q + \Gamma_1^\mu p_\mu + \dots$$

The first contribution to the linear term is one-loop (Fig. 6.3). It has a logarithmic UV divergence, and we may retain only UV  $1/\varepsilon$  poles. According to (6.34), the result should be equal to

$$\tilde{Z}_a^k p \cdot v + \tilde{Z}_b^k m_q \psi.$$

From Fig. 6.3, we obtain a gauge-invariant  $\Gamma(p, 0)$ ; its linear term is

$$iC_F g_0^2 \int \frac{d^d k}{(2\pi)^d} \left( \not{k}_\perp - \frac{k_\perp^2 \not{\psi}}{k \cdot v} \right) \frac{\not{k} \not{p} \not{k} - k^2 m_q}{(k^2)^3 k \cdot v}.$$

Similarly to the previous calculation, we obtain

$$\Gamma_1 m_q + \Gamma_1^\mu p_\mu = \frac{4}{3} iC_F g_0^2 \left( p \cdot v + \frac{1}{2} m_q \psi \right) \int \frac{d^d k}{(2\pi)^d} \frac{1}{(k^2)^2} \left( \frac{k^2}{(k \cdot v)^2} - 1 \right).$$

Averaging the first term over the directions of  $k$ , we obtain  $-(d-2) \rightarrow -2$  (Sect. 4.3). Finally,

$$\tilde{\gamma}_a^k = -8C_F \frac{\alpha_s}{4\pi} + \dots, \quad \tilde{\gamma}_b^k = -4C_F \frac{\alpha_s}{4\pi} + \dots.$$

The two-loop calculation of  $\tilde{\gamma}_a^k$  was performed in [2]:

$$\begin{aligned} \tilde{\gamma}_a^k &= -8C_F \frac{\alpha_s}{4\pi} \\ &+ C_F \left[ \left( -\frac{32}{9}\pi^2 - \frac{32}{3} \right) C_F + \left( \frac{16}{3}\pi^2 - \frac{608}{9} \right) C_A + \frac{160}{9} T_F n_l \right] \left( \frac{\alpha_s}{4\pi} \right)^2 \\ &+ \dots \end{aligned} \tag{6.38}$$

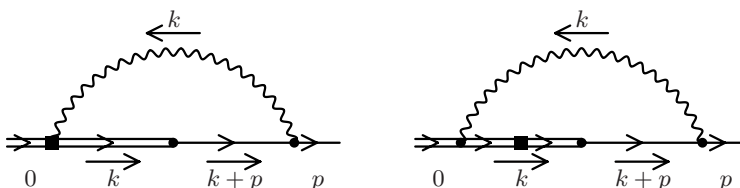


Fig. 6.3. Matrix element of  $\mathcal{O}_{20}^k$

Finally, we shall discuss bilocal operators with a chromomagnetic-interaction insertion  $\mathcal{O}_m$  (4.11), again following [2]. The four operators

$$\begin{aligned}\mathcal{O}_1^m &= -\frac{1}{4}\bar{q}\left(-iv \cdot \overleftrightarrow{D}\right)\sigma_{\mu\nu}\Gamma(1+\not{v})\sigma^{\mu\nu}\tilde{Q} = \frac{i}{4}v \cdot \partial\left(\bar{q}\sigma_{\mu\nu}\Gamma(1+\not{v})\sigma^{\mu\nu}\tilde{Q}\right), \\ \mathcal{O}_2^m &= -\frac{i}{4}\bar{q}\left(-i\overleftrightarrow{D}_\nu\right)\gamma_\mu\not{v}\Gamma(1+\not{v})\sigma^{\mu\nu}\tilde{Q}, \\ \mathcal{O}_3^m &= \frac{1}{4}m_q\bar{q}\sigma_{\mu\nu}\not{v}\Gamma(1+\not{v})\sigma^{\mu\nu}\tilde{Q}, \\ \mathcal{O}_4^m &= i\int dx T\{\tilde{j}(0), \mathcal{O}_m(x)\}\end{aligned}\quad (6.39)$$

are closed under renormalization for any  $\Gamma$ . Note that the indices  $\mu, \nu$  live in the subspace orthogonal to  $v$ , owing to  $\not{v}\tilde{Q} = \tilde{Q}$ . When we calculate radiative corrections to matrix elements of  $\mathcal{O}_4^m$ , there is always one chromomagnetic vertex (with the Dirac structure  $\sigma^{\mu\nu}$ ) to the right of  $\Gamma$ , and a heavy-quark propagator(s) containing  $1+\not{v}$  between  $\Gamma$  and this vertex. If the light quark is massless, the number of  $\gamma$ -matrices to the left of  $\Gamma$  remains even; in terms proportional to  $m_q$  it becomes odd. The only local operators satisfying these conditions are  $\mathcal{O}_{1,2,3}^m$ . They are just  $O_{3,2,4}^{\Gamma'}$  (6.23), with

$$\Gamma'_\alpha = -\frac{1}{4}i\gamma^\mu\not{v}\Gamma(1+\not{v})\sigma_{\mu\alpha}.$$

They renormalize among themselves, according to (6.25). The bilocal operator  $\mathcal{O}_4^m$  needs the additional local counterterms  $\mathcal{O}_{1,2,3}^m$ , so that

$$\begin{aligned}Z &= \begin{pmatrix} \tilde{Z}_j & 0 & 0 & 0 \\ \tilde{Z}_b & \tilde{Z}_j + \tilde{Z}_a & \tilde{Z}_c & 0 \\ 0 & 0 & \tilde{Z}_j Z_m & 0 \\ \tilde{Z}_b^m & \tilde{Z}_a^m & \tilde{Z}_c^m & \tilde{Z}_j \tilde{Z}_m \end{pmatrix}, \\ Z^{-1} &= \begin{pmatrix} \tilde{Z}_j^{-1} & 0 & 0 & 0 \\ \tilde{Z}_b & \tilde{Z}_j^{-1} + \bar{Z}_a & \bar{Z}_c & 0 \\ 0 & 0 & \tilde{Z}_j^{-1} Z_m^{-1} & 0 \\ \bar{Z}_b^m & \bar{Z}_a^m & \bar{Z}_c^m & \tilde{Z}_j^{-1} \tilde{Z}_m^{-1} \end{pmatrix}, \\ \gamma &= \tilde{\gamma}_j + \begin{pmatrix} 0 & 0 & 0 & 0 \\ \tilde{\gamma}_b & \tilde{\gamma}_a & \tilde{\gamma}_c & 0 \\ 0 & 0 & \gamma_m & 0 \\ \tilde{\gamma}_b^m & \tilde{\gamma}_a^m & \tilde{\gamma}_c^m & \tilde{\gamma}_m \end{pmatrix}.\end{aligned}\quad (6.40)$$

Do not confuse the anomalous dimension  $\gamma_m$  (5.16) of the  $\overline{\text{MS}}$  mass (Sect. 5.1) with the anomalous dimension  $\tilde{\gamma}_m$  (4.67) of the chromomagnetic-interaction operator (Sect. 4.6)!

Let us calculate the anomalous dimensions  $\tilde{\gamma}_{a,b,c}^m$  at one loop. To this end, we take the on-shell matrix element of  $O_4^m$  from  $\tilde{Q}$  with  $\tilde{p} = 0$  to  $q$  with a small on-shell momentum  $p$ , and expand it in  $p$  and  $m_q$  up to the linear term. It starts at one loop (Fig. 6.4), and is logarithmically divergent; we retain only its UV  $1/\varepsilon$  pole. This should give us

$$\frac{1}{4} \left[ \tilde{Z}_a^m i p_\mu \gamma_\nu - \tilde{Z}_b^m p \cdot v \sigma_{\mu\nu} + \tilde{Z}_c^m m_q \sigma_{\mu\nu} \not{p} \right] \Gamma(1 + \not{p}) \sigma^{\mu\nu}. \quad (6.41)$$

The vertex correction of Fig. 6.4 is obviously gauge-invariant; its linear part is

$$\frac{1}{2} C_F g_0^2 \int \frac{d^d k}{(2\pi)^d} \frac{k_\mu \gamma_\nu (k \not{p} k - k^2 m_q)}{(k^2)^3 k \cdot v} \Gamma(1 + \not{p}) \sigma^{\mu\nu}.$$

Now we decompose  $k = (k \cdot v)v + k_\perp$  and average over the directions of  $k_\perp$ . The HQET denominator cancels. The Dirac algebra may be done in four dimensions; we anticommute  $\not{p}$  to the left (where it gives  $m_q$ ), and take into account the fact that the indices  $\mu, \nu$  live only in the subspace orthogonal to  $v$ . At one loop, there are not enough  $\gamma$ -matrices to the left of  $\Gamma$  to give the third structure in (6.41). Using the UV divergence (4.51), we obtain

$$\frac{i}{4} C_F \frac{\alpha_s}{4\pi\varepsilon} (-p \cdot v \gamma_\mu \gamma_\nu + p_\mu \gamma_\nu \not{p}) \Gamma(1 + \not{p}) \sigma^{\mu\nu}.$$

Therefore, the anomalous dimensions are

$$\tilde{\gamma}_a^m = -2C_F \frac{\alpha_s}{4\pi} + \dots, \quad \tilde{\gamma}_b^m = -2C_F \frac{\alpha_s}{4\pi} + \dots, \quad \tilde{\gamma}_c^m = \mathcal{O}(\alpha_s^2).$$

The two-loop calculation of  $\tilde{\gamma}_{a,b}^m$  was performed in [2]:

$$\begin{aligned} \tilde{\gamma}_a^m &= -2C_F \frac{\alpha_s}{4\pi} \\ &+ C_F \left[ \left( -\frac{8}{9}\pi^2 + \frac{22}{3} \right) C_F + \left( \frac{2}{9}\pi^2 - \frac{110}{9} \right) C_A + \frac{4}{9} T_F n_l \right] \left( \frac{\alpha_s}{4\pi} \right)^2 + \dots \\ \tilde{\gamma}_b^m &= -2C_F \frac{\alpha_s}{4\pi} \\ &+ C_F \left[ \left( -\frac{40}{9}\pi^2 - \frac{16}{3} \right) C_F + \left( \frac{10}{9}\pi^2 - \frac{50}{9} \right) C_A + \frac{4}{9} T_F n_l \right] \left( \frac{\alpha_s}{4\pi} \right)^2 + \dots \end{aligned} \quad (6.42)$$

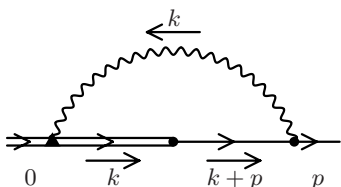


**Fig. 6.4.** Matrix element of  $O_{40}^m$

## 6.4 Spin-0 Currents

First, we shall consider the three-scalar QCD currents with  $\Gamma = 1$ ,  $\gamma^0$  (in the  $v$  rest frame). The leading term in (5.57) contains  $\tilde{j} = \bar{q}\tilde{Q}$ ; the  $1/m$  correction contains the five operators

$$\begin{aligned}\mathcal{O}_1 &= \bar{q}i\cancel{D}\tilde{Q} = i\partial_\alpha(\bar{q}\gamma^\alpha\tilde{Q}) , \quad \mathcal{O}_2 = \bar{q}\left(-i\cancel{D}_0\right)\tilde{Q} = -i\partial_0\tilde{j}, \quad \mathcal{O}_3 = m_q\tilde{j}, \\ \mathcal{O}_4 &= i\int dx T\{\tilde{j}(0), \mathcal{O}_k(x)\} , \quad \mathcal{O}_5 = i\int dx T\{\tilde{j}(0), \mathcal{O}_m(x)\} .\end{aligned}\quad (6.43)$$

The first three operators are renormalized as  $\mathcal{O}_{10} = \tilde{Z}_j\mathcal{O}_1$ ,  $\mathcal{O}_{20} = \tilde{Z}_j\mathcal{O}_2$ ,  $\mathcal{O}_{30} = \tilde{Z}_jZ_m\mathcal{O}_3$ . The bilocal operator  $\mathcal{O}_4$  is  $\mathcal{O}_3^k$  (6.33) with  $\Gamma = 1$ ; it needs counterterms proportional to the local operators  $\mathcal{O}_1^k = \mathcal{O}_2$  and  $\mathcal{O}_2^k = \mathcal{O}_3$ :

$$\mathcal{O}_{30} = \tilde{Z}_j\mathcal{O}_3 + \tilde{Z}_a^k\mathcal{O}_2 + \tilde{Z}_b^k\mathcal{O}_3 .$$

The bilocal operator  $\mathcal{O}_5$  also needs a counterterm proportional to  $\mathcal{O}_{2,3}$ , and

$$Z = \begin{pmatrix} \tilde{Z}_j & 0 & 0 & 0 & 0 \\ 0 & \tilde{Z}_j & 0 & 0 & 0 \\ 0 & 0 & \tilde{Z}_jZ_m & 0 & 0 \\ 0 & \tilde{Z}_a^k & \tilde{Z}_b^k & \tilde{Z}_j & 0 \\ 0 & \tilde{Z}_1^m & \tilde{Z}_2^m & 0 & \tilde{Z}_j\tilde{Z}_m \end{pmatrix} , \quad \gamma = \tilde{\gamma}_j + \begin{pmatrix} 0 & 0 & 0 & 0 & 0 \\ 0 & 0 & 0 & 0 & 0 \\ 0 & 0 & \gamma_m & 0 & 0 \\ 0 & \tilde{\gamma}_a^k & \tilde{\gamma}_b^k & 0 & 0 \\ 0 & \tilde{\gamma}_1^m & \tilde{\gamma}_2^m & 0 & \tilde{\gamma}_m \end{pmatrix} . \quad (6.44)$$

Do not confuse  $\gamma_m$  with  $\tilde{\gamma}_m$ !

From (6.2) and (6.5),

$$\begin{aligned}B_1^1 &= B_4^1 = C_1 , \quad B_5^1 = C_m C_1 ; \\ B_1^{\gamma^0} &= C_{\gamma^0} - 2C_{\gamma^1} , \quad B_4^{\gamma^0} = C_{\gamma^0} , \quad B_5^{\gamma^0} = C_m C_{\gamma^0} .\end{aligned}\quad (6.45)$$

The renormalization-group equations for these coefficients,

$$\frac{\partial B^\Gamma(\mu, \mu')}{\partial \log \mu'} = \gamma^T(\alpha'_s(\mu')) B^\Gamma(\mu, \mu') \quad (6.46)$$

(where the superscript T means the transposed matrix), fix columns 1, 4, and 5 in the anomalous-dimension matrix (6.44).

The operators  $\mathcal{O}_{1,2,3,4}^m$  (6.39) with  $\Gamma = 1$  are related to  $\mathcal{O}_{2,3,5}$  (6.43):

$$\begin{aligned}\mathcal{O}_{10}^m &= -(1-\varepsilon)(3-2\varepsilon)\mathcal{O}_{20} , \quad \mathcal{O}_{20}^m = (1-\varepsilon)(-\mathcal{O}_{20} + \mathcal{O}_{30}) , \\ \mathcal{O}_{30}^m &= (1-\varepsilon)(3-2\varepsilon)\mathcal{O}_{30} , \quad \mathcal{O}_{40}^m = \mathcal{O}_{50} .\end{aligned}\quad (6.47)$$

We have

$$\begin{aligned}\mathcal{O}_4^m(\mu) &= \mathcal{O}_5(\mu) + \left[ \tilde{Z}_j^{-1} \tilde{Z}_m^{-1} \tilde{Z}_1^m - (1-\varepsilon) \tilde{Z}_j (\bar{Z}_a^m + (3-2\varepsilon) \bar{Z}_b^m) \right] \mathcal{O}_2(\mu) \\ &\quad + \left[ \tilde{Z}_j^{-1} \tilde{Z}_m^{-1} \tilde{Z}_2^m + (1-\varepsilon) \tilde{Z}_j Z_m (\bar{Z}_a^m + (3-2\varepsilon) \bar{Z}_c^m) \right] \mathcal{O}_3(\mu).\end{aligned}\tag{6.48}$$

Therefore,

$$\begin{aligned}\tilde{Z}_j^{-1} \tilde{Z}_m^{-1} \tilde{Z}_1^m - (1-\varepsilon) \tilde{Z}_j (\bar{Z}_a^m + (3-2\varepsilon) \bar{Z}_b^m) \quad \text{and} \\ \tilde{Z}_j^{-1} \tilde{Z}_m^{-1} \tilde{Z}_2^m + (1-\varepsilon) \tilde{Z}_j Z_m (\bar{Z}_a^m + (3-2\varepsilon) \bar{Z}_c^m)\end{aligned}$$

must be finite at  $\varepsilon \rightarrow 0$ . This allows one to reconstruct  $\tilde{\gamma}_{1,2}^m$  in (6.44) from  $\tilde{\gamma}_{a,b,c}^m$  in (6.40) and (6.42):

$$\begin{aligned}\tilde{\gamma}_1^m &= -\tilde{\gamma}_a^m - 3\tilde{\gamma}_b^m + \Delta\tilde{\gamma}_1^m, \quad \tilde{\gamma}_2^m = \tilde{\gamma}_a^m + 3\tilde{\gamma}_c^m + \Delta\tilde{\gamma}_2^m, \\ \Delta\tilde{\gamma}_1^m &= \left[ \frac{1}{2} (\tilde{\gamma}_{m0} - 2\beta'_0) (\tilde{\gamma}_{a0}^m + 5\gamma_{b0}^m) - \frac{1}{3} \tilde{\gamma}_{a0} \tilde{\gamma}_{a0}^m \right] \left( \frac{\alpha_s}{4\pi} \right)^2 + \mathcal{O}(\alpha_s^3), \\ \Delta\tilde{\gamma}_2^m &= \frac{1}{6} \tilde{\gamma}_{a0}^m (2\tilde{\gamma}_{a0} + \gamma_{m0} - 3\tilde{\gamma}_{m0} + 6\beta'_0) \left( \frac{\alpha_s}{4\pi} \right)^2 + \mathcal{O}(\alpha_s^3).\end{aligned}\tag{6.49}$$

The finite part, at the next-to-leading order, is

$$\mathcal{O}_4^m(\mu) = \mathcal{O}_4(\mu) + \frac{1}{2} (\tilde{\gamma}_{a0}^m + 5\gamma_{b0}^m) \frac{\alpha_s(\mu)}{4\pi} \mathcal{O}_2(\mu) - \frac{1}{2} \tilde{\gamma}_{a0}^m \frac{\alpha_s(\mu)}{4\pi} \mathcal{O}_3(\mu).\tag{6.50}$$

The unknown coefficients  $B_{2,3}^\Gamma(\mu, \mu')$  for  $\Gamma = 1, \gamma^0$  are obtained by solving the renormalization-group equations

$$\begin{aligned}\frac{\partial B_2^\Gamma}{\partial \log \mu'} &= \tilde{\gamma}_j B_2^\Gamma + \tilde{\gamma}_a^k B_4^\Gamma + \tilde{\gamma}_1^m B_5^\Gamma, \\ \frac{\partial B_3^\Gamma}{\partial \log \mu'} &= (\tilde{\gamma}_j + \gamma_m) B_3^\Gamma + \tilde{\gamma}_b^k B_4^\Gamma + \tilde{\gamma}_2^m B_5^\Gamma.\end{aligned}\tag{6.51}$$

The running of the coefficients  $B_{4,5}$  of the bilocal operators does not depend on the coefficients of the local operators (see (6.46)), as expected (6.45); the “amount” of  $\mathcal{O}_{2,3}$  contained in the bilocal operators  $\mathcal{O}_{4,5}$  is  $\mu'$ -dependent, and hence the equations (6.51) for  $B_{2,3}$  contain  $B_{4,5}$  in the right-hand side.

The initial conditions  $B_{2,3}^\Gamma(m, m)$  are obtained by matching at  $\mu = \mu' = m$ . We write down the sum in (5.57) at  $m_q = 0$  via the bare operators:

$$\begin{aligned}C_F \frac{g_0^2 m^{-2\varepsilon}}{(4\pi)^{d/2}} \Gamma(\varepsilon) b_\Gamma \mathcal{O}_{20} &\pm \mathcal{O}_{10} + \mathcal{O}_{40} + \mathcal{O}_{50} \\ &= \left( C_F b_\Gamma - \frac{\tilde{\gamma}_0^k + \tilde{\gamma}_0^m}{2} \right) \frac{\alpha'_s(m)}{4\pi\varepsilon} \mathcal{O}_2(m) + (\text{other operators}).\end{aligned}$$

Taking  $\tilde{\gamma}_0^k + \tilde{\gamma}_0^m = 0$  into account, we see that both  $b_\Gamma$  should vanish at  $\varepsilon = 0$ . The  $\mathcal{O}(\varepsilon)$  terms of (6.10) give [5, 7]

$$\begin{aligned} B_2^1(m, m) &= 8C_F \frac{\alpha'_s(m)}{4\pi} + \dots, \\ B_2^{\gamma^0}(m, m) &= 12C_F \frac{\alpha'_s(m)}{4\pi} + \dots \end{aligned} \quad (6.52)$$

The initial values  $B_3^\Gamma(m, m)$  are also  $\mathcal{O}(\alpha_s)$ ; we do not consider them here.

In the leading-logarithmic approximation (LLA),

$$\begin{aligned} C_m(\mu') &= x^{\tilde{\gamma}_{m0}}, \quad C_\Gamma(m, \mu') = x^{\tilde{\gamma}_{j0}}, \quad \frac{m_q(\mu')}{m_q(m)} = x^{-\gamma_{m0}}, \\ x &= \left( \frac{\alpha'_s(\mu')}{\alpha'_s(m)} \right)^{-1/(2\beta'_0)} \end{aligned} \quad (6.53)$$

(see (4.71), (5.58), (5.19)). The coefficients  $B^\Gamma(\mu, \mu')$  for  $\Gamma = 1, \gamma^0$  are [4, 7], from (6.45) and (6.51),

$$\begin{aligned} \frac{B_4^\Gamma(\mu, \mu')}{C_\Gamma(\mu, \mu')} &= \pm \frac{B_1^\Gamma(\mu, \mu')}{C_\Gamma(\mu, \mu')} = 1, \quad \frac{B_5^\Gamma(\mu, \mu')}{C_\Gamma(\mu, \mu')} = x^{\tilde{\gamma}_{m0}}, \\ \frac{B_2^\Gamma(\mu, \mu')}{C_\Gamma(\mu, \mu')} &= \tilde{\gamma}_{a0}^k \log x - \frac{\tilde{\gamma}_{a0}^m + 3\tilde{\gamma}_{b0}^m}{\tilde{\gamma}_{m0}} (x^{\tilde{\gamma}_{m0}} - 1), \\ \frac{B_3^\Gamma(\mu, \mu')}{C_\Gamma(\mu, \mu')} &= \frac{\tilde{\gamma}_{b0}^k}{\gamma_{m0}} (x^{\gamma_{m0}} - 1) + \frac{\tilde{\gamma}_{a0}^m}{\tilde{\gamma}_{m0} - \gamma_{m0}} (x^{\tilde{\gamma}_{m0}} - x^{\gamma_{m0}}). \end{aligned} \quad (6.54)$$

The next-to-leading-order (NLO) results at  $m_q = 0$  can be found in [2, 3].

An exact relation between  $B_{2,3}^1$  and  $B_{2,3}^{\gamma^0}$  can be derived. The QCD vector current and the scalar current are related by the equations of motion

$$i\partial_\alpha j_0^\alpha = i\partial_\alpha j^\alpha = (m_0 - m_{q0}) j_0 = (m(\mu) - m_q(\mu)) j(\mu), \quad (6.55)$$

where  $m(\mu)$  is the  $\overline{\text{MS}}$  running mass of the heavy quark. We separate  $j^\alpha = (j \cdot v)v^\alpha + j_\perp^\alpha$  and substitute the expansions (5.57) with (6.43) and (6.45). The matrix element of (6.55) from a heavy quark with momentum  $mv$  to an on-shell light quark with momentum  $p$  reads

$$\begin{aligned} mC_{\gamma^0}(\mu, \mu') &\left\{ 1 + \frac{1}{2m} \left[ \left( \frac{B_2^{\gamma^0}(\mu, \mu')}{C_{\gamma^0}(\mu, \mu')} + 2 \left( \frac{C_{\gamma^1}(\mu, \mu')}{C_{\gamma^0}(\mu, \mu')} - 1 \right) \right) p \cdot v \right. \right. \\ &\quad \left. \left. + \frac{B_3^{\gamma^0}(\mu, \mu')}{C_{\gamma^0}(\mu, \mu')} m_q(\mu') + r \right] \right\} \\ &= m(\mu)C_1(\mu, \mu') \left\{ 1 + \frac{1}{2m} \left[ \frac{B_2^1(\mu, \mu')}{C_1(\mu, \mu')} p \cdot v \right. \right. \\ &\quad \left. \left. + \left( \frac{B_3^1(\mu, \mu')}{C_1(\mu, \mu')} - 2 \right) m_q(\mu') + r \right] \right\}, \end{aligned}$$

where

$$r = \frac{\left\langle q | i \int dx T \{ \tilde{J}(\mu'), (\mathcal{O}_k + C_m(\mu') \mathcal{O}_m(\mu'))_x \} | Q \right\rangle - p_\alpha \left\langle q | \tilde{J}^\alpha(\mu') | Q \right\rangle}{\left\langle q | \tilde{J}(\mu') | Q \right\rangle},$$

and  $\tilde{J}^\alpha = \bar{q} \gamma^\alpha \tilde{Q}$ . At the leading order in  $1/m$ , this yields

$$\frac{m}{m(\mu)} = \frac{C_1(m, m)}{C_{\gamma^0}(m, m)}; \quad (6.56)$$

see (5.74) and (5.75). At the first order, we obtain [3]

$$\begin{aligned} \frac{B_2^1(\mu, \mu')}{C_1(\mu, \mu')} - \frac{B_2^{\gamma^0}(\mu, \mu')}{C_{\gamma^0}(\mu, \mu')} &= 2 \left( \frac{C_{\gamma^1}(\mu, \mu')}{C_{\gamma^0}(\mu, \mu')} - 1 \right), \\ \frac{B_3^1(\mu, \mu')}{C_1(\mu, \mu')} - \frac{B_3^{\gamma^0}(\mu, \mu')}{C_{\gamma^0}(\mu, \mu')} &= 2. \end{aligned} \quad (6.57)$$

Note that (6.11) is just the one-loop case of the first result.

Now we shall discuss B-meson matrix elements; therefore, we replace  $\bar{q}$  by  $\bar{q} \gamma_5^{AC}$  and set  $m_q = 0$ . The leading current is  $\tilde{J} = \bar{q} \gamma_5^{AC} \tilde{Q}$ , and the definitions of  $\mathcal{O}_i$  (6.43) are changed accordingly. The matrix element of  $\tilde{J}$  is

$$\langle 0 | \tilde{J}(\mu) | B \rangle = -i\sqrt{m_B} F(\mu); \quad (6.58)$$

see (5.71). When taking matrix elements of  $\mathcal{O}_{1,2}(\mu)$ , we replace the derivative acting on the whole operator by the difference between the momenta of the states, so that  $i\partial_\alpha \rightarrow \bar{A}v_\alpha$ , and obtain

$$\langle 0 | \mathcal{O}_1(\mu) | B \rangle = -\langle 0 | \mathcal{O}_2(\mu) | B \rangle = -i\sqrt{m_B} \bar{A}F(\mu). \quad (6.59)$$

The operator  $\mathcal{O}_4(\mu)$  is just  $\mathcal{O}_2^k(\mu)$  with  $\Gamma = \gamma_5^{AC}$  (Sect. 6.3), and the first formula in (6.14) gives

$$\langle 0 | \mathcal{O}_4(\mu) | B \rangle = -i\sqrt{m_B} F(\mu) G_k(\mu). \quad (6.60)$$

Note that  $\mathcal{O}_{jk}(\mu)$  and  $\mathcal{O}_{jm}(\mu)$  in (6.14) should be understood as  $\mathcal{O}_2^k(\mu)$  and  $\mathcal{O}_3^m(\mu)$  (Sect. 6.3). Therefore, we obtain from (6.50)

$$\begin{aligned} \langle 0 | \mathcal{O}_5(\mu) | B \rangle &= -i\sqrt{m_B} F(\mu) G_{m0}(\mu), \\ G_{m0}(\mu) &= G_m(\mu) + R_{m0}(\alpha_s'(\mu)) \bar{A}, \quad R_{m0}(\alpha_s) = \frac{1}{2} (\tilde{\gamma}_{a0}^m + 5\tilde{\gamma}_{b0}^m) \frac{\alpha_s}{4\pi} + \dots \end{aligned} \quad (6.61)$$

The hadronic parameters  $G_k(\mu)$ ,  $G_{m0}(\mu)$  obey the renormalization-group equations

$$\begin{aligned} \frac{dG_k(\mu)}{d\log\mu} &= \tilde{\gamma}^k(\alpha'_s(\mu))\bar{A}, \\ \frac{dG_{m0}(\mu)}{d\log\mu} + \tilde{\gamma}_m(\alpha'_s(\mu))G_{m0}(\mu) &= \tilde{\gamma}^m(\alpha'_s(\mu))\bar{A}. \end{aligned} \quad (6.62)$$

Their solution in the LLA is

$$\begin{aligned} G_k(\mu) &= \hat{G}_k - \bar{A}\frac{\tilde{\gamma}_0^k}{2\beta'_0}\log\frac{\alpha'_s(\mu)}{4\pi}, \\ G_{m0}(\mu) &= \hat{G}_m\left(\frac{\alpha'_s(\mu)}{4\pi}\right)^{\tilde{\gamma}_{m0}/(2\beta'_0)} + \frac{\tilde{\gamma}_0^m}{\tilde{\gamma}_{m0}}\bar{A}, \end{aligned} \quad (6.63)$$

where  $\hat{G}_{k,m}$  are  $\mu$ -independent and thus are just some (non-perturbative) numbers times  $\Lambda_{\overline{\text{MS}}}$ .

Taking the matrix element of (5.57), we obtain

$$\begin{aligned} \left\{ \begin{array}{c} f_B^P(\mu) \\ f_B \end{array} \right\} &= \frac{C_\Gamma(\mu, \mu')F(\mu')}{\sqrt{m_B}} \\ &\times \left[ 1 + \frac{1}{2m} \left( C_A^\Gamma(\mu')\bar{A} + G_k(\mu') + C_m(\mu')G_{m0}(\mu') \right) \right], \end{aligned} \quad (6.64)$$

where  $\Gamma = 1, \gamma^0$ , and

$$C_A^1(\mu') = 1 - \frac{B_2^1(\mu, \mu')}{C_1(\mu, \mu')}, \quad C_A^{\gamma^0}(\mu') = 1 - 2\frac{C_{\gamma^1}(\mu, \mu')}{C_{\gamma^0}(\mu, \mu')} - \frac{B_2^{\gamma^0}(\mu, \mu')}{C_{\gamma^0}(\mu, \mu')}.$$

Substituting the solutions of the renormalization-group equations, we arrive at the explicitly  $\mu, \mu'$ -independent LLA results

$$\begin{aligned} \left\{ \begin{array}{c} \hat{f}_B^P \\ f_B \end{array} \right\} &= \left( \frac{\alpha'_s(m)}{4\pi} \right)^{\tilde{\gamma}_{j0}/(2\beta'_0)} \frac{\hat{C}_\Gamma \hat{F}}{\sqrt{m_B}} \\ &\times \left\{ 1 + \frac{1}{2m} \left[ \left( -\frac{\tilde{\gamma}_0^k}{2\beta'_0} \log \frac{\alpha'_s(m)}{4\pi} \pm 1 + \frac{\tilde{\gamma}_0^m}{\tilde{\gamma}_{m0}} \right) \bar{A} \right. \right. \\ &\quad \left. \left. + \hat{G}_k + \hat{G}_m \left( \frac{\alpha'_s(m)}{4\pi} \right)^{\tilde{\gamma}_{m0}/(2\beta'_0)} \right] \right\}. \end{aligned} \quad (6.65)$$

The NLO results can be found in [2, 3].

The matrix element of (6.55) is (5.74). Substituting (6.64) and using the relation (6.57), we obtain

$$\frac{f_B^P(\mu)}{f_B} = \frac{C_1(\mu, \mu')}{C_{\gamma^0}(\mu, \mu')} \left( 1 + \frac{\bar{A}}{m} \right).$$

The ratio of the quark masses is given by (6.56); naturally, it contains no  $1/m$  corrections with B-meson hadronic parameters; it is just a series in  $\alpha_s(m)$ . Therefore, we recover  $m_B = m + \bar{A}$ .

## 6.5 Spin-1 Currents

Similarly, for the three-vector currents with  $\Gamma = \gamma^i$ ,  $\gamma^i\gamma^0$  the leading term in (5.57) contains  $\tilde{j}^i = \bar{q}\gamma^i\tilde{Q}$ , and the  $1/m$  correction contains the seven operators

$$\begin{aligned}\mathcal{O}_1^i &= \bar{q}\text{i}D^i\tilde{Q}, \quad \mathcal{O}_2^i = \bar{q}\text{i}\not{D}\gamma^i\tilde{Q} = \text{i}\partial_\alpha(\bar{q}\gamma^\alpha\gamma^i\tilde{Q}), \\ \mathcal{O}_3^i &= \bar{q}\left(-\text{i}\overleftrightarrow{D}^i\right)\tilde{Q}, \quad \mathcal{O}_4^i = \bar{q}\left(-\text{i}\overleftrightarrow{D}_0\right)\gamma^i\tilde{Q} = -\text{i}\partial_0\tilde{j}^i, \quad \mathcal{O}_5^i = m_q\tilde{j}^i, \\ \mathcal{O}_6^i &= \text{i}\int dx T\{\tilde{j}^i(0), \mathcal{O}_k(x)\}, \quad \mathcal{O}_7^i = \text{i}\int dx T\{\tilde{j}^i(0), \mathcal{O}_m(x)\}. \end{aligned}\quad (6.66)$$

Note that

$$\mathcal{O}_1^i - \mathcal{O}_3^i = \text{i}\partial^i\left(\bar{q}\tilde{Q}\right). \quad (6.67)$$

From (6.2) and (6.5),

$$\begin{aligned}B_1^{\gamma^i} &= 2C_{\gamma^0}, \quad -B_2^{\gamma^i} = B_6^{\gamma^i} = C_{\gamma^i}, \quad B_7^{\gamma^i} = C_m C_{\gamma^i}, \\ -\frac{1}{2}B_1^{\gamma^i\gamma^0} &= B_2^{\gamma^i\gamma^0} = B_6^{\gamma^i\gamma^0} = C_{\gamma^i\gamma^0}, \quad B_7^{\gamma^i\gamma^0} = C_m C_{\gamma^i\gamma^0}. \end{aligned}\quad (6.68)$$

The anomalous-dimension matrix of the dimension-4 operators (6.66) has the structure

$$\gamma = \tilde{\gamma}_j + \begin{pmatrix} 0 & 0 & \tilde{\gamma}_a & \tilde{\gamma}_b & \tilde{\gamma}_c & 0 & 0 \\ 0 & 0 & 0 & 0 & 0 & 0 & 0 \\ 0 & 0 & \tilde{\gamma}_a & \tilde{\gamma}_b & \tilde{\gamma}_c & 0 & 0 \\ 0 & 0 & 0 & 0 & 0 & 0 & 0 \\ 0 & 0 & 0 & 0 & 0 & 0 & 0 \\ 0 & 0 & 0 & 0 & \gamma_m & 0 & 0 \\ 0 & 0 & 0 & \tilde{\gamma}_a^k & \tilde{\gamma}_b^k & 0 & 0 \\ 0 & 0 & \tilde{\gamma}_3^m & \tilde{\gamma}_4^m & \tilde{\gamma}_5^m & 0 & \tilde{\gamma}_m \end{pmatrix}. \quad (6.69)$$

The operators (6.23) with  $\Gamma = 1$  are

$$\mathcal{O}_1^\Gamma = \mathcal{O}_1^i, \quad \mathcal{O}_2^\Gamma = \mathcal{O}_3^i, \quad \mathcal{O}_3^\Gamma = \mathcal{O}_4^i, \quad \mathcal{O}_4^\Gamma = \mathcal{O}_5^i;$$

the operators (6.33) with  $\Gamma = \gamma^i$  are

$$\mathcal{O}_1^k = \mathcal{O}_4^i, \quad \mathcal{O}_2^k = \mathcal{O}_5^i, \quad \mathcal{O}_3^k = \mathcal{O}_6^i.$$

Therefore, the relevant parts of (6.69) can be taken from (6.26) and (6.36). The bilocal operator  $\mathcal{O}_6^i = \mathcal{O}_3^k$  (with  $\Gamma = \gamma^i$ ) needs counterterms proportional to  $\mathcal{O}_1^k = \mathcal{O}_4^i$  and  $\mathcal{O}_2^k = \mathcal{O}_5^i$  (see (6.35)), but not  $\mathcal{O}_3^i$ . The operators  $\mathcal{O}_{2,4}^i$  are renormalized multiplicatively with  $\tilde{\gamma}_j$ , which determines the second and the fourth row. The same holds for  $\mathcal{O}_1^i - \mathcal{O}_3^i$  (6.67), and hence the first and the

third row coincide. Furthermore, the form of  $B_{1,2,6,7}$  (see (6.68)) fixes columns 1, 2, 6, and 7. In particular, the (non-mixing) anomalous dimension  $\gamma_{11}$  of  $\mathcal{O}_1^i$  is  $\tilde{\gamma}_j$ ; therefore, the fact that the element  $\gamma_{11}$  of the matrix (6.26) is  $\tilde{\gamma}_j$  follows from reparametrization invariance (this proves the statement made in Sect. 6.2).

The operators  $\mathcal{O}_{1,2,3,4}^m$  (6.39) with  $\Gamma = \gamma^i$  are related to  $\mathcal{O}_{3,4,5,7}^i$ :

$$\begin{aligned}\mathcal{O}_{10}^m &= (1 - \varepsilon)(1 + 2\varepsilon)\mathcal{O}_{40}^i, & \mathcal{O}_{20}^m &= (1 - 2\varepsilon)\mathcal{O}_{30}^i + \varepsilon\mathcal{O}_{40}^i + \varepsilon\mathcal{O}_{50}^i, \\ \mathcal{O}_{30}^m &= (1 - \varepsilon)(1 + 2\varepsilon)\mathcal{O}_{50}^i, & \mathcal{O}_{40}^m &= \mathcal{O}_{70}^i.\end{aligned}\quad (6.70)$$

We have

$$\begin{aligned}\mathcal{O}_4^m(\mu) &= \mathcal{O}_7^i(\mu) + \left[ \tilde{Z}_j^{-1} \tilde{Z}_m^{-1} \tilde{Z}_3^m + (1 - 2\varepsilon)(\tilde{Z}_j + \tilde{Z}_a) \bar{Z}_a^m \right] \mathcal{O}_3^i(\mu) \\ &\quad + \left[ \tilde{Z}_j^{-1} \tilde{Z}_m^{-1} \tilde{Z}_4^m + \left( \varepsilon \tilde{Z}_j + (1 - 2\varepsilon) \tilde{Z}_b \right) \bar{Z}_a^m \right. \\ &\quad \quad \left. + (1 - \varepsilon)(1 + 2\varepsilon) \tilde{Z}_j \bar{Z}_b^m \right] \mathcal{O}_4^i(\mu) \\ &\quad + \left[ \tilde{Z}_j^{-1} \tilde{Z}_m^{-1} \tilde{Z}_5^m + \left( \varepsilon \tilde{Z}_j Z_m + (1 - 2\varepsilon) \tilde{Z}_c \right) \bar{Z}_a^m \right. \\ &\quad \quad \left. + (1 - \varepsilon)(1 + 2\varepsilon) \tilde{Z}_j Z_m \bar{Z}_c^m \right] \mathcal{O}_5^i(\mu).\end{aligned}\quad (6.71)$$

These three coefficients must be finite at  $\varepsilon \rightarrow 0$ . This allows one to reconstruct  $\tilde{\gamma}_{3,4,5}^m$  in (6.69) from  $\tilde{\gamma}_{a,b,c}^m$  in (6.40):

$$\begin{aligned}\tilde{\gamma}_3^m &= \tilde{\gamma}_a^m + \Delta\tilde{\gamma}_3^m, & \tilde{\gamma}_4^m &= \tilde{\gamma}_b^m + \Delta\tilde{\gamma}_4^m, & \tilde{\gamma}_5^m &= \tilde{\gamma}_c^m + \Delta\tilde{\gamma}_5^m, \\ \Delta\tilde{\gamma}_3^m &= \tilde{\gamma}_{a0}^m (\tilde{\gamma}_{a0} - \tilde{\gamma}_{m0} + 2\beta'_0) \left( \frac{\alpha_s}{4\pi} \right)^2 + \mathcal{O}(\alpha_s^3), \\ \Delta\gamma_4^m &= \left[ \frac{1}{2} (\tilde{\gamma}_{a0}^m + \tilde{\gamma}_{b0}^m) (\tilde{\gamma}_{m0} - 2\beta'_0) - \frac{1}{3} \tilde{\gamma}_{a0} \gamma_{a0}^m \right] \left( \frac{\alpha_s}{4\pi} \right)^2 + \mathcal{O}(\alpha_s^3), \\ \Delta\gamma_5^m &= -\frac{1}{6} \tilde{\gamma}_{a0}^m (2\tilde{\gamma}_{a0} + \gamma_{m0} - 3\tilde{\gamma}_{m0} + 6\beta'_0) \left( \frac{\alpha_s}{4\pi} \right)^2 + \mathcal{O}(\alpha_s^3).\end{aligned}\quad (6.72)$$

The finite part, at the next-to-leading order, is

$$\begin{aligned}\mathcal{O}_3^m(\mu) &= \mathcal{O}_6^i(\mu) - \tilde{\gamma}_{a0}^m \frac{\alpha'_s(\mu)}{4\pi} \mathcal{O}_3^i(\mu) + \frac{1}{2} (\tilde{\gamma}_{a0}^m + \tilde{\gamma}_{b0}^m) \frac{\alpha'_s(\mu)}{4\pi} \mathcal{O}_4^i(\mu) \\ &\quad + \frac{1}{2} \tilde{\gamma}_{a0}^m \frac{\alpha'_s(\mu)}{4\pi} \mathcal{O}_5^i(\mu).\end{aligned}\quad (6.73)$$

The unknown coefficients  $B_{3,4,5}^\Gamma(\mu, \mu')$  for  $\Gamma = \gamma^i, \gamma^i \gamma^0$  are obtained by solving the renormalization-group equations

$$\frac{\partial B_3^\Gamma}{\partial \log \mu'} = (\tilde{\gamma}_j + \tilde{\gamma}_a) B_3^\Gamma + \tilde{\gamma}_a B_1^\Gamma + \tilde{\gamma}_3^m B_7^\Gamma,$$

$$\begin{aligned}\frac{\partial B_4^\Gamma}{\partial \log \mu'} &= \tilde{\gamma}_j B_4^\Gamma + \tilde{\gamma}_b (B_1^\Gamma + B_3^\Gamma) + \tilde{\gamma}_a^k B_6^\Gamma + \tilde{\gamma}_4^m B_7^\Gamma, \\ \frac{\partial B_5^\Gamma}{\partial \log \mu'} &= (\tilde{\gamma}_j + \gamma_m) B_5^\Gamma + \tilde{\gamma}_c (B_1^\Gamma + B_3^\Gamma) + \tilde{\gamma}_b^k B_6^\Gamma + \tilde{\gamma}_5^m B_7^\Gamma.\end{aligned}\quad (6.74)$$

The initial conditions  $B_{3,4}^\Gamma(m, m)$  are obtained by matching at  $\mu = \mu' = m$ . We write down the sum in (5.57) at  $m_q = 0$  via the bare operators:

$$\begin{aligned}C_F \frac{g_0^2 m^{-2\varepsilon}}{(4\pi)^{d/2}} \Gamma(\varepsilon) (b_{\Gamma,2} \mathcal{O}_{30}^i + b_{\Gamma,1} \mathcal{O}_{40}^i) &\pm \mathcal{O}_{10} \mp \mathcal{O}_{20} + \mathcal{O}_{50} + \mathcal{O}_{60} \\ &= \frac{\alpha'_s(m)}{4\pi\varepsilon} \left[ \left( C_F b_{\Gamma,2} \mp \tilde{\gamma}_{a0} - \frac{\tilde{\gamma}_{10}^m}{2} \right) \mathcal{O}_3^i(m) \right. \\ &\quad \left. + \left( C_F b_{\Gamma,1} \mp \tilde{\gamma}_{b0} - \frac{\tilde{\gamma}_0^k + \tilde{\gamma}_{20}^m}{2} \right) \mathcal{O}_4^i(m) + (\text{other operators}) \right].\end{aligned}$$

The values of  $b_{\Gamma,i}$  at  $\varepsilon = 0$  have to cancel these anomalous dimensions. The  $\mathcal{O}(\varepsilon)$  terms of (6.10) give

$$\begin{aligned}B_3^{\gamma^i}(m, m) &= 4C_F \frac{\alpha'_s(m)}{4\pi} + \dots, \quad B_4^{\gamma^i}(m, m) = -4C_F \frac{\alpha'_s(m)}{4\pi} + \dots, \\ B_3^{\gamma^i \gamma^0}(m, m) &= 2C_F \frac{\alpha'_s(m)}{4\pi} + \dots, \quad B_4^{\gamma^i \gamma^0}(m, m) = -6C_F \frac{\alpha'_s(m)}{4\pi} + \dots\end{aligned}\quad (6.75)$$

The initial values  $B_5^\Gamma(m, m)$  are also  $\mathcal{O}(\alpha_s)$ ; we do not consider them here.

In the LLA, the coefficients  $B^\Gamma(\mu, \mu')$  for  $\Gamma = \gamma^i, \gamma^i \gamma^0$  are [4, 7], from (6.68) and (6.74),

$$\begin{aligned}\frac{B_6^\Gamma(\mu, \mu')}{C_\Gamma(\mu, \mu')} &= \pm \frac{1}{2} \frac{B_1^\Gamma(\mu, \mu')}{C_\Gamma(\mu, \mu')} = \mp \frac{B_2^\Gamma(\mu, \mu')}{C_\Gamma(\mu, \mu')} = 1, \quad \frac{B_7^\Gamma(\mu, \mu')}{C_\Gamma(\mu, \mu')} = x^{\tilde{\gamma}_{m0}}, \\ \frac{B_3^\Gamma(\mu, \mu')}{C_\Gamma(\mu, \mu')} &= \pm 2 \left( x^{\tilde{\gamma}_{a0}} - 1 \right) + \frac{\tilde{\gamma}_{a0}^m}{\tilde{\gamma}_{a0} - \tilde{\gamma}_{m0}} \left( x^{\tilde{\gamma}_{a0}} - x^{\tilde{\gamma}_{m0}} \right), \\ \frac{B_4^\Gamma(\mu, \mu')}{C_\Gamma(\mu, \mu')} &= \tilde{\gamma}_{a0}^k \log x - \frac{1}{3} \left( \frac{\tilde{\gamma}_{a0}^m}{\tilde{\gamma}_{a0} - \tilde{\gamma}_{m0}} \pm 2 \right) \left( x^{\tilde{\gamma}_{a0}} - 1 \right) \\ &\quad + \left( \frac{1}{3} \frac{\tilde{\gamma}_{a0} \tilde{\gamma}_{a0}^m}{\tilde{\gamma}_{a0} - \tilde{\gamma}_{m0}} + \tilde{\gamma}_{b0}^m \right) \frac{x^{\tilde{\gamma}_{m0}} - 1}{\tilde{\gamma}_{m0}}. \\ \frac{B_5^\Gamma(\mu, \mu')}{C_\Gamma(\mu, \mu')} &= \frac{\tilde{\gamma}_{b0}^k}{\gamma_{m0}} (x^{\gamma_{m0}} - 1) - \frac{1}{3} \left( \frac{\tilde{\gamma}_{a0}^m}{\tilde{\gamma}_{a0} - \tilde{\gamma}_{m0}} \pm 2 \right) \left( x^{\tilde{\gamma}_{a0}} - x^{\gamma_{m0}} \right) \\ &\quad + \frac{1}{3} \frac{(\tilde{\gamma}_{a0} - \gamma_{m0}) \tilde{\gamma}_{a0}^m}{\tilde{\gamma}_{a0} - \tilde{\gamma}_{m0}} \frac{x^{\tilde{\gamma}_{m0}} - x^{\gamma_{m0}}}{\tilde{\gamma}_{m0} - \gamma_{m0}}.\end{aligned}\quad (6.76)$$

The NLO results at  $m_q = 0$  can be found in [2, 3].

Now we shall discuss  $B^*$ -meson matrix elements, and therefore set  $m_q = 0$ . According to (5.71), the leading HQET matrix element is

$$\langle 0 | \tilde{J}^i(\mu) | B^* \rangle = i\sqrt{m_{B^*}} F(\mu) e^i, \quad (6.77)$$

where  $e$  is the  $B^*$  polarization vector. The operators  $\mathcal{O}_{2,4}^i$  are full derivatives:

$$\langle 0 | \mathcal{O}_2^i(\mu) | B^* \rangle = \langle 0 | \mathcal{O}_4^i(\mu) | B^* \rangle = -i\sqrt{m_{B^*}} \bar{A}F(\mu) e^i. \quad (6.78)$$

The matrix elements of  $\mathcal{O}_1^i$  and  $\mathcal{O}_3^i$  are equal, owing to (6.67). Let us define [6]

$$\langle 0 | \mathcal{O}_1^\Gamma(\mu) | M \rangle = \frac{F_2(\mu)}{2} \text{Tr} \gamma_\perp^\alpha \Gamma \mathcal{M}, \quad (6.79)$$

for the matrix element of  $\mathcal{O}_1^\Gamma$  (6.23). If we take  $\Gamma = \gamma_\alpha \Gamma'$ , then

$$\langle 0 | \mathcal{O}_1^\Gamma(\mu) | M \rangle = \frac{3}{2} F_2(\mu) \text{Tr} \Gamma' \mathcal{M}.$$

Taking into account (6.31) and

$$\langle 0 | \mathcal{O}'_1(\mu) | M \rangle = \langle 0 | \mathcal{O}'_2(\mu) | M \rangle = -\frac{1}{2} \bar{A}F(\mu) \text{Tr} \Gamma' \mathcal{M},$$

we obtain, at the next-to-leading order,

$$F_2(\mu) = -\frac{1}{3} \bar{A}F(\mu) R(\alpha'_s(\mu)), \quad R(\alpha_s) = 1 + \frac{1}{3} \gamma_{a0} \frac{\alpha_s}{4\pi} + \mathcal{O}(\alpha_s^2). \quad (6.80)$$

Finally [3],

$$\langle 0 | \mathcal{O}_1^i(\mu) | B^* \rangle = \langle 0 | \mathcal{O}_3^i(\mu) | B^* \rangle = -\frac{i}{3} \sqrt{m_{B^*}} \bar{A}F(\mu) R(\alpha_s(\mu)) e^i. \quad (6.81)$$

The operator  $\mathcal{O}_6^i(\mu)$  is just  $\mathcal{O}_2^k(\mu)$  with  $\Gamma = \gamma^i$  (Sect. 6.3), and the first formula in (6.14) gives

$$\langle 0 | \mathcal{O}_5^i(\mu) | B^* \rangle = i\sqrt{m_{B^*}} F(\mu) G_k(\mu) e^i. \quad (6.82)$$

The second formula, together with (6.73), gives

$$\begin{aligned} \langle 0 | \mathcal{O}_7^i | B^* \rangle &= -\frac{i}{3} \sqrt{m_{B^*}} F(\mu) G_{m1}(\mu) e^i, \\ G_{m1}(\mu) &= G_m(\mu) + R_{m1}(\alpha'_s(\mu)) \bar{A}, \\ R_{m1}(\alpha_s) &= -\frac{1}{2} (\tilde{\gamma}_{a0}^m + 3\tilde{\gamma}_{b0}^m) \frac{\alpha_s}{4\pi} + \dots \end{aligned} \quad (6.83)$$

Taking the matrix element of (5.57), we obtain

$$\left\{ \begin{array}{l} f_{B^*} \\ f_{B^*}^T(\mu) \end{array} \right\} = \frac{C_\Gamma(\mu, \mu') F(\mu')}{\sqrt{m_{B^*}}} \times \left[ 1 + \frac{1}{2m} \left( C_A^\Gamma(\mu') \bar{A} + G_k(\mu') - \frac{1}{3} C_m(\mu') G_{m1}(\mu') \right) \right], \quad (6.84)$$

where  $\Gamma = \gamma^i$ ,  $\gamma^i \gamma^0$ , and

$$C_A^\Gamma(\mu') = \pm 1 - \frac{B_4^\Gamma(\mu, \mu')}{C_\Gamma(\mu, \mu')} - \frac{1}{3} \left( 2 \left\{ \begin{array}{c} C_{\gamma^0}(\mu, \mu') / C_{\gamma^1}(\mu, \mu') \\ -1 \end{array} \right\} + \frac{B_3^\Gamma(\mu, \mu')}{C_\Gamma(\mu, \mu')} \right) R(\alpha'_s(\mu')).$$

Substituting the solutions of the renormalization-group equations, we arrive at the explicitly  $\mu$ ,  $\mu'$ -independent LLA results

$$\left\{ \begin{array}{l} f_{B^*} \\ \hat{f}_{B^*}^T \end{array} \right\} = \left( \frac{\alpha'_s(m)}{4\pi} \right)^{\tilde{\gamma}_{j0}/(2\beta'_0)} \frac{\hat{C}_\Gamma \hat{F}}{\sqrt{m_{B^*}}} \times \left\{ 1 + \frac{1}{2m} \left[ \left( -\frac{\tilde{\gamma}_0^k}{2\beta'_0} \log \frac{\alpha'_s(m)}{4\pi} + \frac{1}{3} \left( \pm 1 - \frac{\tilde{\gamma}_0^m}{\tilde{\gamma}_{m0}} \right) \right) \bar{A} \right. \right. \\ \left. \left. + \hat{G}_k - \frac{1}{3} \hat{G}_m \left( \frac{\alpha'_s(m)}{4\pi} \right)^{\tilde{\gamma}_{m0}/(2\beta'_0)} \right] \right\}. \quad (6.85)$$

The ratio  $f_{B^*}/f_B$  is

$$\frac{f_{B^*}}{f_B} = \frac{\hat{C}_{\gamma^1}}{\hat{C}_{\gamma^0}} \left\{ 1 + \frac{2}{3m} \left[ \left( 1 - \frac{\gamma_0^m}{\gamma_{m0}} \right) \bar{A} - \hat{G}_m \left( \frac{\alpha'_s(m)}{4\pi} \right)^{\tilde{\gamma}_{m0}/(2\beta'_0)} \right] \right\}. \quad (6.86)$$

The NLO results can be found in [2, 3].

## References

1. G. Amorós, M. Neubert: Phys. Lett. B **420**, 340 (1998) [121](#), [127](#), [130](#)
2. T. Becher, M. Neubert, A.A. Petrov: Nucl. Phys. B **611**, 367 (2001) [121](#), [131](#), [132](#), [133](#), [134](#), [137](#), [139](#), [142](#), [144](#)
3. F. Campanario, A.G. Grozin, T. Mannel: Nucl. Phys. B **663**, 280 (2003); Erratum: Nucl. Phys. B **670**, 331 (2003) [137](#), [138](#), [139](#), [142](#), [143](#), [144](#)
4. A.F. Falk, B. Grinstein: Phys. Lett. B **247**, 406 (1990) [121](#), [137](#), [142](#)
5. M. Golden, B. Hill: Phys. Lett. B **254**, 225 (1991) [121](#), [124](#), [136](#)
6. M. Neubert: Phys. Rev. D **46**, 1076 (1992) [125](#), [143](#)
7. M. Neubert: Phys. Rev. D **49**, 1542 (1994) [121](#), [122](#), [124](#), [136](#), [137](#), [142](#)

# 7 Heavy–Heavy Currents

In this chapter, we discuss heavy–heavy quark currents. They have many interesting applications. Matrix elements of the vector and axial  $b \rightarrow c$  currents describe exclusive semileptonic  $B$  decays, which provide one of the ways to measure the CKM matrix element  $|V_{cb}|$ . Matrix elements of the electromagnetic  $b$ - and  $c$ -currents describe  $B\bar{B}$  and  $D\bar{D}$  production in  $e^+e^-$  annihilation.

## 7.1 Heavy–Heavy Current in HQET

Now we are going to consider the current

$$\tilde{J} = \tilde{Z}_J^{-1}(\cosh \vartheta) \tilde{J}_0, \quad \tilde{J}_0 = \tilde{Q}_{v0}^+ \tilde{Q}_{v0}, \quad \cosh \vartheta = v \cdot v', \quad (7.1)$$

where  $\tilde{Q}_v$  and  $\tilde{Q}_{v'}$  are scalar static-quark fields with velocities  $v$  and  $v'$ . This current is clearly discussed in [9]. Let the sum of all one-particle-irreducible vertex diagrams with this current (not including external leg propagators) be  $\tilde{\Gamma} = 1 + \tilde{\Lambda}$ . The one-loop vertex function in the coordinate space (Fig. 7.1) is

$$\begin{aligned} \tilde{\Lambda}(t, t'; \cosh \vartheta) &= iC_F g_0^2 D_{\mu\nu}^0(vt + v't') v^\mu v'^\nu \theta(t) \theta(t') \\ &= -C_F \frac{g_0^2}{8\pi^{d/2}} \Gamma(d/2 - 1) \theta(t) \theta(t') \\ &\times \frac{(1 + a_0)x^2 \cosh \vartheta + (d - 2)(1 - a_0)(t + t' \cosh \vartheta)(t' + t \cosh \vartheta)}{(-x^2)^{d/2}}, \\ x^2 &= t^2 + t'^2 + 2tt' \cosh \vartheta \end{aligned} \quad (7.2)$$

(see (3.51)). In the momentum space,

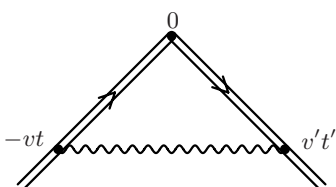


**Fig. 7.1.** One-loop heavy–heavy vertex

$$\tilde{A}(\omega, \omega'; \cosh \vartheta) = \int dt dt' e^{i\omega t + i\omega' t'} \tilde{A}(t, t'; \cosh \vartheta). \quad (7.3)$$

When the vertex function  $\tilde{\Gamma}(\omega, \omega'; \cosh \vartheta)$  is expressed via the renormalized quantities  $\alpha_s(\mu)$ ,  $a(\mu)$ , it should become  $\tilde{Z}_\Gamma \tilde{\Gamma}_r(\omega, \omega'; \cosh \vartheta)$ , where  $\tilde{Z}_\Gamma$  is minimal and  $\tilde{\Gamma}_r(\omega, \omega'; \cosh \vartheta)$  is finite at  $\varepsilon \rightarrow 0$ . The renormalization constant of the current (7.1) is  $\tilde{Z}_J = \tilde{Z}_Q \tilde{Z}_\Gamma$ . The UV divergences of  $\tilde{\Gamma}(\omega, \omega'; \cosh \vartheta)$  do not depend on the residual energies  $\omega, \omega'$ , and we may set them to zero. An IR cut-off is then necessary to avoid IR  $1/\varepsilon$  terms. At one loop, substituting (7.2) into (7.3) and proceeding to the variables

$$t = \tau \frac{1+\xi}{2}, \quad t' = \tau \frac{1-\xi}{2},$$

we obtain

$$\begin{aligned} \tilde{A}(0, 0; \cosh \vartheta) &= -C_F \frac{g_0^2}{16\pi^{d/2}} \Gamma\left(\frac{d}{2} - 1\right) \int_0^T \frac{d\tau}{\tau^{d-3}} \\ &\times \int_{-1}^{+1} d\xi \frac{(1+a_0) \cosh \vartheta (c^2 - s^2 \xi^2) + (d-2)(1-a_0)(c^4 - s^4 \xi^2)}{(-c^2 + s^2 \xi^2)^{d/2}}, \end{aligned}$$

where  $c = \cosh(\vartheta/2)$ ,  $s = \sinh(\vartheta/2)$ , and the upper limit  $T$  provides an IR cut-off. We need only the  $1/\varepsilon$  UV pole given by the integral

$$\int_0^T d\tau \tau^{-1+2\varepsilon} \Big|_{\text{UV}} = \frac{T^{2\varepsilon}}{2\varepsilon} = \frac{1}{2\varepsilon} + \mathcal{O}(\varepsilon^0). \quad (7.4)$$

We may put  $d = 4$  in the rest of the formula:

$$\begin{aligned} \tilde{Z}_\Gamma(\cosh \vartheta) &= 1 - C_F \frac{\alpha_s}{4\pi\varepsilon} \int_{-1}^{+1} d\xi \\ &\times \left[ (1+a) \frac{\cosh \vartheta}{2 \cosh^2(\vartheta/2)} \frac{1}{1 - \xi^2 \tanh^2(\vartheta/2)} \right. \\ &\quad \left. + (1-a) \frac{1 - \xi^2 \tanh^4(\vartheta/2)}{[1 - \xi^2 \tanh^2(\vartheta/2)]^2} \right]. \end{aligned}$$

Changing the integration variable  $\xi = \tanh \psi / \tanh(\vartheta/2)$ , we obtain

$$\begin{aligned} \tilde{Z}_\Gamma(\cosh \vartheta) &= 1 - C_F \frac{\alpha_s}{4\pi\varepsilon} \int_{-\vartheta/2}^{+\vartheta/2} d\psi \left[ 2 \coth \vartheta + \frac{1-a}{\sinh \vartheta} \cosh 2\psi \right] \\ &= 1 - C_F \frac{\alpha_s}{4\pi\varepsilon} (2\vartheta \coth \vartheta + 1 - a). \end{aligned} \quad (7.5)$$

When this  $\tilde{Z}_\Gamma$  is multiplied by  $\tilde{Z}_Q$  (3.65), the gauge dependence cancels, and we obtain the anomalous dimension [12]

$$\tilde{\gamma}_J(\alpha_s; \cosh \vartheta) = 4C_F \frac{\alpha_s}{4\pi} (\vartheta \coth \vartheta - 1). \quad (7.6)$$

The heavy–heavy current with  $v' = v$  ( $\vartheta = 0$ ) is not renormalized. The integral of  $\tilde{J}v^0$  over the whole space is the full number of heavy quarks, which is always 1 and does not depend on  $\mu$ . We can see how this happens. At one loop, the vertex (7.2) at  $\vartheta = 0$  becomes just the HQET quark self-energy (3.62):

$$\tilde{\Lambda}(t, t'; \vartheta = 0) = -i\tilde{\Sigma}(t + t')\theta(t)\theta(t'). \quad (7.7)$$

In fact, this Ward identity holds to all orders. Let us consider an arbitrary diagram for  $\tilde{\Sigma}(t + t')$  in the coordinate space. The vertices along the heavy-quark line have times  $t_0 < t_1 < \dots < t_{n-1} < t_n$ ,  $t_0 = -t$ ,  $t_n = t'$ , and integration with respect to  $t_1, \dots, t_{n-1}$  is performed. The integrand is an integral over the coordinates of all vertices not belonging to the heavy-quark line. Now consider all diagrams for  $\tilde{\Lambda}(t, t'; \vartheta = 0)$  obtained by inserting the heavy–heavy current vertex with  $\vartheta = 0$  at time 0 into all the possible places along the heavy-quark line. These diagrams have the same integrand, and integration regions  $t_0 < t_1 < \dots < t_{i-1} < 0 < t_i < \dots < t_{n-1} < t_n$  ( $i = 1, \dots, n$ ). These regions span the whole integration region of the original diagram. Therefore, the sum of this set of vertex diagrams is equal to the original self-energy diagram.

Applying the Fourier transformation (7.3) to (7.7), we obtain

$$\begin{aligned} \tilde{\Lambda}(\omega, \omega'; \vartheta = 0) &= -\frac{\tilde{\Sigma}(\omega') - \tilde{\Sigma}(\omega)}{\omega' - \omega} \\ \text{or } \tilde{\Gamma}(\omega, \omega'; \vartheta = 0) &= \frac{\tilde{S}^{-1}(\omega') - \tilde{S}^{-1}(\omega)}{\omega' - \omega}. \end{aligned} \quad (7.8)$$

This can be proved directly, in the same way as for the QED Ward identity (see Fig. 3.16). We start from an arbitrary diagram for  $\tilde{\Sigma}(\omega)$ , and construct a set of diagrams for  $\tilde{\Lambda}(\omega, \omega'; \vartheta = 0)$  by inserting the heavy–heavy vertex into all propagators along the heavy-quark line in turn (Fig. 7.2; a dot near a heavy-quark propagator means that its residual energy is shifted by  $\omega' - \omega$ ). Each diagram is a difference, because

$$i\tilde{S}(\omega' + \omega_i) \cdot i\tilde{S}(\omega + \omega_i) = \frac{i}{\omega - \omega'} [i\tilde{S}(\omega' + \omega_i) - i\tilde{S}(\omega + \omega_i)].$$

All terms cancel each other, except the extreme ones (Fig. 7.2), and we arrive at (7.8). In particular,

$$\tilde{\Lambda}(\omega, \omega; \vartheta = 0) = -\frac{d\tilde{\Sigma}(\omega)}{d\omega} \quad \text{or} \quad \tilde{\Gamma}(\omega, \omega; \vartheta = 0) = \frac{d\tilde{S}^{-1}(\omega)}{d\omega}.$$

Multiplying (7.8) by  $\tilde{Z}_Q$  transforms  $\tilde{S}^{-1}$  into  $\tilde{S}_r^{-1}$ , and hence makes  $\tilde{\Gamma}$  finite. Therefore,  $\tilde{Z}_J(\vartheta = 0) = 1$ , or

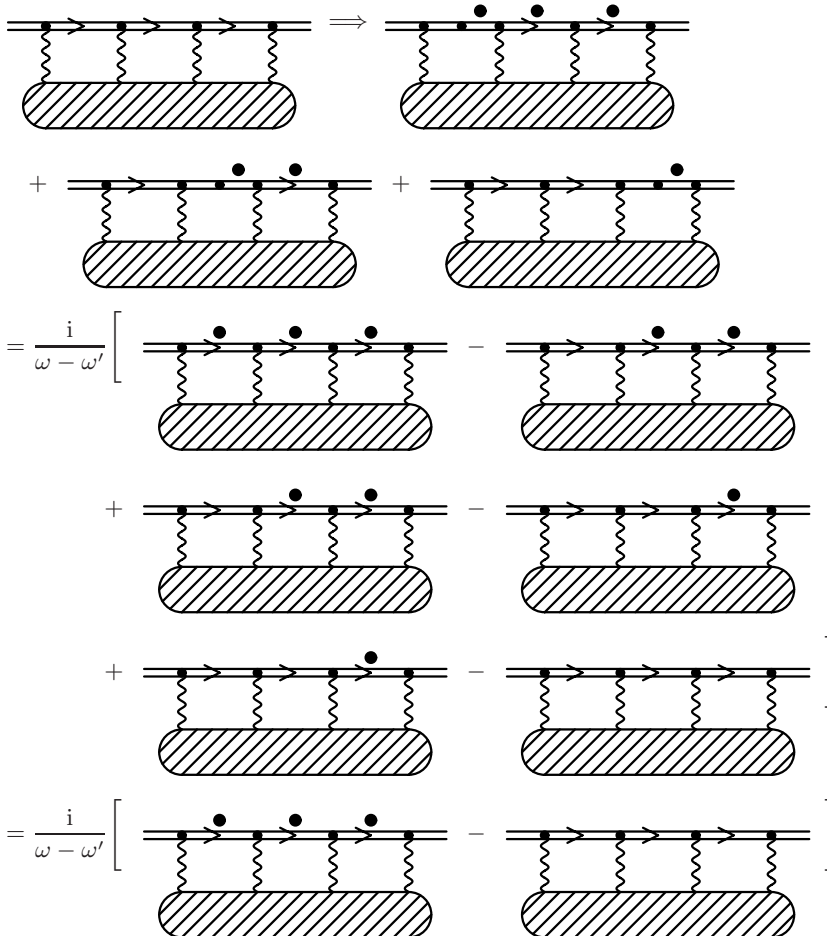


**Fig. 7.2.** Ward identity for the heavy–heavy vertex at  $\vartheta = 0$

$$\tilde{\gamma}_J(\alpha_s; \vartheta = 0) = 0, \quad (7.9)$$

to all orders in  $\alpha_s$ .

The heavy–heavy current has especially simple properties in heavy-electron effective theory (Sect. 3.5). Let us consider the full (non-amputated) Green function of  $\tilde{Q}$ ,  $\tilde{Q}^+$ , and  $\tilde{J}$ . After singling out the obvious  $\delta$ -functions, it can be written as  $G(t, t'; \cosh \vartheta)$  (Fig. 7.3). The exponentiation argument (see Fig. 3.14) holds for this heavy-quark world line with an angle, too. Therefore,

$$G(t, t'; \cosh \vartheta) = \theta(t)\theta(t') \exp \left[ \frac{e_0^2}{(4\pi)^{d/2}} F(t, t'; \cosh \vartheta) \right], \quad (7.10)$$

where  $F(t, t'; \cosh \vartheta)$  is just the one-loop correction. Let us divide (7.10) by

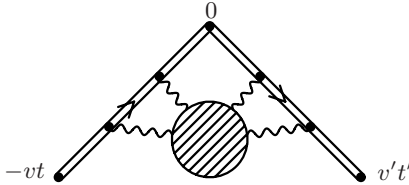


**Fig. 7.3.** Green function with insertion of the heavy–heavy current

$$G(t, t'; \vartheta = 0) = i\tilde{S}(t + t')\theta(t)\theta(t')$$

at  $t > 0, t' > 0$ :

$$\begin{aligned} \mathcal{G}(t, t'; \cosh \vartheta) &= \frac{G(t, t'; \cosh \vartheta)}{i\tilde{S}(t + t')} \\ &= \exp \left[ \frac{e_0^2}{(4\pi)^{d/2}} (\mathcal{F}(t, t'; \cosh \vartheta) - \mathcal{F}(t, t'; \vartheta = 0)) \right], \end{aligned} \quad (7.11)$$

where  $\mathcal{F}(t, t'; \cosh \vartheta)$  is the one-loop correction which has the  $\tilde{J}$  vertex inside (shown in Fig. 7.1); corrections to the external legs cancel here. If this ratio is re-expressed via the renormalized quantities (this is trivial, because in this theory  $e = e_0$  and  $a = a_0$ ), it should be equal to  $\tilde{Z}_J \mathcal{G}_r(t, t'; \cosh \vartheta)$ , where  $\mathcal{G}_r(t, t'; \cosh \vartheta)$  is finite at  $\varepsilon \rightarrow 0$ . Therefore,

$$\begin{aligned} \tilde{Z}_J &= \exp \left[ \frac{\alpha}{4\pi\varepsilon} (f(\cosh \vartheta) - f(\vartheta = 0)) \right], \\ \varepsilon e^{\gamma\varepsilon} \mathcal{F}(t, t'; \cosh \vartheta) &= f(\cosh \vartheta) + \mathcal{O}(\varepsilon). \end{aligned}$$

The anomalous dimension is exactly equal to the one-loop contribution,

$$\tilde{\gamma}_J(\cosh \vartheta) = \frac{\alpha}{\pi} (\vartheta \coth \vartheta - 1). \quad (7.12)$$

This is the well-known soft-photon radiation factor.

In the real HQET, the Green function can be written as

$$G(t, t'; \cosh \vartheta) = \exp \left[ C_F \frac{g_0^2}{(4\pi)^{d/2}} F + C_F \frac{g_0^4}{(4\pi)^d} (C_A F_A + T_F n_l F_l) + \dots \right] \quad (7.13)$$

(by the non-abelian exponentiation theorem [7, 6]). If the colour factors of all two-loop diagrams with two gluons attached to the heavy-quark line were equal to  $C_F^2$  (as in the abelian case), they would produce the  $F^2$  term in the expansion of the exponential. In the non-abelian case, the colour factors of some diagrams also contain a non-abelian part  $C_F C_A$ , which should be taken into account separately (these parts contribute to  $F_A$ ). The ratio (7.11) can be

written similarly. Only the diagrams with the  $\tilde{J}$  vertex inside the correction (Fig. 7.4) contribute to  $\mathcal{F}_A$  and  $\mathcal{F}_I$  (the diagrams of Figs. 7.4b,d should be taken with the non-abelian part of their colour factors,  $C_F C_A$ ). Therefore, the renormalization constant has a similar structure:

$$\begin{aligned} \tilde{Z} = \exp & \left[ C_F \frac{\alpha_s}{4\pi\varepsilon} (f(\cosh \vartheta) - f(\vartheta = 0)) \right. \\ & + C_F \left( \frac{\alpha_s}{4\pi\varepsilon} \right)^2 \left( C_A (f_A(\cosh \vartheta) - f_A(\vartheta = 0)) \right. \\ & \left. \left. + T_F n_l (f_l(\cosh \vartheta) - f_l(\vartheta = 0)) \right) + \dots \right]. \end{aligned} \quad (7.14)$$

In particular, this means that the two-loop anomalous dimension contains no  $C_F^2$  term.

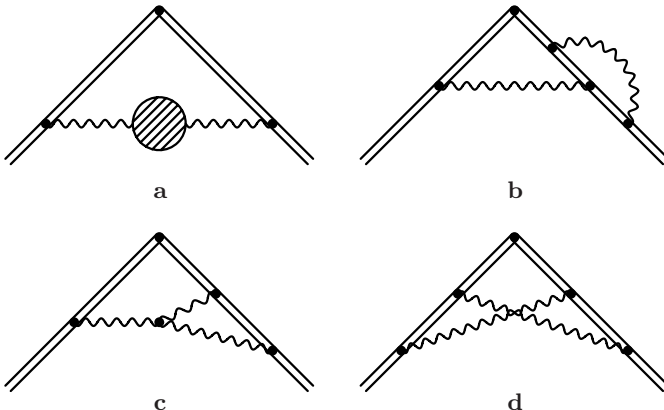


**Fig. 7.4.** Diagrams contributing to the exponent

These diagrams were calculated in [9] (except the easiest one, Fig. 7.4a with the quark-loop correction, which gives  $f_l(\cosh \vartheta)$  and was found in [8]). The diagrams of Figs. 7.4a,b,d can be calculated straightforwardly in the coordinate space, similarly to the one-loop case discussed above (for Fig. 7.4a, this is slightly easier than the momentum-space method used in [9], see Sect. 8.4). The diagram of Fig. 7.4c is more difficult; it was calculated in the momentum space in [9]. The result is

$$\tilde{\gamma}_J(\alpha_s; \cosh \vartheta) = 4C_F \frac{\alpha_s}{4\pi} (\vartheta \coth \vartheta - 1)$$

$$\begin{aligned}
& + C_F \left\{ C_A \left[ \left( \frac{268}{9} - \frac{2}{3}\pi^2 \right) (\vartheta \coth \vartheta - 1) + 8 \right. \right. \\
& \quad + 4 \coth \vartheta (\vartheta \coth \vartheta + 1) [\text{Li}_2(1 - e^{2\vartheta}) - \text{Li}_2(1 - e^{-2\vartheta})] \\
& \quad - 8 \coth^2 \vartheta [\text{Li}_3(1 - e^{2\vartheta}) + \text{Li}_3(1 - e^{-2\vartheta})] \\
& \quad \left. \left. - 8 \sinh 2\vartheta \int_0^\vartheta d\psi \frac{\psi \coth \psi - 1}{\sinh^2 \vartheta - \sinh^2 \psi} \log \frac{\sinh \vartheta}{\sinh \psi} \right] \right. \\
& \quad \left. - \frac{80}{9} T_F n_l (\vartheta \coth \vartheta - 1) \right\} \left( \frac{\alpha_s}{4\pi} \right)^2 + \dots
\end{aligned} \tag{7.15}$$

It has been written here in a form explicitly even in  $\vartheta$ . It can be rewritten via just one trilogarithm using

$$\begin{aligned}
& \text{Li}_3(1 - e^{2\vartheta}) + \text{Li}_3(1 - e^{-2\vartheta}) \\
& = -\text{Li}_3(e^{-2\vartheta}) - 2\vartheta^2 \log(1 - e^{-2\vartheta}) - \frac{4}{3}\vartheta^3 - \frac{\pi^2}{3}\vartheta + \zeta_3,
\end{aligned}$$

but then this symmetry is not obvious. Similarly, using

$$\begin{aligned}
& \text{Li}_2(1 - e^{2\vartheta}) + \text{Li}_2(1 - e^{-2\vartheta}) = -2\vartheta^2, \\
& \text{Li}_2(1 - e^{-2\vartheta}) + \text{Li}_2(e^{-2\vartheta}) = \vartheta \log(1 - e^{-2\vartheta}) + \frac{\pi^2}{6},
\end{aligned} \tag{7.16}$$

the result (7.15) can be rewritten via just one dilogarithm – any of  $\text{Li}_2(1 - e^{2\vartheta})$ ,  $\text{Li}_2(1 - e^{-2\vartheta})$ , or  $\text{Li}_2(e^{-2\vartheta})$ .

At small angles,

$$\begin{aligned}
\tilde{\gamma}_J(\alpha_s; \cosh \vartheta) &= \tilde{\gamma}_0(\alpha_s)\vartheta^2 + \mathcal{O}(\vartheta^4), \\
\tilde{\gamma}_0(\alpha_s) &= \frac{4}{3}C_F \frac{\alpha_s}{4\pi} + C_F \left[ C_A \left( \frac{376}{27} - \frac{8}{9}\pi^2 \right) - \frac{80}{27}T_F n_l \right] \left( \frac{\alpha_s}{4\pi} \right)^2 + \dots
\end{aligned} \tag{7.17}$$

At large angles,

$$\tilde{\gamma}_J(\alpha_s; \cosh \vartheta) = \tilde{\gamma}_\infty(\alpha_s)\vartheta + \mathcal{O}(\vartheta^0) \tag{7.18}$$

to all orders in  $\alpha_s$ , as argued in [9]; with two-loop accuracy,

$$\tilde{\gamma}_\infty(\alpha_s) = 4C_F \frac{\alpha_s}{4\pi} + C_F \left[ C_A \left( \frac{268}{9} - \frac{4}{3}\pi^2 \right) - \frac{80}{9}T_F n_l \right] \left( \frac{\alpha_s}{4\pi} \right)^2 + \dots \tag{7.19}$$

It is remarkable that one of the finest perturbative-HQET papers [9] was written several years before the HQET ‘gold rush’ of 1990–91. The one-loop result (7.6) is, perhaps, the anomalous dimension that has been known for the longest time – it follows from classical electrodynamics (Sect. 1.2).

## 7.2 Flavour-Diagonal Currents at Zero Recoil

In physical applications, we are interested in matrix elements of QCD currents, such as  $b \rightarrow c$  transition currents  $J(\mu) = Z_j^{-1}(\mu) \bar{c}_0 \Gamma b_0$ . Their anomalous dimensions are the same as for light quarks (Sect. 5.1). When the initial and final quark momenta are  $p = m_b v + \tilde{p}$ ,  $p' = m_c v' + \tilde{p}'$ , with small residual momenta  $\tilde{p}$  and  $\tilde{p}'$ , the QCD currents can be expanded in  $1/m_b$  and  $1/m_c$ , the coefficients being HQET heavy–heavy currents with the appropriate quantum numbers:

$$\begin{aligned} J(\mu) &= \sum_i H_i(\cosh \vartheta, \mu, \mu') \tilde{J}_i(\mu') \\ &+ \frac{1}{2m_b} \sum_i G_i(\cosh \vartheta, \mu, \mu') \mathcal{O}_i(\mu') + \frac{1}{2m_c} \sum_i G'_i(\cosh \vartheta, \mu, \mu') \mathcal{O}'_i(\mu') \\ &+ \dots \end{aligned} \quad (7.20)$$

In HQET,  $\alpha'_s(\mu')$  is the same as in QCD with  $n_l = n_f - 2$  flavours. The  $\mu'$ -dependence of  $\tilde{J}_i$  is governed by the HQET anomalous dimension  $\tilde{\gamma}_J$  (Sect. 7.1). The coefficients  $H_i, G_i, G'_i, \dots$  are found by matching – equating on-shell matrix elements of the left-hand and right-hand sides.

For a generic Dirac matrix  $\Gamma$  satisfying (5.5), there are four leading HQET currents in (7.20):

$$\begin{aligned} \bar{c} \Gamma b &= \sum_i H_i \bar{c}_{v'} \Gamma_i \tilde{b}_v + \dots, \\ \Gamma_i &= \Gamma, \quad \not{p} \Gamma, \quad \Gamma \not{p}', \quad \not{p} \Gamma \not{p}'. \end{aligned} \quad (7.21)$$

In particular, for the vector and the axial currents, we have

$$\begin{aligned} \bar{c} \gamma^\alpha b &= \bar{c}_{v'} [H_1^V \gamma^\alpha + H_2^V v^\alpha + H_3^V v'^\alpha] \tilde{b}_v + \dots, \\ H_1^V &= H_1 - H_2 - H_3 - (2 \cosh \vartheta + 1) H_4, \\ H_2^V &= 2(H_2 + H_4), \quad H_3^V = 2(H_3 + H_4); \\ \bar{c} \gamma_5^{AC} \gamma^\alpha b &= \bar{c}_{v'} \gamma_5^{AC} [H_1^A \gamma^\alpha + H_2^A v^\alpha + H_3^A v'^\alpha] \tilde{b}_v + \dots, \\ H_1^A &= H_1 + H_2 + H_3 + (2 \cosh \vartheta - 1) H_4, \\ H_2^A &= -2(H_2 - H_4), \quad H_3^A = 2(H_3 - H_4). \end{aligned} \quad (7.22)$$

First we shall consider the simple case  $v' = v$ ,  $\vartheta = 0$ ; the general case will be discussed in Sects. 7.4 and 7.5. For  $\Gamma$  satisfying (5.5), only one leading-order HQET current  $\tilde{J}$  with the same  $\Gamma$  appears in (7.20).  $\Gamma$  should commute with  $\not{p}$ ; otherwise, by inserting two  $(1 + \not{p})/2$  projectors around it in  $\tilde{J}$ , we see that the leading term vanishes. The HQET current  $\tilde{J}$ , and hence the matching coefficient  $H$ , does not depend on  $\mu'$ .

We begin with the simplest case of flavour-diagonal currents  $J = \bar{Q} \Gamma Q$ . The on-shell matrix element of the QCD current is

$$\langle Q, p = mv | J | Q, p = mv \rangle = Z_Q^{\text{os}} Z_j^{-1} \bar{u} \Gamma(mv, mv) u,$$

where  $\Gamma(p', p) = \Gamma + \Lambda(p', p)$  is the bare proper-vertex function, and the on-shell heavy-quark field renormalization constant  $Z_Q^{\text{os}}$  has been calculated in Sect. 4.2. For  $\Gamma$  satisfying (5.5),  $\bar{u} \Gamma(mv, mv) u = \bar{u} \Gamma u \cdot \Gamma(m^2)$ ,  $\Gamma(m^2) = 1 + \Lambda(m^2)$ . This QCD matrix element should be equal to  $H \langle \tilde{Q}, \tilde{p} = 0 | \tilde{J} | \tilde{Q}, \tilde{p} = 0 \rangle$ , where the HQET on-shell matrix element is

$$\langle \tilde{Q}, \tilde{p} = 0 | \tilde{J} | \tilde{Q}, \tilde{p} = 0 \rangle = \tilde{Z}_Q^{\text{os}} \bar{u}_v \tilde{\Gamma}(0, 0) u_v$$

(here HQET has  $n_l = n_f - 1$  flavours;  $\tilde{Z}_J(\vartheta = 0) = 1$ ). Both matrix elements are UV finite, but may contain IR divergences, which are the same because HQET was designed to reproduce QCD in the IR region. At this point  $\tilde{p} = 0$ ,  $\tilde{p}' = 0$ , and all loop corrections in  $\tilde{\Gamma}(0, 0)$  and  $\tilde{Z}_Q^{\text{os}}$  vanish (except those containing loops of other massive flavours; such contributions first appear at two loops).

The one-loop diagram for  $\bar{u} \Lambda u$  is shown in Fig. 7.5. It has the structure

$$\bar{u} \left( \sum_i x_i L_i \Gamma R_i \right) u, \quad L_i \times R_i = 1 \times 1, \quad \gamma^\mu \times \gamma_\mu, \quad \gamma^\mu \gamma^\nu \times \gamma_\nu \gamma_\mu$$

( $\not{p}$  can always be anticommutated to  $u$  or  $\bar{u}$ ). Taking the double traces with

$$\begin{aligned} \bar{L}_i \times \bar{R}_i &= (1 + \not{p}) \times (1 + \not{p}), \quad \gamma^\alpha (1 + \not{p}) \times (1 + \not{p}) \gamma_\alpha, \\ &\quad \gamma^\alpha \gamma^\beta (1 + \not{p}) \times (1 + \not{p}) \gamma_\beta \gamma_\alpha, \end{aligned}$$

we see that the matrix  $M^{-1}$  is the same as in (5.30). Therefore, this diagram can be calculated, once, and for all  $\Gamma$ , using the projector

$$\begin{aligned} P = \frac{1}{2(d-1)(d-2)} &[ (d-2)(3d-2-4h^2)(1+\not{p}) \times (1+\not{p}) \\ &+ 4h(d-2h)\gamma^\alpha (1+\not{p}) \times (1+\not{p}) \gamma_\alpha \\ &+ (-d+2-4h+4h^2)\gamma^\alpha \gamma^\beta (1+\not{p}) \times (1+\not{p}) \gamma_\beta \gamma_\alpha ] \end{aligned}$$

(see Sect. 5.3). The scalar integrals can be calculated using (4.15). The result is obviously gauge-invariant:

$$\Lambda(m^2) = C_F \frac{g_0^2 m^{-2\varepsilon}}{(4\pi)^{d/2}} \Gamma(\varepsilon) \frac{2(d-2) + (d-3)h(d-4+2h)}{(d-2)(d-3)}. \quad (7.23)$$

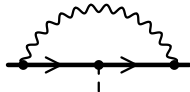


**Fig. 7.5.** Proper vertex of the QCD current at one loop

Multiplying  $\Gamma(m^2)$  by  $Z_Q^{\text{os}}$ , we obtain

$$Z_Q^{\text{os}} \Gamma(m^2) = 1 - C_F \frac{g_0^2 m^{-2\varepsilon}}{(4\pi)^{d/2}} \Gamma(\varepsilon) \frac{(1-h)(d-2+2h)}{d-2} + \dots \quad (7.24)$$

The matrix element of the vector current can be obtained from the Ward identity (5.10) (see (4.25)):

$$\begin{aligned} \Gamma^\mu(p, p) &= \frac{\partial}{\partial p_\mu} [(1 - \Sigma_2(p^2)) (\not{p} - m) + \delta m - m \Sigma_1(p^2)] , \\ \bar{u} \Gamma^\mu(mv, mv) u &= (1 - \Sigma_2(m^2) - 2m^2 \Sigma'_1(m^2)) v^\mu \bar{u} u , \\ Z_Q^{\text{os}} \bar{u} \Gamma^\mu(mv, mv) u &= v^\mu \bar{u} u \end{aligned} \quad (7.25)$$

to all orders. The matrix  $\Gamma = \not{p}$  has  $h = -d/2 + 1$ ; substituting this into (7.24) we see that our one-loop result satisfies this requirement.

Recall that we are only considering matrices  $\Gamma$  commuting with  $\gamma^0 = \not{p}$  (in the  $v$  rest frame), for which  $\bar{u} \Gamma u$  does not vanish. Such matrices have

$$h(d) = \eta \left( n - \frac{d}{2} \right) , \quad (7.26)$$

where  $\eta = (-1)^{n+1}$  for an antisymmetrized product of  $n$   $\gamma$ -matrices, and  $\eta = (-1)^n$  for such a product multiplied by  $\gamma_5^{\text{AC}}$ . Comparing the matrix elements (7.24) for  $\Gamma = 1$  ( $h = 2 - \varepsilon$ ) and  $\gamma_5^{\text{AC}} \gamma_5^{\text{HV}}$  ( $h = 2 + \varepsilon$ ), we reproduce (5.36); for  $\Gamma = \gamma^0$  ( $h = -1 + \varepsilon$ ) and  $\gamma_5^{\text{AC}} \gamma_5^{\text{HV}} \gamma^0$  ( $h = -1 - \varepsilon$ ), we reproduce (5.38); for  $\Gamma = \gamma_5^{\text{AC}} \boldsymbol{\gamma}$  ( $h = 1 - \varepsilon$ ) and  $\gamma_5^{\text{HV}} \boldsymbol{\gamma}$  ( $h = 1 + \varepsilon$ ), we reproduce (5.38) again; and for  $\Gamma = \gamma_5^{\text{AC}} \gamma^0 \boldsymbol{\gamma}$  ( $h = \varepsilon$ ) and  $\gamma_5^{\text{HV}} \gamma^0 \boldsymbol{\gamma}$  ( $h = -\varepsilon$ ), we reproduce  $Z_T = 1$  (Sect. 5.3).

The product (7.24), when expressed via the renormalized  $\alpha_s(\mu)$ , should be equal to  $Z_j(\alpha_s(\mu)) H(\mu)$  (which does not depend on  $\mu'$ ). Its UV divergence reproduces (5.8). It is most natural to perform matching at  $\mu = \mu' = m$ . The matching coefficient is

$$H_\Gamma(m) = 1 + C_F \frac{\alpha_s(m)}{4\pi} (n-2)(n-\eta) + \dots \quad (7.27)$$

This calculation can be done at two loops; the calculation of the necessary integrals was discussed in Sect. 4.2. The diagrams can be obtained from those for the quark self-energy (Fig. 3.6) by inserting the current vertex into all propagators along the quark line. For other  $\mu$ , the matching coefficient can be found using the renormalization group.

The integral of the 0th component of the QCD vector current  $J^\mu$  over all space is the number of heavy quarks (minus antiquarks). The same is true for the HQET current  $\tilde{J}v^\mu$ . Therefore,

$$H_{\gamma^0}(\mu) = 1 \quad (7.28)$$

exactly, for all  $\mu$ . Technically, this follows from the Ward identity (7.25). For the axial current [1],

$$\begin{aligned} H_{\gamma_5^{\text{AC}}\gamma}(m) &= 1 - 2C_F \frac{\alpha_s(m)}{4\pi} \\ &+ C_F \left[ C_F \left( -\frac{29}{3} + 32\zeta_2 - \frac{16}{3} \right) + C_A \left( -\frac{143}{9} - 8\zeta_2 + \frac{8}{3}I \right) \right. \\ &\quad \left. + T_F \left( \frac{920}{9} - 64\zeta_2 \right) + \frac{28}{9}T_F n_l \right] \left( \frac{\alpha_s(m)}{4\pi} \right)^2 + \dots \end{aligned} \quad (7.29)$$

(see (4.20)).

### 7.3 Flavour-Changing Currents at Zero Recoil

Now we shall discuss a more challenging case of flavour-changing QCD currents  $J = \bar{c}\Gamma b$ , but still at  $v' = v$ .

The one-loop vertex (Fig. 7.5) contains integrals

$$\int \frac{d^d k}{[m_b^2 - (k + m_b v)^2]^{n_1} [m_c^2 - (k + m_c v)^2]^{n_2} (-k^2)^{n_3}}.$$

The denominators are linearly dependent. We can multiply the integrand by

$$1 = \frac{m_b [m_c^2 - (k + m_c v)^2] - m_c [m_b^2 - (k + m_b v)^2]}{(m_b - m_c)(-k^2)},$$

thus lowering  $n_1$  or  $n_2$ , until one of these denominators disappears. The remaining integrals are single-mass (4.12). The vertex is, of course, symmetric with respect to  $m_b \leftrightarrow m_c$ :

$$\begin{aligned} \Lambda &= C_F \frac{g_0^2}{(4\pi)^{d/2}} \frac{\Gamma(\varepsilon)}{d-3} \frac{m_b^{1-2\varepsilon} \Phi(m_c/m_b) - m_c^{1-2\varepsilon} \Phi(m_b/m_c)}{m_b - m_c}, \\ \Phi(r) &= \frac{d-1}{d-5} r - \frac{(1-h)(d-2+2h)}{d-2}. \end{aligned} \quad (7.30)$$

This result reproduces (7.23) at  $m_c \rightarrow m_b$  and (5.64) at  $m_c \rightarrow 0$ . The checks with  $Z_P$ ,  $Z_A$ , and  $Z_T$  are passed as before.

The on-shell matrix element expressed via the renormalized  $\alpha_s(\mu)$  is

$$\begin{aligned} (Z_b^{\text{os}} Z_c^{\text{os}})^{1/2} \Gamma &= 1 + C_F \frac{\alpha_s(\mu)}{4\pi\varepsilon} \left( \frac{m_b m_c}{\mu^2} \right)^{-\varepsilon} \frac{1}{1-2\varepsilon} \\ &\times \left[ \frac{r^\varepsilon \Phi(r) - r^{1-\varepsilon} \Phi(r^{-1})}{1-r} - \frac{1}{2} (r^\varepsilon + r^{-\varepsilon}) (3-2\varepsilon) \right], \end{aligned} \quad (7.31)$$

where  $r = m_c/m_b$ . It is most convenient to perform matching at

$$\mu_0 = \sqrt{m_b m_c}, \quad (7.32)$$

when the matching coefficients are symmetric with respect to  $m_b \leftrightarrow m_c$ . The UV divergence of (7.31) (see (7.30)) once more gives us the anomalous dimension (5.8). The finite part gives the matching coefficient, which does not depend on  $\mu'$ :

$$H_T(\mu_0) = 1 - C_F \left[ n(n-4)L \coth \frac{L}{2} - n(3n-10) + \eta(n-2) \right] \frac{\alpha_s(\mu_0)}{4\pi} + \dots \quad (7.33)$$

(where  $L = -\log r$ ). This result reproduces (7.27) at  $r \rightarrow 1$ . For the vector and axial currents, the matching coefficients do not depend on  $\mu$ :

$$H_{\gamma^0} = 1 + 6C_F \left[ \frac{L}{2} \coth \frac{L}{2} - 1 \right] \frac{\alpha_s(\mu_0)}{4\pi} + \dots, \\ H_{\gamma_5^A \gamma} = 1 + 6C_F \left[ \frac{L}{2} \coth \frac{L}{2} - \frac{4}{3} \right] \frac{\alpha_s(\mu_0)}{4\pi} + \dots \quad (7.34)$$

When  $m_c \sim m_b$ , the vertex can be expanded in  $m_b - m_c$ . Owing to the  $m_b \leftrightarrow m_c$  symmetry, the result can be written as a series in  $\rho = (m_b - m_c)^2/(m_b m_c)$ :

$$H_{\gamma^0} = 1 + C_F \left( \frac{1}{2}\rho - \frac{1}{20}\rho^2 + \dots \right) \frac{\alpha_s(\mu_0)}{4\pi} + \mathcal{O}(\alpha_s^2), \\ H_{\gamma_5^A \gamma} = 1 + C_F \left( -2 + \frac{1}{2}\rho - \frac{1}{20}\rho^2 + \dots \right) \frac{\alpha_s(\mu_0)}{4\pi} + \mathcal{O}(\alpha_s^2). \quad (7.35)$$

The two-loop correction can be calculated straightforwardly, because the resulting two-loop integrals are single-mass on-shell ones (Sect. 4.2). However, calculating many terms of such expansions requires efficient computer-algebra programming. For the vector and axial currents, the two-loop matching coefficients expanded up to  $\rho^4$  have been calculated in [1]. For the vector current, the expansion starts from  $\mathcal{O}(\rho)$ , in accord with (7.28).

These two-loop matching coefficients have also been calculated exactly [2] (and independently checked in [5]). The results are rather complicated: they contain trilogarithms. The  $n_l$  contributions to (7.34) are simple:

$$-\frac{4}{3}C_F T_F n_l \left( \frac{L}{2} \coth \frac{L}{2} - 1 \right) \left( \frac{\alpha_s}{4\pi} \right)^2, \\ -\frac{2}{3}C_F T_F n_l \left( 5L \coth \frac{L}{2} - \frac{44}{3} \right) \left( \frac{\alpha_s}{4\pi} \right)^2; \quad (7.36)$$

see Sect. 8.8.

Until now, we have matched the QCD currents  $J$  onto HQET, where both the  $b$  and the  $c$  are considered static, in a single step, at a scale somewhere between  $m_b$  and  $m_c$ . This method is good when  $m_c \sim m_b$ : it gives us the exact dependence of the matching coefficients on  $r = m_c/m_b$ . These coefficients are known at two loops; all terms of order  $(\alpha_s/\pi)^n$  with  $n \geq 3$  are neglected. When  $r \ll 1$  ( $m_c \ll m_b$ ), the matching coefficients are [2]

$$\begin{aligned}
H_{\gamma^0} &= 1 + C_F (3L - 6) \frac{\alpha_s(\mu_0)}{4\pi} \\
&+ C_F \left[ C_F \left( \frac{9}{2}L^2 + \left( 16\zeta_2 - \frac{41}{2} \right)L - 16I - 24\zeta_3 + 58\zeta_2 + 29 \right) \right. \\
&\quad \left. + C_A \left( \left( -4\zeta_2 + \frac{5}{6} \right)L + 8I - 24\zeta_3 - \zeta_2 - \frac{23}{3} \right) \right. \\
&\quad \left. + T_F \left( 4L^2 - \frac{26}{3}L - 37\zeta_2 + \frac{1147}{18} \right) \right. \\
&\quad \left. + T_F n_l \left( -\frac{2}{3}L + \frac{4}{3} \right) \right] \left( \frac{\alpha_s(\mu_0)}{4\pi} \right)^2 + \mathcal{O}(\alpha_s^3), \\
H_{\gamma_5^{\text{AC}} \gamma} &= 1 + C_F (3L - 8) \frac{\alpha_s(\mu_0)}{4\pi} \\
&+ C_F \left[ C_F \left( \frac{9}{2}L^2 + \left( 16\zeta_2 - \frac{53}{2} \right)L - \frac{32}{3}I - 24\zeta_3 + \frac{46}{3}\zeta_2 + \frac{154}{3} \right) \right. \\
&\quad \left. + C_A \left( \left( -4\zeta_2 + \frac{49}{6} \right)L + \frac{16}{3}I - 24\zeta_3 + 15\zeta_2 - \frac{332}{9} \right) \right. \\
&\quad \left. + T_F \left( 4L^2 - 14L - \frac{79}{3}\zeta_2 + \frac{971}{18} \right) \right. \\
&\quad \left. + T_F n_l \left( -\frac{10}{3}L + \frac{88}{9} \right) \right] \left( \frac{\alpha_s(\mu_0)}{4\pi} \right)^2 + \mathcal{O}(\alpha_s^3), \tag{7.37}
\end{aligned}$$

where  $L = -\log r$ ,  $n_l$  includes neither the  $b$  nor the  $c$ , and  $\alpha_s(\mu_0)$  has  $n_f = n_l + 2$  flavours (this quantity is somewhat artificial because  $\mu_0$  is below  $m_b$ ). We may want to sum leading powers of  $L$ . In other words, when the scales  $m_b$  and  $m_c$  are widely separated, it is desirable to take into account the running of  $\alpha_s(\mu)$  and of the currents between these two scales correctly.

This can be achieved by a two-step matching. First we match  $J$  onto the effective theory in which the  $b$ -quark is considered static while the  $c$ -quark is still dynamic (HQET-1) at the scale  $\mu = m_b$ :

$$J(m_b) = C_F(m_b, \mu) \tilde{J}(\mu) + \frac{1}{2m_b} \sum_i B_i(m_b, \mu) \mathcal{O}_i(\mu) + \dots, \tag{7.38}$$

where  $\tilde{J} = \bar{c} T \bar{b}$ . Some of the dimension-4 operators  $\mathcal{O}_i$  have matrix elements proportional to  $m_c$ , so that this is an expansion in  $r = m_c/m_b$ . There are  $n_i = n_f - 1 = n_l + 1$  flavours in this intermediate theory. Then we match it

onto the effective theory in which the c is also considered static (HQET-2) at the scale  $\mu = m_c$ :

$$\tilde{j}(m_c) = E(m_c)\tilde{J}, \quad \mathcal{O}_i(m_c) = m_c F_i(m_c)\tilde{J}, \quad \dots, \quad (7.39)$$

where  $\tilde{J} = \bar{\tilde{c}}\Gamma\tilde{b}$ , and terms of the order  $\Lambda_{\text{QCD}}/m_c$  are neglected. Therefore,

$$H_\Gamma(m_b, m_c) = C_\Gamma(m_b, m_c)E(m_c) + \frac{r}{2} \sum_i B_i(m_b, m_c)F_i(m_c) + \dots \quad (7.40)$$

The matching coefficients  $C_\Gamma(m_b, m_b)$  for all currents have been considered in Sect. 5.6. The running is given by (5.58):

$$\begin{aligned} &C_\Gamma(m_b, \mu) \\ &= C_\Gamma(m_b, m_b)x^{\tilde{\gamma}_{j0}} \left[ 1 + \frac{\tilde{\gamma}_{j0}}{2\beta_0''} \left( \frac{\tilde{\gamma}_{j1}}{\tilde{\gamma}_{j0}} - \frac{\beta_1''}{\beta_0''} \right) \frac{\alpha_s''(m_b) - \alpha_s''(\mu)}{4\pi} + \dots \right], \\ &x = \left( \frac{\alpha_s''(\mu)}{\alpha_s''(m_b)} \right)^{-1/(2\beta_0'')} . \end{aligned} \quad (7.41)$$

where  $\alpha_s''$ ,  $\beta''$ , and the anomalous dimension  $\tilde{\gamma}_j$  (5.45) involve  $n_i$  flavours. Now we are going to find  $E(m_c)$  (it does not depend on the Dirac matrix  $\Gamma$ ).

To this end, the HQET-1 on-shell matrix element  $(Z_c^{\text{os}}\tilde{Z}_b^{\text{os}})^{1/2}\tilde{Z}_j^{-1}\bar{u}\tilde{\Gamma}_1(m_c v, 0)u_v$  from  $\tilde{b}$  with  $\tilde{p} = 0$  to c with  $p = m_c v$  is equated to  $E_\Gamma$  times the HQET-2 on-shell matrix element  $\tilde{Z}'_Q^{\text{os}}\bar{u}_v\tilde{\Gamma}_2(0, 0)u_v$  from  $\tilde{b}$  with  $\tilde{p} = 0$  to  $\tilde{c}$  with  $\tilde{p} = 0$  (in this theory, the number of flavours is  $n_l = n_i - 1$ ;  $\tilde{Z}_J(\vartheta = 0) = 1$ ). All loop corrections in HQET-2 vanish (unless there is a massive flavour lighter than c). For any  $\Gamma$ , in HQET-1 we have  $\bar{u}\tilde{\Gamma}_1(m_c v, 0)u_v = \bar{u}\Gamma u_v \cdot \tilde{\Gamma}_1$ .

The one-loop diagram for the vertex correction is shown in Fig. 7.6:

$$\tilde{\Gamma}_1(m_c v, 0) = \left[ 1 - iC_F g_0^2 \int \frac{d^d k}{(2\pi)^d} \frac{\not{v}(\not{k} + m_c \not{v} + m_c)}{[m_c^2 - (k + m_c v)^2](k \cdot v)(-k^2)} \right] \Gamma.$$

We may replace  $\not{k}$  by  $k \cdot v \not{v}$ , because the integral of  $k_\perp$  vanishes. In the integrals

$$\int \frac{d^d k}{[m_c^2 - (k + m_c v)^2]^{n_1} (k \cdot v)^{n_2} (-k^2)^{n_3}},$$

the denominators are linearly dependent. We can multiply the integrand by



Fig. 7.6. Proper vertex of the HQET-1 current at one loop

$$1 = \frac{[m_c^2 - (k + m_c v)^2] + 2m_c k \cdot v}{-k^2}$$

until one of the quark denominators disappears. Integrals without the massive-quark denominator are scale-free and vanish; those without the HQET denominator have been discussed in Sect. 4.2. We obtain

$$\tilde{\Gamma}_1 = 1 - C_F \frac{g_0^2 m_c^{-2\varepsilon}}{(4\pi)^{d/2}} \Gamma(\varepsilon) \frac{d-1}{(d-3)(d-5)}, \quad (7.42)$$

or

$$(Z_c^{\text{os}})^{1/2} \tilde{\Gamma}_1 = 1 - \frac{1}{2} C_F \frac{g_0^2 m_c^{-2\varepsilon}}{(4\pi)^{d/2}} \Gamma(\varepsilon) \frac{d-1}{d-5}.$$

The  $1/\varepsilon$  pole is cancelled by  $\tilde{Z}_j^{-1}$ , and we obtain the matching coefficient

$$E(m_c) = 1 - 4C_F \frac{\alpha_s''(m_c)}{4\pi} + \dots \quad (7.43)$$

Collecting all the pieces together, we obtain

$$\begin{aligned} H_{\gamma^0}(m_b, m_c) &= x^{\tilde{\gamma}_{j0}} \left[ 1 - 2C_F \frac{\alpha_s(m_b)}{4\pi} - 4C_F \frac{\alpha_s''(m_c)}{4\pi} \right. \\ &\quad \left. + \frac{\tilde{\gamma}_{j0}}{2\beta_0''} \left( \frac{\tilde{\gamma}_{j1}}{\tilde{\gamma}_{j0}} - \frac{\beta_1''}{\beta_0''} \right) \frac{\alpha_s''(m_b) - \alpha_s''(m_c)}{4\pi} + \dots \right], \\ H_{\gamma_5^{\text{AC}}\gamma}(m_b, m_c) &= x^{\tilde{\gamma}_{j0}} \left[ 1 - 4C_F \frac{\alpha_s(m_b)}{4\pi} - 4C_F \frac{\alpha_s''(m_c)}{4\pi} \right. \\ &\quad \left. + \frac{\tilde{\gamma}_{j0}}{2\beta_0''} \left( \frac{\tilde{\gamma}_{j1}}{\tilde{\gamma}_{j0}} - \frac{\beta_1''}{\beta_0''} \right) \frac{\alpha_s''(m_b) - \alpha_s''(m_c)}{4\pi} + \dots \right]. \end{aligned} \quad (7.44)$$

If we express  $\alpha_s''(m_c)$  via  $\alpha_s''(m_b)$  with two-loop accuracy using the  $n_i$ -flavour  $\beta$ -function, then use  $\alpha_s''(m_b) = \alpha_s(m_b) + \mathcal{O}(\alpha_s^3)$ , and finally express  $\alpha_s(m_b)$  via  $\alpha_s(\mu_0)$  using the  $n_f$ -flavour  $\beta$ -function, then we reproduce all leading and next-to-leading logarithms in (7.37), i.e., the one-loop term and the  $L^2$  and  $L$  terms at two loops.

Now we shall discuss the  $\mathcal{O}(r)$  term in (7.40) in the LLA [3]. It is sufficient to know the matching coefficients  $F_i(m_c)$  at the tree level. In the case of spin-0 currents (Sect. 6.4), the only operators producing  $\mathcal{O}(m_c)$  contributions are  $\mathcal{O}_{2,3}$ . In  $\mathcal{O}_3$ , we may replace the  $\overline{\text{MS}}$  mass  $m_c(m_c)$  by the pole mass  $m_c$ :

$$\mathcal{O}_3(m_c) = m_c \tilde{j}(m_c). \quad (7.45)$$

In  $\mathcal{O}_2$ , we may replace  $-i\overleftrightarrow{D}$  by the c-quark momentum  $m_c v$ :

$$\mathcal{O}_2(m_c) = m_c \tilde{\mathcal{J}}(m_c). \quad (7.46)$$

For the vector current  $\bar{c}\gamma^0 b$ , the coefficients  $B_{2,3}^T(m_b, m_c)$  are given by (6.54) (the lower sign, with  $\mu = m_c$  and  $n_i$  flavours), and the  $\mathcal{O}(r)$  term in  $H_{\gamma^0}(m_b, m_c)$  is

$$\begin{aligned} & \frac{r}{2} \left( B_2^{\gamma^0}(m_b, m_c) + B_3^{\gamma^0}(m_b, m_c) \right) \\ &= \frac{r}{2} x^{\tilde{\gamma}_{j0}} \left[ \tilde{\gamma}_{a0}^k \log x + \frac{\gamma_{m0} (\tilde{\gamma}_{a0}^m + 3\tilde{\gamma}_{b0}^m)}{\tilde{\gamma}_{m0} (\tilde{\gamma}_{m0} - \gamma_{m0})} \left( x^{\tilde{\gamma}_{m0}} - 1 \right) \right. \\ & \quad \left. + \left( \frac{\tilde{\gamma}_{a0}^m + 3\tilde{\gamma}_{b0}^m}{\gamma_{m0} - \tilde{\gamma}_{m0}} + \frac{\gamma_{b0}^k}{\gamma_{m0}} \right) (x^{\gamma_{m0}} - 1) \right] \\ &= ry^{-2} \left( -\frac{8}{3} \log y - \frac{5}{9} + \frac{32}{9} y^3 - 3y^4 \right), \quad y = \left( \frac{\alpha_s''(m_b)}{\alpha_s''(m_c)} \right)^{3/25}. \end{aligned} \quad (7.47)$$

For the axial current  $\bar{c}\gamma_5^{AC}\gamma^i b$ , the leading HQET current is  $\tilde{\mathcal{J}}^i = \bar{c}\gamma_5^{AC}\gamma^i \tilde{b}$ , and the subleading operators are obtained from (6.66) by the substitution  $\bar{c} \rightarrow \bar{c}\gamma_5^{AC}$ , except  $\mathcal{O}_5^i = -m_c \tilde{\mathcal{J}}^i$ . With this definition, the anomalous-dimension matrix (6.69) is the same as in Sect. 6.5. Only  $\mathcal{O}_{3,4,5}^i$  can produce  $\mathcal{O}(m_c)$  contributions:

$$\mathcal{O}_3^i(m_c) = 0, \quad \mathcal{O}_4^i(m_c) = -\mathcal{O}_5^i(m_c) = m_c \tilde{\mathcal{J}}^i(m_c). \quad (7.48)$$

The coefficients  $B_{3,4,5}^T(m_b, m_c)$  in the LLA are given by (6.76) (with the upper sign), and the  $\mathcal{O}(r)$  term in  $H_{\gamma_5^{AC}\gamma}(m_b, m_c)$  is

$$\begin{aligned} & \frac{r}{2} \left( B_4^{\gamma^i}(m_b, m_c) - B_5^{\gamma^i}(m_b, m_c) \right) \\ &= \frac{r}{2} x^{\tilde{\gamma}_{j0}} \left[ \tilde{\gamma}_{a0}^k \log x + \frac{1}{3} \left( \frac{\tilde{\gamma}_{a0}^m}{\gamma_{m0} - \tilde{\gamma}_{m0}} + \frac{\tilde{\gamma}_{a0}^m + 3\tilde{\gamma}_{b0}^m}{\tilde{\gamma}_{m0}} \right) \left( x^{\tilde{\gamma}_{m0}} - 1 \right) \right. \\ & \quad \left. + \left( \frac{1}{3} \frac{\tilde{\gamma}_{a0} \tilde{\gamma}_{a0}^m}{\tilde{\gamma}_{m0} (\tilde{\gamma}_{m0} - \tilde{\gamma}_{a0})} + \frac{1}{3} \frac{\tilde{\gamma}_{a0}^m}{\tilde{\gamma}_{m0} - \gamma_{m0}} - \frac{\tilde{\gamma}_{b0}^m}{\tilde{\gamma}_{m0}} - \frac{\tilde{\gamma}_{b0}^k}{\gamma_{m0}} - \frac{2}{3} \right) (x^{\gamma_{m0}} - 1) \right] \\ &= ry^{-2} \left( -\frac{8}{3} \log y + \frac{2}{9} - \frac{14}{27} y^3 + \frac{8}{27} y^4 \right). \end{aligned} \quad (7.49)$$

How can results of these two approaches be combined? We start from the single-step matching results (7.34), with the two-loop corrections [2]. These results are expressed via  $\alpha_s(\mu_0)$ , and contain all powers of  $r$ . Then we take the two-step matching results (7.44), and subtract from them the terms of order  $\alpha_s(\mu_0)$  and  $\alpha_s^2(\mu_0)$ , which are already accounted for in the single-step results. By adding this difference, we take into account an infinite sequence of radiative corrections of order  $\mathcal{O}(r^0)$  with leading and next-to-leading powers of the logarithm  $L$ . Similarly, we take the  $\mathcal{O}(r)$  two-step matching results (7.47) and (7.49), and subtract from them the terms of order  $\alpha_s(\mu_0)$  and  $\alpha_s^2(\mu_0)$ , which are already accounted for. By adding this difference, we take into account corrections of order  $\mathcal{O}(r)$  with leading powers of  $L$  at all orders in  $\alpha_s$ .

## 7.4 Flavour-Diagonal Currents at Non-Zero Recoil

Now we are going to consider flavour-diagonal currents at  $\vartheta \neq 0$  [4]. The on-shell QCD matrix element  $Z_Q^{\text{os}} Z_J^{-1}(\mu) \bar{u}(\Gamma + \Lambda(mv', mv)) u$  should be equal to  $\tilde{Z}_J^{-1}(\mu') \bar{u}_{v'} [\sum_i H_i(\mu, \mu') \Gamma_i] u_v$  ( $\tilde{Z}_Q^{\text{os}} = 1$  and  $\tilde{\Lambda}(0, 0) = 0$ , if there are no other massive flavours). The one-loop vertex correction  $\Lambda(mv', mv)$  (Fig. 7.5) is obviously gauge-invariant. Using the Feynman parametrization (2.13), we have

$$\begin{aligned} \Lambda &= iC_F g_0^2 \int \frac{d^d k}{(2\pi)^d} \frac{\gamma_\mu(k + m\psi' + m)\Gamma(k + m\psi + m)\gamma^\mu}{(-k^2)(-k^2 - 2m v \cdot k)(-k^2 - 2m v' \cdot k)} \\ &= 2iC_F g_0^2 \int dx dx' \frac{d^d k'}{(2\pi)^d} \\ &\quad \times \frac{\gamma_\mu(k' + m(1-x')\psi' - mx\psi + m)\Gamma(k' + m(1-x)\psi - mx'\psi' + m)\gamma^\mu}{(a^2 - k'^2)^3}, \\ k' &= k + m(xv + x'v'), \\ a^2 &= m^2(xv + x'v')^2 = m^2(x^2 + x'^2 + 2xx' \cosh \vartheta). \end{aligned}$$

We calculate the loop integral using (2.16), and substitute  $x = \xi(1+z)/2$  and  $x' = \xi(1-z)/2$ ; the  $\xi$  integration is trivial ( $a^2 = m^2\xi^2 a_+ a_-$ ,  $a_\pm = \cosh(\vartheta/2) \pm z \sinh(\vartheta/2)$ ):

$$\begin{aligned} \Lambda &= C_F \frac{g_0^2 m^{-2\varepsilon}}{(4\pi)^{d/2}} \Gamma(1+\varepsilon) \\ &\times \left[ \Gamma \int_{-1}^{+1} \frac{dz}{(a_+ a_-)^{1+\varepsilon}} \left( \frac{a_+ a_- h^2}{2\varepsilon(1-\varepsilon)} - \frac{(1-z^2)h}{8(1-\varepsilon)} + \frac{\cosh \vartheta}{\varepsilon(1-2\varepsilon)} + \frac{1}{1-2\varepsilon} \right) \right. \\ &\quad - (\psi\Gamma + \Gamma\psi') \frac{1}{2} \int_{-1}^{+1} \frac{dz}{(a_+ a_-)^{1+\varepsilon}} \left( \frac{(1+z^2)h}{4(1-\varepsilon)} + \frac{1}{1-2\varepsilon} \right) \\ &\quad \left. - \psi\Gamma\psi' \frac{h}{8(1-\varepsilon)} \int_{-1}^{+1} \frac{dz (1-z^2)}{(a_+ a_-)^{1+\varepsilon}} \right]. \end{aligned} \quad (7.50)$$

Here the function  $h(d)$  (5.5) is given by (7.26). The checks with  $Z_P$ ,  $Z_A$ , and  $Z_T$  are passed as for  $\vartheta = 0$ . At  $\vartheta = 0$ ,  $a_+ = a_- = 1$ , and (7.23) is reproduced.

It is not difficult to calculate the integrals with the accuracy needed for the terms finite at  $\varepsilon \rightarrow 0$ :

$$\begin{aligned} \int_{-1}^{+1} \frac{dz}{(a_+ a_-)^\varepsilon} &= 2 - 2\varepsilon \left( \frac{\vartheta(\cosh \vartheta + 1)}{\sinh \vartheta} - 2 \right) + \mathcal{O}(\varepsilon^2), \\ \int_{-1}^{+1} \frac{dz}{(a_+ a_-)^{1+\varepsilon}} &= 2 \frac{\vartheta + \varepsilon F(\vartheta)}{\sinh \vartheta} + \mathcal{O}(\varepsilon^2), \\ F(\vartheta) &= \text{Li}_2(-e^{-\vartheta}) - \text{Li}_2(-e^\vartheta) - \vartheta \log(2(\cosh \vartheta + 1)), \\ \int_{-1}^{+1} \frac{z^2 dz}{(a_+ a_-)^{1+\varepsilon}} &= \frac{4}{\cosh \vartheta - 1} \left( \frac{\vartheta}{\sinh \vartheta} - 1 \right) + \frac{2\vartheta}{\sinh \vartheta} + \mathcal{O}(\varepsilon). \end{aligned} \quad (7.51)$$

The dilogarithms here are not independent:

$$\text{Li}_2(-e^\vartheta) + \text{Li}_2(-e^{-\vartheta}) = -\frac{\vartheta^2}{2} - \frac{\pi^2}{6}.$$

It is most natural to perform matching at  $\mu = \mu' = m$ . Using  $Z_Q^{\text{os}}$  (4.29),  $Z_J$  (5.8), and  $\tilde{Z}_J$  (7.6), we see that the  $1/\varepsilon$  poles cancel in  $H_i$ :

$$\begin{aligned} H_1 &= 1 + H_4 + C_F \frac{\alpha_s(m)}{4\pi} \left[ \left( 3 - \vartheta \frac{\cosh \vartheta + 1}{\sinh \vartheta} \right) (n-2)^2 + 2(n-2) \right. \\ &\quad \left. + \frac{2\vartheta}{\sinh \vartheta} + 4(\vartheta \coth \vartheta - 1) + 2F(\vartheta) \coth \vartheta \right], \\ H_2 = H_3 &= -H_4 - C_F \frac{\alpha_s(m)}{4\pi} \frac{\vartheta}{\sinh \vartheta} \left[ \frac{\eta(n-2)}{2} + 1 \right], \\ H_4 &= C_F \frac{\alpha_s(m)}{4\pi} \left( \frac{\vartheta}{\sinh \vartheta} - 1 \right) \frac{\eta(n-2)}{2(\cosh \vartheta - 1)}. \end{aligned} \quad (7.52)$$

At  $\vartheta \rightarrow 0$ ,  $H_1 + H_2 + H_3 + H_4$  reproduces (7.27). In particular, we obtain the following [4, 10] from (7.22) for the vector ( $n = 1$ ,  $\eta = 1$ ) and axial ( $n = 1$ ,  $\eta = -1$ ) currents:

$$\begin{aligned} H_1^V &= 1 + C_F \frac{\alpha_s(m)}{4\pi} \left[ \frac{3\vartheta}{\sinh \vartheta} + 3\vartheta \coth \vartheta - 4 + F(\vartheta) \coth \vartheta \right], \\ H_2^V = H_3^V &= -C_F \frac{\alpha_s(m)}{4\pi} \frac{\vartheta}{\sinh \vartheta}, \\ H_1^A &= H_1^V - C_F \frac{\alpha_s(m)}{4\pi} \frac{4\vartheta}{\sinh \vartheta}, \\ H_2^A = -H_3^A &= C_F \frac{\alpha_s(m)}{4\pi} \left[ \frac{2}{\cosh \vartheta - 1} \left( \frac{\vartheta}{\sinh \vartheta} - 1 \right) + \frac{3\vartheta}{\sinh \vartheta} \right]. \end{aligned} \quad (7.53)$$

## 7.5 Flavour-Changing Currents at Non-Zero Recoil

Now we shall discuss a more challenging case of flavour-changing QCD currents  $J = \bar{c}\Gamma b$ . The momentum transfer squared is

$$\begin{aligned} q^2 &= (m_b v - m_c v')^2 = 2m_b m_c (\cosh L - \cosh \vartheta) \\ &= 4m_b m_c \sinh \frac{L + \vartheta}{2} \sinh \frac{L - \vartheta}{2}, \quad L = \log \frac{m_b}{m_c}. \end{aligned} \quad (7.54)$$

In the decay channel,  $\vartheta$  varies from 0 to  $L$  (this case corresponds to  $q^2 = 0$ );  $\vartheta > L$  is the scattering channel.

The one-loop vertex correction  $\Lambda(m_c v', m_b v)$  (Fig. 7.5) is obviously gauge-invariant:

$$\Lambda = iC_F g_0^2 \int \frac{d^d k}{(2\pi)^d} \frac{\gamma_\mu (\not{k} + m_c \not{v}' + m_c) \Gamma(\not{k} + m_b \not{v} + m_b) \gamma^\mu}{(-k^2)(-k^2 - 2m_b v \cdot k)(-k^2 - 2m_c v' \cdot k)}$$

$$\begin{aligned}
&= 2iC_F g_0^2 \int dx dx' \frac{d^d k'}{(2\pi)^d} \\
&\times \frac{\gamma_\mu (\not{k}' + m_c(1-x')\not{v}' - m_b x\not{v} + m_c) \Gamma(\not{k}' + m_b(1-x)\not{v} - m_c x'\not{v}' + m_b) \gamma^\mu}{(a^2 - k'^2)^3}, \\
k' &= k + m_b x v + m_c x' v', \\
a^2 &= (m_b x v + m_c x' v')^2 = m_b^2 x^2 + m_c^2 x'^2 + 2 m_b m_c x x' \cosh \vartheta.
\end{aligned}$$

We calculate the loop integral using (2.16), and substitute  $x = \xi(1+z)/2$ ,  $x' = \xi(1-z)/2$ , and

$$a^2 = m_b m_c \xi^2 a_+ a_-, \quad a_\pm = \cosh \frac{L \pm \vartheta}{2} + z \sinh \frac{L \pm \vartheta}{2}.$$

The  $\xi$  integration is trivial:

$$\begin{aligned}
A &= C_F \frac{g_0^2 (m_b m_c)^{-\varepsilon}}{(4\pi)^{d/2}} \Gamma(1+\varepsilon) \\
&\times \left[ \Gamma \int_{-1}^{+1} \frac{dz}{(a_+ a_-)^{1+\varepsilon}} \left( \frac{a_+ a_- h^2}{2\varepsilon(1-\varepsilon)} - \frac{(1-z^2)h}{8(1-\varepsilon)} + \frac{\cosh \vartheta}{\varepsilon(1-2\varepsilon)} \right. \right. \\
&\quad \left. \left. + \frac{\cosh L + z \sinh L}{1-2\varepsilon} \right) \right. \\
&- \not{v} \Gamma \frac{1}{2} \int_{-1}^{+1} \frac{dz}{(a_+ a_-)^{1+\varepsilon}} \left( \frac{e^L(1+z)^2 h}{4(1-\varepsilon)} + \frac{1-z}{1-2\varepsilon} \right) \\
&- \Gamma \not{v}' \frac{1}{2} \int_{-1}^{+1} \frac{dz}{(a_+ a_-)^{1+\varepsilon}} \left( \frac{e^{-L}(1-z)^2 h}{4(1-\varepsilon)} + \frac{1+z}{1-2\varepsilon} \right) \\
&\left. - \not{v} \Gamma \not{v}' \frac{h}{8(1-\varepsilon)} \int_{-1}^{+1} \frac{dz}{(a_+ a_-)^{1+\varepsilon}} (1-z^2) \right]. \tag{7.55}
\end{aligned}$$

Here the function  $h(d)$  (5.5) is given by (7.26). The checks with  $Z_P$ ,  $Z_A$ , and  $Z_T$  are passed as before. At  $m_c = m_b$  ( $L = 0$ ), this expression coincides with (7.50). At  $\vartheta = 0$ ,

$$a_+ = a_- = \cosh \frac{L}{2} + z \sinh \frac{L}{2}, \tag{7.56}$$

and (7.30) is reproduced.

The case  $q^2 = 0$  ( $\vartheta = L$ ) is also easy:

$$a_+ = \cosh L + z \sinh L, \quad a_- = 1,$$

and the integrals can be calculated:

$$\begin{aligned}
\int_{-1}^{+1} \frac{dz}{a_+^\varepsilon} &= \frac{2 \sinh(1-\varepsilon)L}{(1-\varepsilon) \sinh L} = 2 [1 - \varepsilon(L \coth L - 1)] + \mathcal{O}(\varepsilon^2), \\
\int_{-1}^{+1} \frac{dz}{a_+^{1+\varepsilon}} &= \frac{2 \sinh L \varepsilon}{\varepsilon \sinh L} = \frac{2L}{\sinh L} + \mathcal{O}(\varepsilon^2),
\end{aligned}$$

$$\begin{aligned} \int_{-1}^{+1} \frac{z dz}{a_+^{1+\varepsilon}} &= \frac{2}{\sinh^2 L} \left[ \frac{\sinh(1-\varepsilon)L}{1-\varepsilon} - \frac{\cosh L \sinh L \varepsilon}{\varepsilon} \right] \\ &= -\frac{2}{\sinh L} (L \coth L - 1) + \mathcal{O}(\varepsilon), \\ \int_{-1}^{+1} \frac{z^2 dz}{a_+^{1+\varepsilon}} &= \frac{2}{\sinh^3 L} \left[ \frac{\sinh(2-\varepsilon)L}{2-\varepsilon} - \frac{2 \cosh L \sinh(1-\varepsilon)L}{1-\varepsilon} \right. \\ &\quad \left. + \frac{\cosh^2 L \sinh L \varepsilon}{\varepsilon} \right] \\ &= \frac{2 \cosh L}{\sinh^2 L} (L \coth L - 1) + \mathcal{O}(\varepsilon). \end{aligned}$$

The matching coefficients at  $\mu = \mu' = \mu_0$  are

$$\begin{aligned} H_1 &= 1 + H_4 + C_F \frac{\alpha_s(\mu_0)}{4\pi} \left[ (2 - L \coth L)(n-2)^2 + 2(n-2) \right. \\ &\quad \left. + 2(2L \coth L - 1) \right], \\ H_2 = H_3(L \rightarrow -L) &= -C_F \frac{\alpha_s(\mu_0)}{4\pi} \left[ \frac{2L e^{-L} + (e^{2L} - 3) \sinh L}{8 \sinh^3 L} \eta(n-2) \right. \\ &\quad \left. + \frac{L e^L - \sinh L}{\sinh^2 L} \right], \\ H_4 &= C_F \frac{\alpha_s(\mu_0)}{4\pi} \frac{L - \sinh L \cosh L}{4 \sinh^3 L} \eta(n-2). \end{aligned} \tag{7.57}$$

At  $L \rightarrow 0$ ,  $H_1 + H_2 + H_3 + H_4$  reproduces (7.27).

In general, the integrals are

$$\begin{aligned} \int_{-1}^{+1} \frac{dz}{(a_+ a_-)^\varepsilon} &= 2 - 2\varepsilon \left( \frac{L \sinh L - \vartheta \sinh \vartheta}{\cosh L - \cosh \vartheta} - 2 \right) + \mathcal{O}(\varepsilon^2), \\ \int_{-1}^{+1} \frac{dz}{(a_+ a_-)^{1+\varepsilon}} &= 2 \frac{\vartheta + \varepsilon F(L, \vartheta)}{\sinh \vartheta} + \mathcal{O}(\varepsilon^2), \\ F(L, \vartheta) &= \text{Li}_2 \left( \frac{e^\vartheta - e^L}{e^\vartheta - e^{-\vartheta}} \right) - \text{Li}_2 \left( \frac{e^{-L} - e^{-\vartheta}}{e^\vartheta - e^{-\vartheta}} \right) \\ &\quad + (L + \vartheta) \log \frac{\sinh[(L + \vartheta)/2]}{\sinh \vartheta}, \\ \int_{-1}^{+1} \frac{z dz}{(a_+ a_-)^{1+\varepsilon}} &= 2 \frac{L \sinh \vartheta - \vartheta \sinh L}{\sinh \vartheta (\cosh L - \cosh \vartheta)} + \mathcal{O}(\varepsilon), \\ \int_{-1}^{+1} \frac{z^2 dz}{(a_+ a_-)^{1+\varepsilon}} &= \frac{2}{\cosh L - \cosh \vartheta} \left[ \frac{\vartheta}{\sinh \vartheta} \frac{\sinh^2 L + \sinh^2 \vartheta}{\cosh L - \cosh \vartheta} \right. \\ &\quad \left. - \frac{2L \sinh L}{\cosh L - \cosh \vartheta} + 2 \right] + \mathcal{O}(\varepsilon). \end{aligned}$$

The limiting cases considered previously are reproduced. In particular,  $F(L, L) = 0$ ,  $F(L, \vartheta) = 2\vartheta[L(\cosh L + 1)/(2 \sinh L) - 1] + \mathcal{O}(\vartheta^2)$  at  $\vartheta \rightarrow 0$ , and  $F(0, \vartheta) = F(\vartheta)$  (7.51).

It is most natural to perform matching at  $\mu = \mu' = \mu_0$  (7.32). For any other  $\mu, \mu'$ , the matching coefficients are determined by the renormalization group:

$$\begin{aligned} H_i(\mu, \mu') &= \hat{H}_i \left( \frac{\alpha_s(\mu)}{\alpha_s(\mu_0)} \right)^{\gamma_{jn0}/(2\beta_0)} K_{\gamma_{jn}}(\alpha_s(\mu)) \\ &\quad \times \left( \frac{\alpha'_s(\mu')}{\alpha'_s(\mu_0)} \right)^{-\tilde{\gamma}_{J0}/(2\beta'_0)} K'_{-\tilde{\gamma}_J}(\alpha'_s(\mu')) , \\ \hat{H}_i &= H_i(\mu_0, \mu_0) K_{-\gamma_{jn}}(\alpha_s(\mu_0)) K'_{\tilde{\gamma}_J}(\alpha'_s(\mu_0)) \end{aligned} \quad (7.58)$$

(see (4.72)). Using  $Z_Q^{\text{os}}$  (4.29),  $Z_J$  (5.8), and  $\tilde{Z}_J$  (7.6), we see that the  $1/\varepsilon$  poles cancel in  $H_i(\mu_0, \mu_0)$ :

$$\begin{aligned} H_1 &= 1 + H_4 + C_F \frac{\alpha_s(\mu_0)}{4\pi} \left[ \left( 3 - \frac{L \sinh L - \vartheta \sinh \vartheta}{\cosh L - \cosh \vartheta} \right) (n-2)^2 \right. \\ &\quad \left. + 2(n-2) + 2 \frac{L \sinh L - \vartheta \sinh \vartheta}{\cosh L - \cosh \vartheta} + 2\vartheta \coth \vartheta - 4 + 2F(L, \vartheta) \coth \vartheta \right] , \\ H_2 &= H_3(L \rightarrow -L) = C_F \frac{\alpha_s(\mu_0)}{4\pi} \left[ \left( \vartheta \frac{\sinh L + \cosh \vartheta - e^L \cosh^2 \vartheta}{\sinh \vartheta (\cosh L - \cosh \vartheta)} \right. \right. \\ &\quad \left. \left. + L \frac{e^L \cosh \vartheta - 1}{\cosh L - \cosh \vartheta} - e^L \right) \frac{\eta(n-2)}{2(\cosh L - \cosh \vartheta)} \right. \\ &\quad \left. + \left( \vartheta \frac{\cosh \vartheta - e^L}{\sinh \vartheta} + L \right) \frac{1}{\cosh L - \cosh \vartheta} \right] , \\ H_4 &= C_F \frac{\alpha_s(\mu_0)}{4\pi} \left[ 1 + \frac{\vartheta(\cosh L \cosh \vartheta - 1) - L \sinh L \sinh \vartheta}{\sinh \vartheta (\cosh L - \cosh \vartheta)} \right] \\ &\quad \times \frac{\eta(n-2)}{2(\cosh L - \cosh \vartheta)} . \end{aligned} \quad (7.59)$$

In the flavour-diagonal case ( $L = 0$ ), the result (7.52) is reproduced; at  $q^2 = 0$  ( $\vartheta \rightarrow L$ ), the formula (7.57) follows. At  $\vartheta \rightarrow 0$ ,  $H_1 + H_2 + H_3 + H_4$  reproduces (7.33).

In particular, for the vector and axial currents, we have [10]

$$\begin{aligned} H_1^V &= 1 + C_F \frac{\alpha_s(\mu_0)}{4\pi} \left[ \vartheta \frac{2 \cosh L (\cosh \vartheta + 1) - \cosh \vartheta (3 \cosh \vartheta + 2) + 1}{\sinh \vartheta (\cosh L - \cosh \vartheta)} \right. \\ &\quad \left. + \frac{L \sinh L}{\cosh L - \cosh \vartheta} - 4 + 2F(L, \vartheta) \coth \vartheta \right] , \end{aligned}$$

$$\begin{aligned}
H_2^V &= H_3^V(L \rightarrow -L) = C_F \frac{\alpha_s(\mu_0)}{4\pi} \left[ \frac{(e^L - 1) \sinh L}{(\cosh L - \cosh \vartheta)^2} \left( \frac{\vartheta \sinh L}{\sinh \vartheta} - L \right) \right. \\
&\quad + \frac{1}{\cosh L - \cosh \vartheta} \left( -\frac{\vartheta(2e^L + 3 + 3e^{-L})(e^L - 1)}{2 \sinh \vartheta} + L(e^L + 2) + e^L - 1 \right) \\
&\quad \left. + \frac{\vartheta(e^L - 2)}{\sinh \vartheta} \right], \\
H_1^A &= H_1^V - C_F \frac{\alpha_s(\mu_0)}{4\pi} \frac{4\vartheta}{\sinh \vartheta}, \\
H_2^A &= -H_3^A(L \rightarrow -L) = C_F \frac{\alpha_s(\mu_0)}{4\pi} \left[ \frac{(e^L + 1) \sinh L}{(\cosh L - \cosh \vartheta)^2} \left( \frac{\vartheta \sinh L}{\sinh \vartheta} - L \right) \right. \\
&\quad + \frac{1}{\cosh L - \cosh \vartheta} \left( -\frac{\vartheta(2e^L - 3 + 3e^{-L})(e^L + 1)}{2 \sinh \vartheta} + L(e^L - 2) + e^L + 1 \right) \\
&\quad \left. + \frac{\vartheta(e^L + 2)}{\sinh \vartheta} \right]. \tag{7.60}
\end{aligned}$$

The easiest way to see that  $H_1^V$  (7.60) (with two dilogarithms) is indeed equivalent to the result in [10] (with three dilogarithms) is to subtract the two results, differentiate the difference with respect to  $\vartheta$  and  $L$  (these derivatives simplify to 0), and compare the values at  $\vartheta \rightarrow 0$  and  $L \rightarrow 0$ .

As discussed in Sect. 7.3, the single-step matching of QCD currents onto HQET with both the  $b$  and the  $c$  considered static is good when  $r \sim 1$ , because it gives the exact dependence of the matching coefficients (for example, at one loop, as in (7.59) and (7.60)) on  $r$ . At  $r \ll 1$ , it is better to use the two-step matching. We are considering the QCD current  $J = \bar{c}\Gamma b$ , where  $\Gamma$  satisfies (5.5) ( $\Gamma$  may be the antisymmetrized product of  $n$   $\gamma$ -matrices, possibly multiplied by  $\gamma_5^{AC}$ ; see (7.26)). First we match it onto HQET-1, the effective theory with a static  $b$  and dynamic  $c$ , at  $m_b$ . To this end, we decompose  $\Gamma$  into components (6.3) commuting and anticommuting with  $\not{p}$ :

$$\begin{aligned}
J(m_b) &= C_+(m_b, \mu) \tilde{j}_+(\mu) + C_-(m_b, \mu) \tilde{j}_-(\mu) \\
&\quad + \frac{1}{2m_b} \sum_i B_i(m_b, \mu) \not{\partial}_i(\mu) + \dots, \\
\tilde{j}_\pm &= \bar{c} \frac{1 \pm \not{p}}{2} \Gamma \tilde{b}_v \tag{7.61}
\end{aligned}$$

(see (5.57)). The running is given by (5.58), with  $n_i$  flavours in HQET-1. Finally, we match these operators onto HQET-2, where both the  $b$  and the  $c$  are considered static, at  $m_c$ :

$$\begin{aligned}
\tilde{j}_\pm(m_c) &= E_\pm(m_c) \tilde{J}_\pm(m_c) + \mathcal{O}(1/m_c), \\
\not{\partial}_i(m_c) &= m_c \sum_j F_{ij}(m_c) \tilde{J}_j(m_c) + \mathcal{O}(m_c^0). \tag{7.62}
\end{aligned}$$

We obtain (see (7.20))

$$\begin{aligned} H_{1,2}(m_b, m_c) &= \frac{1}{2} [C_+(m_b, m_c) E_+(m_c) \pm C_-(m_b, m_c) E_-(m_c)] + \mathcal{O}(r), \\ H_{3,4}(m_b, m_c) &= \mathcal{O}(r). \end{aligned} \quad (7.63)$$

With this method, we obtain only a few terms in expansion in  $r = m_c/m_b$ ; on the other hand, the leading (and next-to-leading, etc.) logarithmic terms (in  $L = -\log r$ ) can be summed.

In order to match the HQET-1 current  $\tilde{j} = \tilde{Z}_j^{-1} \bar{c}_0 \Gamma \tilde{b}_{v0}$  onto HQET-2, we calculate its on-shell matrix element from b with residual momentum  $\tilde{p} = 0$  to c with momentum  $m_c v'$ :  $\tilde{Z}_j^{-1} (\tilde{Z}_c^{\text{os}} \tilde{Z}_b^{\text{os}})^{1/2} \cdot \bar{u} \tilde{\Gamma}_1(m_c v', 0) u_v$ . This matrix element should be equal to  $E_\Gamma$  times the corresponding matrix element of the HQET-2 current  $\tilde{J} = \tilde{Z}_j^{-1} (\cosh \vartheta) \bar{c}_{v'0} \Gamma \tilde{b}_{v0}$ , which is  $\tilde{Z}_j^{-1} (\cosh \vartheta) (\tilde{Z}_c^{\text{os}} \tilde{Z}_b^{\text{os}})^{1/2} \cdot \bar{u}_{v'} \tilde{\Gamma}_2(0, 0) u_v$ . All loop corrections in HQET-2 vanish:  $\tilde{\Gamma}_2(0, 0) = 1$ ,  $\tilde{Z}_c^{\text{os}} = \tilde{Z}_b^{\text{os}} = 1$  (unless there is a massive flavour lighter than c; then corrections will start from two loops). The HQET-1 vertex  $\tilde{\Gamma}_1$  can only contain  $\gamma$ -matrices to the left of  $\Gamma$ , owing to the HQET Feynman rules. We can anticommutate  $\not{p}'$  to the left, where it disappears. If  $\Gamma$  either commutes or anticommutes with  $\not{p}$ , then  $\bar{u} \tilde{\Gamma}_1(m_c v', 0) u_v = \bar{u} \Gamma u_v \cdot \tilde{\Gamma}_\pm(m_c^2)$ . Therefore, just one HQET-2 current appears, as shown in (7.62).

At one loop (Fig. 7.6),

$$\tilde{\Gamma}_1(m_c v', 0) = \left[ 1 - i C_F g_0^2 \int \frac{d^d k}{(2\pi)^d} \frac{\not{k} + m_c \not{p}' + m_c}{[m_c^2 - (k + m_c v')^2] (k \cdot v) (-k^2)} \right] \Gamma.$$

Using both the usual (2.13) and the HQET (2.23) Feynman parametrization, this vertex can be rewritten as

$$\begin{aligned} 1 + 4i C_F g_0^2 \int dx dy \frac{d^d k}{(2\pi)^d} \frac{\not{k}' + m_c(1-x)\not{p}' - y\not{p} + m_c}{(-k'^2 + a^2)^3}, \\ k' = k + mxv' + yv, \quad a^2 = (mxv' + yv)^2. \end{aligned}$$

Now we take the  $k'$  integral (2.16); the  $\not{k}'$  term vanishes, and we obtain the following for  $\Gamma_\pm$ :

$$1 + 2C_F \frac{g_0^2}{(4\pi)^{d/2}} \Gamma(1+\varepsilon) \int_0^\infty dy \int_0^1 dx \frac{y - 2m_c(1-x)\cosh \vartheta \mp m_c x}{(y^2 + m_c^2 x^2 + 2m_c x y \cosh \vartheta)^{1+\varepsilon}}.$$

After the substitution  $y = m_c x z$ , the  $x$  integration is trivial:

$$\begin{aligned} \Gamma_\pm &= 1 + 2C_F \frac{g_0^2 m_c^{-2\varepsilon}}{(4\pi)^{d/2}} \Gamma(1+\varepsilon) \int_0^\infty \frac{dz}{(z^2 + 1 + 2z \cosh \vartheta)^{1+\varepsilon}} \\ &\quad \times \left[ \frac{z + 2 \cosh \vartheta \mp 1}{1 - 2\varepsilon} + \frac{\cosh \vartheta}{\varepsilon} \right]. \end{aligned}$$

When  $\vartheta = 0$ , the integral is easily calculated;  $\Gamma$  must commute with  $\psi$  (the upper sign), and (7.42) is reproduced.

We need two integrals with respect to  $z$ . The first one is convergent, and needed with  $\mathcal{O}(\varepsilon)$  accuracy:

$$\begin{aligned} & \int_0^\infty \frac{dz}{(z^2 + 1 + 2z \cosh \vartheta)^{1+\varepsilon}} \\ &= \frac{1}{\sinh \vartheta} \left[ \vartheta + \frac{\varepsilon}{2} (\text{Li}_2(1 - e^{2\vartheta}) - \text{Li}_2(1 - e^{-2\vartheta})) \right] + \mathcal{O}(\varepsilon^2). \end{aligned}$$

It has been written in a form explicitly even in  $\vartheta$ ; owing to (7.16), it can be expressed via a single dilogarithm. The second integral,

$$\int_0^\infty \frac{z dz}{(z^2 + 1 + 2z \cosh \vartheta)^{1+\varepsilon}},$$

is UV divergent at  $\varepsilon = 0$ . We split the integration region into two parts: from 0 to  $A \gg 1$  and from  $A$  to  $\infty$ . In the first region, we may neglect  $\varepsilon$ :

$$\int_0^A \frac{z dz}{z^2 + 1 + 2z \cosh \vartheta} = \log A - \vartheta \coth \vartheta.$$

In the second region, we may neglect 1 as compared with  $z$ :

$$\int_A^\infty \frac{dz}{z^{1+2\varepsilon}} = \frac{1}{2\varepsilon} - \log A.$$

In the sum,  $\log A$  cancels, as expected:

$$\int_0^\infty \frac{z dz}{(z^2 + 1 + 2z \cosh \vartheta)^{1+\varepsilon}} = \frac{1}{2\varepsilon} - \vartheta \coth \vartheta + \mathcal{O}(\varepsilon).$$

Substituting these integrals, we find the vertex

$$\begin{aligned} \tilde{\Gamma}_\pm &= 1 + C_F \frac{\alpha_s''(m_c)}{4\pi} \left[ \frac{2\vartheta \coth \vartheta + 1}{\varepsilon} + 2\vartheta \coth \vartheta + 2 \mp \frac{2\vartheta}{\sinh \vartheta} \right. \\ &\quad \left. + (\text{Li}_2(1 - e^{2\vartheta}) - \text{Li}_2(1 - e^{-2\vartheta})) \coth \vartheta \right]. \end{aligned}$$

The matching constants  $E_\pm = (\tilde{Z}_J / \tilde{Z}_j)(Z_c^{\text{os}})^{1/2} \tilde{\Gamma}_\pm$  are finite [10]:

$$\begin{aligned} E_\pm(m_c) &= 1 + C_F \frac{\alpha_s''(m_c)}{4\pi} \left[ 2\vartheta \coth \vartheta \mp \frac{2\vartheta}{\sinh \vartheta} \right. \\ &\quad \left. + (\text{Li}_2(1 - e^{2\vartheta}) - \text{Li}_2(1 - e^{-2\vartheta})) \coth \vartheta \right]. \end{aligned} \tag{7.64}$$

The upper sign is for  $\Gamma$  commuting with  $\psi$ , and the lower sign is for  $\Gamma$  anticommuting with  $\psi$ . At  $\vartheta = 0$ ,  $E_+(m_c)$  reproduces (7.43).

Collecting all the pieces together, we have the following [10] for  $H_i^{\text{V,A}}(m_b, m_c)$  at  $\mathcal{O}(r^0)$ :

$$\begin{aligned}
H_1^{\text{V}} &= x^{\tilde{\gamma}_{j0}} \left[ 1 - 4C_F \frac{\alpha_s''(m_b)}{4\pi} \right. \\
&\quad + C_F \left( 2\vartheta \coth \frac{\vartheta}{2} + (\text{Li}_2(1 - e^{2\vartheta}) - \text{Li}_2(1 - e^{-2\vartheta})) \coth \vartheta \right) \frac{\alpha_s''(m_c)}{4\pi} \\
&\quad \left. + \frac{\tilde{\gamma}_{j0}}{2\beta_0''} \left( \frac{\tilde{\gamma}_{j1}}{\tilde{\gamma}_{j0}} - \frac{\beta_1''}{\beta_0''} \right) \frac{\alpha_s''(m_b) - \alpha_s''(m_c)}{4\pi} \right], \\
H_2^{\text{V}} &= 2C_F x^{\tilde{\gamma}_{j0}} \left[ \frac{\alpha_s''(m_b)}{4\pi} - \frac{2\vartheta}{\sinh \vartheta} \frac{\alpha_s''(m_c)}{4\pi} \right], \quad H_3^{\text{V}} = 0, \\
H_1^{\text{A}} &= x^{\tilde{\gamma}_{j0}} \left[ 1 - 4C_F \frac{\alpha_s''(m_b)}{4\pi} \right. \\
&\quad + C_F \left( 2\vartheta \tanh \frac{\vartheta}{2} + (\text{Li}_2(1 - e^{2\vartheta}) - \text{Li}_2(1 - e^{-2\vartheta})) \coth \vartheta \right) \frac{\alpha_s''(m_c)}{4\pi} \\
&\quad \left. + \frac{\tilde{\gamma}_{j0}}{2\beta_0''} \left( \frac{\tilde{\gamma}_{j1}}{\tilde{\gamma}_{j0}} - \frac{\beta_1''}{\beta_0''} \right) \frac{\alpha_s''(m_b) - \alpha_s''(m_c)}{4\pi} \right], \\
H_2^{\text{A}} &= 2C_F x^{\tilde{\gamma}_{j0}} \left[ \frac{\alpha_s''(m_b)}{4\pi} + \frac{2\vartheta}{\sinh \vartheta} \frac{\alpha_s''(m_c)}{4\pi} \right], \quad H_3^{\text{A}} = 0. \tag{7.65}
\end{aligned}$$

These results, expanded up to  $\mathcal{O}(\alpha_s)$ , reproduce  $H_i^{\text{V,A}}(m_b, m_c)$  (7.58) (also expanded up to  $\mathcal{O}(\alpha_s)$ ) with  $H_i^{\text{V,A}}(\mu_0, \mu_0)$  (7.60), where

$$F(L, \vartheta) = \frac{1}{2} [\text{Li}_2(1 - e^{2\vartheta}) - \text{Li}_2(1 - e^{-2\vartheta})] + L\vartheta + \mathcal{O}(r), \quad r = e^{-L}.$$

At  $\vartheta \rightarrow 0$ ,  $H_1^{\text{V}} + H_2^{\text{V}} + H_3^{\text{V}}$  (7.65) reproduces  $H_{\gamma^0}$  (7.44), and  $H_1^{\text{A}}$  (7.65) reproduces  $H_{\gamma_5^{\text{AC}}\gamma}$  (7.44).

Now we shall discuss the  $\mathcal{O}(r)$  terms in the LLA [3]. For the vector current  $J^\alpha = \bar{c}\gamma^\alpha b$ , the  $1/m_b$  term in (7.61) is

$$\frac{1}{2m_b} \left[ v^\alpha \sum_i B_i^p(m_b, \mu) \mathcal{O}_i(\mu) + \sum_i B^{\gamma\perp}(m_b, \mu) \mathcal{O}_i^\alpha(\mu) \right].$$

Only  $\mathcal{O}_{2,3}$  (6.43) and  $\mathcal{O}_{3,4,5}^\alpha$  (6.66) produce  $\mathcal{O}(m_c)$  contributions; at the tree level, we may replace  $-i\overleftrightarrow{D}$  by  $m_c v'$ :

$$\begin{aligned}
\mathcal{O}_2(m_c) &= m_c \tilde{J}(m_c) \cosh \vartheta, \quad \mathcal{O}_3(m_c) = m_c \tilde{J}(m_c), \\
\mathcal{O}_3^\alpha(m_c) &= m_c \tilde{J}(m_c)(v'^\alpha - v^\alpha \cosh \vartheta), \\
\mathcal{O}_4^\alpha(m_c) &= m_c \left( \tilde{J}^\alpha(m_c) - \tilde{J}(m_c)v^\alpha \right) \cosh \vartheta, \\
\mathcal{O}_5^\alpha(m_c) &= m_c \left( \tilde{J}^\alpha(m_c) - \tilde{J}(m_c)v^\alpha \right), \tag{7.66}
\end{aligned}$$

where  $\tilde{J} = \bar{\tilde{c}}_{v'} \tilde{b}_v$ ,  $\tilde{J}^\alpha = \bar{\tilde{c}}_{v'} \gamma^\alpha \tilde{b}_v$ . For the axial current  $J^\alpha = \bar{c} \gamma_5^{\text{AC}} \gamma^\alpha b$ , the operators  $\mathcal{O}_i$  and  $\mathcal{O}_i^\alpha$  are obtained from (6.43) and (6.66) by  $\bar{c} \rightarrow \bar{c} \gamma_5^{\text{AC}}$  and  $m_c \rightarrow -m_c$ , and the matching coefficients remain unchanged:

$$B_i^{\gamma_5^{\text{AC}} p} = B_i^p, \quad B_i^{\gamma_5^{\text{AC}} \gamma^\perp} = B_i^{\gamma^\perp}.$$

Therefore,

$$\begin{aligned} H_1^{\text{V,A}}(m_b, m_c) - H_1^{\text{V,A}}(m_b, m_c) \Big|_{\mathcal{O}(r^0)} \\ = \frac{r}{2} \left( B_4^{\gamma^\perp}(m_b, m_c) \cosh \vartheta \pm B_5^{\gamma^\perp}(m_b, m_c) \right) \\ = ry^{-2} \left[ \left( -\frac{8}{3} \log y + \frac{5}{9} - \frac{5}{9}y^2 - \frac{2}{27}y^3 + \frac{2}{27}y^4 \right) \cosh \vartheta \right. \\ \left. \pm \left( \frac{1}{3} - \frac{5}{9}y^2 + \frac{4}{9}y^3 - \frac{2}{9}y^4 \right) \right], \\ H_2^{\text{V,A}}(m_b, m_c) - H_2^{\text{V,A}}(m_b, m_c) \Big|_{\mathcal{O}(r^0)} \\ = \frac{r}{2} \left[ \left( B_2^p(m_b, m_c) - B_3^{\gamma^\perp}(m_b, m_c) - B_4^{\gamma^\perp}(m_b, m_c) \right) \cosh \vartheta \right. \\ \left. \pm \left( B_3^p(m_b, m_c) - B_5^{\gamma^\perp}(m_b, m_c) \right) \right] \\ = ry^{-2} \left[ \left( -\frac{4}{9} - \frac{10}{9}y^2 + \frac{44}{27}y^3 - \frac{2}{27}y^4 \right) \cosh \vartheta \right. \\ \left. \pm \left( \frac{5}{9}y^2 + \frac{20}{9}y^3 - \frac{25}{9}y^4 \right) \right], \\ H_3^{\text{V,A}}(m_b, m_c) = \frac{r}{2} B_3^{\gamma^\perp}(m_b, m_c) = ry^{-2} \left( -1 + \frac{5}{3}y^2 - \frac{2}{3}y^3 \right) \end{aligned} \quad (7.67)$$

(see (7.47)). At  $\vartheta \rightarrow 0$ , the  $\mathcal{O}(r)$  term in  $H_1^{\text{V}} + H_2^{\text{V}} + H_3^{\text{V}}$  (7.47) reproduces (7.47), and  $H_1^{\text{A}}$  (7.47) reproduces (7.49).

The results of these two approaches can be combined [10]. We take the single-step matching results (7.58) and (7.60), express them via  $\alpha_s(\mu_0)$ , and retain only terms up to  $\alpha_s(\mu_0)$ . These results contain all powers of  $r$ . Then we take the two-step matching results (7.65), and subtract from them the terms of order  $\alpha_s(\mu_0)$ , which are already accounted for. By adding this difference, we take into account an infinite sequence of radiative corrections of order  $\mathcal{O}(r^0)$  with leading and next-to-leading powers of the logarithm  $L$ . Similarly, we take the  $\mathcal{O}(r)$  two-step matching results (7.67), and subtract from them the terms of order  $\alpha_s(\mu_0)$ , which are already accounted for. By adding this difference, we take into account corrections of order  $\mathcal{O}(r)$  with leading powers of  $L$  at all orders in  $\alpha_s$ .

## 7.6 $1/m$ Corrections

There are two kinds of operators  $\mathcal{O}_i$  in (7.1): local (having the structure  $\bar{\tilde{c}}_{v'} D \tilde{b}_v$ ), and bilocal,

$$i \int dx T \left\{ \tilde{J}_i(0), \mathcal{O}_{k,m}^b(x) \right\},$$

where  $\mathcal{O}_{k,m}^b$  are the b-quark kinetic energy and chromomagnetic interaction. Similarly, the operators  $\mathcal{O}'_i$  are local ( $\bar{\tilde{c}}_{v'} \overleftrightarrow{D} \tilde{b}_v$ ) or bilocal, containing  $\mathcal{O}_{k,m}^c$ . The coefficients of the bilocal operators are just the leading-order coefficients  $H_i$  times the coefficients of  $\mathcal{O}_{k,m}$  in the Lagrangian (1 and  $C_m$ ).

The coefficients of the local operators  $\bar{\tilde{c}}_{v'} D \tilde{b}_v$  and  $\bar{\tilde{c}}_{v'} \overleftrightarrow{D} \tilde{b}_v$  are completely determined by reparametrization invariance [11]. The leading-order expression (7.21) is not reparametrization-invariant. Instead of  $v$  and  $v'$ , one should use the operators (6.6)

$$\mathcal{V} = v + \frac{iD}{m_b}, \quad \mathcal{V}'^+ = v' - \frac{i\overleftrightarrow{D}}{m_c}. \quad (7.68)$$

Instead of  $\tilde{b}_v$  and  $\bar{\tilde{c}}_{v'}$ , one should use (6.7)

$$\tilde{b}_{\mathcal{V}} = \left( 1 + \frac{i\cancel{D}}{2m_b} \right) \tilde{b}_v, \quad \bar{\tilde{c}}_{\mathcal{V}'} = \bar{\tilde{c}}_{v'} \left( 1 - \frac{i\overleftrightarrow{D}}{2m_c} \right). \quad (7.69)$$

Finally, the argument  $v \cdot v'$  of  $H_i$  should be replaced by

$$\mathcal{V} \cdot \mathcal{V}'^+ = v \cdot v' + \frac{iv' \cdot D}{m_b} - \frac{iv \cdot \overleftrightarrow{D}}{m_c}. \quad (7.70)$$

Then (7.21) becomes a reparametrization-invariant combination

$$\begin{aligned} & \bar{\tilde{c}}_{v'} [H_1 \Gamma + H_2 \not{\Gamma} + H_3 \Gamma \not{\psi} + H_4 \not{\psi} \Gamma \not{\psi}] \tilde{b}_v \\ & + \frac{1}{2m_b} \bar{\tilde{c}}_{v'} \left[ (H_1 \Gamma + H_2 \not{\Gamma} + H_3 \Gamma \not{\psi} + H_4 \not{\psi} \Gamma \not{\psi}) i \cancel{D} \right. \\ & \quad + 2i\cancel{D} (H_2 \Gamma + H_4 \Gamma \not{\psi}) \\ & \quad + 2(H'_1 \Gamma + H'_2 \not{\Gamma} + H'_3 \Gamma \not{\psi} + H'_4 \not{\psi} \Gamma \not{\psi}) iv' \cdot D \left. \right] \tilde{b}_v \\ & + \frac{1}{2m_c} \bar{\tilde{c}}_{v'} \left[ (-i) \overleftrightarrow{D} (H_1 \Gamma + H_2 \not{\Gamma} + H_3 \Gamma \not{\psi} + H_4 \not{\psi} \Gamma \not{\psi}) \right. \\ & \quad + 2(H_3 \Gamma + H_4 \not{\psi} \Gamma) (-i) \overleftrightarrow{D} \\ & \quad + 2(-i)v \cdot \overleftrightarrow{D} (H'_1 \Gamma + H'_2 \not{\Gamma} + H'_3 \Gamma \not{\psi} + H'_4 \not{\psi} \Gamma \not{\psi}) \left. \right] \tilde{b}_v, \end{aligned} \quad (7.71)$$

where the  $H'_i$  are derivatives of  $H_i$  with respect to the argument  $v \cdot v'$ . Operators of the form  $\bar{c}_{v'} D\tilde{b}_v$ ,  $\bar{c}_{v'} \tilde{D}\tilde{b}_v$  are not reparametrization-invariant separately, and can only appear in this combination.

In particular, for the vector current (7.22), we have [11]

$$\begin{aligned} J^\alpha &= H_1^V \tilde{J}_1^\alpha + H_2^V \tilde{J}_2^\alpha + H_3^V \tilde{J}_3^\alpha \\ &+ \frac{1}{2m_b} (H_1^V \mathcal{O}_1^\alpha + H_2^V \mathcal{O}_2^\alpha + H_3^V \mathcal{O}_3^\alpha + 2H_2^V \mathcal{O}_4^\alpha \\ &\quad + 2H_1^{V'} \mathcal{O}_5^\alpha + 2H_2^{V'} \mathcal{O}_6^\alpha + 2H_3^{V'} \mathcal{O}_7^\alpha) \\ &+ \frac{1}{2m_c} (H_1^V \mathcal{O}'_1^\alpha + H_2^V \mathcal{O}'_2^\alpha + H_3^V \mathcal{O}'_3^\alpha + 2H_3^V \mathcal{O}'_4^\alpha \\ &\quad + 2H_1^{V'} \mathcal{O}'_5^\alpha + 2H_2^{V'} \mathcal{O}'_6^\alpha + 2H_3^{V'} \mathcal{O}'_7^\alpha) \\ &+ (\text{bilocal terms}) + \mathcal{O}(1/m_{c,b}^2), \end{aligned} \quad (7.72)$$

where

$$\begin{aligned} J^\alpha &= \bar{c} \gamma^\alpha b, \\ \tilde{J}_1^\alpha &= \bar{\tilde{c}}_{v'} \gamma^\alpha \tilde{b}_v, \quad \tilde{J}_2^\alpha = \bar{\tilde{c}}_{v'} v^\alpha \tilde{b}_v, \quad \tilde{J}_3^\alpha = \bar{\tilde{c}}_{v'} v'^\alpha \tilde{b}_v, \\ \mathcal{O}_1^\alpha &= \bar{\tilde{c}}_{v'} \gamma^\alpha i \not{D} \tilde{b}_v, \quad \mathcal{O}_2^\alpha = \bar{\tilde{c}}_{v'} v^\alpha i \not{D} \tilde{b}_v, \quad \mathcal{O}_3^\alpha = \bar{\tilde{c}}_{v'} v'^\alpha i \not{D} \tilde{b}_v, \\ \mathcal{O}_4^\alpha &= \bar{\tilde{c}}_{v'} i D^\alpha \tilde{b}_v, \\ \mathcal{O}_5^\alpha &= \bar{\tilde{c}}_{v'} \gamma^\alpha i v' \cdot D\tilde{b}_v = v' \cdot \partial \tilde{J}_1^\alpha, \\ \mathcal{O}_6^\alpha &= \bar{\tilde{c}}_{v'} v^\alpha i v' \cdot D\tilde{b}_v = v' \cdot \partial \tilde{J}_2^\alpha, \\ \mathcal{O}_7^\alpha &= \bar{\tilde{c}}_{v'} v'^\alpha i v' \cdot D\tilde{b}_v = v' \cdot \partial \tilde{J}_3^\alpha, \\ \mathcal{O}'_1^\alpha &= \bar{\tilde{c}}_{v'} (-i) \not{\overleftarrow{D}} \gamma^\alpha \tilde{b}_v, \quad \mathcal{O}'_2^\alpha = \bar{\tilde{c}}_{v'} (-i) \not{\overleftarrow{D}} v^\alpha \tilde{b}_v, \quad \mathcal{O}'_3^\alpha = \bar{\tilde{c}}_{v'} (-i) \not{\overleftarrow{D}} v'^\alpha \tilde{b}_v, \\ \mathcal{O}'_4^\alpha &= \bar{\tilde{c}}_{v'} (-i) \not{\overleftarrow{D}}^\alpha \tilde{b}_v, \\ \mathcal{O}'_5^\alpha &= \bar{\tilde{c}}_{v'} (-i) v \cdot \not{\overleftarrow{D}} \gamma^\alpha \tilde{b}_v = -iv \cdot \partial \tilde{J}_1, \\ \mathcal{O}'_6^\alpha &= \bar{\tilde{c}}_{v'} (-i) v \cdot \not{\overleftarrow{D}} v^\alpha \tilde{b}_v = -iv \cdot \partial \tilde{J}_2, \\ \mathcal{O}'_7^\alpha &= \bar{\tilde{c}}_{v'} (-i) v \cdot \not{\overleftarrow{D}} v'^\alpha \tilde{b}_v = -iv \cdot \partial \tilde{J}_3. \end{aligned}$$

Similar formulae hold for the axial current.

If we are interested in matrix elements of  $J^\alpha$  from the ground-state B-meson to the ground-state D or  $D^*$ -meson, we can easily calculate the matrix elements of operators which are full derivatives. Their effect is to replace  $\cosh \vartheta = v_B \cdot v_D$  in the argument of  $H_i^V$  in the leading-order terms by the new variable

$$\cosh \bar{\vartheta} = v_B \cdot v_D + \bar{\Lambda} \left( \frac{1}{m_c} + \frac{1}{m_b} \right) (v_B \cdot v_D - 1). \quad (7.73)$$

With this improved angular variable, the vector current  $J^\alpha$  is equivalent to

$$\begin{aligned}
& H_1^V(\cosh \bar{\vartheta}) \left( \tilde{J}_1^\alpha + \frac{\mathcal{O}_1^\alpha}{2m_b} + \frac{\mathcal{O}'_1^\alpha}{2m_c} \right) \\
& + H_2^V(\cosh \bar{\vartheta}) \left( \tilde{J}_2^\alpha + \frac{\mathcal{O}_2^\alpha + 2\mathcal{O}_4^\alpha}{2m_b} + \frac{\mathcal{O}'_2^\alpha}{2m_c} \right) \\
& + H_3^V(\cosh \bar{\vartheta}) \left( \tilde{J}_3^\alpha + \frac{\mathcal{O}_3^\alpha}{2m_b} + \frac{\mathcal{O}'_3^\alpha + 2\mathcal{O}'_4^\alpha}{2m_c} \right) \\
& + (\text{bilocal terms}) + \mathcal{O}(1/m_{c,b}^2), \tag{7.74}
\end{aligned}$$

when only matrix elements between ground-state mesons are considered. Of course, similar formulae hold for the axial current.

## References

1. A. Czarnecki: Phys. Rev. Lett. **76**, 4124 (1996) [155](#), [156](#)
2. A. Czarnecki, K. Melnikov: Nucl. Phys. B **505**, 65 (1997) [156](#), [157](#), [160](#)
3. A.F. Falk, B. Grinstein: Phys. Lett. B **247**, 406 (1990) [159](#), [169](#)
4. A.F. Falk, B. Grinstein: Phys. Lett. B **249**, 314 (1990) [161](#), [162](#)
5. J. Franzkowski, J.B. Tausk: Eur. Phys. J. C **5**, 517 (1998) [156](#)
6. J. Frenkel, J.C. Taylor: Nucl. Phys. B **246**, 231 (1984) [149](#)
7. J.G.M. Gatheral: Phys. Lett. B **133**, 90 (1983) [149](#)
8. G.P. Korchemsky: Mod. Phys. Lett. A **4**, 1257 (1989) [150](#)
9. G.P. Korchemsky, A.V. Radyushkin: Nucl. Phys. B **283**, 342 (1987) [145](#), [150](#), [151](#)
10. M. Neubert: Phys. Rev. D **46**, 2212 (1992) [162](#), [165](#), [166](#), [168](#), [169](#), [170](#)
11. M. Neubert: Phys. Lett. B **306**, 357 (1993) [171](#), [172](#)
12. A.M. Polyakov: Nucl. Phys. B **164**, 171 (1980) [146](#)

# 8 Renormalons in HQET

It is well known that perturbative series do not converge. They are asymptotic series, i.e., the difference between the exact result and its approximation up to the order  $\alpha_s^L$ , divided by  $\alpha_s^L$ , tends to 0 in the limit  $\alpha_s \rightarrow 0$ . The large-order behaviour of various perturbative series has attracted considerable attention during recent years. Most of the results obtained so far are model-dependent: they are derived in the large- $\beta_0$  limit, i.e., at  $n_f \rightarrow -\infty$ . There are some hints that the situation in real QCD may be not too different from this limit, but this cannot be proved. However, a few results are rigorous consequences of QCD. They are based on the renormalization group; see [14, 4]. In this chapter, we shall discuss some simple technical methods used for calculations in the large- $\beta_0$  limit. Several applications in HQET will be considered in detail. Many more applications are discussed in the excellent review [2], where additional references can be found.

## 8.1 Large- $\beta_0$ Limit

Let us consider a perturbative quantity  $A$  such that the tree diagram for it contains no gluon propagators. We can always normalize the tree value of  $A$  to be 1. Then the perturbative series for the bare quantity  $A_0$  has the form

$$A_0 = 1 + \sum_{L=1}^{\infty} \sum_{n=0}^{L-1} a'_{Ln} n_f^n \left( \frac{g_0^2}{(4\pi)^{d/2}} \right)^L, \quad (8.1)$$

where  $L$  is the number of loops. This series can be rewritten in terms of  $\beta_0 = (11/3)C_A - (4/3)T_F n_f$  instead of  $n_f$ :

$$A_0 = 1 + \sum_{L=1}^{\infty} \sum_{n=0}^{L-1} a_{Ln} \beta_0^n \left( \frac{g_0^2}{(4\pi)^{d/2}} \right)^L. \quad (8.2)$$

Now we are going to consider  $\beta_0$  as a large parameter such that  $\beta_0 \alpha_s \sim 1$ , and consider only a few terms in the expansion in  $1/\beta_0 \sim \alpha_s$ :

$$A_0 = 1 + \frac{1}{\beta_0} f \left( \frac{\beta_0 g_0^2}{(4\pi)^{d/2}} \right) + \mathcal{O} \left( \frac{1}{\beta_0^2} \right). \quad (8.3)$$

This regime is called large- $\beta_0$  limit, and can only hold in QCD with  $n_f \rightarrow -\infty$ . Note that it has nothing in common with the large- $N_c$  limit, because we cannot control the powers of  $N_c$  in the coefficients  $a_{Ln}$ .

There is some empirical evidence [7] that the two-loop coefficients  $a_{21}\beta_0 + a_{20}$  for many quantities are well approximated by  $a_{21}\beta_0$ . It is easy to find  $a'_{21}$  from a diagram with a quark-loop insertion into a gluon propagator in the one-loop correction. Then we can estimate the full two-loop coefficient as  $a_{21}\beta_0 = a'_{21}(n_f - (11/4)(C_A/T_F))$ . This is called naive nonabelianization [7]. Of course, there is no guarantee that this will hold at higher orders. We can only hope that higher perturbative corrections are mainly due to the running of  $\alpha_s$ ; in this respect, gluonic contributions behave as  $-33/2$  flavours, and QCD with  $n_f = 3$  or 4 flavours is not too different from QCD with  $-\infty$  flavours.

It is easy to find the coefficients  $a_{L,L-1}$  of the highest degree,  $\beta_0^{L-1}$ , at  $L$  loops. They are determined by the coefficients  $a'_{L,L-1}$  of  $n_f^{L-1}$ , i.e., by inserting  $L-1$  quark loops into the gluon propagator in the one-loop correction. We shall assume for now that there is only one gluon propagator and there are no three-gluon vertices at one loop. The bare gluon propagator with  $L-1$  quark loops inserted is (see (3.27))

$$\begin{aligned} D_{\mu\nu}^{(L-1)}(p) &= -\frac{1}{(-p^2)^{1+(L-1)\varepsilon}} \left( g_{\mu\nu} + \frac{p_\mu p_\nu}{-p^2} \right) \\ &\quad \times \left( -\frac{4}{3} T_F n_f \frac{g_0^2}{(4\pi)^{d/2}} \frac{D(\varepsilon)}{\varepsilon} e^{-\gamma\varepsilon} \right)^{L-1}, \\ D(\varepsilon) &= 6e^{\gamma\varepsilon} \Gamma(1+\varepsilon) B(2-\varepsilon, 2-\varepsilon) = 1 + \frac{5}{3}\varepsilon + \dots \end{aligned} \quad (8.4)$$

This propagator looks like the free propagator in the Landau gauge  $a_0 = 0$ , with a shifted power of  $-p^2$  (and an extra constant factor). Let the one-loop contribution to  $A_0$  be  $(a_1 + a'_1 a_0) g_0^2 / (4\pi)^{d/2}$ . If we calculate the one-loop contribution in the Landau gauge  $a_1$  with the denominator of the gluon propagator equal to  $(-p^2)^n$  instead of just  $-p^2$  and call it  $a_1(n)$ , then for all  $L > 1$ ,

$$a_{L,L-1} = \left( \frac{D(\varepsilon)}{\varepsilon} e^{-\gamma\varepsilon} \right)^{L-1} a_1(1 + (L-1)\varepsilon). \quad (8.5)$$

Only the one-loop contribution  $a_{10}$  contains the additional gauge-dependent term  $a'_1 a_0$ .

The large- $\beta_0$  limit, as formulated above, does not correspond to summation of any subset of diagrams. If we include not only quark loops, but also gluon and ghost ones (Fig. 3.2), then  $-(4/3)T_F n_f$  in (8.4) is replaced by

$$-\frac{4}{3}P = \beta_0 - \frac{C_A}{3} \left\{ 8\varepsilon + \frac{3-2\varepsilon}{2(1-\varepsilon)} (a_0 + 3) \left[ 1 - \frac{\varepsilon}{2}(a_0 + 3) \right] \right\} \quad (8.6)$$

(see (3.28)). Summing these diagrams yields a gauge-dependent result. This gauge dependence is compensated (for a gauge-invariant  $A_0$ ) by other diagrams, which have more complicated topologies than a simple chain, and are impossible to sum. In the gauge  $a_0 = -3$ , the one-loop running of  $\alpha_s$  is produced by one-loop insertions into the gluon propagator (Fig. 3.2) only, without vertex contributions. Summation of chains of one-loop insertions into the gluon propagator in this gauge is equivalent to the large- $\beta_0$  limit.

In the large- $\beta_0$  limit,  $\beta_1 \sim \beta_0$ ,  $\beta_2 \sim \beta_0^2$ , etc. Therefore, the  $\beta$ -function is equal to

$$\beta = \frac{\beta_0 \alpha_s}{4\pi} \quad (8.7)$$

(this term is of order 1) plus  $\mathcal{O}(1/\beta_0)$  corrections. At the leading order in  $1/\beta_0$ , the renormalization-group equation

$$\frac{d \log Z_\alpha}{d \beta} = -\frac{\beta}{\varepsilon + \beta} \quad (8.8)$$

(see (3.7)) can be explicitly integrated:

$$Z_\alpha = \frac{1}{1 + \beta/\varepsilon}. \quad (8.9)$$

To the leading order in  $1/\beta_0$ ,

$$\alpha_s(\mu) = \frac{2\pi}{\beta_0 \log(\mu/A_{\overline{\text{MS}}})}. \quad (8.10)$$

The perturbative series (8.2) can be rewritten (in the Landau gauge) via the renormalized quantities:

$$A_0 = 1 + \frac{1}{\beta_0} \sum_{L=1}^{\infty} \frac{F(\varepsilon, L\varepsilon)}{L} \left( \frac{\beta}{\varepsilon + \beta} \right)^L + \mathcal{O}\left(\frac{1}{\beta_0^2}\right), \quad (8.11)$$

where

$$F(\varepsilon, u) = ue^{\gamma\varepsilon} a_1 (1 + u - \varepsilon) \mu^{2u} D(\varepsilon)^{u/\varepsilon-1}. \quad (8.12)$$

If  $a \neq 0$ , the term  $a'_1 a \beta / \beta_0 + \mathcal{O}(1/\beta_0^2)$  should be added (the difference between  $a_0$  and  $a$  is  $\mathcal{O}(1/\beta_0)$ ).

We can expand (8.11) in the renormalized  $\alpha_s$ , or in  $\beta$  (8.7), using

$$\left( \frac{\beta}{\varepsilon + \beta} \right)^L = \left( \frac{\beta}{\varepsilon} \right)^L \left[ 1 - L \frac{\beta}{\varepsilon} + \frac{(L)_2}{2} \left( \frac{\beta}{\varepsilon} \right)^2 - \frac{(L)_3}{3!} \left( \frac{\beta}{\varepsilon} \right)^3 + \dots \right]$$

(here  $(x)_n = x(x+1)\cdots(x+n-1) = \Gamma(x+n)/\Gamma(x)$  is the Pochhammer symbol). In the applications we shall consider,  $F(\varepsilon, u)$  is regular at the origin:

$$F(\varepsilon, u) = \sum_{n=0}^{\infty} \sum_{m=0}^{\infty} F_{nm} \varepsilon^n u^m; \quad (8.13)$$

however, I know no general proof of this fact. Substituting these expansions into (8.11), we obtain a quadruple sum expressing  $A_0$  via the renormalized quantities.

The bare quantity  $A_0$  is equal to  $ZA$ , where both  $Z$  and  $A$  have the form  $1 + \mathcal{O}(1/\beta_0)$ . Therefore, we can find  $Z - 1$  with  $1/\beta_0$  accuracy just by retaining all terms with negative powers of  $\varepsilon$  in this quadruple sum. The renormalized  $A - 1$ , with  $1/\beta_0$  accuracy, is given by the terms with  $\varepsilon^0$ . It is enough to find  $Z_1$ , the coefficient of  $1/\varepsilon$  in  $Z$ , in order to obtain the anomalous dimension

$$\gamma = -2 \frac{dZ_1}{d \log \beta}$$

(see (3.15)). Collecting terms with  $\varepsilon^{-1}$  in the quadruple sum for  $A_0$ , we obtain for  $\beta_0 Z_1$

$$\begin{aligned} & \beta F_{00} - \beta^2(F_{10} + F_{01}) + \beta^3(F_{20} + F_{11} + F_{02}) \\ & \quad - \beta^4(F_{30} + F_{21} + F_{12} + F_{03}) + \dots \\ & + \frac{1}{2}\beta^2(F_{10} + 2F_{01}) - \beta^3(F_{20} + 2F_{11} + 4F_{02}) \\ & \quad + \frac{3}{2}\beta^4(F_{30} + 2F_{21} + 4F_{12} + 8F_{03}) + \dots \\ & + \frac{1}{3}\beta^3(F_{20} + 3F_{11} + 9F_{02}) - \beta^4(F_{30} + 3F_{21} + 9F_{12} + 27F_{03}) + \dots \\ & + \frac{1}{4}\beta^4(F_{30} + 4F_{21} + 16F_{12} + 64F_{03}) + \dots \\ & + \dots \\ & = \beta F_{00} - \frac{\beta^2}{2}F_{10} + \frac{\beta^3}{3}F_{20} - \frac{\beta^4}{4}F_{30} + \dots \end{aligned}$$

Therefore, the anomalous dimension is [13]

$$\gamma = -2 \frac{\beta}{\beta_0} F(-\beta, 0) + \mathcal{O}\left(\frac{1}{\beta_0^2}\right). \quad (8.14)$$

Collecting terms with  $\varepsilon^0$  in the quadruple sum for  $A_0$ , we obtain for  $\beta_0(A - 1)$

$$\begin{aligned} & \beta(F_{10} + F_{01}) - \beta^2(F_{20} + F_{11} + F_{02}) + \beta^3(F_{30} + F_{21} + F_{12} + F_{03}) \\ & \quad - \beta^4(F_{40} + F_{31} + F_{22} + F_{13} + F_{04}) + \dots \\ & + \frac{1}{2}\beta^2(F_{20} + 2F_{11} + 4F_{02}) - \beta^3(F_{30} + 2F_{21} + 4F_{12} + 8F_{03}) \\ & \quad + \frac{3}{2}\beta^4(F_{40} + 2F_{31} + 4F_{22} + 8F_{13} + 16F_{04}) + \dots \end{aligned}$$

$$\begin{aligned}
& + \frac{1}{3} \beta^3 (F_{30} + 3F_{21} + 9F_{12} + 27F_{03}) \\
& \quad - \beta^4 (F_{40} + 3F_{31} + 9F_{22} + 27F_{13} + 81F_{04}) + \dots \\
& + \frac{1}{4} \beta^4 (F_{40} + 4F_{31} + 16F_{22} + 64F_{13} + 256F_{04}) + \dots \\
& + \dots \\
& = \beta F_{10} - \frac{\beta^2}{2} F_{20} + \frac{\beta^3}{3} F_{30} - \frac{\beta^4}{4} F_{40} + \dots \\
& \quad + \beta F_{01} + \beta^2 F_{02} + 2\beta^3 F_{03} + 6\beta^4 F_{04} + \dots
\end{aligned}$$

Therefore, the renormalized quantity is [6]

$$\begin{aligned}
A(\mu) &= 1 + \frac{1}{\beta_0} \int_{-\beta}^0 d\varepsilon \frac{F(\varepsilon, 0) - F(0, 0)}{\varepsilon} \\
&+ \frac{1}{\beta_0} \int_0^\infty du e^{-u/\beta} \frac{F(0, u) - F(0, 0)}{u} + \mathcal{O}\left(\frac{1}{\beta_0^2}\right), \tag{8.15}
\end{aligned}$$

where  $\beta = \beta_0 \alpha_s(\mu)/(4\pi)$ .

The renormalization-group equation

$$\frac{d \log A(\mu)}{d \log \alpha_s} = \frac{\gamma(\alpha_s)}{2\beta(\alpha_s)}$$

can be conveniently solved as

$$A(\mu) = \hat{A} \left( \frac{\alpha_s(\mu)}{\alpha_s(\mu_0)} \right)^{\gamma_0/(2\beta_0)} K_\gamma(\alpha_s(\mu)) \tag{8.16}$$

(see (4.72)), where

$$\hat{A} = A(\mu_0) K_{-\gamma}(\alpha_s(\mu_0)).$$

At the first order in  $1/\beta_0$ , we obtain from (8.14)

$$K_\gamma(\alpha_s) = 1 + \frac{1}{\beta_0} \int_{-\beta(\alpha_s)}^0 d\varepsilon \frac{F(\varepsilon, 0) - F(0, 0)}{\varepsilon}.$$

Therefore,

$$\hat{A} = 1 + \frac{1}{\beta_0} \int_0^\infty du e^{-u/\beta(\alpha_s(\mu_0))} \left. \frac{F(0, u) - F(0, 0)}{u} \right|_{\mu_0} + \mathcal{O}\left(\frac{1}{\beta_0^2}\right).$$

Let us suppose that  $m \gg \Lambda_{\overline{\text{MS}}}$  is the characteristic hard scale in the quantity  $A$ . Then  $F(\varepsilon, u)$  contains a factor  $(\mu/m)^{2u}$ . When we take the limit  $\varepsilon \rightarrow 0$ , the factor  $D(\varepsilon)^{u/\varepsilon-1}$  in (8.12) becomes  $\exp[(5/3)u]$ . Therefore,

$$F(0, u) = \left( \frac{e^{5/6} \mu}{m} \right)^{2u} F(u), \quad F(u) = ua_1(1+u)m^{2u}. \quad (8.17)$$

It is most convenient to use

$$\mu_0 = e^{-5/6} m \quad (8.18)$$

in the definition of  $\hat{A}$ . In the rest of this chapter,  $\beta$  will mean  $\beta_0 \alpha_s(\mu_0)/(4\pi)$ . This renormalization-group invariant is

$$\hat{A} = 1 + \frac{1}{\beta_0} \int_0^\infty du e^{-u/\beta} S(u) + \mathcal{O}\left(\frac{1}{\beta_0^2}\right), \quad (8.19)$$

where

$$S(u) = \frac{F(u) - F(0)}{u}. \quad (8.20)$$

Here,

$$e^{-u/\beta} = \left( \frac{e^{5/6} \Lambda_{\overline{\text{MS}}}}{m} \right)^{2u}. \quad (8.21)$$

If we substitute the expansion

$$S(u) = \sum_{L=1}^{\infty} s_L u^{L-1}$$

into the Laplace integral (8.19), we obtain the renormalized perturbative series

$$\hat{A} = 1 + \frac{1}{\beta_0} \sum_{L=1}^{\infty} c_L \beta^L + \mathcal{O}\left(\frac{1}{\beta_0^2}\right), \quad (8.22)$$

$$c_L = (L-1)! s_L = \left( \frac{d}{du} \right)^{L-1} S(u) \Big|_{u=0}. \quad (8.23)$$

Therefore,  $S(u)$  can be obtained from  $\hat{A}$  (8.22) by using

$$S(u) = \sum_{L=1}^{\infty} \frac{c_L u^{L-1}}{(L-1)!}, \quad (8.24)$$

which is called the Borel transform.

We see that the function  $F(\varepsilon, u)$  (8.12) contains all the necessary information about the quantity  $A$  at the order  $1/\beta_0$ . The anomalous dimension (8.14) is determined by  $F(\varepsilon, 0)$ , and the renormalization-group invariant  $\hat{A}$  (8.19) (which gives  $A(\mu)$  (8.16)) by  $F(0, u)$ . These formulae are written in the Landau gauge  $a = 0$ ; if  $a \neq 0$ , additional one-loop terms from the longitudinal part of the gluon propagator (3.21) should be added.

## 8.2 Renormalons

The Laplace integral (8.19) is not well defined if the Borel image  $S(u)$  has singularities on the integration path – the positive half-axis  $u > 0$ . At the first order in  $1/\beta_0$ ,  $S(u)$  typically has simple poles. If

$$S(u) = \frac{r}{u_0 - u} + \dots, \quad (8.25)$$

where the dots mean terms regular at  $u = u_0$ , and  $u_0 > 0$ , then the integral (8.19) is not well defined near  $u_0$ . One way to make sense of this integral is to use its principal value: to make a hole  $[u_0 - \delta, u_0 + \delta]$  and take the limit  $\delta \rightarrow 0$ . However, if we make, for example, a hole  $[u_0 - \delta, u_0 + 2\delta]$  instead, we shall obtain a result which differs from the principal value by the residue of the integrand times  $\log 2$ . Therefore, the sum of the perturbative series (8.19) contains an intrinsic ambiguity of the order of this residue. This ambiguity is equal to

$$\Delta \hat{A} = \frac{re^{-u_0/\beta}}{\beta_0} = \frac{r}{\beta_0} \left( \frac{e^{5/6} \Lambda_{\overline{\text{MS}}}}{m} \right)^{2u_0}. \quad (8.26)$$

These renormalon ambiguities are commensurate with  $1/m$  power corrections – contributions of matrix elements of higher-dimensional operators to the quantity  $A$ . The full result for the physical quantity  $A$  must be unambiguous. Therefore, if one changes the prescription for handling the integral across the renormalon singularity at  $u = u_0$ , one has to change the values of the dimension- $2u_0$  matrix elements accordingly. This shows that renormalons can only happen at integer and half-integer values of  $u$ , corresponding to the dimensionalities of the allowed power corrections. The largest ambiguity is associated with the renormalon closest to the origin.

The renormalon pole (8.25) yields a contribution to the coefficients  $c_L$  of the renormalized perturbative series (8.22) equal to

$$c_L = r \frac{(L-1)!}{u_0^L} \quad (8.27)$$

(see (8.23)). The series (8.25) is, clearly, divergent. Using the Stirling formula for the factorial, we can see that the terms of this series behave as

$$c_L \beta^L \sim r \left( \frac{\beta L}{eu_0} \right)^L$$

at large  $L$ . The best one can do with such a series is to sum it until its minimum term, and to assign it an ambiguity of the order of this minimum term. The minimum happens at  $L \approx u_0/\beta$  loops, and the magnitude of the minimum term is given by (8.26). This is another way to look at this

renormalon ambiguity. The fastest-growing contribution to  $c_L$  comes from the renormalon closest to the origin.

Note that renormalons at  $u_0 < 0$  give sign-alternating factorially-growing coefficients (8.27). For such series, the integral (8.19) provides an unambiguous definition of the summation called the Borel sum.

Renormalon singularities can result from either UV or IR divergences of the one-loop integral. Suppose that the integral behaves as  $\int d^4k/(-k^2)^{n_{UV}}$  at  $k \rightarrow \infty$ , so that the degree of its UV divergence (at  $d = 4$ ) is  $\nu_{UV} = 4 - 2n_{UV}$ . When we insert the renormalon chain, the power changes:  $n_{UV} \rightarrow n_{UV} + (L-1)\varepsilon = n_{UV} + u$  if  $\varepsilon = 0$  (which is the case when one is calculating  $S(u)$ ). This integral can have a UV divergence only at  $u \leq 2 - n_{UV} = \nu_{UV}/2$ . Therefore, UV renormalons can be situated at  $\nu_{UV}/2$  and to the left. Only quantities  $A$  with power-like UV divergences at one loop have UV renormalons at positive  $u$ . The divergence at  $u = 0$  is the usual UV divergence of the one-loop integral, which is eliminated by renormalization; renormalized quantities have no UV renormalon at  $u = 0$ .

Similarly, if the one-loop integral behaves as  $\int d^4k/(-k^2)^{n_{IR}}$  at  $k \rightarrow 0$  (where  $k$  is the virtual gluon momentum), so that the degree of its IR divergence is  $\nu_{IR} = 2n_{IR} - 4$ ,  $S(u)$  can have an IR divergence only at  $u \geq 2 - n = -\nu_{IR}/2$ , and IR renormalons can be situated at  $-\nu_{IR}/2$  and integer and half-integer points to the right of this point. Quantities described by off-shell diagrams have  $n_{IR} = 1$ , and their IR renormalons are at  $u = 1$  and to the right.

We can get a better understanding of the physical meaning of renormalons if we rewrite (8.19) in the form [11]

$$\hat{A} = 1 + \int_0^\infty \frac{d\tau}{\tau} w(\tau) \frac{\alpha_s(\sqrt{\tau}\mu_0)}{4\pi} + \mathcal{O}\left(\frac{1}{\beta_0^2}\right). \quad (8.28)$$

This looks like the one-loop correction, but with the running  $\alpha_s$  under the integral sign. The function  $w(\tau)$  has the meaning of the distribution function of gluon virtualities in the one-loop diagram; it is normalized to the coefficient of  $\alpha_s/(4\pi)$  in the one-loop correction. Inside the  $1/\beta_0$  term in (8.28), we may use the leading-order formula for the running of  $\alpha_s$ :

$$\alpha_s(\sqrt{\tau}\mu_0) = \frac{\alpha_s(\mu_0)}{1 + \beta \log \tau} = \alpha_s(\mu_0) \sum_{n=0}^{\infty} (-\beta \log \tau)^n.$$

Substituting this expansion into (8.28), we see that this representation holds if  $w(\tau)$  is related to the coefficients of the perturbative series  $c_L$  by

$$c_L = \int_0^\infty \frac{d\tau}{\tau} w(\tau) (-\log \tau)^{L-1}. \quad (8.29)$$

Therefore,  $S(u)$  (8.24) becomes

$$S(u) = \int_0^\infty \frac{d\tau}{\tau} w(\tau) \tau^{-u}. \quad (8.30)$$

In other words,  $S(u)$  is the Mellin transform of  $w(\tau)$ . Therefore, the distribution function  $w(\tau)$  is given by the inverse Mellin transform:

$$w(\tau) = \frac{1}{2\pi i} \int_{u_0 - i\infty}^{u_0 + i\infty} du S(u) \tau^u, \quad (8.31)$$

where  $u_0$  should lie in the gap between the IR and UV renormalons.

For  $\tau < 1$ , we can close the integration contour to the right. If  $S(u)$  has IR renormalons  $r_i/(u_i - u)$ , then

$$w(\tau) = \sum_{\text{IR}} r_i \tau^{u_i}. \quad (8.32)$$

The leading term at small  $\tau$  is given by the leftmost IR renormalon. If our quantity  $A$  is IR finite at one loop, all  $u_i > 0$ , and  $w(\tau) \rightarrow 0$  at  $\tau \rightarrow 0$ . Similarly, for  $\tau > 1$ , we can close the contour to the left. If the UV renormalons are  $r_i/(u - u_i)$ , then

$$w(\tau) = \sum_{\text{UV}} r_i \tau^{u_i}. \quad (8.33)$$

The leading term at large  $\tau$  is given by the rightmost UV renormalon. If  $A$  is UV finite at one loop, all  $u_i < 0$ , and  $w(\tau) \rightarrow 0$  at  $\tau \rightarrow \infty$ .

All virtualities (including small ones) contribute to (8.28). The behaviour of the distribution function  $w(\tau)$  in the small-virtuality region  $\tau \rightarrow 0$  is determined by the IR renormalon closest to the origin. The integral (8.28) is ill-defined, just like the original integral (8.19). The one-loop  $\alpha_s$  (8.10) becomes infinite at  $\tau = (e^{5/6} \Lambda_{\overline{\text{MS}}}/m)^2$  (the Landau pole), and we integrate across this pole. This happens at small  $\tau$ ; substituting the asymptotics (8.32) of the distribution function at small virtualities, we see that the residue at this pole, given by the IR renormalon nearest to the origin, is again equal to (8.26).

### 8.3 Light Quarks

First, we shall discuss the massless-quark propagator at the order  $1/\beta_0$ . The one-loop expression for  $\Sigma_V(p^2)$  (Fig. 3.5) in the Landau gauge with the gluon denominator raised to the power  $n = 1 + (L - 1)\varepsilon$  is

$$\frac{a_1(n)}{(4\pi)^{d/2}} = i \frac{C_F}{-p^2} \int \frac{d^d k}{(2\pi)^d} \frac{\frac{1}{4} \text{Tr } \not{p} \gamma^\mu (\not{k} + \not{p}) \gamma^\nu}{[-(k + p)^2] (-k^2)^n} \left( g_{\mu\nu} + \frac{k_\mu k_\nu}{-k^2} \right).$$

Using the one-loop integrals (2.18), we can easily find the function  $F(\varepsilon, u)$  (8.12). Such functions, for all off-shell massless quantities, have the same  $\Gamma$ -function structure, resulting from (2.18) with  $n_2 = 1 + u - \varepsilon$ :

$$F(\varepsilon, u) = \left( \frac{\mu^2}{-p^2} \right)^u e^{\gamma\varepsilon} \frac{\Gamma(1+u)\Gamma(1-u)\Gamma(2-\varepsilon)}{\Gamma(2+u-\varepsilon)\Gamma(3-u-\varepsilon)} D(\varepsilon)^{u/\varepsilon-1} N(\varepsilon, u). \quad (8.34)$$

The first  $\Gamma$ -function in the numerator, with a positive sign in front of  $u$ , comes from the first  $\Gamma$ -function in the numerator of (2.18), with a negative sign in front of  $d$ , and its poles are UV divergences. The second  $\Gamma$ -function in the numerator, with a negative sign in front of  $u$ , comes from the second  $\Gamma$ -function in the numerator of (2.18), with a positive sign in front of  $d$ , and its poles are IR divergences. For  $\Sigma_V(p^2)$ , we obtain

$$N(\varepsilon, u) = -C_F(3-2\varepsilon)(u-\varepsilon). \quad (8.35)$$

At one loop ( $L = u/\varepsilon = 1$ ), the Landau-gauge self-energy vanishes (see (3.47)); at  $L = 2$ , the  $\beta_0$  term in the two-loop result (3.56) is reproduced.

The massless-quark propagator  $S(p) = [(1 - \Sigma_V(p^2))\not{p}]^{-1}$ , with  $1/\beta_0$  accuracy, in the Landau gauge, is equal to  $1/\not{p}$  times (8.11), where  $F(\varepsilon, u)$  is given by (8.34) and (8.35). Terms with negative powers of  $\varepsilon$  in the expression for  $\not{p}S(p)$  via renormalized quantities form  $Z_q$ . The anomalous dimension is given by (8.14):

$$\gamma = -\frac{\beta}{3\beta_0} \frac{N(-\beta, 0)}{B(2+\beta, 2+\beta)\Gamma(3+\beta)\Gamma(1-\beta)} + \mathcal{O}\left(\frac{1}{\beta_0^2}\right).$$

In the general covariant gauge, the one-loop term proportional to  $a$  (3.50) should be added:

$$\begin{aligned} \gamma_q &= C_F \frac{\alpha_s}{4\pi} \left[ 2a + \frac{\beta(1+(2/3)\beta)}{B(2+\beta, 2+\beta)\Gamma(3+\beta)\Gamma(1-\beta)} \right] + \mathcal{O}\left(\frac{1}{\beta_0^2}\right) \\ &= C_F \frac{\alpha_s}{4\pi} \left[ 2a + 3\beta \left( 1 + \frac{5}{6}\beta - \frac{35}{36}\beta^2 + \dots \right) \right]. \end{aligned} \quad (8.36)$$

This perturbative series for  $\gamma_q$  has a radius of convergence equal to the distance from the origin to the nearest singularity, which is situated at  $\beta = -5/2$ ; in other words, it converges for  $|\beta| < 5/2$ . It reproduces the leading  $\beta_0$  terms in the two-loop result (3.57).

The renormalized expression for  $\not{p}S(p)$  is given by (8.15). If we factor out its  $\mu$ -dependence as in (8.16), then the corresponding renormalization-group invariant is given by (8.19) with

$$S(u) = \frac{1}{u} \left[ \frac{N(0, u)}{(1+u)(1-u)(2-u)} - \frac{N(0, 0)}{2} \right] = -\frac{3C_F}{(1+u)(1-u)(2-u)}$$

(8.37)

(here  $\sqrt{-p^2}$  plays the role of  $m$ ). The pole at  $u = -1$  comes from the first  $\Gamma$ -function in the numerator of (8.34), and is a UV renormalon; the poles at  $u = 1, 2$  come from the second  $\Gamma$ -function, and are IR renormalons (Fig. 8.1a). We can also see this from power counting (Sect. 8.2). The light-quark self-energy seems to have a linear UV divergence. However, the leading term of the integrand at  $k \rightarrow \infty$ ,  $\not{k}/(k^2)^2$ , yields 0 after integration, owing to Lorentz invariance. The actual UV divergence is logarithmic,  $\nu_{\text{UV}} = 0$ , and UV renormalons can exist only at  $u \leq 0$ . The UV divergence at  $u = 0$  is removed by renormalization, and the UV renormalons are at  $u < 0$ . The index of the IR divergence of the self-energy, like that of any off-shell quantity, is  $\nu_{\text{IR}} = -2$ , and the IR renormalons are at  $u \geq 1$ . The power corrections to the light-quark propagator form an expansion in  $1/(-p^2)$ , therefore, IR renormalons can appear only at positive integer values of  $u$ . For gauge-invariant quantities, the first power correction contains the gluon condensate  $\langle G^2 \rangle$  of dimension 4, and the first IR renormalon is at  $u = 2$ . The quark propagator is not gauge-invariant, and a renormalon at  $u = 1$  is allowed. The virtuality distribution function (8.31) is

$$w(\tau) = -3C_F \times \begin{cases} \frac{1}{2}\tau - \frac{1}{3}\tau^2, & \tau < 1, \\ \frac{1}{6}\tau^{-1}, & \tau > 1 \end{cases}$$

(Fig. 8.1b).

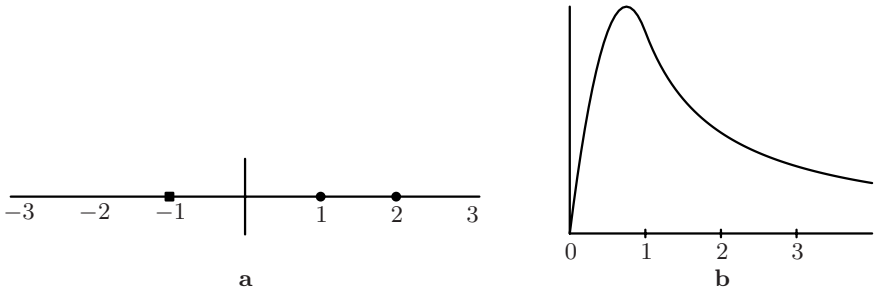


**Fig. 8.1.** UV renormalons (black squares) and IR renormalons (black circles) in the light-quark self-energy (a); the virtuality distribution function (b)

Now we shall discuss light-quark currents (5.1). By repeating the calculation of the vertex function  $\Gamma(p, 0) = \Gamma\Gamma_b(p^2)$  (Sect. 5.3) with the denominator of the gluon propagator raised to the power  $n = 1 + (L - 1)\varepsilon$ , we obtain  $\Gamma_b(p^2)$  in the Landau gauge; it has the form of (8.11) and (8.34), with

$$N_b(\varepsilon, u) = -C_F [2 - u - \varepsilon + 2h(u - h)], \quad (8.38)$$

where  $h$  is defined by (5.32) (if  $a_0 \neq 0$ , the one-loop term proportional to  $a_0$  from (5.34) should be added). If  $L = u/\varepsilon = 1$ , the one-loop result (5.34) is reproduced. For the longitudinal vector current ( $h = 1 - d/2$ ), the result can be obtained from  $\Sigma_V(p^2)$  using the Ward identity (Sect. 5.3). The result for  $\Gamma_a(p^2)$  is a little more complicated, and provides no new insight; we omit it. The anomalous dimension of the current is

$$\gamma_{jn} = \frac{d \log Z_{\Gamma n}}{d \log \mu} + \gamma_q ,$$

where the derivative of  $Z_{\Gamma n}$  is given by (8.14). We arrive at [7]

$$\begin{aligned} \gamma_{jn} &= \frac{2}{3} C_F \frac{\alpha_s}{4\pi} \frac{(n-1)(3-n+2\beta)}{B(2+\beta, 2+\beta)\Gamma(3+\beta)\Gamma(1-\beta)} + \mathcal{O}\left(\frac{1}{\beta_0^2}\right) \\ &= -2C_F \frac{\alpha_s}{4\pi} (n-1) \left[ n-3 + \frac{n-15}{6}\beta - \frac{13n-35}{12}\beta^2 + \dots \right] . \end{aligned} \quad (8.39)$$

This perturbative series converges for  $|\beta| < 5/2$ . It reproduces the leading  $\beta_0$  terms in the two-loop result (5.9). In particular,

$$\gamma_m = -\gamma_{j0} = 2C_F \frac{\alpha_s}{4\pi} \frac{1 + (2/3)\beta}{B(2+\beta, 2+\beta)\Gamma(3+\beta)\Gamma(1-\beta)} + \mathcal{O}\left(\frac{1}{\beta_0^2}\right) . \quad (8.40)$$

The expressions for  $Z_{P,A}$  (Sect. 5.3) in the large- $\beta_0$  limit can be obtained from (5.39):

$$\begin{aligned} Z_A &= 1 - \frac{4}{3} \frac{C_F}{\beta_0} \int_0^\beta \frac{d\beta}{B(2+\beta, 2+\beta)\Gamma(3+\beta)\Gamma(1-\beta)} \\ &= 1 - 4C_F \frac{\alpha_s}{4\pi} \left[ 1 + \frac{1}{12}\beta - \frac{13}{36}\beta^2 + \dots \right] , \\ Z_P &= Z_A^2 . \end{aligned} \quad (8.41)$$

They reproduce the leading  $\beta_0$  terms of (5.42) and (5.41).

## 8.4 HQET Heavy Quark

Now we turn to the HQET static-quark propagator. The one-loop expression for  $\tilde{\Sigma}(\omega)/\omega$  (Fig. 3.12) in the Landau gauge with the gluon denominator raised to the power  $n = 1 + (L-1)\varepsilon$  is

$$\frac{a_1(n)}{(4\pi)^{d/2}} = \frac{iC_F}{\omega^2} \int \frac{d^d k}{(2\pi)^d} \frac{\omega}{k \cdot v + \omega} \frac{v^\mu v^\nu}{(-k^2)^n} \left( g_{\mu\nu} + \frac{k_\mu k_\nu}{-k^2} \right) .$$

Using the one-loop integrals (2.27), we can easily find the function  $F(\varepsilon, u)$  (8.12). Such functions, for all off-shell HQET quantities, have the same  $\Gamma$ -function structure, resulting from (2.27) with  $n_2 = 1 + u - \varepsilon$ :

$$F(\varepsilon, u) = \left( \frac{\mu}{-2\omega} \right)^{2u} e^{\gamma\varepsilon} \frac{u\Gamma(-1+2u)\Gamma(1-u)}{\Gamma(2+u-\varepsilon)} D(\varepsilon)^{u/\varepsilon-1} N(\varepsilon, u). \quad (8.42)$$

The first  $\Gamma$ -function in the numerator, with a positive sign in front of  $u$ , comes from the first  $\Gamma$ -function in the numerator of (2.27), with a negative sign in front of  $d$ , and its poles are UV divergences. The second  $\Gamma$ -function in the numerator, with a negative sign in front of  $u$ , comes from the second  $\Gamma$ -function in the numerator of (2.27), with a positive sign in front of  $d$ , and its poles are IR divergences. For  $\tilde{\Sigma}(\omega)/\omega$ , we obtain

$$N(\varepsilon, u) = -2C_F(3-2\varepsilon). \quad (8.43)$$

If  $a_0 \neq 0$ , the one-loop term proportional to  $a_0$  from (3.61) should be added to  $\tilde{\Sigma}(\omega)$ . This result reproduces (3.61) at  $L = u/\varepsilon = 1$  and the  $\beta_0$  term from (3.73) at  $L = 2$ .

The static-quark propagator  $\tilde{S}(\omega) = [\omega - \tilde{\Sigma}(\omega)]^{-1}$ , with  $1/\beta_0$  accuracy, in the Landau gauge, is equal to  $1/\omega$  times (8.11), where  $F(\varepsilon, u)$  is given by (8.42) and (8.43). Terms with negative powers of  $\varepsilon$  in the expression for  $\omega\tilde{S}(\omega)$  via renormalized quantities form  $\tilde{Z}_Q$ . The anomalous dimension is given by (8.14):

$$\tilde{\gamma} = \frac{\beta}{6\beta_0} \frac{N(-\beta, 0)}{B(2+\beta, 2+\beta)\Gamma(2+\beta)\Gamma(1-\beta)} + \mathcal{O}\left(\frac{1}{\beta_0^2}\right).$$

In the general covariant gauge, the one-loop term proportional to  $a$  (3.67) should be added:

$$\begin{aligned} \tilde{\gamma}_Q &= C_F \frac{\alpha_s}{4\pi} \left[ 2a - \frac{1+(2/3)\beta}{B(2+\beta, 2+\beta)\Gamma(2+\beta)\Gamma(1-\beta)} \right] + \mathcal{O}\left(\frac{1}{\beta_0^2}\right) \\ &= C_F \frac{\alpha_s}{4\pi} \left[ 2(a-3) - 8\beta + \frac{10}{3}\beta^2 + \dots \right]. \end{aligned} \quad (8.44)$$

This perturbative series converges for  $|\beta| < 5/2$ . It reproduces the leading  $\beta_0$  terms in (3.75).

The renormalized expression for  $\omega\tilde{S}(\omega)$  is given by (8.15). If we factor out its  $\mu$ -dependence as in (8.16), then the corresponding renormalization-group invariant is given by (8.19) with [3]

$$\begin{aligned} S(u) &= \frac{\Gamma(-1+2u)\Gamma(1-u)}{\Gamma(2+u)} N(0, u) + \frac{N(0, 0)}{2u} \\ &= -6C_F \left[ \frac{\Gamma(-1+2u)\Gamma(1-u)}{\Gamma(2+u)} + \frac{1}{2u} \right] \end{aligned} \quad (8.45)$$

(here  $-2\omega$  plays the role of  $m$ ). The first  $\Gamma$ -function, with a positive sign in front of  $u$ , produces UV renormalons, while the second one, with a negative sign, produces IR renormalons (Fig. 8.2a). We can understand this from power counting (Sect. 8.2). The static-quark self-energy has a linear UV divergence which is not nullified by Lorentz invariance:  $\nu_{\text{UV}} = 1$ . This is the same divergence as that of the Coulomb energy of a point charge in classical electrodynamics. Therefore, the UV renormalons are situated at  $u \leq 1/2$ . The index of the IR divergence of the self-energy, like that of any off-shell quantity, is  $\nu_{\text{IR}} = -2$ , and the IR renormalons are at  $u \geq 1$ .

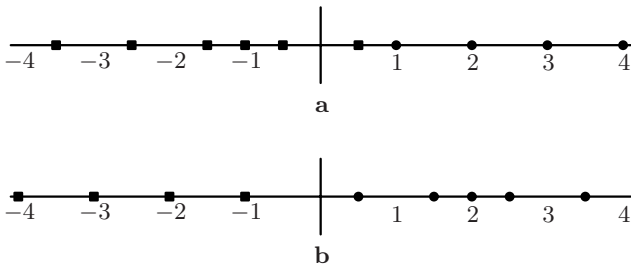


**Fig. 8.2.** Renormalons in the off-shell HQET self-energy (a) and in the on-shell heavy-quark self-energy (b)

Here we encounter a radically new situation: a UV renormalon at  $u > 0$ . This renormalon leads to an ambiguity  $\Delta\tilde{\Sigma}(\omega)/\omega = (r/\beta_0)e^{5/6}\Lambda_{\overline{\text{MS}}}/(-2\omega)$ , where  $r = 4C_F$  is the residue of  $S(u)$  at  $u = 1/2$ . If we change the prescription for handling the pole at  $u = 1/2$ , we have to change the zero-energy level of HQET. Therefore, the HQET residual meson energy has an ambiguity  $\Delta\bar{\Lambda} = \Delta\tilde{\Sigma}(\omega)$  of order  $\Lambda_{\overline{\text{MS}}}/\beta_0$  [3] (see also [5]):

$$\Delta\bar{\Lambda} = -2C_F e^{5/6} \frac{\Lambda_{\overline{\text{MS}}}}{\beta_0}. \quad (8.46)$$

The structure of the leading UV renormalon at  $u = 1/2$  can be investigated beyond the large- $\beta_0$  limit [1]. The renormalization-group invariant corresponding to  $\omega\tilde{S}(\omega)$  is now written as

$$1 + \frac{1}{\beta_0} \int_0^\infty du S(u) \exp \left[ -\frac{4\pi}{\beta_0 \alpha_s(\mu_0)} u \right] \quad (8.47)$$

instead of (8.19), where the exact  $\alpha_s$  is used in the exponent,  $\mu_0 = -2\omega e^{-5/6}$ , and  $\mathcal{O}(1/\beta_0^2)$  is absent. The singularity of  $S(u)$  at  $u = 1/2$  becomes a branch point, so that

$$S(u) = \frac{r}{(1/2 - u)^{1+a}} + \dots,$$

with a cut from  $1/2$  to  $+\infty$ , instead of a simple pole. The renormalon ambiguity of  $\tilde{\Sigma}(\omega)/\omega$  is defined, as before, as the difference between the integrals (8.47) below and above the real axis divided by  $2\pi i$ :

$$\begin{aligned}\Delta \bar{\Lambda} &= \frac{r\omega}{\beta_0} \frac{1}{2\pi i} \int_C \frac{du}{(1/2 - u)^{1+a}} \exp \left[ -\frac{4\pi}{\beta_0 \alpha_s(\mu_0)} u \right] \\ &= \frac{r}{2\beta_0 \Gamma(1+a)} (-2\omega) \exp \left[ -\frac{2\pi}{\beta_0 \alpha_s(\mu_0)} \right] \left( \frac{\beta_0 \alpha_s(\mu_0)}{4\pi} \right)^{-a}\end{aligned}\quad (8.48)$$

(Fig. 8.3; we have used  $\Gamma(-a)\Gamma(1+a) = -\pi/\sin(\pi a)$ ). But this must be just some number times  $\Lambda_{\overline{\text{MS}}}$ , and cannot depend on  $\omega$ !

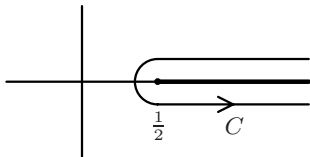


**Fig. 8.3.** Integration contour

We have to use a formula for  $\alpha_s(\mu)$  that is more precise than the one-loop one (8.10). The renormalization-group equation (3.5) is solved by separation of variables:

$$\begin{aligned}\frac{2\pi}{\beta_0} \int \frac{d\alpha_s}{\alpha_s^2} \left[ 1 - \frac{\beta_1}{\beta_0} \frac{\alpha_s}{4\pi} + \mathcal{O}(\alpha_s^2) \right] &= - \int d\log \mu, \\ \frac{2\pi}{\beta_0 \alpha_s(\mu)} + \frac{\beta_1}{2\beta_0^2} \log \frac{\alpha_s(\mu)}{4\pi} + \mathcal{O}(\alpha_s) &= \log \frac{\mu}{\Lambda_{\overline{\text{MS}}}},\end{aligned}$$

and hence

$$\Lambda_{\overline{\text{MS}}} = \mu \exp \left[ -\frac{2\pi}{\beta_0 \alpha_s(\mu)} \right] \left( \frac{\alpha_s(\mu)}{4\pi} \right)^{-\beta_1/(2\beta_0^2)} [1 + \mathcal{O}(\alpha_s)]. \quad (8.49)$$

The UV renormalon ambiguity  $\Delta \bar{\Lambda}$  must be equal to  $\Lambda_{\overline{\text{MS}}}$  times some number:

$$\Delta \bar{\Lambda} = N_0 \Delta_0, \quad \Delta_0 = -2C_F e^{5/6} \frac{\Lambda_{\overline{\text{MS}}}}{\beta_0}. \quad (8.50)$$

The normalization factor  $N_0$  is only known in the large- $\beta_0$  limit:

$$N_0 = 1 + \mathcal{O}(1/\beta_0);$$

In general, it is just some unknown number of order 1. Comparing (8.48) with (8.50), we conclude that at  $u \rightarrow 1/2$ ,

$$S(u) = -\frac{4C_F N'_0}{(1/2-u)^{1+\beta_1/(2\beta_0^2)}} [1 + \mathcal{O}(1/2-u)] , \quad (8.51)$$

where

$$N'_0 = N_0 \Gamma \left( 1 + \frac{\beta_1}{2\beta_0^2} \right) \beta_0^{\beta_1/(2\beta_0^2)} . \quad (8.52)$$

The result for the power is exact; the normalization cannot be found within this approach.

The self-energy with a kinetic-energy insertion  $\tilde{\Sigma}_{k0}$  (Fig. 4.2) can also be easily calculated in the large- $\beta_0$  limit. In the Landau gauge, raising the gluon denominator in (4.6) to the power  $n = 1 + (L-1)\varepsilon$ , we obtain (8.42) with

$$N(\varepsilon, u) = 2C_F(3-2\varepsilon)^2\omega^2 , \quad (8.53)$$

and hence

$$\Delta\tilde{\Sigma}_{k0}(\omega) = -3\omega \Delta\bar{\Lambda} . \quad (8.54)$$

This leads to a UV renormalon ambiguity of the heavy-quark field renormalization constant [9],

$$\Delta\tilde{Z}_Q = -\frac{3}{2} \frac{\Delta\bar{\Lambda}}{m} . \quad (8.55)$$

Let us also discuss the heavy-light current in HQET. If the light quark is massless, we may take  $(1/4) \text{Tr}$  of any diagram for  $\tilde{\Gamma}(\omega, 0)$ . All diagrams with insertions into the gluon propagator of the one-loop diagram (Fig. 5.3b), as well as this one-loop diagram itself in the Landau gauge, vanish owing to the transversality of the gluon propagator; see (5.55). Therefore, to the first order in  $1/\beta_0$ ,  $\tilde{\Gamma}(\omega, 0) = 1$ , and  $\tilde{\gamma}_j = (\tilde{\gamma}_Q + \gamma_q)/2$  in the Landau gauge. This anomalous dimension is gauge-invariant, and [7]

$$\begin{aligned} \tilde{\gamma}_j &= -C_F \frac{\alpha_s}{4\pi} \frac{1 + (2/3)\beta}{B(2+\beta, 2+\beta)\Gamma(3+\beta)\Gamma(1-\beta)} + \mathcal{O}\left(\frac{1}{\beta_0^2}\right) \\ &= -3C_F \frac{\alpha_s}{4\pi} \left[ 1 + \frac{5}{6}\beta - \frac{35}{36}\beta^2 + \dots \right] , \end{aligned} \quad (8.56)$$

from (8.36) and (8.44). This perturbative series converges for  $\beta_0|\alpha_s| < 4\pi$ . It reproduces the leading  $\beta_0$  terms in (5.45). Note that  $\tilde{\gamma}_j = \gamma_{j0}/2$  (8.39) at the first order in  $1/\beta_0$ .

Finally, we discuss the heavy-heavy current in HQET. We consider the vertex (7.3) at  $\omega = \omega' = 0$ , integrated over the region  $t + t' < T$  ( $T$  acts as an IR cut-off). Changing the power of  $-p^2$  in the denominator of the gluon propagator in the Landau gauge from 1 to  $n$  produces, in the coordinate space,

$$\frac{i}{2^{2n-1}\pi^{d/2}} \frac{\Gamma(d/2-n)}{\Gamma(n+1)} \frac{(2n-1)x^2 g_{\mu\nu} + (d-2n)x_\mu x_\nu}{(-x^2 + i0)^{d/2-n+1}},$$

instead of (3.51). Following the derivation in Sect. 7.1, we find the one-loop coefficient

$$a_1(n) = C_F \frac{\Gamma(d/2-n-1)}{\Gamma(n+1)} \left( \frac{i}{2} T \cosh \frac{\vartheta}{2} \right)^{2n+2-d} \int_{-\vartheta/2}^{+\vartheta/2} \frac{d\psi}{\cosh^{2n+2-d} \psi} \\ \times \left[ \left( \frac{d}{2} + n - 1 \right) \coth \vartheta + \frac{d/2 - n}{\sinh \vartheta} \cosh 2\psi \right]$$

(this coefficient becomes real in the Euclidean space  $T \rightarrow -iT_E$ ). Therefore (8.12),

$$F(\varepsilon, u) = -C_F \frac{\Gamma(1-u)}{\Gamma(2+u-\varepsilon)} e^{\gamma\varepsilon} D(\varepsilon)^{u/\varepsilon-1} \left( \frac{i}{2} \mu T \cosh \frac{\vartheta}{2} \right)^{2u} \\ \times \int_{-\vartheta/2}^{+\vartheta/2} \frac{d\psi}{\cosh^{2u} \psi} \left[ (2+u-2\varepsilon) \coth \vartheta + \frac{1-u}{\sinh \vartheta} \sinh 2\psi \right].$$

The anomalous dimension corresponding to  $\tilde{Z}_\Gamma$  is (8.14)

$$\tilde{\gamma}_\Gamma = \frac{1}{3} C_F \frac{\alpha_s}{4\pi} \frac{2(1+\beta)\vartheta \coth \vartheta + 1}{B(2+\beta, 2+\beta)\Gamma(2+\beta)\Gamma(1-\beta)}.$$

In order to obtain  $\tilde{\gamma}_J = \tilde{\gamma}_\Gamma + \tilde{\gamma}_Q$ , we add (8.44):

$$\tilde{\gamma}_J = \frac{2}{3} C_F \frac{\alpha_s}{4\pi} \frac{\vartheta \coth \vartheta - 1}{B(2+\beta, 2+\beta)\Gamma(1+\beta)\Gamma(1-\beta)} \\ = 4C_F \frac{\alpha_s}{4\pi} \left( 1 + \frac{5}{3}\beta - \frac{1}{3}\beta^2 + \dots \right) (\vartheta \coth \vartheta - 1). \quad (8.57)$$

This anomalous dimension vanishes at  $\vartheta = 0$  (Sect. 7.1). It reproduces the  $n_1$  term in (7.15).

## 8.5 On-Shell Heavy Quark in QCD

Now, we turn to the on-shell mass and wave-function renormalization of a heavy quark in QCD at the order  $1/\beta_0$ . To this end, we need to calculate the function  $T(t)$  (4.28) with linear accuracy in  $t$ . Closely following the derivation in Sect. 4.2 (with the gluon denominator raised to the power  $n = 1+(L-1)\varepsilon$ ), we obtain

$$\frac{a_1(n)}{(4\pi)^{d/2}} = -iC_F \int \frac{d^d k}{(2\pi)^d} \frac{\text{Tr}(\not{p} + 1)\gamma^\mu(\not{k} + m)\gamma^\nu}{4mD_1(t)D_2^n} \left[ g_{\mu\nu} + \frac{k_\mu k_\nu}{D_2} \right] \\ = -2iC_F \int \frac{d^d k}{(2\pi)^d} \frac{1}{D_1(t)D_2^n} \left[ 1 - \frac{(d-2)D_2}{4m^2}(1-t) + \mathcal{O}(t^2) \right].$$

Expanding  $1/D_1(t)$  up to the linear term in  $t$  and using the one-loop on-shell integrals (4.15), we find  $a_1(n)$  and  $F(\varepsilon, u)$  (8.12). The functions  $F(\varepsilon, u)$ , for all on-shell quantities, have a common  $\Gamma$ -function structure, resulting from (4.15) with  $n_2 = 1 + u - \varepsilon$ :

$$F(\varepsilon, u) = \left(\frac{\mu}{m}\right)^{2u} e^{\gamma\varepsilon} \frac{\Gamma(1+u)\Gamma(1-2u)}{\Gamma(3-u-\varepsilon)} D(\varepsilon)^{u/\varepsilon-1} N(\varepsilon, u). \quad (8.58)$$

The first  $\Gamma$ -function in the numerator, with a positive sign in front of  $u$ , comes from the second  $\Gamma$ -function in the numerator of (4.15), with a negative sign in front of  $d$ , and its poles are UV divergences. The second  $\Gamma$ -function in the numerator, with a negative sign in front of  $u$ , comes from the first  $\Gamma$ -function in the numerator of (4.15), with a positive sign in front of  $d$ , and its poles are IR divergences. For  $T(t)$ , we obtain [7]

$$N(\varepsilon, u) = 2C_F(3-2\varepsilon)(1-u)[1-(1+u-\varepsilon)t] + \mathcal{O}(t^2). \quad (8.59)$$

The on-shell mass renormalization constant  $Z_m^{\text{os}} = m_0/m = 1 - T(0)$  with  $1/\beta_0$  accuracy is given by (8.11) and (8.58) with  $N(\varepsilon, u)$  equal to minus (8.59) at  $t = 0$ . Retaining only terms with negative powers of  $\varepsilon$ , we obtain the  $\overline{\text{MS}}$  mass renormalization constant  $Z_m$  (because  $Z_m^{\text{os}}$  contains no IR divergences). Using (8.14), we reproduce the mass anomalous dimension (8.40). Retaining terms with  $\varepsilon^0$ , we obtain  $Z_m^{\text{os}}/Z_m(\mu) = m(\mu)/m$  in the form (8.15). As usual, it is convenient to express  $m(\mu)$  via the renormalization-group invariant  $\hat{m}$  (8.16). Then the ratio [3]

$$\begin{aligned} \frac{m}{\hat{m}} &= 1 + \frac{1}{\beta_0} \int_0^\infty du e^{-u/\beta} S(u) + \mathcal{O}\left(\frac{1}{\beta_0^2}\right), \\ S(u) &= 6C_F \left[ \frac{\Gamma(u)\Gamma(1-2u)}{\Gamma(3-u)}(1-u) - \frac{1}{2u} \right]. \end{aligned} \quad (8.60)$$

The first  $\Gamma$ -function, with a positive sign in front of  $u$ , produces UV renormalons, while the second one, with a negative sign, produces IR renormalons (Fig. 8.2b). We can understand this from power counting (Sect. 8.2). The QCD quark self-energy has a logarithmic UV divergence ( $\nu_{\text{UV}} = 0$ ), and hence the UV renormalons are situated at  $u < 0$ . The index of the IR divergence of the on-shell quark self-energy is  $\nu_{\text{IR}} = -1$ , and the IR renormalons are at  $u \geq 1/2$ .

The ratio (8.60) can be represented [11] in the form (8.28). For  $\tau > 1$ , the distribution function is given by the sum (8.33) over the UV renormalons at  $u = -n$ ,  $n = 1, 2, 3, \dots$ :

$$\begin{aligned} w(\tau) &= 6C_F \sum_{n=1}^{\infty} \frac{(n+1)(2n)!}{n!(n+2)!} \left(-\frac{1}{\tau}\right)^n \\ &= \frac{1}{2} C_F \tau^2 \left[ 1 - \frac{6}{\tau^2} - \left(1 - \frac{2}{\tau}\right) \sqrt{1 + \frac{4}{\tau}} \right]. \end{aligned}$$

For  $\tau < 1$ , the distribution function is the sum (8.32) over the IR renormalons at  $u = n + 1/2$  ( $n = 0, 1, 2, \dots$ ) and at  $u = 2$ :

$$\begin{aligned} w(\tau) &= \frac{1}{2} C_F \left[ \tau^2 - 3 \sum_{n=0}^{\infty} \frac{(2n-1)(2n-1)!!(2n-5)!!}{(2n)!} \frac{\tau^{n+1/2}}{(-4)^n} \right] \\ &= \frac{1}{2} C_F \left[ (2-\tau)\sqrt{\tau(4+\tau)} + \tau^2 \right] \end{aligned}$$

(both of these series are easily summed using the Newton binomial expansion). Finally, we obtain (Fig. 8.4)

$$w(\tau) = \frac{1}{2} C_F \left[ (2-\tau)\sqrt{\tau(4+\tau)} + \tau^2 - 6\theta(\tau-1) \right]. \quad (8.61)$$

At  $\tau \rightarrow 0$ ,  $w(\tau) \sim \sqrt{\tau}$ , and at  $\tau \rightarrow \infty$ ,  $w(\tau) \sim 1/\tau$ , according to the positions of the nearest IR and UV renormalons.

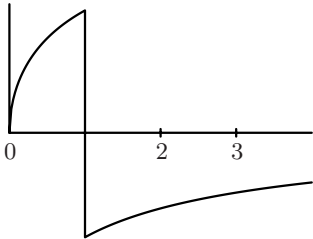


**Fig. 8.4.** Virtuality distribution function

The IR renormalon ambiguity of the on-shell mass is the following [3], from the residue of  $S(u)$  at the leading IR renormalon  $u = 1/2$ :

$$\Delta m = 2C_F e^{5/6} \frac{\Lambda_{\overline{\text{MS}}}}{\beta_0}. \quad (8.62)$$

The meson mass (1.1) is a measurable quantity, and must be unambiguous. In HQET, it is an expansion in  $1/m$ . Its leading term,  $m$ , is a short-distance quantity – a parameter of QCD. The first correction,  $\bar{\Lambda}$ , is a long-distance quantity, determined by the meson structure at the confinement scale. However, the  $\overline{\text{MS}}$  regularization scheme contains no strict momentum cut-offs. As a result, the on-shell mass  $m$  also contains a contribution from large distances, where perturbation theory is ill-defined. This produces the IR renormalon ambiguity (8.62), which is suppressed by  $1/m$  as compared with the leading term. Likewise,  $\bar{\Lambda}$  contains a contribution from small distances, which leads to the UV renormalon ambiguity (8.46). These ambiguities compensate each other in the physical quantity – the meson mass. In other words, in  $\overline{\text{MS}}$  the

separation of the short- and long-distance contributions is ambiguous, even though the full result is not.

This cancellation should hold beyond the large- $\beta_0$  limit. Therefore [1],

$$S(u) = \frac{2C_F N'_0}{(1/2 - u)^{1+\beta_1/(2\beta_0^2)}} [1 + \mathcal{O}(1/2 - u)] , \quad (8.63)$$

where the power is exact. The coefficients in the perturbative series

$$\frac{m}{\hat{m}} = 1 + \frac{1}{\beta_0} \sum_{L=1}^{\infty} c_L \left( \frac{\alpha_s(\mu_0)}{4\pi} \right)^L$$

at  $L \gg 1$  are, according to (8.23),

$$c_{n+1} = 2^{1+a} 2C_F N'_0 (2\beta_0)^n (1+a)_n [1 + \mathcal{O}(1/n)] , \quad a = \frac{\beta_1}{2\beta_0^2} .$$

From the Stirling formula,  $\Gamma(n+1+a) = n^a n! [1 + \mathcal{O}(1/n)]$ , and we arrive at

$$c_{n+1} = 4C_F N_0 n! (2\beta_0)^n (2\beta_0 n)^{\beta_1/(2\beta_0^2)} [1 + \mathcal{O}(1/n)] . \quad (8.64)$$

This result is model-independent.

Our calculation of  $T(t)$  also yields  $Z_Q^{\text{os}} = [1 - T'(0)]^{-1}$  at the first order in  $1/\beta_0$ . It has the form of (8.11) and (8.58) with

$$N_Z(\varepsilon, u) = -2C_F (3 - 2\varepsilon)(1 - u)(1 + u - \varepsilon) \quad (8.65)$$

(see (8.59)). If we retain only negative powers of  $\varepsilon$ , we should obtain  $Z_q(\mu)/\tilde{Z}_Q(\mu)$ , according to (4.35) (because  $\tilde{Z}_Q^{\text{os}} = 1$ ). Therefore, calculating the corresponding anomalous dimension by use of (8.14), we obtain

$$\gamma_q - \tilde{\gamma}_Q = 2C_F \frac{\alpha_s}{4\pi} \frac{(1 + \beta)(1 + (2/3)\beta)}{B(2 + \beta, 2 + \beta)\Gamma(3 + \beta)\Gamma(1 - \beta)} + \mathcal{O}\left(\frac{1}{\beta_0^2}\right) .$$

This difference is gauge-invariant at the  $1/\beta_0$  level; it agrees with (8.36) and (8.44). If we retain terms with  $\varepsilon^0$ , we obtain the finite combination  $Z_Q^{\text{os}} \tilde{Z}_Q(\mu)/Z_q(\mu)$  of the form (8.15); the corresponding renormalization-group invariant (8.19) has [12]

$$S(u) = -6C_F \left[ \frac{\Gamma(u)\Gamma(1-2u)}{\Gamma(3-u)} (1-u^2) - \frac{1}{2u} \right] .$$

## 8.6 Chromomagnetic Interaction

Now we shall discuss [9] the chromomagnetic-interaction coefficient  $C_m(\mu)$  (Sects. 4.4–4.6). It is defined by matching the on-shell scattering amplitudes

in an external chromomagnetic field in QCD and HQET at the linear order in the momentum transfer  $q$ . All loop diagrams in HQET contain no scale and hence vanish. The QCD amplitude at the first order in  $1/\beta_0$  is given by the  $L$ -loop diagrams with  $L - 1$  quark loops (Fig. 8.5). The results have the form (8.58). The diagram of Fig. 8.5a is calculated in the standard way, and gives

$$N_a(\varepsilon, u) = (2C_F - C_A)(3 + 2u - u^2 - 5\varepsilon + 3\varepsilon u - 2\varepsilon u^2 + 2\varepsilon^2 - 2\varepsilon^2 u).$$

We must sum the diagrams of the type shown in 8.5b over  $l$  from 0 to  $L - 1$ . All terms in the sum are equal, so that the summation just gives a factor  $L = u/\varepsilon$ :

$$N_b(\varepsilon, u) = C_A(5 - 2u - 3\varepsilon)\frac{u}{\varepsilon}.$$

In order to calculate the diagrams in Fig. 8.5c, we need the triangle quark loop with linear accuracy in  $q$ ; it is a combination of one-loop propagator integrals (2.18). Again, all terms in the sum over  $l$  from 0 to  $L - 2$  are equal, and the summation just gives a factor  $L - 1$ :

$$N_c(\varepsilon, u) = -C_A \frac{10 - 4u - 28\varepsilon + 9\varepsilon u + 23\varepsilon^3 - 4\varepsilon^2 u - 6\varepsilon^3}{2(1 - \varepsilon)} \left(\frac{u}{\varepsilon} - 1\right).$$

Also, we must include the one-loop on-shell quark wave-function renormalization contribution (8.65) multiplied by the Born scattering amplitude (which is just 1). Finally, we arrive at [9]

$$\begin{aligned} N(\varepsilon, u) &= C_F N_F(\varepsilon, u) + C_A N_A(\varepsilon, u), \\ N_F(\varepsilon, u) &= 4u(1 + u - 2\varepsilon u), \\ N_A(\varepsilon, u) &= \frac{2 - u - \varepsilon}{2(1 - \varepsilon)} (2 + 3u - 5\varepsilon - 6\varepsilon u + 2\varepsilon^2 + 4\varepsilon^2 u). \end{aligned} \quad (8.66)$$

The sum is regular at the origin  $\varepsilon = u = 0$ , unlike the separate contributions. It reproduces the known results for  $L = u/\varepsilon = 1$  and 2 (Sect. 4.4).

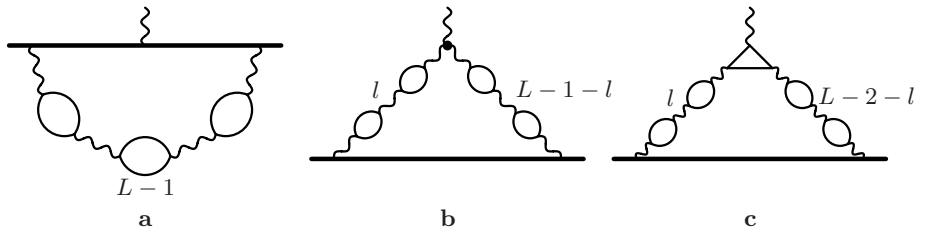


**Fig. 8.5.** Quark scattering in an external gluon field

Now we can easily find the anomalous dimension  $\tilde{\gamma}_m$  and  $C_m(\mu)$  with  $1/\beta_0$  accuracy. The anomalous dimension (8.14) is [9]

$$\begin{aligned}\tilde{\gamma}_m &= C_A \frac{\alpha_s}{2\pi} \frac{\beta(1+2\beta)\Gamma(5+2\beta)}{24(1+\beta)\Gamma^3(2+\beta)\Gamma(1-\beta)} + \mathcal{O}\left(\frac{1}{\beta_0^2}\right) \\ &= C_A \frac{\alpha_s}{2\pi} \left[ 1 + \frac{13}{6}\beta - \frac{1}{2}\beta^2 + \dots \right].\end{aligned}\quad (8.67)$$

It reproduces the leading  $\beta_0$  term of the two-loop result (4.67),

$$\tilde{\gamma}_m = C_A \frac{\alpha_s}{2\pi} \left[ 1 + (13\beta_0 - 25C_A) \frac{\alpha_s}{24\pi} + \dots \right].$$

The perturbative series (8.67) converges for  $\beta_0|\alpha_s| < 4\pi$ .

The renormalization-group invariant  $\hat{C}_m$  corresponding to  $C_m(\mu)$  (see (8.16)) has the form (8.19), with [9]

$$S(u) = \frac{\Gamma(u)\Gamma(1-2u)}{\Gamma(3-u)} \left[ 4u(1+u)C_F + \frac{1}{2}(2-u)(2+3u)C_A \right] - \frac{C_A}{u}. \quad (8.68)$$

The renormalon poles coincide with those in Fig. 8.2b. Taking the residue at the leading IR pole  $u = 1/2$  and comparing with (8.46), we obtain

$$\Delta\hat{C}_m = - \left( 1 + \frac{7}{8} \frac{C_A}{C_F} \right) \frac{\Delta\bar{A}}{m}. \quad (8.69)$$

In physical quantities, such as the mass splitting  $m_{B^*} - m_B$ , this IR renormalon ambiguity is compensated by UV renormalon ambiguities in the matrix elements in the  $1/m$  correction. Detailed investigation of this cancellation allows one to find the exact nature of the singularity of  $S(u)$  at  $u = 1/2$ : it is a branch point, a sum of three terms with different fractional powers of  $1/2 - u$ , where the powers are known exactly, but the normalizations are known only in the large- $\beta_0$  limit. The large- $L$  asymptotics of the perturbative series for  $\hat{C}_m$  can be found. The results have been obtained in [9]. We shall not discuss them here, because they require the use of  $1/m^2$  terms in the HQET Lagrangian. A similar analysis of bilinear heavy-light currents will be presented in the next section.

We can rewrite  $\hat{C}_m$  in the form (8.28), with [9]

$$\begin{aligned}w(\tau) &= C_F w_F(\tau) + C_A w_A(\tau), \\ w_F(\tau) &= 2\tau \left[ \frac{2+4\tau+\tau^2}{\sqrt{\tau(4+\tau)}} - 2 - \tau \right], \\ w_A(\tau) &= \frac{\tau}{4} \left[ \frac{14+5\tau}{\sqrt{\tau(4+\tau)}} - 5 \right] - \theta(\tau-1)\end{aligned}\quad (8.70)$$

(Fig. 8.6; these formulae can be derived in the same way as for (8.61)).

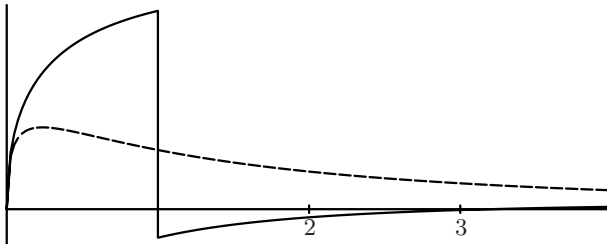


**Fig. 8.6.** Distribution functions  $w_F$  (dashed line) and  $w_A$  (solid line)

## 8.7 Heavy–Light Currents

Hadronic matrix elements of QCD operators, such as quark currents  $j$ , can be expanded in  $1/m$  (see (5.57)),

$$\langle j \rangle = C \langle \tilde{j} \rangle + \frac{1}{2m} \sum B_i \langle \emptyset_i \rangle + \mathcal{O}\left(\frac{1}{m^2}\right), \quad (8.71)$$

to separate short-distance contributions – the matching coefficients  $C, B_i, \dots$ , from long-distance contributions – HQET matrix elements  $\langle \tilde{j} \rangle, \langle \emptyset_i \rangle, \dots$ . The QCD matrix element  $\langle j \rangle$  contains no renormalon ambiguities, because the operator  $j$  has the lowest dimensionality in its channel. In schemes without strict separation of large and small momenta, such as  $\overline{\text{MS}}$ , this procedure artificially introduces IR renormalon ambiguities into matching coefficients and UV renormalon ambiguities into HQET matrix elements. When calculating the matching coefficients  $C, \dots$ , we integrate over all loop momenta, including small momenta. Therefore, the matching coefficients contain, in addition to the main short-distance contributions, also contributions from large distances, where the perturbation theory is ill-defined. The latter contributions produce IR renormalon singularities, which lead to ambiguities  $\sim (\Lambda_{\overline{\text{MS}}}/m)^n$  in the matching coefficients  $C, \dots$ . Similarly, HQET matrix elements of higher-dimensional operators  $\langle \emptyset_i \rangle, \dots$  contain, in addition to the main large-distance contributions, also contributions from short distances, which produce several UV renormalon singularities at positive  $u$ . The latter contributions lead to ambiguities of the order  $\Lambda_{\overline{\text{MS}}}^n$  times lower-dimensional matrix elements (e.g.,  $\langle \tilde{j} \rangle$ ). These two kinds of renormalon ambiguities have to cancel in physical full-QCD matrix elements  $\langle j \rangle$  (8.71) [12].

Let us consider the QCD/HQET matching coefficients  $C_\Gamma(\mu)$  (5.59). Closely following the derivation in Sect. 5.6 (with the gluon denominator raised to the power  $n = 1 + (L - 1)\varepsilon$ ), we obtain for  $\Gamma(mv, 0)$  (5.63)

$$\frac{a_1(n)}{(4\pi)^{d/2}}$$

$$= \frac{iC_F}{2(d-1)} \int \frac{d^d k}{(2\pi)^d} \frac{2(d-1) + (dD_2/m^2 + 4)h - 2(D_2/m^2 + 4)h^2}{D_1 D_2^n}.$$

At the first order in  $1/\beta_0$ ,  $\Gamma(mv, 0)$  has the form of (8.11) and (8.58) with [7]

$$N(\varepsilon, u) = -C_F (2 - u - \varepsilon + 2uh - 2h^2), \quad (8.72)$$

where (5.62)  $h = \eta(n - 2 + \varepsilon)$ . In order to obtain the renormalized matrix element  $(Z_Q^{\text{os}})^{1/2} \Gamma(mv, 0)$ , we must add  $N_Z(\varepsilon, u)/2$  (8.65).

To the accuracy considered,  $\tilde{\Gamma}(0, 0) = 1$  and  $Z_q^{\text{os}} = Z'_q^{\text{os}} = \tilde{Z}_Q^{\text{os}} = 1$ . Retaining only negative powers of  $\varepsilon$  in  $(Z_Q^{\text{os}})^{1/2} \Gamma(mv, 0)$ , we obtain  $Z_j(\mu)/\tilde{Z}_j(\mu)$ , according to (5.59). The corresponding anomalous dimension (8.14) is

$$\gamma_{jn} - \tilde{\gamma}_j = C_F \frac{\alpha_s}{12\pi} \frac{2 + \beta - 2(n - 2 - \beta)^2 + (3 + 2\beta)(1 + \beta)}{B(2 + \beta, 2 + \beta)\Gamma(3 + \beta)\Gamma(1 - \beta)} + \mathcal{O}\left(\frac{1}{\beta_0^2}\right), \quad (8.73)$$

in agreement with (8.39) and (8.56). Retaining  $\varepsilon^0$  terms, we obtain  $C_\Gamma(\mu)$  in the form (8.15). The corresponding renormalization-group invariant (8.16) has the form (8.19), with [7]

$$S(u) = -C_F \left\{ \frac{\Gamma(u)\Gamma(1-2u)}{\Gamma(3-u)} [5 - u - 3u^2 + 2u\eta(n-2) - 2(n-2)^2] - \frac{5 - 2(n-2)^2}{2u} \right\}. \quad (8.74)$$

Comparing the residue at the leading IR renormalon  $u = 1/2$  with  $\Delta\bar{\Lambda}$  (8.46), we obtain the ambiguity of the matching coefficient [7],

$$\Delta C_\Gamma(\mu) = \frac{1}{3} \left[ \frac{15}{4} + \eta(n-2) - 2(n-2)^2 \right] \frac{\Delta\bar{\Lambda}}{m}. \quad (8.75)$$

The matching coefficients for the currents containing  $\gamma_5^{\text{AC}}$  and  $\gamma_5^{\text{HV}}$  have identical  $S(u)$  and  $\hat{C}_\Gamma$ ; they differ only by  $K_\gamma(\alpha_s)$  in (8.16). From (8.72) and (5.69), we can trivially reproduce (8.41). Taking into account (5.75),

$$\frac{m}{m(\mu)} = \frac{C_1(\mu)}{C_{\gamma^0}(\mu)},$$

the result (8.72) also reproduces the corresponding formula for  $m/m(\mu)$ , namely (8.59) with  $t = 0$ .

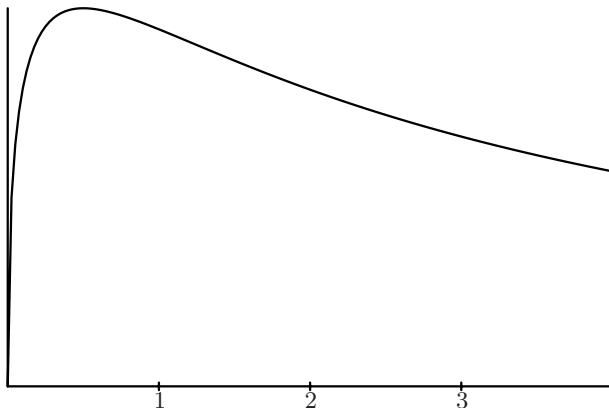
The ratio  $f_{B^*}/f_B$  (5.76) is given by (8.19), with [12]

$$S(u) = 4C_F \frac{\Gamma(1+u)\Gamma(1-2u)}{\Gamma(3-u)}. \quad (8.76)$$

This ratio can be rewritten in the form (8.28). Summing the series (8.32) and (8.33) over the residues of  $S(u)$ , we obtain [11]

$$w(\tau) = -\frac{2}{3}C_F \left[ (1+\tau)\sqrt{\tau(4+\tau)} - \tau(3+\tau) \right] \quad (8.77)$$

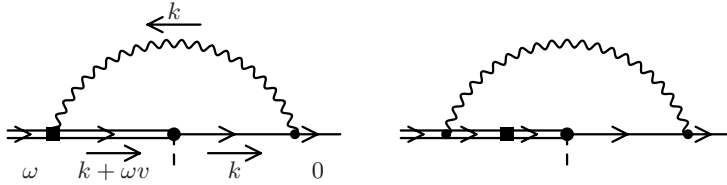
(Fig. 8.7).



**Fig. 8.7.** Virtuality distribution function for  $f_{B^*}/f_B$

Now we turn to the matrix elements of the dimension-4 HQET operators  $\langle 0 | \mathcal{O}_{4,5} | B \rangle$  (see (6.43)). The UV contributions to these matrix elements are independent of the external states, and we may use quark states instead of the hadron states used in (6.60), (6.61). By dimensional analysis, the UV renormalon ambiguities of the matrix elements of  $\mathcal{O}_{4,5}$  are proportional to  $\Delta\bar{\Lambda}$  times the matrix element of the lower-dimensional operator  $\tilde{j}$  with the same external states. We consider a transition from an off-shell heavy quark with residual energy  $\omega < 0$  to a light quark with zero momentum, this is enough to ensure the absence of IR divergences. For  $\mathcal{O}_4$ , all loop corrections to the vertex function (see Fig. 8.8) vanish. The kinetic-energy vertices contain no Dirac matrices, and we may take  $(1/4) \text{Tr}$  on the light-quark line; this yields  $k^\alpha$  at the vertex, and the gluon propagator with insertions is transverse. There is one more contribution: the matrix element  $F$  of  $\tilde{j}$  should be multiplied by the heavy-quark wave-function renormalization  $\tilde{Z}_Q^{1/2}$ , which has a UV renormalon ambiguity (8.55). This gives  $-(3/4)(\Delta\bar{\Lambda}/m)F$  as the ambiguity of the matrix element of  $\mathcal{O}_4$ . This must be equal to  $F \Delta G_k/(2m)$ , and we obtain [12]

$$\Delta G_k(\mu) = -\frac{3}{2}\Delta\bar{\Lambda} \quad (8.78)$$

**Fig. 8.8.** Matrix element of  $\mathcal{O}_4$ 

(this ambiguity is  $\mu$ -independent at the first order in  $1/\beta_0$ ).

For  $\mathcal{O}_5$ , a straightforward calculation of the diagram in Fig. 8.9 gives the bare matrix element of the usual form (8.11) and (8.42), with

$$N(\varepsilon, u) = -2d_F C_F C_m^0 \frac{\omega}{m} \quad (8.79)$$

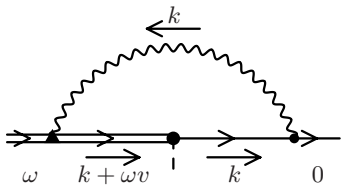
(see (6.16)). The renormalization-group invariant matrix element has the form (8.19) with  $\mu_0 = -2\omega e^{-5/6}$  and

$$S(u) = -2d_F C_F C_m(\mu_0) \frac{\omega}{m} \left( \frac{\Gamma(-1+2u)\Gamma(1-u)}{\Gamma(2+u)} + \frac{1}{2u} \right). \quad (8.80)$$

Taking the residue at the pole  $u = 1/2$ , we find a UV renormalon ambiguity of  $(d_F/3)C_m(\mu_0)(\Delta\bar{\Lambda}/m)$  times the matrix element of  $\tilde{j}$ . Using (6.17), we obtain [12]

$$\Delta G_m(\mu) = 2 \Delta \bar{\Lambda} \quad (8.81)$$

(again,  $\mu$ -independent at this order).

**Fig. 8.9.** Matrix element of  $\mathcal{O}_5$ 

In the full QCD matrix elements (6.17), the IR renormalon ambiguities (8.75) of the leading matching coefficients  $C_F$  are compensated, at the order  $1/\beta_0$ , by the UV renormalon ambiguities of the subleading matrix elements  $\Delta\bar{\Lambda}$  (8.46) and  $\Delta G_{k,m}$  (8.78), (8.81). This cancellation must hold beyond the large- $\beta_0$  limit. The subleading matrix elements are controlled by the renormalization group. The requirement of cancellation allows one to investigate the structure of the leading IR renormalon singularity of  $C_F$  [8].

In the large- $\beta_0$  limit,

$$\Delta\hat{G}_k = -\frac{3}{2}\Delta\bar{A}, \quad \Delta\hat{G}_m = \left(2 - \frac{\gamma_0^m}{\gamma_{m0}}\right)\Delta\bar{A};$$

see (8.78), (8.81), (6.63). In general, these ambiguities must be equal to  $\Lambda_{\overline{\text{MS}}}$  times some numbers:

$$\Delta\hat{G}_k = -\frac{3}{2}N_1\Delta_0, \quad \Delta\hat{G}_m = N_2\left(2 - \frac{\gamma_0^m}{\gamma_{m0}}\right)\Delta_0 \quad (8.82)$$

(see 8.50). The normalization factors  $N_{1,2}$  are known only in the large- $\beta_0$  limit:

$$N_i = 1 + \mathcal{O}(1/\beta_0);$$

in general, they are just some unknown numbers of order 1. Using (8.49), we can represent the UV renormalon ambiguities of the  $1/m$  corrections in (6.65) and (6.85) as  $\exp[-2\pi/(\beta_0\alpha_s(\mu_0))]$  times a sum of terms with different fractional powers of  $\alpha_s(\mu_0)/(4\pi)$ . It is convenient to replace  $\log[\alpha_s(\mu_0)/(4\pi)]$  by  $[(\alpha_s(\mu_0)/(4\pi))^\delta - 1]/\delta$ , and take the limit  $\delta \rightarrow 0$  at the end of the calculation.

In order to cancel this ambiguity, we must have a branch point

$$S_\Gamma(u) = \sum_i \frac{r_i}{(1/2 - u)^{1+a_i}} \quad (8.83)$$

instead of a simple pole (8.74). Then (see (8.48))

$$\Delta\hat{C}_\Gamma = \frac{1}{\beta_0} \exp\left[-\frac{2\pi}{\beta_0\alpha_s(\mu_0)}\right] \sum_i \frac{r_i}{\Gamma(1+a_i)} \left(\frac{\beta_0\alpha_s(\mu_0)}{4\pi}\right)^{-a_i}. \quad (8.84)$$

The requirement for cancellation of the ambiguities in (6.65) gives the following for  $\Gamma = 1, \gamma^0$ :

$$\begin{aligned} S_\Gamma(u) &= \frac{C_F}{(1/2 - u)^{1+\beta_1/(2\beta_0^2)}} \\ &\times \left\{ \left[ -\frac{\gamma_0^k}{2\beta_0} \left( \log \frac{1/2 - u}{\beta_0} - \psi \left( 1 + \frac{\beta_1}{2\beta_0^2} \right) \right) \pm 1 + \frac{\gamma_0^m}{\gamma_{m0}} \right] N'_0 \right. \\ &\left. - \frac{3}{2}N'_1 + \left( 2 - \frac{\gamma_0^m}{\gamma_{m0}} \right) N'_2 (1/2 - u)^{\gamma_{m0}/(2\beta_0)} \right\}. \end{aligned} \quad (8.85)$$

A similar requirement for (6.85) gives the following for  $\Gamma = \gamma^i, \gamma^i\gamma^0$ :

$$S_\Gamma(u) = \frac{C_F}{(1/2 - u)^{1+\beta_1/(2\beta_0^2)}}$$

$$\times \left\{ \left[ -\frac{\gamma_0^k}{2\beta_0} \left( \log \frac{1/2-u}{\beta_0} - \psi \left( 1 + \frac{\beta_1}{2\beta_0^2} \right) \right) + \frac{1}{3} \left( \pm 1 - \frac{\gamma_{m0}^m}{\gamma_{m0}} \right) \right] N'_0 \right. \\ \left. - \frac{3}{2} N'_1 - \frac{1}{3} \left( 2 - \frac{\gamma_0^m}{\gamma_{m0}} \right) N'_2 (1/2-u)^{\gamma_{m0}/(2\beta_0)} \right\}. \quad (8.86)$$

Here

$$N'_1 = N_1 \Gamma \left( 1 + \frac{\beta_1}{2\beta_0^2} \right) \beta_0^{\beta_1/(2\beta_0^2)}, \\ N'_2 = N_2 \Gamma \left( 1 + \frac{\beta_1}{2\beta_0^2} - \frac{\gamma_{m0}}{2\beta_0} \right) \beta_0^{\beta_1/(2\beta_0^2) - \gamma_{m0}/(2\beta_0)}$$

(see (8.52)). The next-to-leading terms were derived in [8]. In the large- $\beta_0$  limit, the simple-pole behaviour with the residue (8.75) is reproduced.

The asymptotics of the perturbative coefficients  $c_L^\Gamma$  at  $L \gg 1$  is determined by the renormalon singularity closest to the origin. Similarly to (8.64), we obtain, for  $\Gamma = 1, \gamma^0$ ,

$$c_{n+1}^\Gamma = 2C_F n! (2\beta_0)^n (2\beta_0 n)^{\beta_1/(2\beta_0^2)} \left[ \left( \frac{\gamma_0^k}{2\beta_0} \log(2\beta_0 n) \pm 1 + \frac{\gamma_0^m}{\gamma_{m0}} \right) N_0 \right. \\ \left. - \frac{3}{2} N_1 + \left( 2 - \frac{\gamma_0^m}{\gamma_{m0}} \right) N_2 (2\beta_0 n)^{-\gamma_{m0}/(2\beta_0)} \right], \quad (8.87)$$

and for  $\Gamma = \gamma^i, \gamma^i \gamma^0$ ,

$$c_{n+1}^\Gamma = 2C_F n! (2\beta_0)^n (2\beta_0 n)^{\beta_1/(2\beta_0^2)} \\ \times \left[ \left( \frac{\gamma_0^k}{2\beta_0} \log(2\beta_0 n) + \frac{1}{3} \left( \pm 1 - \frac{\gamma_0^m}{\gamma_{m0}} \right) \right) N_0 \right. \\ \left. - \frac{3}{2} N_1 - \frac{1}{3} \left( 2 - \frac{\gamma_0^m}{\gamma_{m0}} \right) N_2 (2\beta_0 n)^{-\gamma_{m0}/(2\beta_0)} \right]. \quad (8.88)$$

The  $\mathcal{O}(1/n)$  corrections were calculated in [8].

For the ratio  $f_{B^*}/f_B$  (6.86), the Borel image of the perturbative series is

$$S(u) = \frac{4}{3} \frac{C_F}{(1/2-u)^{1+\beta_1/(2\beta_0^2)}} \\ \times \left[ \left( 1 - \frac{\gamma_0^m}{\gamma_{m0}} \right) N'_0 - \left( 2 - \frac{\gamma_0^m}{\gamma_{m0}} \right) N'_2 (1/2-u)^{\gamma_{m0}/(2\beta_0)} \right], \quad (8.89)$$

and the asymptotics of the coefficients is

$$c_{n+1} = \frac{8}{3} C_F n! (2\beta_0)^n (2\beta_0 n)^{\beta_1/(2\beta_0^2)} \\ \times \left[ \left( 1 - \frac{\gamma_0^m}{\gamma_{m0}} \right) N_0 - \left( 2 - \frac{\gamma_0^m}{\gamma_{m0}} \right) N_2 (2\beta_0 n)^{-\gamma_{m0}/(2\beta_0)} \right]. \quad (8.90)$$

## 8.8 Heavy–Heavy Currents

First we consider the leading matching coefficients for the currents  $\bar{c}\Gamma b$  at  $\vartheta = 0$  at the order  $1/\beta_0$  [10]. By repeating the calculation in Sect. 7.3, we can easily calculate the one-loop coefficient for the vertex function (Fig. 7.5) with the gluon denominator raised to a power  $n$ :

$$\begin{aligned} a_1(n) &= C_F \frac{\Gamma(d-2n-1)\Gamma(-d/2+n+1)}{\Gamma(d-n-1)} \\ &\quad \times \frac{m_b^{d-2n-1}\Phi(m_c/m_b) - m_c^{d-2n-1}\Phi(m_b/m_c)}{m_b - m_c}, \\ \Phi(r) &= \frac{d-1}{d-2n-3}r + \frac{2h^2 + (d-2n-2)h - d+n+1}{d-n-1}, \end{aligned} \quad (8.91)$$

generalizing (7.30). Adding the on-shell wave-function renormalization (8.65) for the b and c, we obtain

$$F(\varepsilon, u) = \left( \frac{\mu^2}{m_b m_c} \right)^u e^{\gamma_\varepsilon} \frac{\Gamma(1+u)\Gamma(1-2u)}{\Gamma(3-u-\varepsilon)} D(\varepsilon)^{u/\varepsilon-1} N(\varepsilon, u), \quad (8.92)$$

$$\begin{aligned} N(\varepsilon, u) &= 2C_F \left[ \left( (n-2)^2 - u\eta(n-2) + 2\varepsilon(n-2) - u\varepsilon\eta \right. \right. \\ &\quad \left. \left. - \frac{4-u^2-4\varepsilon-2u\varepsilon^2}{1+2u} \right) R_1 \right. \\ &\quad \left. + (3-2\varepsilon) \frac{1-2u}{1+2u} (1-u-u^2+u\varepsilon) R_0 \right], \end{aligned} \quad (8.93)$$

where

$$R_0 = \cosh \frac{L}{2}, \quad R_1 = \frac{\sinh [(1-2u)L]/2}{\sinh(L/2)},$$

for the on-shell QCD matrix element (which is equal to the matching coefficient, because all loop corrections in HQET vanish). The corresponding anomalous dimension (8.14) reproduces  $\gamma_{jn}$  (8.39), because  $\tilde{\gamma}_J = 0$  at  $\vartheta = 0$ . The function  $S(u)$  (8.20) for the matching coefficient is

$$\begin{aligned} S(u) &= C_F \left\{ 2 \frac{\Gamma(u)\Gamma(1-2u)}{\Gamma(3-u)} \left[ \left( (n-2)^2 - u\eta(n-2) - \frac{4-u^2}{1+2u} \right) R_1 \right. \right. \\ &\quad \left. \left. + 3 \frac{(1-2u)(1-u-u^2)}{1+2u} R_0 \right] - \frac{(n-1)(n-3)}{u} \right\} \end{aligned} \quad (8.94)$$

with

$$\mu_0 = e^{-5/6} \sqrt{m_b m_c}$$

(see (8.18)). There is no pole at  $u = 1/2$ , the leading IR renormalon is at  $u = 1$ . Therefore, the IR renormalon ambiguity of the matching coefficients at  $\vartheta = 0$  is  $\sim (\Lambda_{\overline{\text{MS}}}/m_{c,b})^2/\beta_0$ .

For the vector and axial currents [10],

$$\begin{aligned} S_{\gamma^0}(u) &= 6C_F \frac{\Gamma(u)\Gamma(1-2u)}{\Gamma(3-u)} \frac{1-u-u^2}{1+2u} \left[ -R_1 + (1-2u)R_0 \right] \\ &= 6C_F \left( \frac{L}{2} \coth \frac{L}{2} - 1 \right) \left( 1 - \frac{3}{2}u + \dots \right), \\ S_{\gamma_5^{\text{AC}}\gamma}(u) &= 2C_F \frac{\Gamma(u)\Gamma(1-2u)}{(1+2u)\Gamma(3-u)} \\ &\quad \times \left[ -(3-u+u^2)R_1 + (1-2u)(1-u-u^2)R_0 \right] \\ &= C_F \left[ 3L \coth \frac{L}{2} - 8 - \left( \frac{5}{2}L \coth \frac{L}{2} - 6 \right) u + \dots \right]. \end{aligned} \quad (8.95)$$

The matching coefficients do not depend on  $\mu, \mu'$ , and are given by (8.19):

$$\begin{aligned} H_{\gamma^0} &= 6C_F \frac{\alpha_s(\mu_0)}{4\pi} \left( \frac{L}{2} \coth \frac{L}{2} - 1 \right) \left( 1 - \frac{3}{2}\beta + \dots \right), \\ H_{\gamma_5^{\text{AC}}\gamma} &= C_F \frac{\alpha_s(\mu_0)}{4\pi} \left[ 3L \coth \frac{L}{2} - 8 - \left( \frac{5}{2}L \coth \frac{L}{2} - 6 \right) \beta + \dots \right]. \end{aligned} \quad (8.96)$$

Re-expressing  $\alpha_s(\mu_0)$  via  $\alpha_s(\sqrt{m_b m_c})$ , we recover (7.36).

Now we consider the general case  $\vartheta \neq 0$  [12]. Closely following the derivation in Sect. 7.5, we obtain  $H_i$ , which have the form (8.11), without the leading 1 for  $H_{2,3,4}$ ; the functions  $F_i(\varepsilon, u)$  have the form (8.92), with

$$\begin{aligned} N_1(\varepsilon, u) &= C_F \left\{ \int_{-1}^{+1} \frac{dz}{(a_+ a_-)^{1+u}} \right. \\ &\quad \times \left[ a_+ a_- h^2 (1-2u) - \frac{(1-z^2)h}{4} u (1-2u) \right. \\ &\quad + (1+u-\varepsilon)(2-u-\varepsilon) \cosh \vartheta \\ &\quad \left. \left. + (\cosh L + z \sinh L) u (2-u-\varepsilon) \right] \right. \\ &\quad \left. - (3-2\varepsilon)(1-u)(1+u-\varepsilon)(r^u + r^{-u}) \right\}, \end{aligned}$$

$$\begin{aligned} N_2(\varepsilon, u) &= -C_F \frac{u}{2} \int_{-1}^{+1} \frac{dz}{(a_+ a_-)^{1+u}} \\ &\quad \times \left[ \frac{e^L (1+z)^2 h}{2} (1-2u) + (1-z)(2-u-\varepsilon) \right], \end{aligned}$$

$$\begin{aligned}
N_3(\varepsilon, u) &= -C_F \frac{u}{2} \int_{-1}^{+1} \frac{dz}{(a_+ a_-)^{1+u}} \\
&\quad \left[ \frac{e^{-L}(1-z)^2 h}{2} (1-2u) + (1+z)(2-u-\varepsilon) \right], \\
N_4(\varepsilon, u) &= -C_F \frac{hu(1-2u)}{4} \int_{-1}^{+1} \frac{dz (1-z^2)}{(a_+ a_-)^{1+u}}.
\end{aligned} \tag{8.97}$$

At one loop ( $u = \varepsilon$ ), the result (7.55) is reproduced. At  $\vartheta = 0$ , the integrals can be easily calculated (see (7.56)), and  $N_1 + N_2 + N_3 + N_4$  reproduces (8.93). The anomalous dimension (8.14) corresponding to (8.97) is  $\gamma_{jn} - \tilde{\gamma}_J$ ; see (8.39) and (8.57). The functions (8.20),

$$S_i(u) = \frac{\Gamma(u)\Gamma(1-2u)}{\Gamma(3-u)} N_i(0, u) - \frac{N_i(0, 0)}{2u},$$

have a leading IR renormalon pole at  $u = 1/2$ , thus producing the ambiguities (8.26)

$$\Delta H_i = -\frac{N_i(0, 1/2)}{3C_F} \frac{\Delta \bar{A}}{\sqrt{m_b m_c}}$$

in the matching coefficients. It is easy to calculate  $N_i(0, 1/2)$  using the integrals

$$\int_{-1}^{+1} \frac{dz}{(a_+ a_-)^{3/2}} = \frac{4 \cosh(L/2)}{\cosh \vartheta + 1}, \quad \int_{-1}^{+1} \frac{z dz}{(a_+ a_-)^{3/2}} = -\frac{4 \sinh(L/2)}{\cosh \vartheta + 1}.$$

We obtain [12]

$$\begin{aligned}
\Delta H_1 &= \left( \frac{1}{\cosh \vartheta + 1} - \frac{3}{4} \right) \left( \frac{1}{m_c} + \frac{1}{m_b} \right) \Delta \bar{A}, \\
\Delta H_2 &= \frac{1}{\cosh \vartheta + 1} \frac{\Delta \bar{A}}{2m_c}, \quad \Delta H_3 = \frac{1}{\cosh \vartheta + 1} \frac{\Delta \bar{A}}{2m_b}, \quad \Delta H_4 = 0.
\end{aligned} \tag{8.98}$$

They do not depend on the Dirac matrix  $\Gamma$  in the current. As expected,  $\Delta H_1 + \Delta H_2 + \Delta H_3 + \Delta H_4$  vanishes at  $\vartheta = 0$ .

In matrix elements of QCD currents (7.20), these IR renormalon ambiguities in the leading matching coefficients  $H_i$  must be compensated by UV renormalon ambiguities in matrix elements of the subleading operators  $\mathcal{O}_i$ ,  $\mathcal{O}'_i$ . There are two kinds of subleading operators – local and bilocal. First we consider local operators, whose coefficients are completely fixed by reparametrization invariance (Sect. 7.6). These local operators contain either  $D_\mu$  or  $\overleftrightarrow{D}_\mu$ . Let us decompose these derivatives into components in the  $(v, v')$  plane and orthogonal to this plane. The projection of  $D_\mu$  onto the longitudinal plane is

$$D_\mu \rightarrow \frac{(v_\mu v' \cdot D + v'_\mu v \cdot D) \cosh \vartheta - v_\mu v \cdot D - v'_\mu v' \cdot D}{\sinh^2 \vartheta},$$

and similarly for  $\overleftarrow{D}_\mu$ . All operators containing longitudinal derivatives can be rewritten, using the equations of motion, as full derivatives of the leading currents  $\tilde{J}_i$ . When we are interested in matrix elements from a ground-state meson to a ground-state meson, we may make the replacement

$$i\partial_\mu \tilde{J}_i \rightarrow \bar{\Lambda}(v - v')_\mu \tilde{J}_i.$$

In this case, projecting onto the longitudinal plane means

$$iD_\mu \rightarrow \bar{\Lambda} \frac{v_\mu \cosh \vartheta - v'_\mu}{\cosh \vartheta + 1}, \quad -i\overleftarrow{D}_\mu \rightarrow \bar{\Lambda} \frac{v'_\mu \cosh \vartheta - v_\mu}{\cosh \vartheta + 1}.$$

The longitudinal part of the local  $1/m_{b,c}$  contribution (7.71) to the QCD matrix element  $\langle J \rangle$  is easily derived by this substitution. It clearly has a UV renormalon ambiguity proportional to  $\Delta\bar{\Lambda}$ . Matrix elements of operators with transverse derivatives cannot be written as matrix elements of the leading currents  $\tilde{J}_i$  times some scalar factors, they require new, independent form factors. Therefore, they contain no UV renormalon ambiguities, which would need to have the form of  $\Delta\bar{\Lambda}$  times lower-dimensional matrix elements of  $\tilde{J}_i$ . The above derivation is exact (and not only valid in the large- $\beta_0$  limit). At the first order in  $1/\beta_0$ , we may replace  $H_1$  by 1,  $H_{2,3,4}$  by 0,  $H'_i$  by 0. The contribution of the local subleading operators to the ambiguity of  $\langle J \rangle$  in this approximation is [12]

$$\begin{aligned} & \left(1 - \frac{1}{\cosh \vartheta + 1}\right) \left(\frac{1}{m_c} + \frac{1}{m_b}\right) \frac{\Delta\bar{\Lambda}}{2} \langle \tilde{J}_1 \rangle \\ & - \frac{1}{\cosh \vartheta + 1} \left(\frac{\Delta\bar{\Lambda}}{2m_c} \langle \tilde{J}_2 \rangle + \frac{\Delta\bar{\Lambda}}{2m_b} \langle \tilde{J}_3 \rangle\right). \end{aligned} \quad (8.99)$$

Now we turn to bilocal subleading operators, and consider the operator

$$i \int dx \text{ T} \left\{ \tilde{J}_1(0), \mathcal{O}_{kc}(x) \right\}$$

with the insertion of the c-quark kinetic energy. This operator appears in the expansion (7.20), with a coefficient  $H_1$ . The one-loop vertex (Fig. 8.10) with the gluon denominator raised to the power  $n$  is

$$\begin{aligned} \frac{a_1(n)}{(4\pi)^{d/2}} &= i \frac{C_F}{2m_c} \int \frac{d^d k}{(2\pi)^d} \left( k_\perp^\mu - \frac{k_\perp^2 v'^\mu}{k \cdot v' + \omega'} \right) \\ &\times \frac{v^\nu}{(k \cdot v + \omega)(k \cdot v' + \omega')(-k^2)^n} \left( g_{\mu\nu} + \frac{k_\mu k_\nu}{-k^2} \right), \end{aligned}$$

where  $k_\perp = k - (k \cdot v') v'$ . We are interested in the UV renormalon at  $u = 1/2$ ; therefore, to make the subsequent formulae shorter, we shall calculate

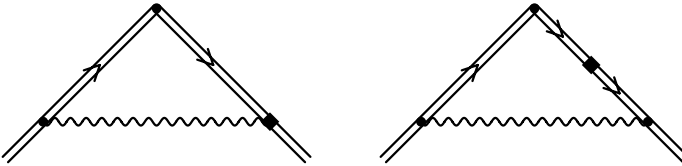


**Fig. 8.10.** Kinetic-energy insertions into the c-quark line

$F(u)$  (8.17) instead of the full function  $F(\varepsilon, u)$ , and omit terms regular at  $u = 1/2$ . We also set  $\omega' = \omega$  for simplicity, and obtain

$$\begin{aligned} F(u) = & -i \frac{C_F}{2m_c} u (-2\omega)^{2u} \left[ \int \frac{d^4 k}{\pi^2} \frac{1}{(-k \cdot v' - \omega)(-k^2)^{1+u}} \right. \\ & \left. + \int \frac{d^4 k}{\pi^2} \frac{\cosh \vartheta}{(-k \cdot v - \omega)(-k \cdot v' - \omega)^2 (-k^2)^u} + \dots \right], \end{aligned}$$

where the dots mean integrals without linear UV divergences at  $u = 0$  (and hence they have no UV renormalon singularity at  $u = 1/2$ ), and  $-2\omega$  plays the role of  $m$  in the definition (8.17).

The first integral is trivial (see (2.27)):

$$-\frac{i}{\pi^2} (-2\omega)^{-1+2u} \int \frac{d^4 k}{(-k \cdot v' - \omega)(-k^2)^{1+u}} = 2 \frac{\Gamma(-1+2u)\Gamma(1-u)}{\Gamma(1+u)}.$$

For the second integral, we use the HQET Feynman parametrization (2.23):

$$\begin{aligned} I = & -\frac{i}{\pi^2} (-2\omega)^{-1+2u} \int \frac{d^4 k}{(-k \cdot v - \omega)(-k \cdot v' - \omega)^2 (-k^2)^u} \\ = & -8 \frac{i}{\pi^2} (-2\omega)^{-1+2u} \frac{\Gamma(3+u)}{\Gamma(u)} \\ & \times \int \frac{y' dy dy' d^4 k}{[-k^2 - 2yv \cdot k - 2y'v' \cdot k - 2\omega(y+y')]^{3+u}} \\ = & 8u (-2\omega)^{-1+2u} \int \frac{y' dy dy'}{[y^2 + y'^2 + 2yy' \cosh \vartheta - 2\omega(y+y')]^{1+u}}. \end{aligned}$$

The substitution  $y = (-2\omega)\xi(1-z)/2$ ,  $y' = (-2\omega)\xi(1+z)/2$  gives

$$I = 2u \int \frac{\xi^{1-u} d\xi (1+z) dz}{[(\cosh^2(\vartheta/2) - z^2 \sinh^2(\vartheta/2)) \xi + 1]^{1+u}}.$$

The substitution  $(\cosh^2(\vartheta/2) - z^2 \sinh^2(\vartheta/2)) \xi = \eta$  then leads to a factored form

$$I = 2u \int_0^\infty \frac{\eta^{1-u} d\eta}{(\eta + 1)^{1+u}} \int_{-1}^{+1} \frac{dz}{[\cosh^2(\vartheta/2) - z^2 \sinh^2(\vartheta/2)]^{2-u}},$$

where

$$\int_0^\infty \frac{\eta^{1-u} d\eta}{(\eta+1)^{1+u}} = \frac{\Gamma(-1+2u)\Gamma(2-u)}{\Gamma(1+u)}.$$

Collecting all contributions, we obtain (8.20)

$$\begin{aligned} S(u) = C_F \frac{-2\omega}{m_c} & \frac{\Gamma(-1+2u)\Gamma(1-u)}{\Gamma(1+u)} \\ & \times \left[ 1 + u(1-u) \cosh \vartheta \int_{-1}^{+1} \frac{dz}{[\cosh^2(\vartheta/2) - z^2 \sinh^2(\vartheta/2)]^{2-u}} \right] \\ & + \dots, \end{aligned} \quad (8.100)$$

where the dots mean terms regular at  $u = 1/2$ .

The residue at the pole  $u = 1/2$  can be obtained using

$$\int_{-1}^{+1} \frac{dz}{[\cosh^2(\vartheta/2) - z^2 \sinh^2(\vartheta/2)]^{3/2}} = \frac{1}{\cosh \vartheta + 1}.$$

The corresponding UV renormalon ambiguity is given by (8.26), with  $-2\omega$  instead of  $m$ . Adding also the external-line renormalization effect  $\Delta \tilde{Z}_c/2$  (8.55), we obtain

$$\left( \frac{1}{2} - \frac{1}{\cosh \vartheta + 1} \right) \frac{\Delta \bar{\Lambda}}{2m_c}.$$

The contribution of the bilocal operator containing the b-quark kinetic energy contains  $m_b$  instead of  $m_c$ . Therefore, the contribution of all bilocal operators with kinetic-energy insertions to the ambiguity of  $\langle J \rangle$  is [12]

$$\left( \frac{1}{2} - \frac{1}{\cosh \vartheta + 1} \right) \left( \frac{1}{m_c} + \frac{1}{m_b} \right) \frac{\Delta \bar{\Lambda}}{2} \langle \tilde{J}_1 \rangle. \quad (8.101)$$

Matrix elements of bilocal operators with a c- or b-quark chromomagnetic insertion cannot be represented as matrix elements of the leading currents  $\tilde{J}_i$  times scalar factors – they require new, independent form factors. Therefore, they have no UV renormalon ambiguities, which would need to be equal to  $\Delta \bar{\Lambda}$  times lower-dimensional matrix elements.

Summing the ambiguity  $\sum \Delta H_i \langle \tilde{J}_i \rangle$  (8.98) of the QCD matrix element  $\langle J \rangle$  due to the IR renormalon in the leading matching coefficients  $H_i$  at  $u = 1/2$ , the ambiguity (8.99) due to the UV renormalon in the local sub-leading operators at  $u = 1/2$ , and the contribution of the bilocal subleading operators (8.101), we see that the ambiguities cancel, at the first order in  $1/\beta_0$ , for any Dirac structure  $\Gamma$  of the current  $J$  [12].

## References

1. M. Beneke: Phys. Lett. B **344**, 341 (1995) [188](#), [194](#)
2. M. Beneke: Phys. Rep. **317**, 1 (1999) [175](#)
3. M. Beneke, V.M. Braun: Nucl. Phys. B **426**, 301 (1994) [187](#), [188](#), [192](#), [193](#)
4. M. Beneke, V.M. Braun, N. Kivel: Phys. Lett. B **404**, 315 (1997) [175](#)
5. I. Bigi, M.A. Shifman, N.G. Uraltsev, A.I. Vainshtein: Phys. Rev. D **50**, 2234 (1994) [188](#)
6. D.J. Broadhurst: Z. Phys. C **58**, 339 (1993) [179](#)
7. D.J. Broadhurst, A.G. Grozin: Phys. Rev. D **52**, 4082 (1995) [176](#), [186](#), [190](#), [192](#), [198](#)
8. F. Campanario, A.G. Grozin, T. Mannel: Nucl. Phys. B **663**, 280 (2003); Erratum: Nucl. Phys. B **670**, 331 (2003) [200](#), [202](#)
9. A.G. Grozin, M. Neubert: Nucl. Phys. B **508**, 311 (1997) [190](#), [194](#), [195](#), [196](#)
10. M. Neubert: Phys. Lett. B **341**, 367 (1995) [203](#), [204](#)
11. M. Neubert: Phys. Rev. D **51**, 5924 (1995) [182](#), [192](#), [199](#)
12. M. Neubert, C.T. Sachrajda: Nucl. Phys. B **438**, 235 (1995) [194](#), [197](#), [198](#), [199](#), [200](#), [204](#), [205](#), [206](#), [208](#)
13. A. Palanques-Mestre, P. Pascual: Commun. Math. Phys. **95**, 277 (1984) [178](#)
14. G. Parisi: Phys. Lett. B **76**, 65 (1978) [175](#)

# Index

- $\beta$ -function 36–37, 77–78, 177
- $\gamma_5$  matrix 1, 95–96, 98, 100–101, 106–107, 111–115, 126, 154–155, 186, 198
- analytical properties of diagrams 24, 26–27
- anomalous dimension 37–39, 126–127, 178
  - chromomagnetic operator 80–81, 133, 135, 195–196
  - electron field 56–58
  - gluon field 37–39, 41–45
  - heavy–heavy current 146–151, 191, 205
  - heavy–light current 103, 190
  - heavy–light dimension-4 local operators 127–131
  - heavy–light operators with chromomagnetic insertion 133–134, 136, 141
  - heavy–light operators with kinetic-energy insertion 132–133
  - heavy-quark field 52, 54–55, 187
  - mass 93–95, 133, 135, 186, 192
  - quark current 92–93, 101, 112, 186, 203, 205
  - quark field 46–47, 50, 184, 194
- axial anomaly 96–97
- background field 71–72
- BGSUV sum rule 15–16
- bilocal operators 121–122, 125, 131–135
- Bjorken sum rule 13–14
- Bloch–Nordström model 55, 148–149
- Borel transform 180
- chromomagnetic
  - form factor 74–76
  - interaction 3, 7–8, 62–63, 76, 79–81, 83–84, 194–196
  - colour factors 48
  - coordinate space 24, 26, 47, 52, 55–56, 145–150, 190–191
  - Cutkosky rules 24, 26–27
  - Cvitanović algorithm 48
- decay constant 8–9, 116–118, 139, 143–144, 198–199, 202
- decoupling 84–85
- chromomagnetic coefficient 89
- coupling constant 87–89
- gluon field 85–86
- heavy–light current 107
- heavy-quark field 87
- mass 105–106
- quark current 103–105
- quark field 86–87
- scalar current 105–106
- vector current 105
- dimensional regularization 1, 23
- Dirac form factor 74–76
- divergences
  - infrared 24, 26, 64, 70–71, 74, 76, 80, 104, 108, 130, 153, 182, 184–185, 187, 192
  - ultraviolet 24, 26, 64, 70–71, 77–78, 80, 92–93, 97, 103, 129–130, 132, 146, 153–154, 156, 159, 165, 182, 184–185, 187–188, 192, 206–207
- Euclidean space 23, 63, 69, 191
- evanescent operators 95
- exponentiation theorem 55–56, 148–150

- Feynman
  - gauge 53–54
  - parametrization 22–23, 64, 161, 167
  - HQET 25, 167, 207
  - rules 20–21, 60, 63
- Foldy–Wouthuysen transformation 63, 80, 122
- form factor 9–11
  - chromomagnetic 74–76
  - Dirac 74–76
  - Isgur–Wise 10–11
- gauge
  - $a = -3$  177
  - Feynman ( $a = 1$ ) 53–54
  - Landau ( $a = 0$ ) 46, 176–177, 180, 183–187, 190–191
  - Yennie ( $a = 3$ ) 52, 58
- heavy quark
  - kinetic energy 7, 60
  - propagator 20–21, 50–55, 186–188
  - self-energy 50–55, 60–61, 70–71, 87, 186–187
  - spin symmetry 3–4, 21, 59–60, 115–116
- homogeneity relation 29
  - HQET 32
- hyperfine splitting 3–5, 7–8, 83–84
- inclusive decays 12–13
- integration by parts 28–29, 65–67
  - HQET 31–32
- inversion 64–65
- Isgur–Wise form factor 10–11
- isospin 5
- Lagrangian
  - HQET 20, 50, 60, 62–63
  - QCD 19, 35–36, 67, 71–72
- Landau
  - gauge 46, 176–177, 180, 183–187, 190–191
  - pole 183
- Larin’s relation 29–30
- lattice simulations 22
- leading logarithms 82–83, 137, 139, 142, 144
- mass shell 19–20, 62
- matching
  - $S$ -matrix elements 59, 80, 194–195
  - dimension-4 operators 159–160, 169–170
  - quark currents
    - dynamic–dynamic  $\Rightarrow$  static–dynamic 107–109, 122–124, 136–137, 142, 157, 166, 197–198
    - dynamic–dynamic  $\Rightarrow$  static–static 152–157, 159–162, 164–166, 168–170, 203–205
    - static–dynamic  $\Rightarrow$  static–static 157–159, 166–168
- Mellin transform 182–183
- partial fractions 33, 155, 158–159
- propagator
  - electron 55–56
  - gluon 39–45, 85, 176–177
  - heavy quark 20–21, 50–55, 186–188
  - quark 21, 45–50, 67–69, 183–185
- renormalization
  - constants 35, 37–39, 50, 126–136, 141
  - coupling constant 36–37, 74, 77–78, 189
  - gluon field 41–45, 74
  - group 37–39, 81–83, 126–127, 131–132, 135–136, 138–139, 141–142, 165, 179
  - heavy–heavy current 146–151
  - heavy–light current 102–103
  - heavy-quark field 70–71, 190
  - mass 46, 67–69, 93–95, 116, 128, 192–194, 198
  - on-shell 67–69, 191–194
  - quark current 91–93
  - quark field 46–47, 50, 68–69, 194
  - scalar current 93–94
  - scale 36
  - vector current 93
- renormalon ambiguity 181–183, 189
  - cancellation 193–194, 196–197, 200–202, 205, 208
  - infrared 193, 196, 198, 204–205
  - ultraviolet 188–190, 199–200, 206, 208

- reparametrization invariance 59–62, 78–79, 122–123, 141, 171–173
- residual mass 21–22, 62
- self-energy
  - gluon 39–45, 70, 85–86
  - heavy quark 50–55, 60–61, 70–71, 87, 186–187
  - quark 45–50, 67–69, 86–87, 183–184, 191–192
- Shmushkevich factory 8
- sum rule
  - BGSUV 15–16
  - Bjorken 13–14
  - Uraltsev 14–15
  - Voloshin 15–16
- superflavour symmetry 4, 59–60
- triangle relations 28–29
  - HQET 31–32
- Uraltsev sum rule 14–15
- vacuum diagram 23, 69–70
- vertex
  - electron–photon 56
  - heavy–heavy current 145–146, 152–155, 161–165, 190–191, 203–205
  - heavy–light current 102–103, 190, 197–198
  - HQET 76–79, 87–88
  - light-quark current 92–93, 104–105, 185–186
  - quark–gluon 72–74
  - static–heavy current 158–159, 167–168
- virtuality distribution function 182–183, 185, 192–193, 196, 199
- Voloshin sum rule 15–16
- Ward identity 56, 73–74, 76, 78–79, 93, 100, 105, 124, 137–139, 147–148, 154–155, 186
- Wick rotation 23, 63
- Yennie gauge 52, 58

# Springer Tracts in Modern Physics

---

- 160 **Physics with Tau Leptons**  
By A. Stahl 2000. 236 figs. VIII, 315 pages
- 161 **Semiclassical Theory of Mesoscopic Quantum Systems**  
By K. Richter 2000. 50 figs. IX, 221 pages
- 162 **Electroweak Precision Tests at LEP**  
By W. Hollik and G. Duckeck 2000. 60 figs. VIII, 161 pages
- 163 **Symmetries in Intermediate and High Energy Physics**  
Ed. by A. Faessler, T.S. Kosmas, and G.K. Leontaris 2000. 96 figs. XVI, 316 pages
- 164 **Pattern Formation in Granular Materials**  
By G.H. Ristow 2000. 83 figs. XIII, 161 pages
- 165 **Path Integral Quantization and Stochastic Quantization**  
By M. Masujima 2000. 0 figs. XII, 282 pages
- 166 **Probing the Quantum Vacuum**  
Perturbative Effective Action Approach in Quantum Electrodynamics and its Application  
By W. Dittrich and H. Gies 2000. 16 figs. XI, 241 pages
- 167 **Photoelectric Properties and Applications of Low-Mobility Semiconductors**  
By R. Könenkamp 2000. 57 figs. VIII, 100 pages
- 168 **Deep Inelastic Positron-Proton Scattering in the High-Momentum-Transfer Regime of HERA**  
By U.F. Katz 2000. 96 figs. VIII, 237 pages
- 169 **Semiconductor Cavity Quantum Electrodynamics**  
By Y. Yamamoto, T. Tassone, H. Cao 2000. 67 figs. VIII, 154 pages
- 170 **d-d Excitations in Transition-Metal Oxides**  
A Spin-Polarized Electron Energy-Loss Spectroscopy (SPEELS) Study  
By B. Fromme 2001. 53 figs. XII, 143 pages
- 171 **High- $T_c$  Superconductors for Magnet and Energy Technology**  
By B. R. Lehnndorff 2001. 139 figs. XII, 209 pages
- 172 **Dissipative Quantum Chaos and Decoherence**  
By D. Braun 2001. 22 figs. XI, 132 pages
- 173 **Quantum Information**  
An Introduction to Basic Theoretical Concepts and Experiments  
By G. Alber, T. Beth, M. Horodecki, P. Horodecki, R. Horodecki, M. Rötteler, H. Weinfurter, R. Werner, and A. Zeilinger 2001. 60 figs. XI, 216 pages
- 174 **Superconductor/Semiconductor Junctions**  
By Thomas Schäpers 2001. 91 figs. IX, 145 pages
- 175 **Ion-Induced Electron Emission from Crystalline Solids**  
By Hiroshi Kudo 2002. 85 figs. IX, 161 pages
- 176 **Infrared Spectroscopy of Molecular Clusters**  
An Introduction to Intermolecular Forces  
By Martina Havenith 2002. 33 figs. VIII, 120 pages
- 177 **Applied Asymptotic Expansions in Momenta and Masses**  
By Vladimir A. Smirnov 2002. 52 figs. IX, 263 pages
- 178 **Capillary Surfaces**  
Shape – Stability – Dynamics, in Particular Under Weightlessness  
By Dieter Langbein 2002. 182 figs. XVIII, 364 pages
- 179 **Anomalous X-ray Scattering for Materials Characterization**  
Atomic-Scale Structure Determination  
By Yoshio Waseda 2002. 132 figs. XIV, 214 pages
- 180 **Coverings of Discrete Quasiperiodic Sets**  
Theory and Applications to Quasicrystals  
Edited by P. Kramer and Z. Papadopolos 2002. 128 figs., XIV, 274 pages

- 181 **Emulsion Science**  
Basic Principles. An Overview  
By J. Bibette, F. Leal-Calderon, V. Schmitt, and P. Poulin 2002. 50 figs., IX, 140 pages
- 182 **Transmission Electron Microscopy of Semiconductor Nanostructures**  
An Analysis of Composition and Strain State  
By A. Rosenauer 2003. 136 figs., XII, 238 pages
- 183 **Transverse Patterns in Nonlinear Optical Resonators**  
By K. Staliūnas, V. J. Sánchez-Morcillo 2003. 132 figs., XII, 226 pages
- 184 **Statistical Physics and Economics**  
Concepts, Tools and Applications  
By M. Schulz 2003. 54 figs., XII, 244 pages
- 185 **Electronic Defect States in Alkali Halides**  
Effects of Interaction with Molecular Ions  
By V. Dierolf 2003. 80 figs., XII, 196 pages
- 186 **Electron-Beam Interactions with Solids**  
Application of the Monte Carlo Method to Electron Scattering Problems  
By M. Dapor 2003. 27 figs., X, 110 pages
- 187 **High-Field Transport in Semiconductor Superlattices**  
By K. Leo 2003. 164 figs., XIV, 240 pages
- 188 **Transverse Pattern Formation in Photorefractive Optics**  
By C. Denz, M. Schwab, and C. Weilnau 2003. 143 figs., XVIII, 331 pages
- 189 **Spatio-Temporal Dynamics and Quantum Fluctuations in Semiconductor Lasers**  
By O. Hess, E. Gehrig 2003. 91 figs., XIV, 232 pages
- 190 **Neutrino Mass**  
Edited by G. Altarelli, K. Winter 2003. 118 figs., XII, 248 pages
- 191 **Spin-orbit Coupling Effects in Two-dimensional Electron and Hole Systems**  
By R. Winkler 2003. 66 figs., XII, 224 pages
- 192 **Electronic Quantum Transport in Mesoscopic Semiconductor Structures**  
By T. Ihn 2003. 90 figs., XII, 280 pages
- 193 **Spinning Particles – Semiclassics and Spectral Statistics**  
By S. Keppeler 2003. 15 figs., X, 190 pages
- 194 **Light Emitting Silicon for Microphotonics**  
By S. Ossicini, L. Pavesi, and F. Priolo 2003. 206 figs., XII, 284 pages
- 195 **Uncovering CP Violation**  
Experimental Clarification in the Neutral K Meson and B Meson Systems  
By K. Kleinknecht 2003. 67 figs., XII, 144 pages
- 196 **Ising-type Antiferromagnets**  
Model Systems in Statistical Physics and in the Magnetism of Exchange Bias  
By C. Binek 2003. 52 figs., X, 120 pages
- 197 **Electroweak Processes in External Electromagnetic Fields**  
By A. Kuznetsov and N. Mikheev 2003. 24 figs., XII, 136 pages
- 198 **Electroweak Symmetry Breaking**  
The Bottom-Up Approach  
By W. Kilian 2003. 25 figs., X, 128 pages
- 199 **X-Ray Diffuse Scattering from Self-Organized Mesoscopic Semiconductor Structures**  
By M. Schmidbauer 2003. 102 figs., X, 204 pages
- 200 **Compton Scattering**  
Investigating the Structure of the Nucleon with Real Photons  
By F. Wissmann 2003. 68 figs., VIII, 142 pages
- 201 **Heavy Quark Effective Theory**  
By A. Grozin 2004. 72 figs., X, 213 pages